THE MECHANICS OF BIPEDALISM IN RELATION TO LOAD-CARRYING: BIOMECHANICAL OPTIMA IN HOMINID EVOLUTION

Thesis submitted in accordance with the requirements of
the University of Liverpool
for the degree of

Doctor in Philosophy

by

WANG Weijie

March 1999

Dedicated to my Dad and Mum:

Wang Liang & Chen Xiuqun.

献给父亲和母亲:

王亮和陈秀群

It is during doing scientific research that many people obtain the peace of mind.

Albert Einstein (1879-1955)

ACKNOWLEDGEMENTS

The first person to whom I would like to say a big 'thank-you' is Dr. Robin Crompton. At the beginning of my programme, he gave me strong support both in terms of financing the project and in the research itself. In the middle, he always gave me good advice. Especially in the later phases, he patiently reviewed my thesis word by word and understood what I tried to express in my poor English. Only with his help did the thesis come to look like it does today.

The Natural Environment Research Council, and in part, the Biotechnology and Biological Sciences Research Council and The Leverhulme Trust supported the research programme through grants to Dr. R.H. Crompton, Dr. M.M. Gunther and Professor R. McN. Alexander.

In my experiments in primates, Chester Zoo (The North of England Zoological Society, Twycross Zoo (The Midlands Zoological Society) provided invaluable research hospitality and assistance.

Without support from friendly colleagues, this thesis would never have been finished. I owe particular thanks to Dr. M.M. Gunther for introducing some interesting topics to me, and would also like to thank Dr. T. Carey for exchanging experience in study and research, and Dr. S. Thorpe for discussions on muscles. I am grateful to Dr. J. Ohman for helpful suggestions. I am grateful to Dr. C. Wood for work on reconstructing KNM WT-15000, and to Mr. R. Savage for help with computing and I especially thank Dr Li Yu for much help in carrying out experiments and discussing academic problems.

I would like to thank the staff of the Department of Human Anatomy and Cell Biology, including the former Head of Department, Prof. B. A. Wood for inviting me to visit in 1993; the current Head, Prof. P. Cobbold for various useful discussions; Mr. R. Burniston and Mr. C. Thompson for assisting with measurements and Mr. B. Read for technical help.

I would like to thank Prof. McN. Alexander for reviewing some of my draught papers and giving wise advice on biomechanical principles, which have been of benefit to the whole of my research.

I am grateful to two examiners, Prof. Preuschoft H and Dr.Gunther M for patiently reading my thesis and bringing many good comments in the viva.

In addition, I would like to extend my thanks to Drs. Shirley and Robin Crompton and Mrs. Shi Qing and Dr. Li Yu for helping my family overcome many difficulties in everyday life.

In the last, I would like to give my affectionate thanks to my wife Ms. Hu Tongjian and daughter Wang Yue, who have accompanied me for the last few years and, of course supported my study in countless ways.

ABSTRACT: Wang Weijie (Ph.D): Mechanics of Bipedalism in Relation to Load-Carrying: Biomechanical Optima in Hominid Evolution

The acquisition of bipedalism is the 'Rubicon' of hominization. Using kiniesiological recording, rigid-body dynamic modelling, calculations of energy transformation of segment and body centres of mass, computational optimization and dynamic modelling at the musculoskeletal level, I compare the mechanics of loaded and unloaded erect and bent-hip, bent-knee (BHBK) bipedal walking in humans, common chimpanzees, and early hominids including *Australopithecus afarensis* and *Homo erectus*.

Experiments show that BHBK walking has the lowest effectiveness irrespective of criterion, suggesting that selection would have favoured early adoption of erect walking. In loaded BHBK walking, moments at the knee are larger and last longer than in erect loaded walking, and moments last almost through the whole of stance. As a result, total joint power is almost 1.5 times greater in BHBK loaded walking, and energy recovery two times lower. Thus, selection against BHBK walking would probably be increased by load-carrying. Comparison of humans with chimpanzees shows that the parameters of chimpanzee joints are less effective. Larger peak moments act at the knee, and larger powers at the hip. Among various modes of human walking, comfortable walking has the best effect on energy transformation and BHBK walking the worst. Chimpanzees had the least effective transformation. Considering positive work done as the effort output from the body to power walking, BHBK walking expends more work done than erect walking. Positive and negative work may play different functional roles.

Simulated ground reaction forces (GRFs) during erect walking by AL-288-1 and WT-15000 are very similar to GRFs measured during erect walking for living adults, suggesting that both fossil species had human-like gaits. WT-15000 has smaller joint powers and moments than AL-288, and androids with a relatively short trunk tended to walk with higher mechanical effectiveness. Selection may thus have operated to increase the length of the lower limb relative to the trunk. Using as dual criteria a match between upper and lower limb swing time, and ability to carry loads in the hand, AL-288 could only have carried weights of 15%-50% upper limb weight while maintaining swing symmetry, but WT-15000 and modern humans weights 3 times upper limb weight. Carrying ability of chimpanzees is worse than that of AL-288-1. The intermembral index of modern humans, at 68-70, is around the smallest, and optimal for hand-carrying. Under reduced selection pressure for hand-carrying, we might expect humans to evolve a longer upper limb, to improve unloaded swing symmetry.

The results from musculoskeletal models show that total of muscle forces and powers in BHBK is larger than in erect walking.

All other things being equal, if achievement of minimum motive power was a selective criterion, human stature might tend to increase slightly in the future but at a lower rate. If mobility and loaded stability were the selective criteria, there should be no size increase.

与搬运相关的两足行走力学：生物力学优化和早期人类进化

王威杰

两足行走是人类起源的重要特征.本文运用运动学试验,多刚体动力学模拟,能量转换分析,计算机优化,和肌肉骨骼模型等方法,比较了搬运和非搬运情况下,人,猩猩和原始人(包括非洲南方古猿,AL-288-1, 和早期直立人, WT15000) 的直立行走和弯膝行走.

试验显示弯膝行走有较差的力学效果.这意味着进化选择可能倾向直立行走.在弯膝搬运行走时,膝关节承受较大的,和较长时间的力矩,使关节功率几乎是直立行走的1.5倍.在能量转换上,直立行走效率几乎是弯膝行走的2倍.

猩猩的行走效果比人更差.它有更高的膝力矩和消耗更大的功率.就人的各种步态来讲,"适意"性行走有着最好的能量转换效果.这可能是人们选择这种步态作为日常使用的原因.假如考虑正功作为身体输出的部分,弯膝行走使身体付出更多的功.

用计算机模拟技术,南方古猿,早期直立人和现代人已被建成多刚体机器人.早期原始人的化石骨骼提供了他们的体形尺寸.根据这些尺寸,依靠计算机,可建成模型.当模型作行走时,模拟出的地面反作用力与试验所得的力非常相似.这使得研究原始人的步行成为可能.模拟结果表明,当作同样行走时,早期直立人比南方古猿消耗较少的关节功率.尤其是当他们作搬运行走时,早期直立人的身体比例可能更适合携带行走.他的较短的上体可能有助于作搬运.另外,根据对上下肢的理论分析,早期直立人可能手握更重的物体行走,而保持上下肢的谐调运动.

利用计算机技术和解剖知识,可以估计肌肉参数,例如肌肉速度,力和功.假设早期原始人有着与现代人相似的肌肉连接,可以建成肌肉骨骼模型.当运动数据已知时,利用数学方法,可以模拟肌肉运动.对南方古猿的分析结果表明,弯膝行走需要更大的肌肉力和功率.这表明直立行走有其生物力学的背景.

根据对行走功和早期原始人骨骼比例的分析，假如力图提高行走效率，人类的身高可能有长高的趋势。另方面，若考虑运动和承载性能，这种趋势可能是相当慢的。

另外，本文所用方法可被广泛用于体育，医学，人机工程和行为控制等领域。

CONTENTS

Abbreviation

Symbols

β	Angular acceleration
$\Delta\theta$	A small change of joint angle
ΔE	The range of energy
Δt	A small change of time
η	A coefficient, the ratio of VCM to the range of energy
π	3.14159
ρ	Density of mass
ω	Angular velocity
3D	Three dimensions
a	Acceleration
a_m	Muscle moment arm
AP	Absolute power
BL	Body weight and limb length
BV	Body weight and velocity
C	A computer programing langrage
CM	The centre of mass
d	Characteristic diameter
$D(p_i,p_j)$	Distance between two point i and j
DCM	Displacement of the centre of mass
EMG	Electromyography
F	Force
F(X)	Object function
f(X,G)	Object function
F_g	Ground reaction force
F_m	Force in a muscle
g	Gravity constant, 9.8 m/s
G	A set of functions
G_a, G_b	Constraint conditions for G
g_i	Function i
g_{ia}, g_{ib}	Constraint conditions for g_i
GRF	Ground reaction force
I	The moment of inertia
I_c	The moment of iertia of carriying mass about a rotating center
I_i	The moment of iertia in a segemnt i
IMI	The intermembral index
KE	Kinetic energy
L	Characteristic length
LHS	Left heel strike
L_i	Limb length of a segment i
L_m	Length in a muscle
L_p	The ratio of limb lengths

LTO	Left toe takeoff
m	Mass
m	Mass of a segment or a whole body
M	Moment or torque
m_c	The mass carried
m_i	The mass of a segment i
M_{oi}	Moment about a segment centre of mass
M_p	The ratio of carried mass to limb mass
MYA, Mya or MYR	Million years ago
N	A force unit, Newton
NP	Negative power
NW	Negative work done
P_d	Dimensionless power
PE	Potential energy or gravitative energy
p_i	Point i on a segment
Pi	Potential force or gravitative forces on a segment
P_m	Power for a muscle
PP	Positive power
PRM	Power required for motion
PW	Positive work done
R	Rotation matrix between different reference frames
RHS	Right heel strike
r_i	The radius from the position on which a force acts to a segment CM
R_p	Robusticity coefficient, d/L
RTO	Right toe takeoff
RUL	Ratio of the upper trunk length to the lower limb length
s	Displacement
SD	Standard deviation
SF	Swing factor, the proportion of swing time and total cycle time
Stance	A phase of a foot contacting on the ground during walking
Swing	A phase of a foot swing in the air during walking
t	Time
v	Velocity
v_c	The velocity of the centre of mass
VCM	The average velocity of the centre of mass
v_m	Velocity of a muscle
X	A set of variables
X_a, X_b	Constraint conditions for X
x_i	Variable i
x_{ia}, x_{ib}	Constraint conditions for x_i
ε	A coefficient, the ratio of the range of changes in kinetic and potential energies to the range of change in the sum of two energies

Names of muscle groups

GA	Gastrocnemius
GU	Gluteus maximus
HA	Biceps femoris/semitendinosus/semimem branosus
RF	Rectus femoris
SO	Soleus
TA	Tibialis anterior
VS	Vestus lateralis/medialis

Gaits

b	Acceleration from standing
bb	Acceleration from standing in BHBK walking
be	Deceleration to stopping in BHBK walking
BHBK	Bent-hip and bent-knee
BLW	Bent-hip and bent-knee loaded walking
BW	Bent-hip and bent-knee walking
ch	Walking like chimpanzee
CW	Comfortable walking
e	Deceleration to stopping
fa	Fast walking
FW or FAS	Fast walking
NLW	Normal loaded walking or erect loaded walking
no	Normal walking
NW	Normal walking or erect walking
sl	Slow walking
SW or SLO	Slow walking

CHAPTER 1 INTRODUCTION

Even a journey of a thousand miles begins where you are standing.

Chinese Proverb

1. 1 The evolution of bipedalism

1. 1. 1 Reasons for the acquisition of bipedalism

The origin and evolution of bipedalism has been discussed ever since Darwin (1871) and remains a topic of hot debate. There are many different views about the reasons for the acquisition of bipedalism, summarized by in Table 1.1, taken from Rose (1991).

However, while speculation as to the reasons why bipedalism was acquired is an amusing pastime, it is less appropriate for scientific enquiry than are the sequential changes in anatomical structure and function that lead to one, and only one, of the three lineages of living African great apes performing efficient bipedal walking, and habitually using bipedal walking rather than any of the other alternative modes of progression. Humans cannot fly unaided, but can run, climb, jump, hop, swim and walk quadrupedally. How did human evolution lead to the selection of bipedal walking among all these alternatives? Since walking is a mechanical process, where work is done on the external environment to propel the body, these questions needs to be answered from a mechanical perspective.

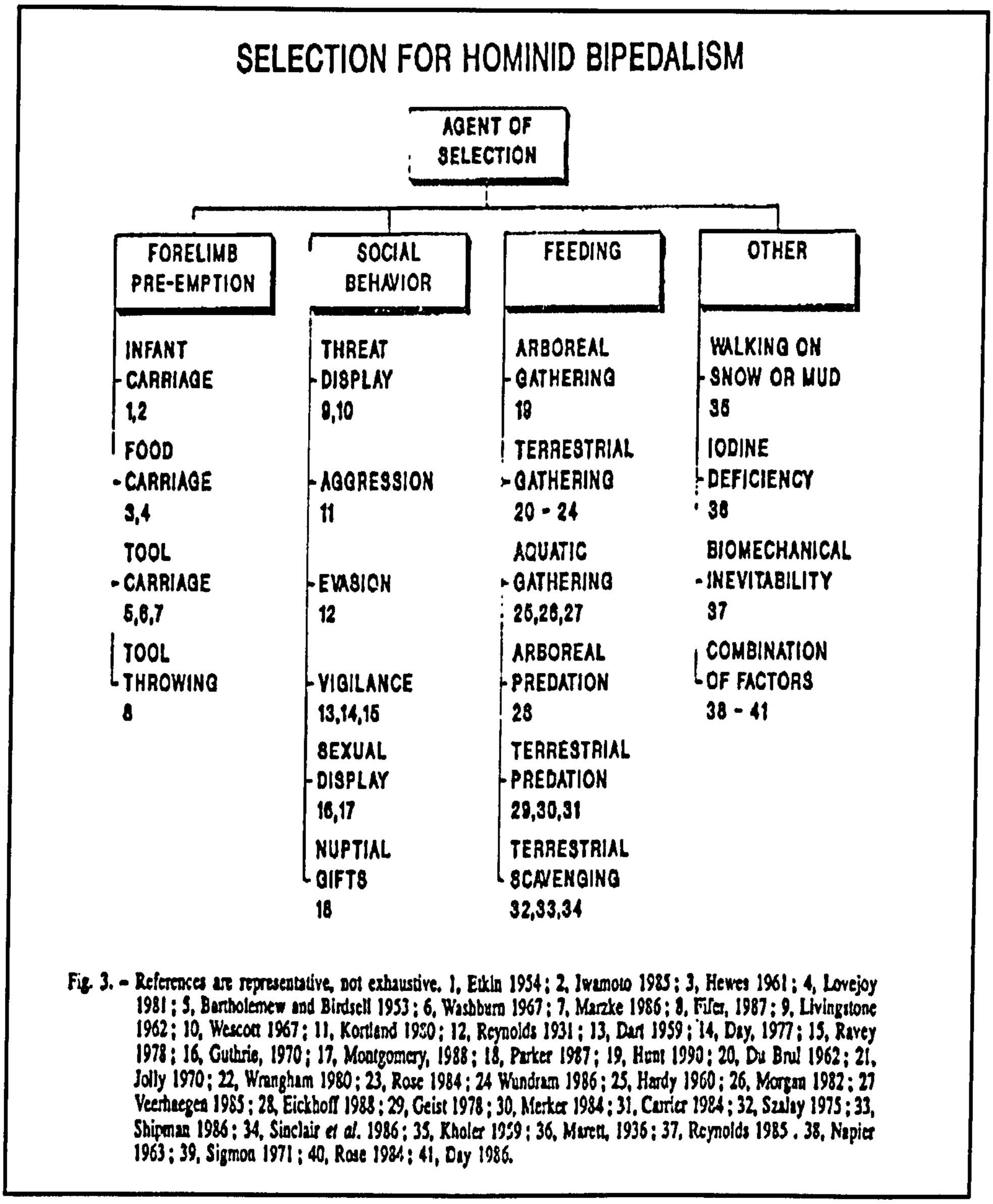

Fig. 3. – References are representative, not exhaustive. 1, Etkin 1954; 2, Iwamoto 1985; 3, Hewes 1961; 4, Lovejoy 1981; 5, Bartholemew and Birdsell 1953; 6, Washburn 1967; 7, Marzke 1986; 8, Fifer, 1987; 9, Livingstone 1962; 10, Wescott 1967; 11, Kortland 1980; 12, Reynolds 1931; 13, Dart 1959; 14, Day, 1977; 15, Ravey 1978; 16, Guthrie, 1970; 17, Montgomery, 1988; 18, Parker 1987; 19, Hunt 1990; 20, Du Brul 1962; 21, Jolly 1970; 22, Wrangham 1980; 23, Rose 1984; 24 Wundram 1986; 25, Hardy 1960; 26, Morgan 1982; 27 Veerhaegen 1985; 28, Eickhoff 1988; 29, Geist 1978; 30, Merker 1984; 31, Carrier 1984; 32, Szalay 1975; 33, Shipman 1986; 34, Sinclair *et al.* 1986; 35, Kholer 1959; 36, Marett, 1936; 37, Reynolds 1985. 38, Napier 1963; 39, Sigmon 1971; 40, Rose 1984; 41, Day 1986.

Table 1.1 Reasons for the acquisition of human bipedalism, from Rose (1991)

1.1.2 The fossil record

In order to investigate the evolution of bipedalism, we have one source of historical data: the fossil record. While fragmentary evidence of the postcranial skeleton of early hominids has long been available (see, e.g. Broom 1938 a and b, Broom and Schepers 1946, 1950; Day and Leakey 1973) it is only within the last quarter century that reasonably complete fossil skeletons have been discovered. The two best known remain *Australopithecus afarensis* AL-288-1 ('Lucy') from the Hadar region of Ethiopia (Johanson et al 1982 and 1987) and *Homo erectus* KNM M15000 from Nariokotome in Kenya (Walker and Leakey, 1986). The fossils have provided us with much information about the skeletons of early hominids a few million years ago (MYA).

1.1.2.1 AL-288-1 Australopithecus afarensis *'Lucy'*

The 40% complete skeleton AL-288-1 dates to around 3.4-3.6 MYA, and bipedality is attested to by several diagnostic features, such as the unequal size of the femoral condyles, which would have produced a habitually adducted posture of the thighs. However, AL-288-1 had relatively long upper limbs and shorter lower limbs than modem humans, her phalanges were curved, and her trunk was shaped like a truncated cone, rather than being anteroposteriorly flattened as in ourselves (see, e.g. Jungers 1982; Jungers and Stern 1983; Wolpoff 1983a and b). Thus, while there is general agreement that the postcranial skeleton shows features adaptive to

bipedalism as well as to arboreal climbing, the mechanical nature of any such bipedalism has still not been agreed upon. Lovejoy (e.g. 1981), Latimer and Lovejoy (1989) and Latimer (1991) hold that this early hominid was an erect terrestrial biped, whose supposed adaptations to climbing were essentially anachronistic. On the other hand, Stern and Susman (1983) conclude that Lucy's gait was most likely characterised by a "bent-hip, bent-knee" (BHBK) posture (1983, page 312). The distinction has an analogue in the distinction between the kinematics of bipedal walking by common chimpanzees and that of humans: while humans walk with relatively straight knees and extended hips, common chimpanzees maintain flexed postures of the knee and hip joint, in which the leg rarely, if ever, passes behind the hip joint (Jenkins, 1972; Kimura et al., 1979 Tardieu, 1987; Tardieu et al. 1993). The dynamics of human and common chimpanzee bipedalism are also distinctive: during chimpanzee bipedalism the vertical components of the ground reaction forces (GRFs) are described by an essentially flat-topped, single-peaked curve, while that of normal human walking is always two-peaked (Kimura et al. 1979; Kimura 1986; Alexander 1991; Li et al. 1996). Distinctions in ground reaction forces in turn imply the possibility of differences in mechanical effectiveness.

Cavagna and colleagues (1976) integrated ground reaction forces against the foot during human walking, and estimated from this the proportion of the external work done by the body 'recovered' by transformation of kinetic to potential energy and vice-versa. They found that while recovery is very variable, the greatest recovery

(48-70%) occurs at speeds around 1.4 m/s. falling off very steeply to about 5-10% over 2.8 m/s., and below 1.1 m/s. In a later paper, Cavagna et al. (1977) argued that exchange of potential and kinetic energies is made possible by the 'inverted pendulum' mechanism of human striding gait. Alexander and Jayes (1980) characterised this type of bipedalism as 'stiff' walking, and contrasted it with flexed-knee bipedalism as 'compliant' walking. They suggested (and see Alexander, 1992) that energy transformation should only obtain in 'stiff' walking, where fluctuations in potential and kinetic energies are out of phase[1]. Alexander (1991) also proposed that the kinematic and kinetic characteristics of non-human primate gaits are functionally related; the flat-topped GRF curves of non-human bipedalism being the product of flexed-knee (compliant) gaits just as the two-humped GRF curves characteristic of human bipedalism are the product of straight-knee, "stiff" gaits. Indeed, Yaguramaki et al. (1995) showed that the shape of GRF curves is affected by posture, flexed-knee postures reducing the height of the second peak. Thus, we should expect that the flexed-knee, compliant bipedalism of common chimpanzees would lack effective energy transformation. However, Kimura (1996) used a method similar to that of Cavagna et al. (1976) to determine the ontogeny of recovery in bipedal walking by trained chimpanzees. He found, despite greater

---

[1] Several studies have investigated compliant effects in running and hopping: for example, McMahon et al. (1986) showed that running with bent knees may increase oxygen consumption by up to 50%; Farley et al. (1991) found that the human body behaves as a simple spring-mass system at a wide range of hopping speeds, but ground contact time increased at subjectively preferred speeds, and Farley and Gonzalez (1996) have shown that in human running, the angle swept by the leg spring decreases at higher stride frequencies, while the stiffness of the leg spring increases sharply. However, the mechanics of energy conservation in running are very different from those in walking (Cavagna et al. 1977; Farley and McMahon 1992) savings being made by return of energy by elastic recoil of muscle-tendon springs, rather than by exchange of potential and kinetic energies.

variability than for Cavagna's humans, that recovery increases with age between 1 and 5 years, the youngest obtaining 20% recovery or less, the eldest as much as 70%, and argued that older chimpanzees are better able to sustain extended knee postures.

Alexander and Jayes' (1980) distinction between compliant and stiff gaits was quickly applied to interpretation of Lucy's likely mode of bipedalism. As Schmitt, Stern and Larson (1996, p. 209) put it, Susman et al. (1984) "*suggested that use of a compliant gait that included hip and knee yield during walking would result in reduced substrate reaction forces and that this in turn might explain the absence of anatomical evidence for human-like sacroiliac stabilization in AL-288-1*". In an abstract, Schmitt, Stern and Larson (1996) returned to this argument, reporting that human subjects reduced vertical force by 10-25% of body weight during compliant walking, and suggesting that: "*The use of a compliant gait could have facilitated the transition from a nonbipedal gait to a fully bipedal one*" (p. 209). However, since the integral of vertical ground reaction forces on time is a constant for any given subject[2], if the magnitude of any peak falls, the curve must therefore rise by the same amount somewhere else. Either the second peak will increase, or the valley in the curve will decrease. Only peak loads, or their timing, could be affected. Thus, "substrate reaction forces" are not "reduced" in compliant walking, but rather changed in timing.

---

[2] essentially, body weight.

Crompton et al. (1998) used predictive dynamic modelling to assess the mechanical effectiveness of AL-288-1 under both hypotheses, on the basis of data on segment proportions from the literature. They found that AL-288-1's proportions were incompatible with the kinematics of chimpanzee bipedalism, but compatible with the kinematics of either erect or BHBK human gait. In the latter case, neither the ankle nor the knee joint would have contributed substantial mechanical work to propulsion of the body, and net energy absorption was predicted for these joints, which would have resulted in increased heat load. They thus concluded that such an ineffective gait is unlikely to have lead to selection for 'bipedal' features in the postcranial skeleton.

An unpublished thesis by Carey (1999) in the same laboratory has confirmed, from physiological measurements on modern humans, that 'BHBK' walking does indeed lead to doubling or near-doubling of oxygen consumption and lactate production, and substantially increased core body temperature.

1.1.2.2 KNM WT-15000 Homo erectus

KNM WT-15000 dates to about 1. 6-1.8 MYA (Walker and Leakey, 1986). This skeleton represents early African *Homo erectus*. Unlike *Australopithecus afarensis*,

Homo erectus is known from East and South-East Asia and southern Europe as well as East Africa. The skeleton of WT-15000 is 75% complete. It is characterised by a shorter trunk and longer leg than either AL-288-1 or modem humans, although the morphology of individual bones is rather similar to those of modern humans (Walker and Leakey 1986).

Hunt (1994) suggested that early hominid bipedalism may have had its origin in a subset of the behaviours he has observed in chimpanzees in the wild. Hunt showed that bipedalism in chimpanzees occurs predominantly in the form of 'postural' bipedalism, which chimpanzees adopt while reaching to feed from trees. In the chimpanzees Hunt observed, functional bipedal locomotion was a rare activity which consisted of relatively ungainly "shuffling between trees" (Wood, 1994 p. 588). Hunt proposed that the "poor bipedal mechanics" (Hunt 1994 p. 198) of *A. afarensis* may be explained by an analogy to the 'postural bipedalism' of chimpanzees. He identified several functional features of the postcranial anatomy of *A. afarensis* which he believes could be linked with a postural rather than locomotor bipedalism, and went on to suggest that locomotor bipedalism (the 'preeminent bipedalism' of Prost [Prost 1980, p. 1861), did not appear until the emergence of early African *Homo* erectus), between 1.9 and 1.8 million years ago. The latter suggestion receives support from comparative physiological studies by Wheeler, who suggests that the thermoregulatory benefits of larger body size (Wheeler, 1992) and the taller physique (Wheeler 1993), when linked with

increasing locomotor efficiency, allowed early African *H.* erectus to range more widely.

Recently, there has been accumulating evidence, from Java and Georgia, that H. *erectus* had a much earlier dispersal in the Old World than had been conventionally accepted. In particular, work by Swisher and colleagues (Swisher et al. 1994) suggest that this species is as old in Java as it is in Africa. This early dispersal coincides with a period, between 3.6 MYA and 1.9-1.8 MYA, in which there was a major reorganization in the anatomy and function of the postcranial skeleton of early hominids, as witnessed by the contrast between the "mosaic" nature of the skeleton of Lucy (whose human-like knees go together with chimp-like thorax and arms, and an unique abductor mechanism at the hip) and the almost entirely modern-human aspect of the skeleton of WT-15000.

Since, in studies of human evolution, stone tools remain our most direct evidence of early hominid ranging behaviour, we should expect such changes to be reflected in the pattern of distribution of stone tools across the landscape. A simple and robust measure of ranging behaviour can be derived from studying the distance between a given assemblage of stone tools and the source of the material of which the tools were made. Caution must be employed in interpreting such evidence. McGrew (1993) for example noted that chimpanzees, despite their small day- and home-ranges, can move material across a landscape in additive small journeys, and he concludes that early hominid transport may reflect a similar phenomenon. But the

manufacturers of both the Oldowan and Acheulean industries do appear to have transported raw materials.

The best documented cases of Oldowan raw material transport are from Olduvai Bed I, where distances of 3km - 12 km have been established (Leakey 1971; Hay 1976). East Turkana also provides instances of the importation of raw material onto flood plains of the ancient lake, over distances of up to 20 km. (Harris and Ilerbich 1978). However, in Acheulean sites, evidence suggests that transport occurs more often - and over much greater distances. At Gadeb, in eastern Ethiopia, dated at about 1.5 MYA, several obsidian bifaces apparently document a transport distance of over 100 km (Clark 1980). At Olorgesailie, it was noted that occurrences of quartz brought over 40 km. At Kilombe, similarly, two obsidian bifaces appear among many hundreds made from local lavas, and the implication is again that long distance transport occurred (Gowlett, 1982). A later example from Arago, in France, suggests that artefacts were being transported systematically for distances of up to 30 km (Wilson, 1988). The archaeological record thus indicates that transport both becomes more common, and occurs over much greater distances, during the period in which early African *H. erectus* skeleton acquired its more modern-human looking postcranial morphology.

Schultz (1937 and later) is the first man who carefully observed and compared the differences of body proportions between humans and high primates. His works has

brought many interesting topics which are worthy to be researched.

1.2. Research Topic

This thesis is therefore primarily intended to address the question of whether the acquisition of the longer-legged, shorter-trunked morphology of WT-15000 does indeed increase mechanical effectiveness in load-carrying.

1.2.1 Assumptions

Natural selection acts at many different levels, and may favour adaptations which improve access to resources such as food or mates, or escape from predators, rather than directly enhancing speed or force. However, in this thesis, I shall assume that natural selection acts upon the locomotor system so as ultimately to enhance mechanical performance capabilities (Alexander, 1991) in behaviours which are adaptively important. Thus, I shall model the process of evolution of the locomotor system as a process of mechanical optimization, and consider the two alternative modes of bipedal walking in early hominids, erect walking and 'bent-hip, bent-knee' walking in these terms. Since we cannot know what the selective forces were on given species at given times, I shall make the further assumption, which I believe to be reasonable, that all other things being equal, natural selection will tend

to optimize the locomotor system so that forces and energy costs are reduced for a given level of performance.

1.2.2 Scope

Both the geometry (lengths, shapes and angles) of individual body segments and the way the segments are articulated, may influence the mechanics of bipedalism (Preuschoft 1970, 1971a and b, 1978, Preuschoft and Witte, 1991). For example, if segments become longer, we might expect a longer step length. But if muscles joining these segments permit only limited excursions, step length may not change. Thus, the present study is concerned not only with segment proportions, but muscle attachments.

The primary research tool shall be predictive dynamic modelling, incorporating an optimization approach, based on kinematic and kinetic data from humans and other living hominoids.

However, with respect to the latter, many problems still remain concerning the comparative biomechanics of unloaded bipedalism in modern humans and our best-known relative, the common chimpanzee. We need much more knowledge, in particular, concerning joint angles, joint velocities, joint torques, joint power and required energy. We need to know how muscles in the lower limb work in erect

walking (NW) and bent-hip, bent-knee (BHBK) walking. We need to know whether the skeletal proportions of early hominids, modern humans and chimpanzees are better suited to BHBK walking or to NW. And, most ambitiously, since details of postcranial morphology and the energetic costs of bipedalism alike depend on the capabilities of muscles and muscle groups, we should begin to estimate muscle forces for early hominids.

1.2.3 Research Plan

The research is divided into several logical stages.

Firstly, I derive and implement a general program for gait analysis, capable of digitizing video sequences, calculating joint angles, joint velocities, joint moments and joint powers, analysing energy transformation and so on.

Secondly, kinetic and kinematic signals is acquired using this program in a wide range of experiments, including investigations of human erect unloaded (NW) and loaded walking (NLW), human BHBK loaded walking (BLW) and common chimpanzee BHBK walking. Some data for unloaded walking were previously available in our laboratory and are reanalyzed with different ways, but most of the required experiments were performed *de novo* for this study by myself, and other members of our research group.

Thirdly, three kinds of models, including particle, multi-rigid-body and musculoskeletal models, will be built, employing appropriate mechanical methods. The kinematic and kinetic data will be applied to the different models according to the questions being asked.

The order of work usually follows the scheme:

1) digitization of video records to provide kinematic data;

2) calculation of all fundamental parameters, including joint motion, joint angular velocity, joint moments, etc.

3) energy analysis using a particle-mechanics approach;

4) construction of androids (multi-rigid-body models) using the commercial dynamic modelling software ADAMS, and simulation studies using these models;

5) analysis of muscle parameters, including muscle forces, velocities, lengths, moments and powers.

Fig. 1.1 shows the primary research pathways.

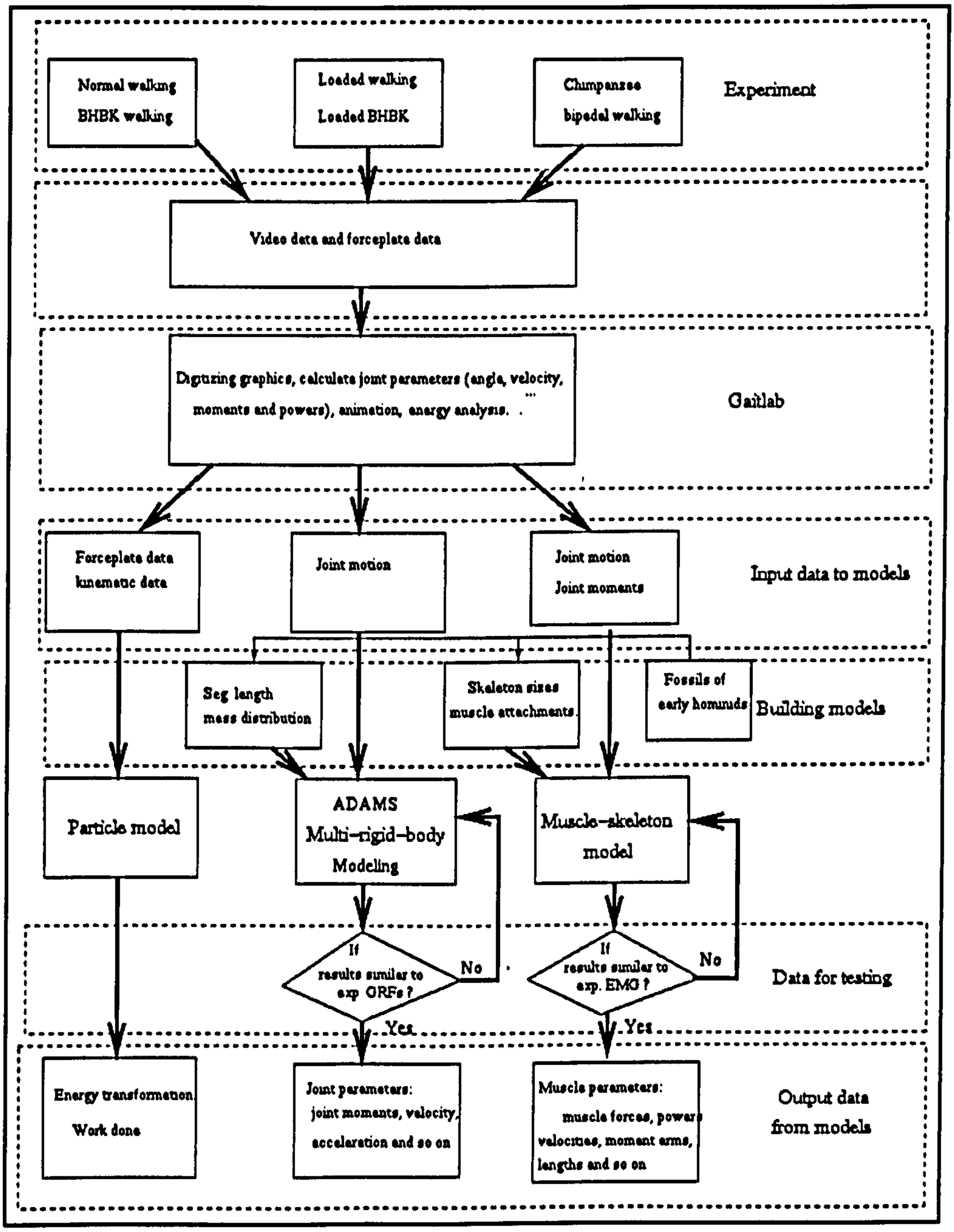

FIGURE 1.1 Main research pathways.

CHAPTER 2. RESEARCH METHOD OVERVIEW

Before starting work, you must ready your tools.

Chinese Proverb

2.1. Basic biomechanics

2.1.1 Mechanics and biological subjects

Classical mechanics offers many effective methods, especially those derived from Newton's Laws, which enable us to solve some basic problems involved in kinematics and kinetics for biological subjects. When classical mechanics was first systematically applied to the analysis of biological subjects in the early 1970's , a so-called 'new' biomechanics developed, which since has matured very quickly (Alexander 1968; papers in Alexander and Goldspink 1977; Alexander et al. 1992; McMahon 1984; Winter 1990, 1991; Nigg & Herzog 1994) and applied in the analysis of human evolution (see, eg. Kimura 1986; Yamazaki 1985). In particular, Preuschoft (1971) addressed the consequences of body shape and posture for the mechanical stresses operating within and across segments.

In order to apply the theories of mechanics to biological subjects, we first have to measure them, to obtain necessary data. As our subjects are living creatures, most often humans, it is usually impossible (let alone unethical) to obtain internal forces directly, since this would require vivisection. However, given necessary data, such as kinematics and ground reaction forces (GRFs), some internal parameters, such as joint moments, may be derived indirectly, from data obtained non-invasively. In the last 25 years, however, the introduction of equipment and techniques such as high-speed videography, the force platform, electromyography (EMG) and magnetic resonance imaging, have enabled us to obtain much of the necessary data (Cavagna et al. 1976; see papers in Alexander and Goldspink 1977; Winter 1990, 1991; Nigg and Herzog 1994) using dynamic analysis.

2.1.2 Inverse and forwards dynamics

In order to work out such internal parameters, we have noted that we may calculate from external kinematic (joint motion) and kinetic (forceplate) data. Calculation of

internal parameters, for example joint forces and moments, from external data is known as inverse dynamics (Winter 1990; Nigg and Herzog 1994; Alexander 1992; McMahon 1984). We generally require to assume that all segments are rigid. Inverse dynamics, as a modelling technique, usually requires verification of predicted results, such as mechanical energy costs, against appropriate real-world physiological data, which in this case would be metabolic energy costs, obtained by methods such as measurement of oxygen consumption (see, e. g. Chapter 1) before predictions may legitimately be used to explain biological cases.

In contrast to inverse dynamics, we may consider the case where, as muscle activity in biological subjects is stimulated by signals from the central nervous system, central stimuli may elicit and control muscles and hence lead to an external action, from which external kinematic and kinetic results may be obtained. Predicting the latter parameters from input stimuli such as EMG patterns is known as forward dynamics (Hash, 1996 and 1998; Winter, 1990).

In this thesis, I employ mainly inverse dynamics and partial forward dynamics.

2.1.3 A purpose-written software' package: 'Gaitlab'

Graphic analysis of motion is a basic tool in biomechanics. In other words, when analysing cinematographic film or video-recordings of a subject's behaviour, we may obtain the kinematic characteristics of the behaviour, such as displacement, velocity and acceleration at crucial points in the performance. With data from graphic analyses of motion data, many other kinematic parameters, such as angle, angular velocity and angular acceleration at joints, may easily be derived.

If the mass distribution of a subject is given, with the addition of kinematic parameters, the location and displacements of the body or segment centre of mass (CM) can be calculated during the whole sequence of motion. Moreover, given both

kinematic data and ground reaction forces (GRFs) measured by forceplate, kinetic parameters for joints may be obtained, and the energy exchange in the body CM may be analysed.

In order to perform such calculations reliably, I have designed and implemented my own software, called 'Gaitlab', which covers most aspects of basic kinematic and kinetic analysis (see Appendix A). The software includes modules which can digitize sequences of video, analyse GRFs from a forceplate, calculate joint parameters (joint angle, velocity, moment and power) and estimate the energy exchange during walking. Some new modules are being developed and added.

2.2 Joint dynamics

Joints play the key roles in the motion of biological subjects, and so, investigation of joint parameters is an important, if basic element of biomechanics studies (Winter, 1990; Nigg and Herzog 1994).

Following Newton's laws, there are identical equations for each segment:

$$\sum F_i = ma \qquad (2.1)$$

$$\sum M_{oi} + \sum F_i R_i = \beta I \qquad (2.2)$$

where: F_i represents all forces acting on a segment, including external forces and mass gravity force; Mo_i the moment about the centre of a segment, produced by all forces; R_i the radius from the position on which a force acts to the centre of a segment; β the angular acceleration about a segment centre of mass; and I the moment of inertia about a segment centre of mass (see Fig. 2.1).

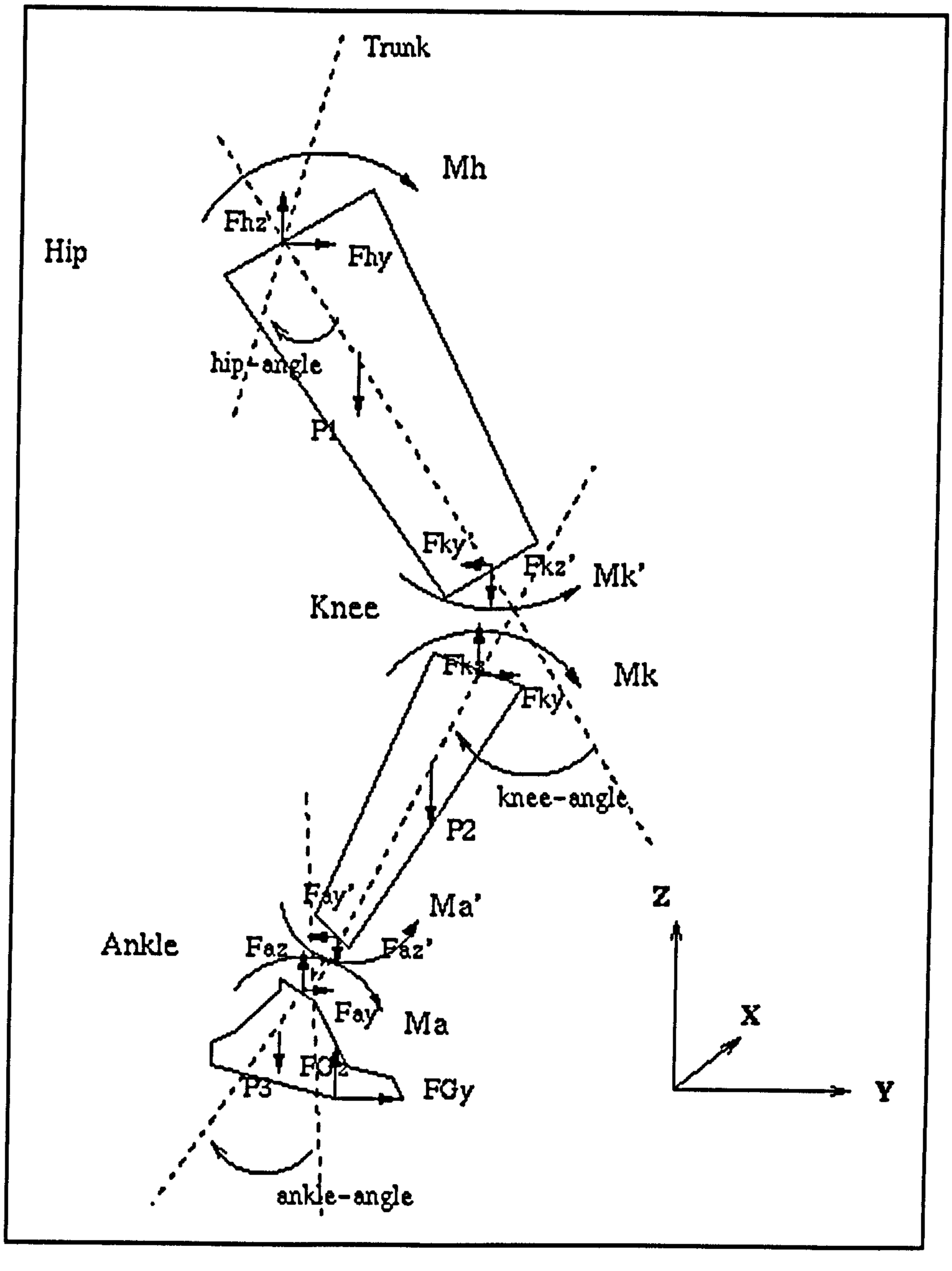

FIGURE 2.1 Graphic definitions of measured or calculated parameters

If these equations are applied to the sagittal plane for each segment, we can work

out the three unknown variables (F_{iz}; F_{iy} and Mo_i) at each joint from the equation groups for each segment. Thus, with the measured GRF, we can calculate all unknown variables centripetally from the most distal segment and joint, subject to the assumption that every segment may be treated as rigid.

In Gaitlab, joint angles and angular velocity are obtained by stereophotogrammetric reconstruction of segment coordinates for succeeding video fields after application of a filter. Joint angles are defined as the angle between the proximodistal long axes of two adjacent segments. The origin of the local reference system is fixed at the most proximal joint, and the main reference system is defined as x: lateral, y: sagittal and z: vertical.

The general processes are as follows: (1) recording frontal and sagittal video images, and converting them into useful data by digitization of segment landmarks while simultaneously recording GRFs; (2) computing all joint moments from the recorded data centripetally; And (3) calculating mechanical joint power as the dot product of the joint relative velocities and moments during a stride.

There are many methods by which to compute the power of joints (see, e. g. Cappozzo, 1975; and Zarrugh, 1981). The main arguments in the literature have involved how to define segments and how to explain positive and negative power. This chapter does not discuss these methods (however, for some discussion see Chapter 6), but instead applies a standard method in biomechanics and mechanical engineering, that of Winter (1990):

$$Power = \frac{1}{N}\sum \frac{M_{oi}\omega_i}{weight} \qquad (2.3)$$

where weight: body weight; ω: angular velocity; N: the total of a sequence of frames.

Power may be expressed as absolute, negative, positive and mean power. To permit comparison of different subjects, moments were normalized by body weight and lower limb length, and joint powers normalized over a full stride and expressed in relation to body weight, and the average velocity of the body centre of mass (CM).

2.3 Particle mechanics

2.3.1 Assumptions

It is said that 'small is beautiful'. In this spirit, we attempt to use a method as simple as possible. One of the simplest is particle mechanics, in which a complex system is considered as a physical particle with mass. Generally, the whole human body is considered as a particle: the body CM its location, the body weight its mass, and all contact- and non-contact forces acting on the body are also considered to apply to the particle. On this basis, we may readily calculate the particle's displacement, velocity and acceleration and all other kinetic parameters.

At the same time, very obvious errors will exist, since this technique ignores any rotations of segments, which can produce rather large changes of energy without necessarily affecting the CM: for example, when we lift weights by the hands and swing the arms symmetrically.

2.3.2 Work done and energy in particle mechanics

Given external forces, such as GRFs, and treating the whole body as a particle, Newton's Laws may be written in the same way as those in the different planes:

$$F_z - mg = ma_z \qquad (2.4)$$
$$F_y = ma_y \qquad (2.5)$$
$$F_x = ma_x \qquad (2.6)$$

where F: GRFs acting on the subject and measured by forceplate; m: mass of the subject; a_i: acceleration of CM. F is the total ground force, the sum of the GRFs after taking into consideration the phase of double support. The acceleration of CM, a_i, can then be obtained. By integrating a_i once more, we can obtain velocity (2.7) and displacement(2.8) :

$$v(t) - v_0(t_0) = \int \frac{F(t)}{m} dt \qquad (2.7)$$
$$s(t) - s(t_0) = \int v(t) dt \qquad (2.8)$$

where v: velocity; s: displacement.

By the definition of mechanical energy, the translational kinetic energy and the gravitative potential energy of the CM of a subject are as follows:

$$W = \int F ds \qquad (2.9)$$
$$KE = \frac{1}{2} m v_c^2 \qquad (2.10$$
$$PE = mgz_c \qquad (2.11)$$

where W: work done; PE: potential energy; KE: kinetic energy; v_c: the velocity of CM, in the horizontal and vertical directions; z_c: the displacement of CM in the vertical direction.

From (2.4)-(2.10), we can calculate all variables during walking. The method has been applied in many situations (see, eg. Cavagna et al. 1976; Kimura 1996), and

will be employed in Chapter 5 and Chapter 6 of this thesis.

2.4. Multi-rigid-body mechanics

2.4.1 The segment rigidity assumption

We may obtain more accurate results if a subject and its segments is considered as a system rather than as a particle. However, when considering body segments -- which not only move but also change shape -- it is important to make the assumption that every segment is rigid, in other words, that neither shape nor mass change under any external influences, such as forces, moments and impacts. This assumption, once made, enables us to apply almost all the methods of classical mechanics to biomechanical research.

2.4.2 ADAMS: A commercial dynamic analysis software package

ADAMS (MDI 1995) was designed as a general package for the analysis of mechanical systems. ADAMS's mechanical calculation techniques rely primarily on Langrange methods (see ADAMS manual, 1995). It can calculate all mechanical parameters of a mechanical system, such as contact forces between parts, and joint moments, subject to the conditions users apply.

In the module ADAMS-ANDROID, users create an android with all necessary segments, then apply sources of drive, e.g. joint motion functions or joint moments, to the android. The model can then simulate the motion of a real subject. If all inputted data satisfy theoretical mechanical requirements, the android can move in manner similar to normal motion of real humans; if not, the android will fail to do so, for example, falling down, jumping or rotating in strange ways.

I apply the software to the reconstruction of the gait of early hominids in chapters 7

and 8.

2.5 Computational simulation

As early hominids lived several million years ago, and their behaviour cannot be investigated directly, computational simulation may offer one of the best chances of studying their behaviour.

A wide range of simulation models exist in the biomechanics literature, from the simple (e. g. Alexander, 1980; Preuschoft and Witte 1991) to the complex (eg. Hase, 1996 and 1998). Computational simulation has been developed largely since the later 1970's, but Yamazaki (1985) was the first to have performed computer simulation of primate bipedal walking. Hase (1996 and 1998) made a major advance by applying a forward-dynamics model, driven by simulated nervous signals, to consideration of the mechanical pressures on the evolution of human bipedalism. However, the model has not been applied to the analysis of the fossil record. Crompton et al. (1998) however reported simulation studies of bipedal walking by AL-288-1 using ADAMS, and the present thesis builds on this approach using some additional techniques.

2.6 Muscle mechanics

The gross mechanics and electrical activities of muscles have of course been investigated by many authors (eg. Basmajian 1974; Joseph 1975; MacConaill and Basmajian 1977; Alexander 1984a; McMahon, 1984; Winter 1991), and the time sequence of muscle activity (Stern & Susman 1983) during bipedal walking has been particularly extensively investigated. However, the mechanical characteristics of muscles during gait, such as the forces they exert, have been less extensively investigated.

Of all studies of the mechanics of muscle, the most famous is the modelling and

physiological study of Hill (1938, 1950). The model describes muscle in terms of elastic and contractile elements, and in application the model has predicted experimental results very well (Hill, 1938; Hof and Berg 1981; Khalil and Martinez 1976; Olney and Winter 1985). However, too many parameters have to be determined to apply Hill's model to a multi-muscle systems, such as the lower limbs.

Since the later 1970's, many authors have tried different approaches to he multi-muscle problem, which may be divided into two kinds: 1) inverse dynamics approaches, driving muscles from external kinematic and kinetic data (eg. Seireg and Arvikar, 1973; Hardt 1978a and b; Crowninshield 1978; Jacobs and Bobbert, 1996; Patriarco et al. 1981) and 2) forward dynamics approaches: given muscle activity signals, parameters such as muscle forces, external kinematic and kinetic responses, are obtained (Hase 1996 and 1998; Hof and Berg 1981; Khalil and Martinez 1976; Olney and Winter 1985). In chapter 9, this thesis tries the former approach.

2.7 Mathematical optimization

2.7.1 Evolution and optimality

It is arguable that the evolution of human bipedalism can be expected to follow a trajectory along which human motion becomes less costly and more effective. Here gains in effectiveness can be expected to include reduction of joint moments, increase of the ratio of the displacement of CM to work done, decrease of power expended at joints and so on. We may regard these changes as mechanical optimization of bipedalism, and propose a programme of research on its evolution.

2.7.2 A mathematical method

In general, mathematical optimization may be described as follows.

Object function: F(X)

Subject to: a limited range of function F and variables X;

The general approach to calculation is as follows:

1) Given a initial value $X^{(0)}$;

2) Calculate aim value $F^{(0)}$;

3) Given $X^{(1)}$ and calculate $F^{(1)}$;

3) Decide whether the aim satisfies requirements;

4) If answer to 3) is 'no', optimally push $X^{(1)}$ to $X^{(2)}$

4-1) Let $X^{(1)}=>X^{(0)}$ and $F^{(1)}=>F^{(0)}$

4-2) Let $X^{(2)}=>X^{(1)}$,return 3)

5) if answer to 3) is 'yes' obtain optimum solution X_o and aim value F_o.

In a particular problem, I need to modify the procedure to fulfill special requirements.

2.8 Method selection and testing

In a short chapter it is impossible to cover all relevant developments in biomechanics; neither can I apply all relevant techniques in this thesis. Depending on our aims, we must select given methods, best suited for solving our particular problem.

The "best" method must further be verified by comparison of calculated results to real-world data, including physical and physiological experiments. If a result obtained by using a predictive technique is in agreement with the relevant experimental data, the technique may be considered as acceptable.

CHAPTER 3.

EXPERIMENTS IN VARIOUS MODES OF BIPEDAL WALKING

No experiment, no science.

Chinese Proverb

3.1 General experiments

3.1.1 Purpose of experiments

The experiments assess the kinematic and kinetic characteristics of various modes of unloaded and loaded bipedal walking, with special reference to the distinction between erect and 'bent-hip, bent-knee' gaits.

3.1.2 Methods

The experimental setup is schematized in Figure 3.1.

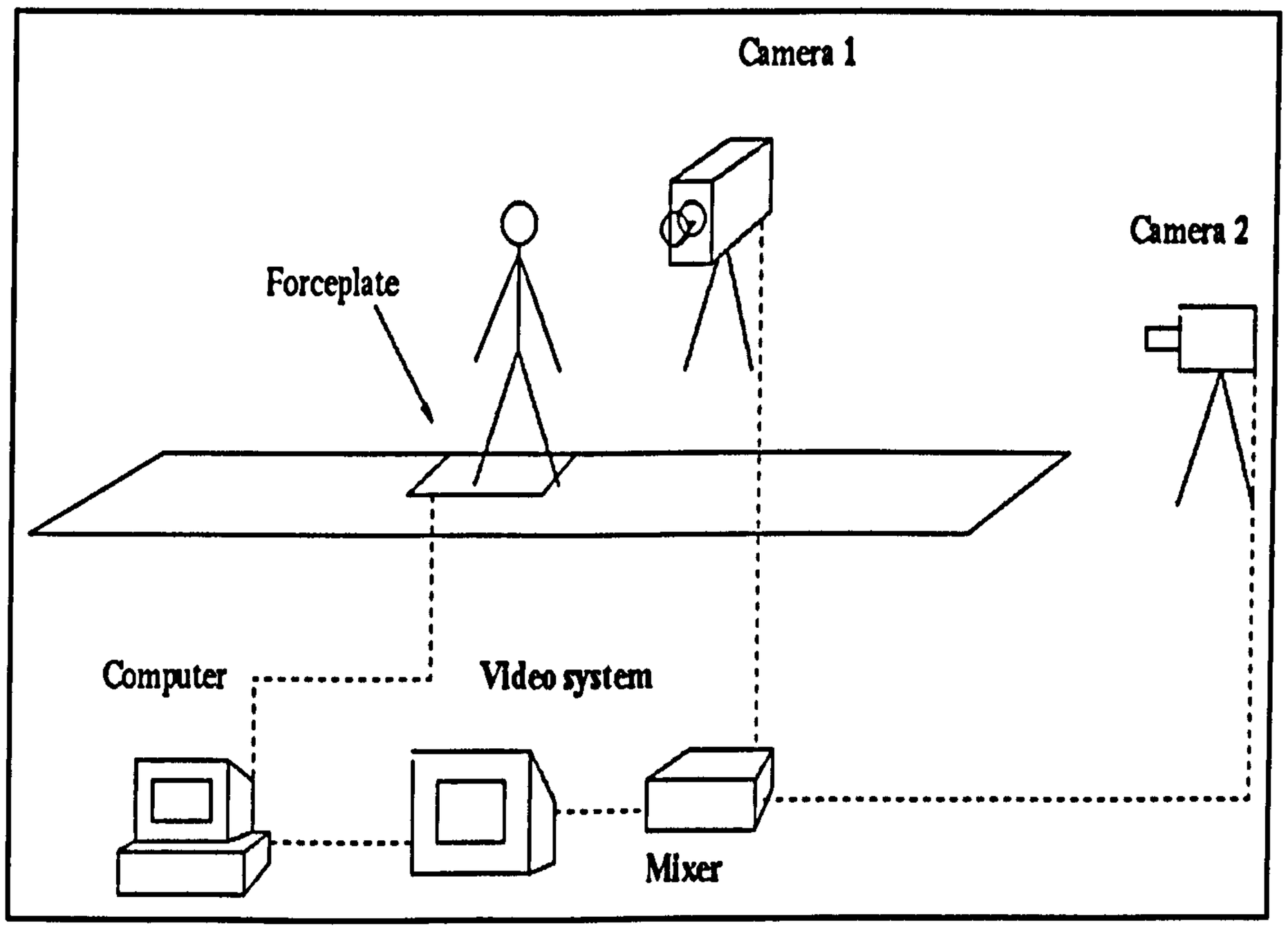

FIGURE 3.1 Schematic of biomechanical experiments

3.1.2.1 Obtaining kinematics

An experimental lane was designed for bipedal walking in our laboratory. A 12 m modular walkway constructed sturdily of plywood was set up in a 30 metre long laboratory. Two Genlocked Panasonic F10 standard PAL (50 fields per second) video cameras were set up orthogonally, one in the frontal plane and one in the sagittal plane respectively. The signals from the video cameras were fed to a Panasonic S1 production mixer for split-screen display and recording, and clocks superimposed. The output was fed to a Panasonic AG 6400 PAL video recorder.

An high speed video system, loaned to us by the Joint Research Councils Equipment Loan Pool: a Kodak Motion Analyzer with two imagers, was used for studies of bipedal running, at 300 frames/second.

Recorded video was captured using the digital framestore (Indy Video) of a Silicon Graphics Indy workstation, and separated into fields and saved as tagged JPEG files for analysis using 'Gaitlab'.

3.1.2.2 Obtaining ground reaction forces

A forceplate (Kistler 9281B) was set flush with the surface of the walkway (see Fig. 3.1) to record forces from any foot contact. The 8 channels of signal from the 4 piezoelectric force transducers were amplified by a Kistler 9865B charge amplifier and then passed to the hard disk of a computer via an AD converter, under control of DIA-DAGO (GfS, Aachen) or Kistler Bioware software. The Kistler forceplate has a high natural frequency (over 500 Hz) and high accuracy (see Kistler 9821B manual, 1995). To obtain information on the double support phase, fast-response LEDs were set within the field of view of at least one of the cameras, and so wired as to be illuminated instantly on any contact with the forceplate.

3.1.3 Data analysis

My own purpose-written software program, 'Gaitlab' (see Chapter 2 and Appendix A) was used to analyze kinematic and kinetic data. The software displays digitized landmarks, reconstructed as 3D coordinates by photogrammetry as 2 or 3D stick-figure output and calculates parameters such as joint angle and angular velocity. In addition, Gaitlab resolves the multi-channel forceplate data into to the three main contact forces and other useful parameters (see Appendix A) and can display GRF vectors and stick-figures together to facilitate understanding of the relationship between the joint motion and external forces (see Chapter 2 and Appendix A for details).

3.2 Human loaded walking

3.2.1 Graphic analysis

Subjects

Unloaded walking

The subjects were 8 adult men and women, aged 20-40, height 1.6-1.85 m. Every subject walked barefoot along the wooden walkway, inset with a Kistler forceplate and with two video cameras set along the frontal and sagittal axes (as described above) at four self-determined speeds, slow, comfortable, fast and BHBK. When

walking normally, the subjects' hip angles ranged at will, from -20 to 45 degrees (thigh/trunk), knee angle from 0 to 60 degrees (crus/thigh) and ankle angle from -12 to 26 degrees (foot/crus, see also Fig. 2.1). When walking BHBK, the subjects hip angles ranged from 23 to 69 degrees, knee angles from 35 to 92 degrees and ankle angles from -2.86 to 34 degrees. These experiments were carried out by all group members and are reported in part in Li et al. (1996) and Wang et al.(1996).

Loaded walking

The subjects were 6 adult males, who were required to walk in two ways, normal erect walking and 'bent-hip, bent-knee' walking with 10 or 20 kg loads carried in different modes: including around the neck, above the shoulder and under the arm. However, only the above-shoulder carrying has been analyzed in this thesis. They walked barefoot along same walkway setup, again at self-determined speeds. The statistics for subjects and speeds were as follows: mean height 1.730 m (SD 0.02), mean weight 73.69 kg (SD 8.5), mean velocity 1.45 m/s (SD 0.38). These studies were primarily carried out by myself. In both cases, joint coordinates and GRFs were assessed during one stride, at 50 Hz and 500 Hz respectively, and filtered using an Butterworth filter (cut-off frequency 8 to 10 Hz). Experimental procedures are illustrated in Fig. 3.2 a-c, and, for the loaded-walking experiment, subjects' general parameters: body weights, statures, and average velocities of the body CM, are listed in Table 3.1.

TABLE 3.1. Comparison of basic experimental conditions between normal loaded walking and bent-hip, bent-knee loaded walking (N = 8)

	NLW		BLW	
	mean	sd	mean	sd
Velocity CM (m/s)	1.3061	0.21	1.1418	0.20
Cadence(step/min)	53.56	4.03	50.43	8.30
DCM (m)	1.4588	0.17	1.3620	0.15

Notes:
1.weight:77.5±6.60, height: 1.785±0.06;
2. NLW: normal loaded walking; BLW: BHBK loaded walking;

With my application program 'Gaitlab' I obtained, first of all, some fundamental kinematic characteristics for the latter experiments, comparing loaded erect and BHBK walking. Typical stick-figure representations are provided in Fig. 3.3 a-d (erect) and 3.4 a-d (BHBK) in each plane and in 3D, which representations reveal segment motion and joint traces. Some basic features are evident from these comparisons, as described below.

3.2.2 Ground reaction forces (GRF)

General patterns of GRFs in erect and BHBK loaded walking are compared in Fig. 3.5.

3.2.3 Graphics and GRFs together

Figs 3.6 and 3.7 show stick-figure representations together with GRF vectors. From these, it is apparent that when subjects walk BHBK, the hip and/or knee will bear
bigger moments. In contrast, in normal walking, the subject experiences lower joint moments. Further analysis of joint dynamics is carried out in Chapter 4.

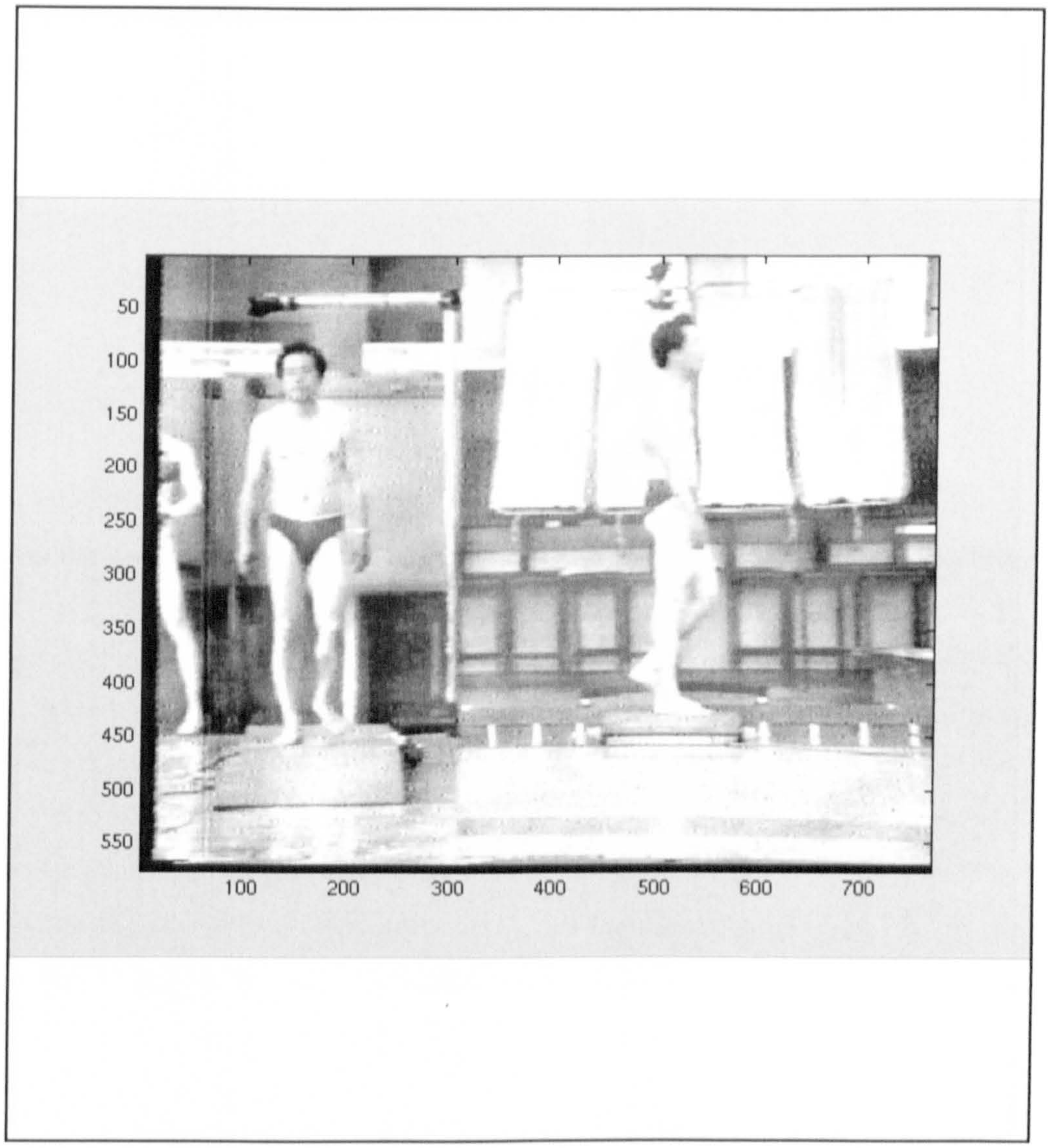

FIGURE 3.2.a Normal erect walking (NW).

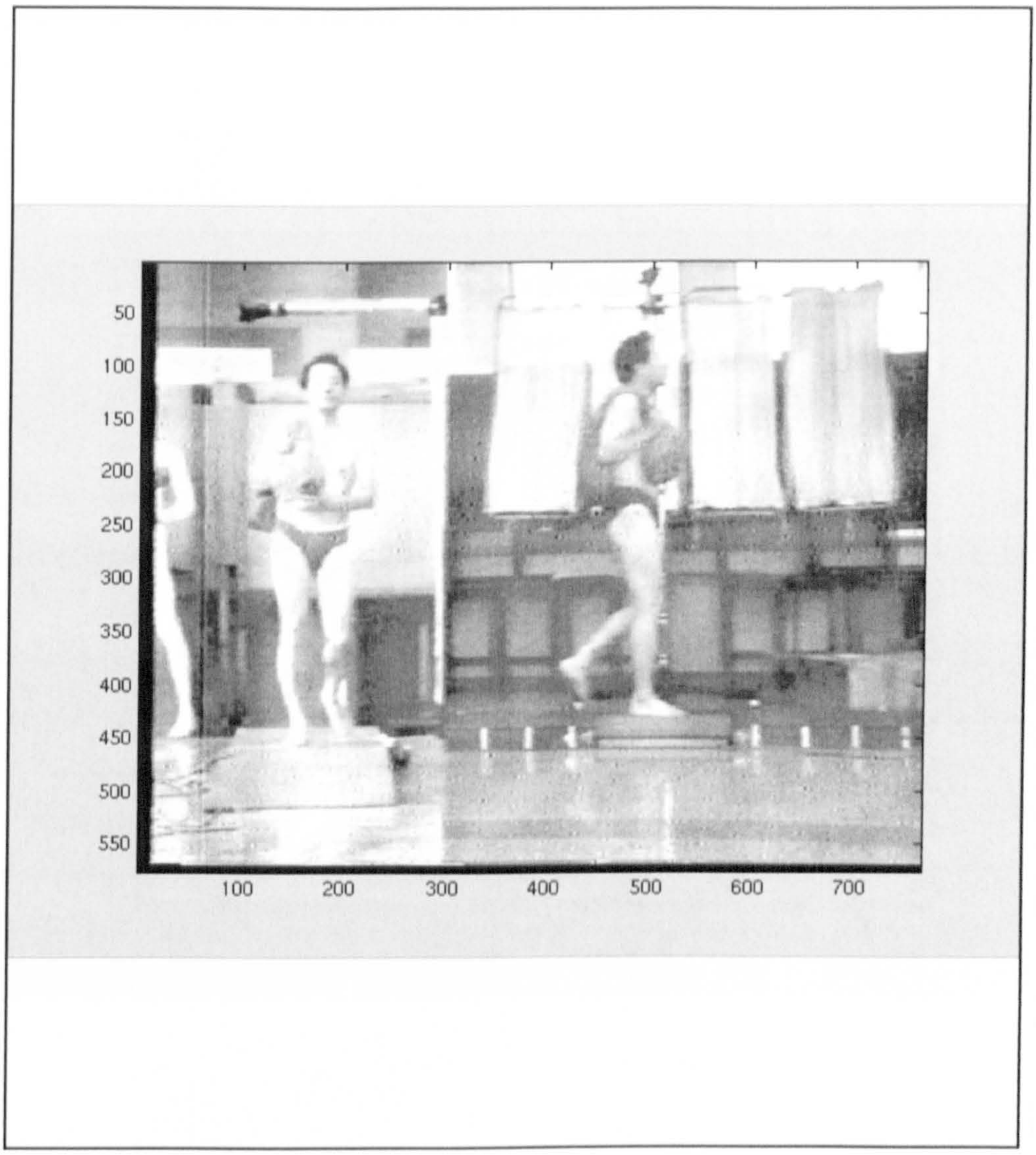

FIGURE 3.2.b Erect loaded walking.

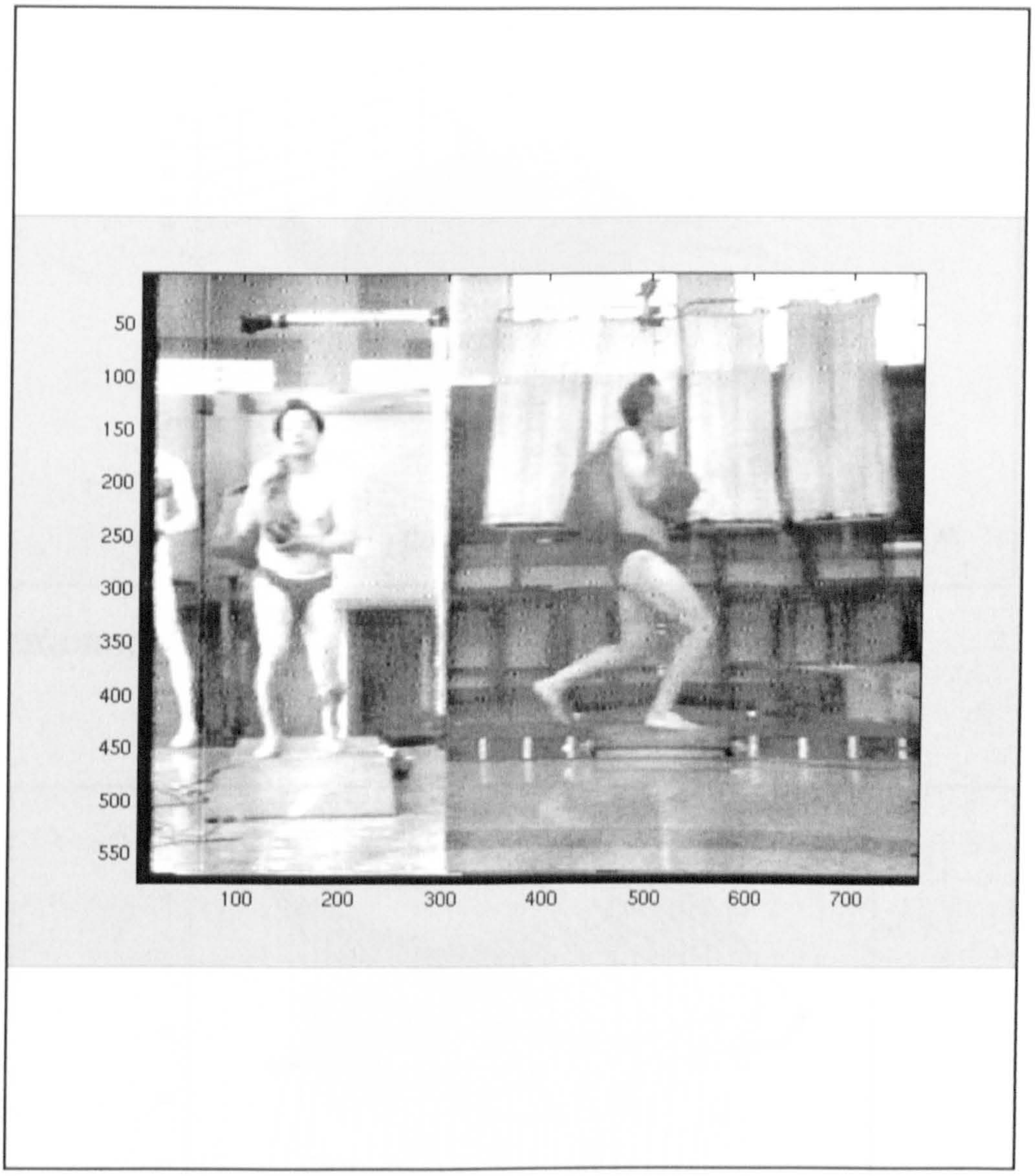

FIGURE 3.2.c Loaded 'bent-hip, bent-knee' walking.

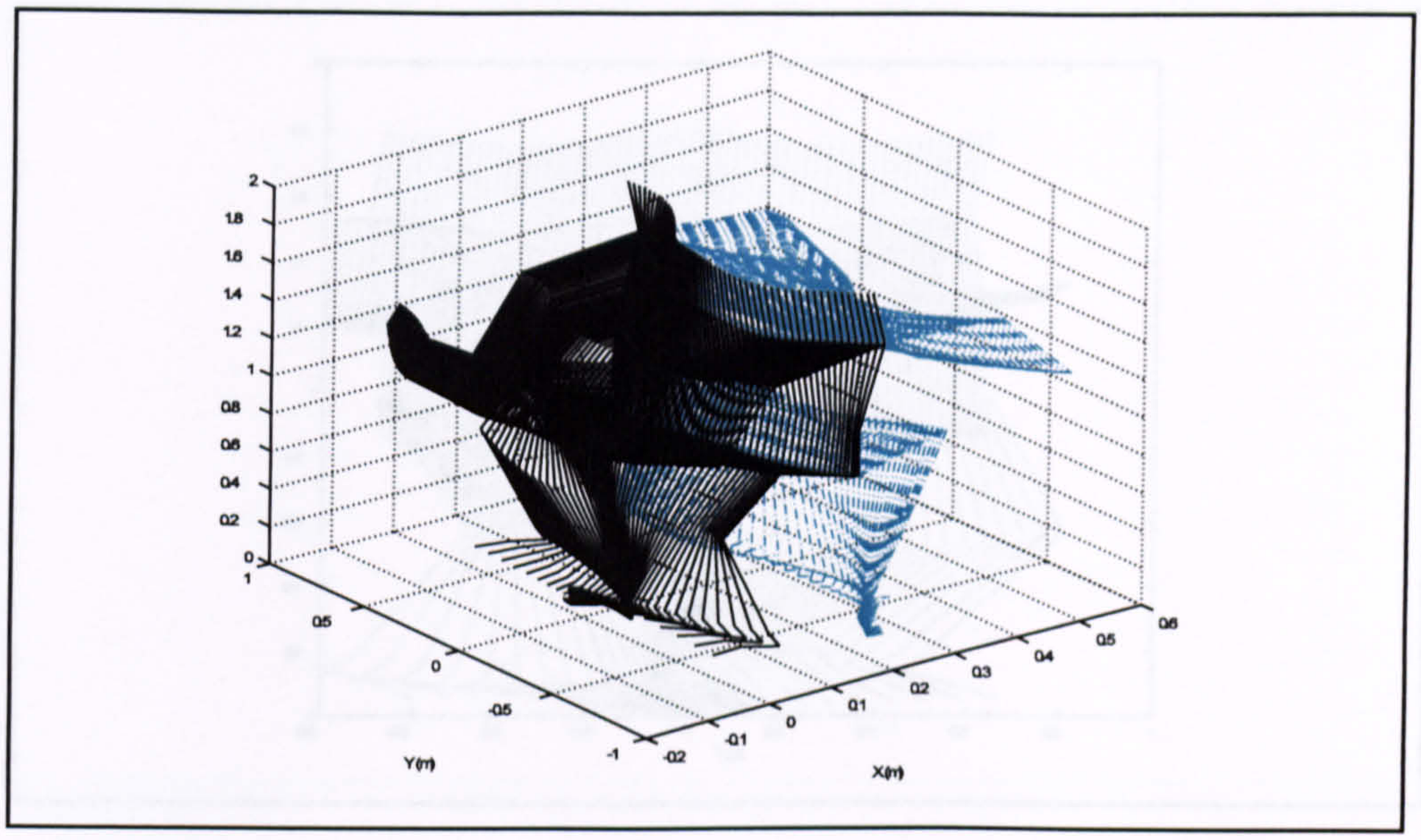

FIGURE 3.3.a All views (3D view) of normal loaded walking (NLW)

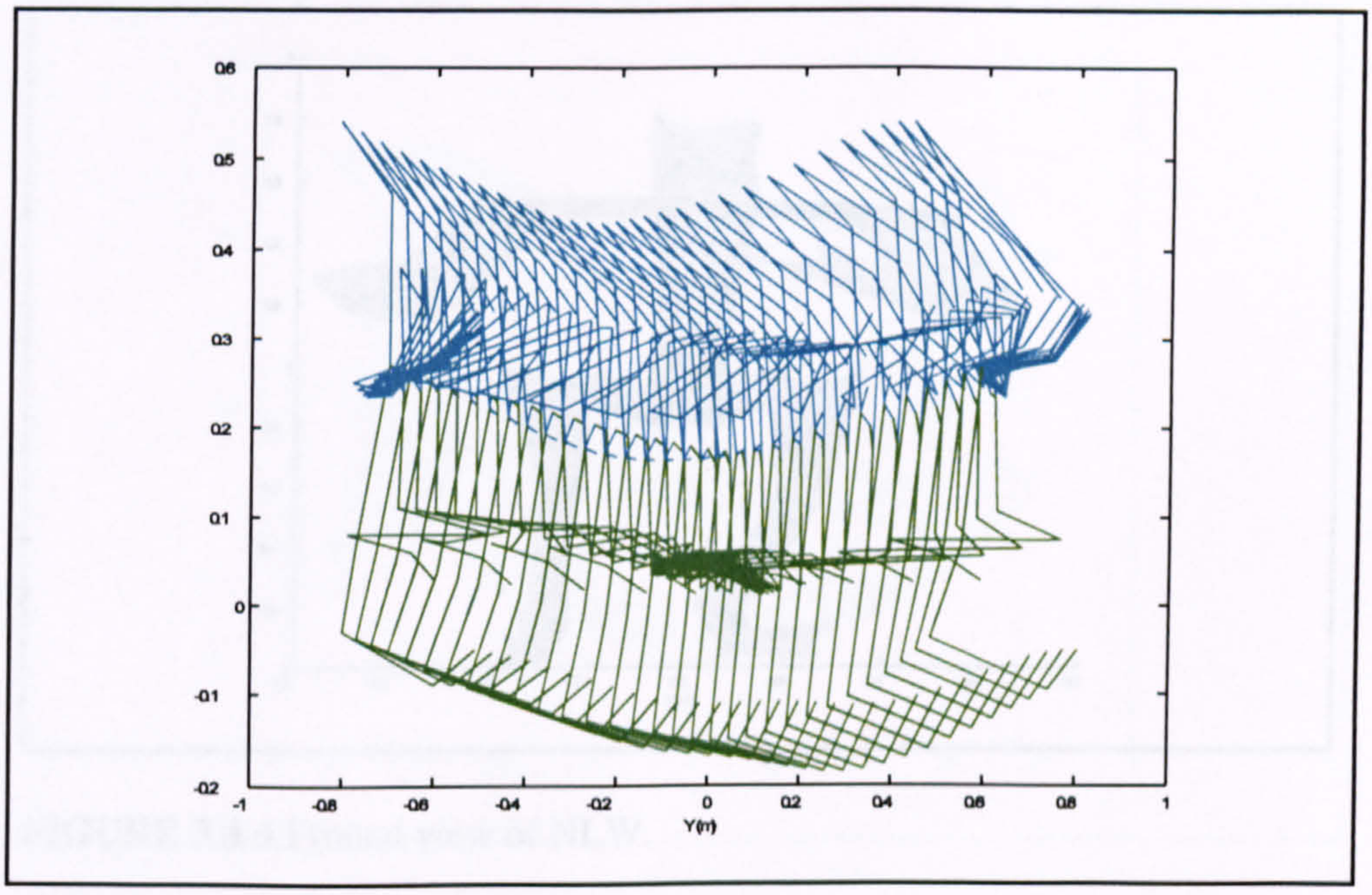

FIGURE 3.3.b Top view of NLW.

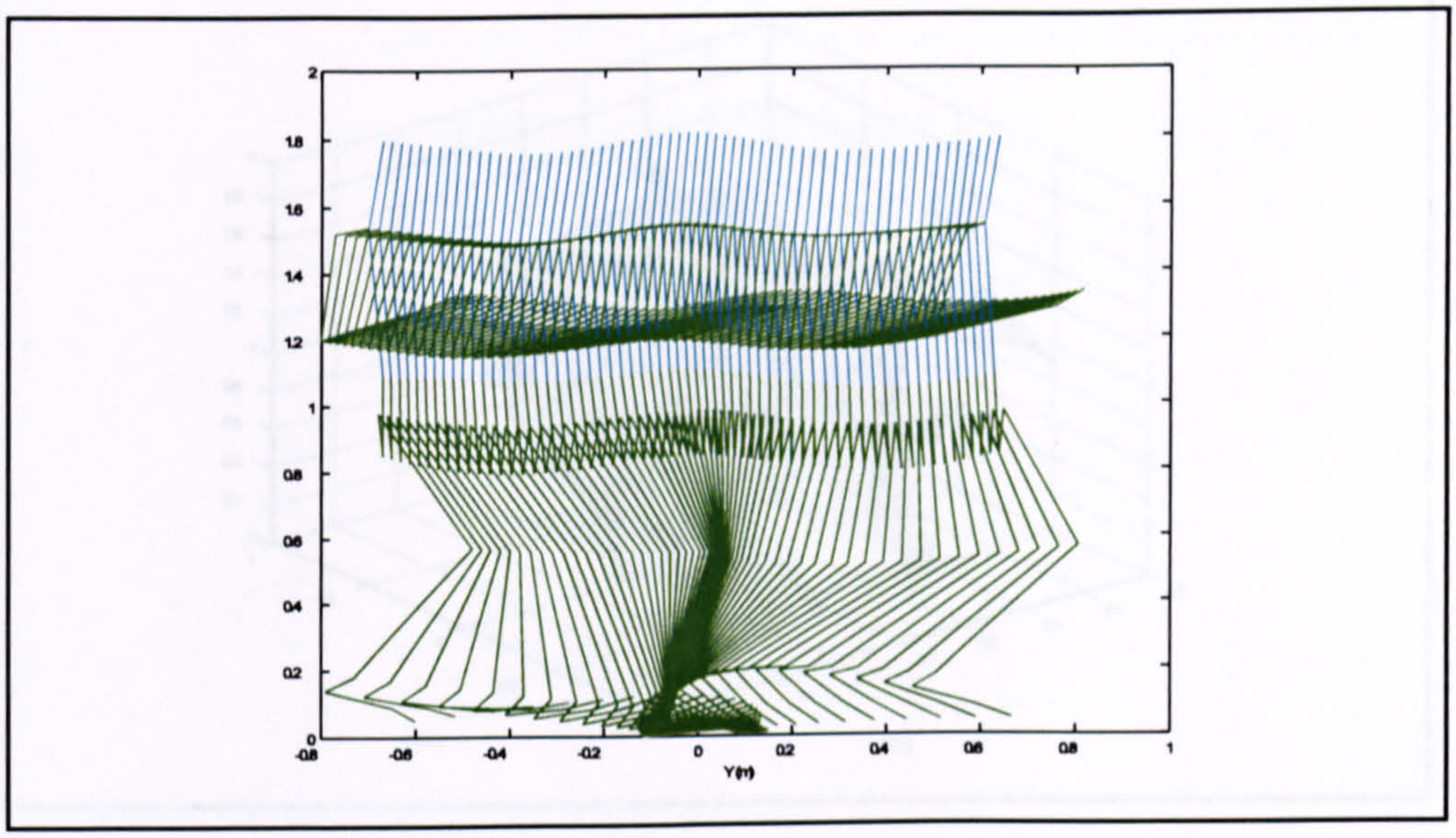

FIGURE 3.3.c Sagittal view of NLW.

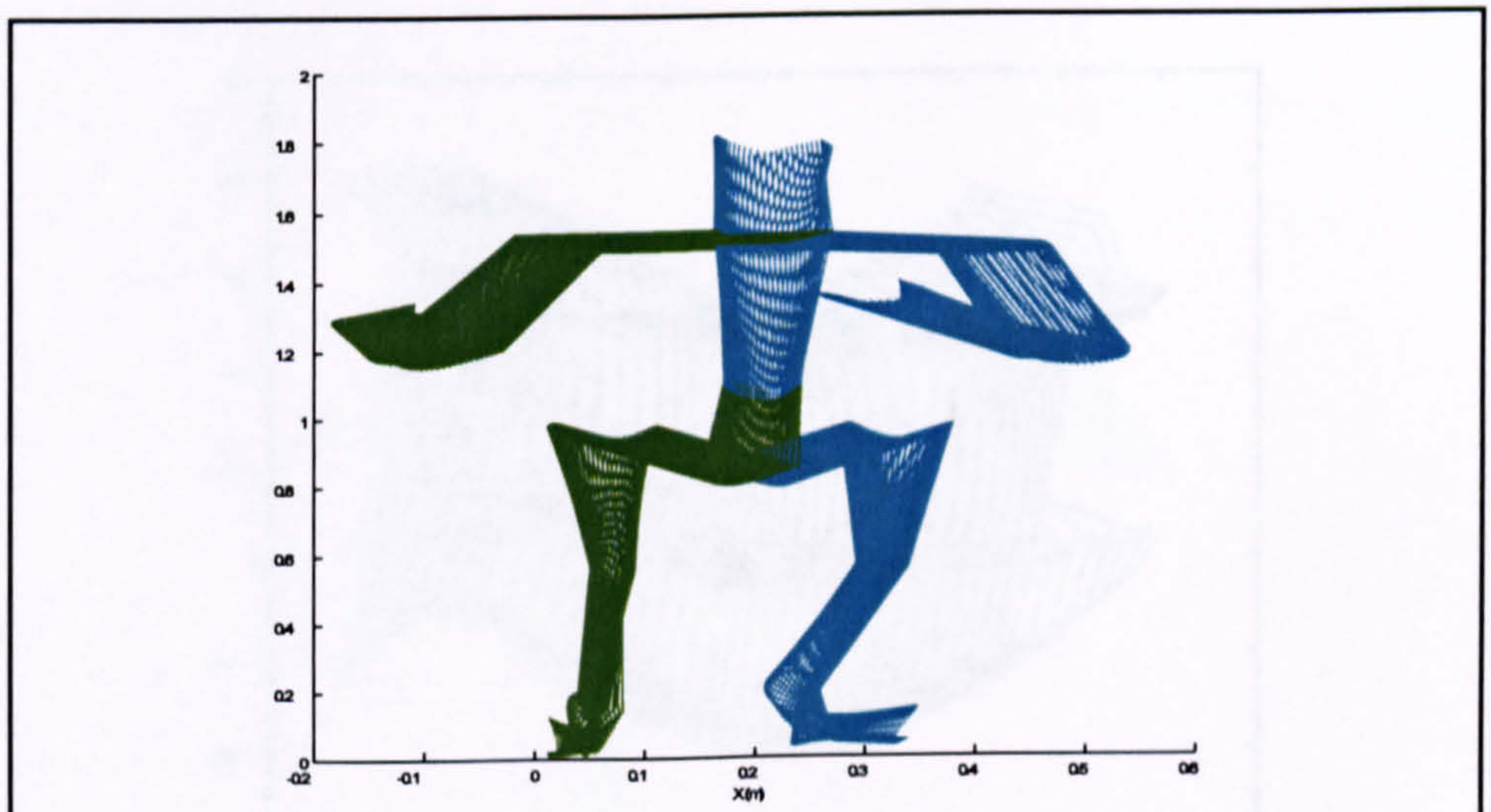

FIGURE 3.3.d Frontal view of NLW.

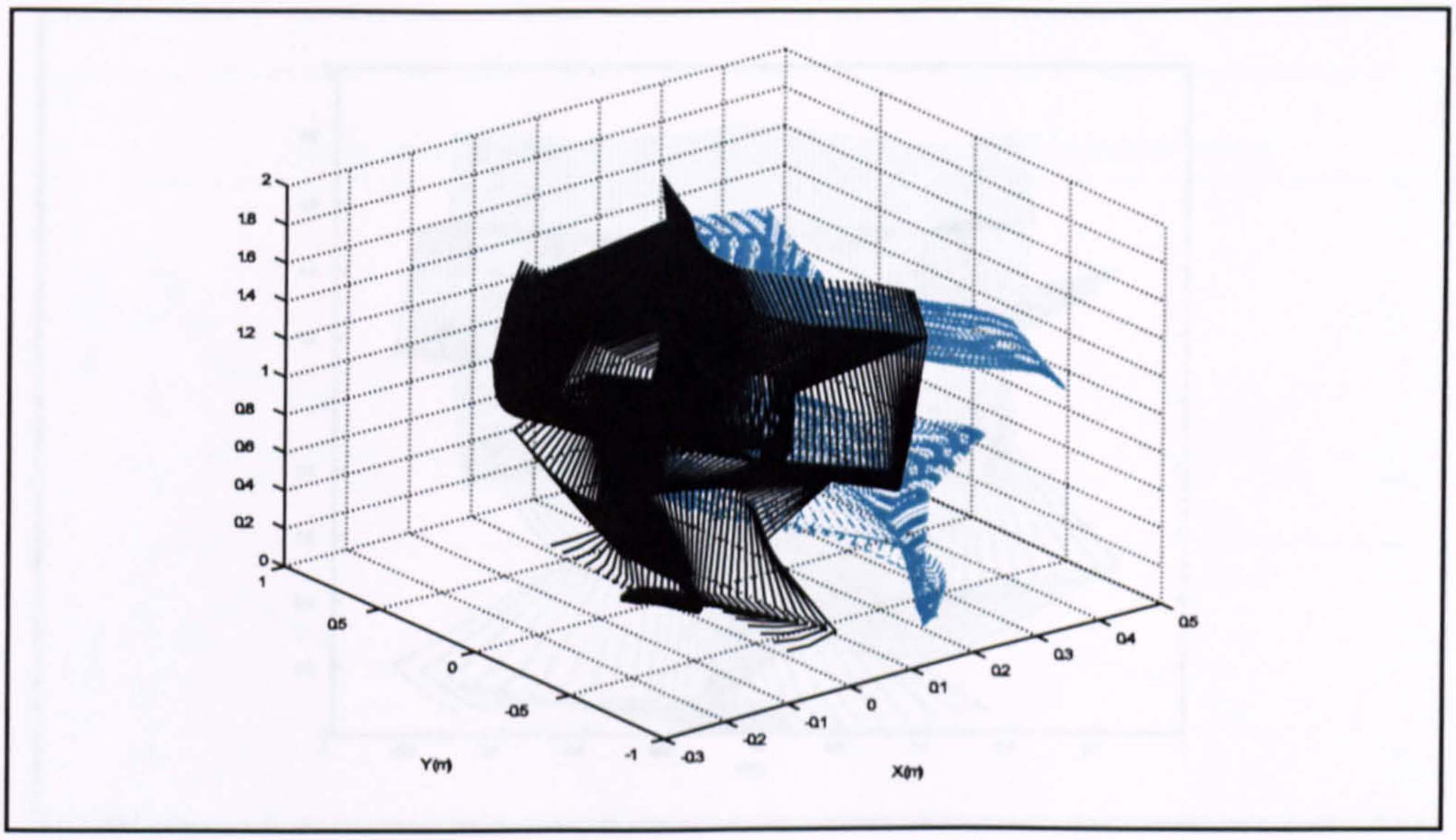

FIGURE 3.4.a 3D view of BHBK loaded walking (BLW).

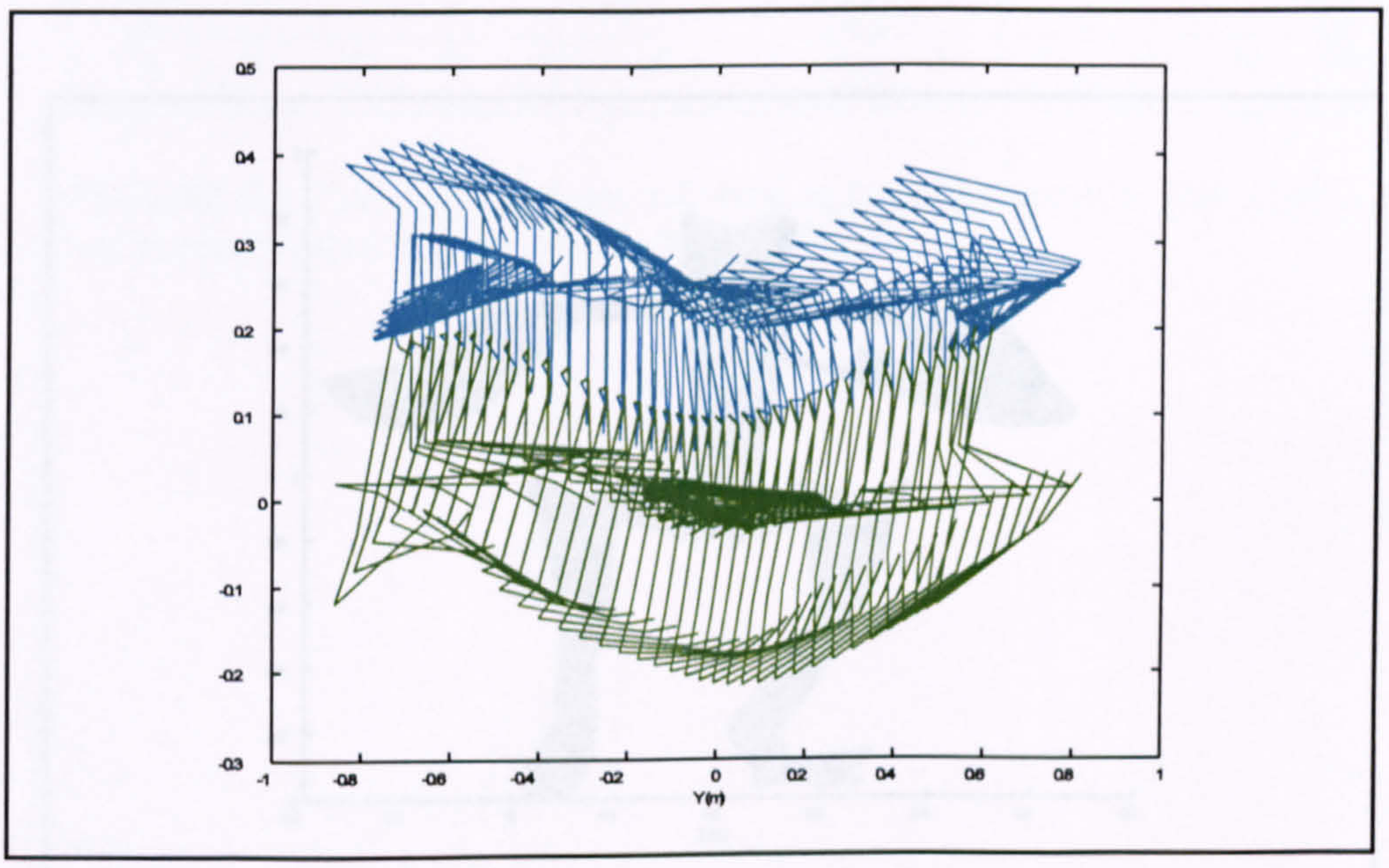

FIGURE 3.4.b Top view of BLW.

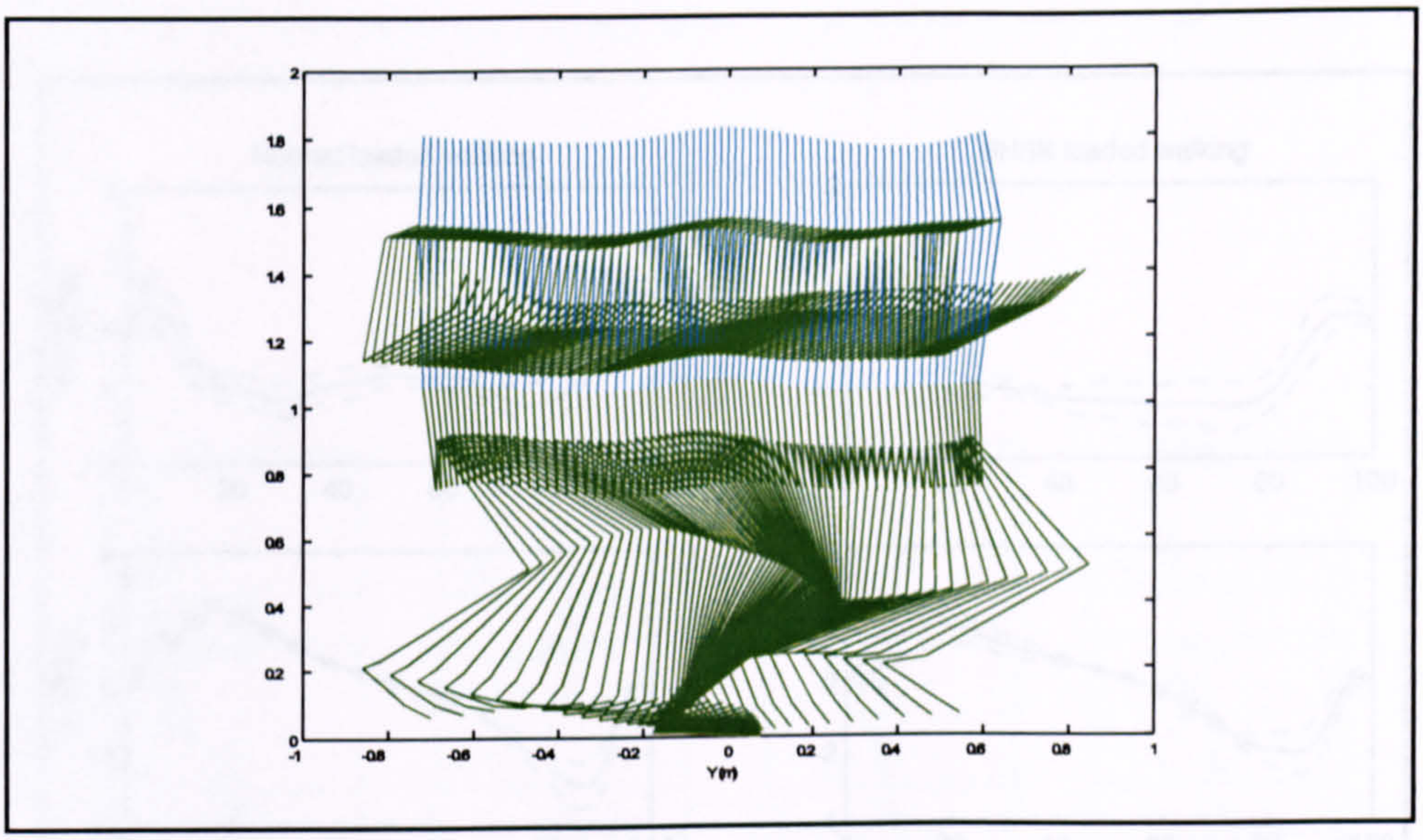

FIGURE 3.4.c Sagittal view of BLW.

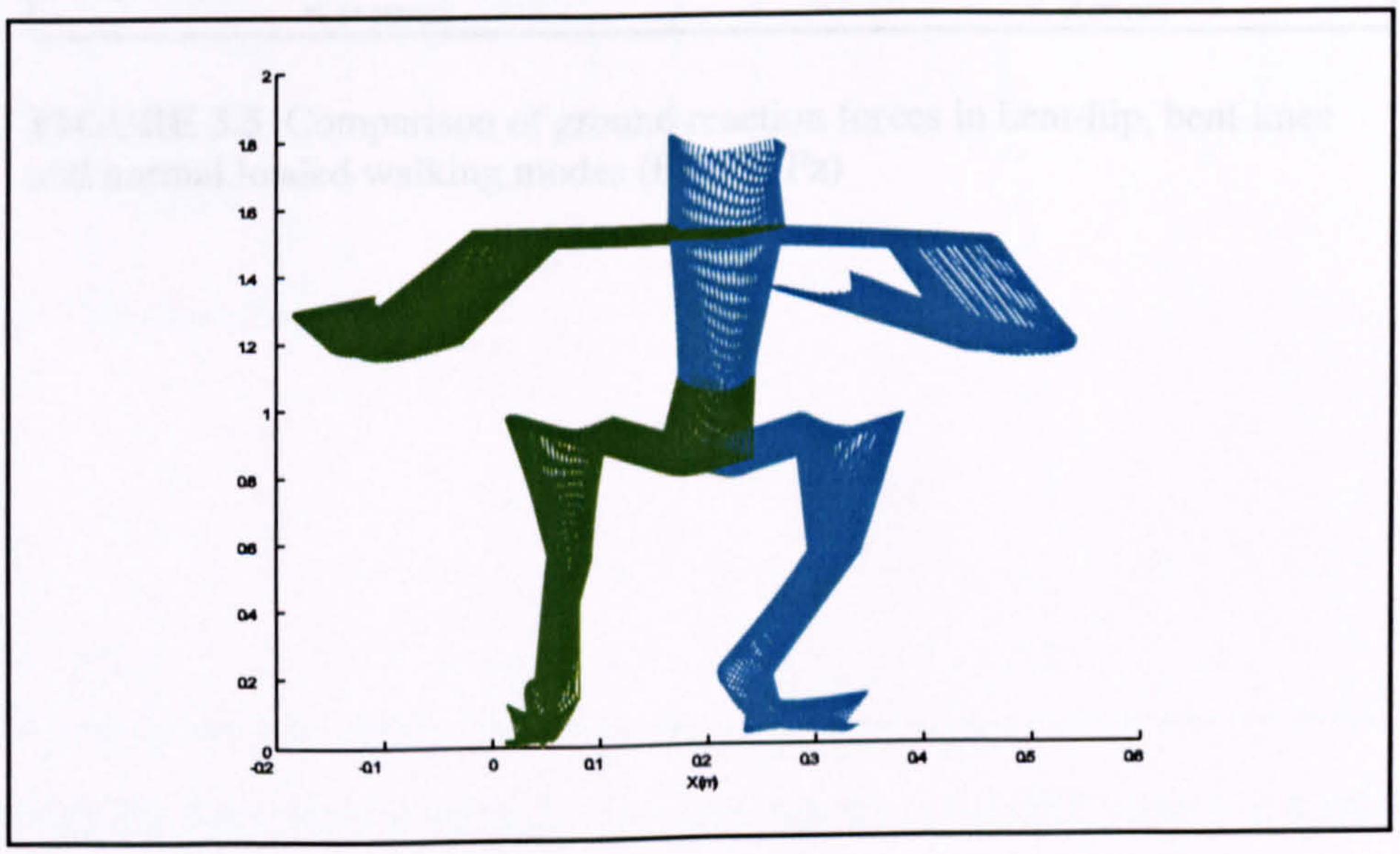

FIGURE 3.4.d Frontal view of BLW.

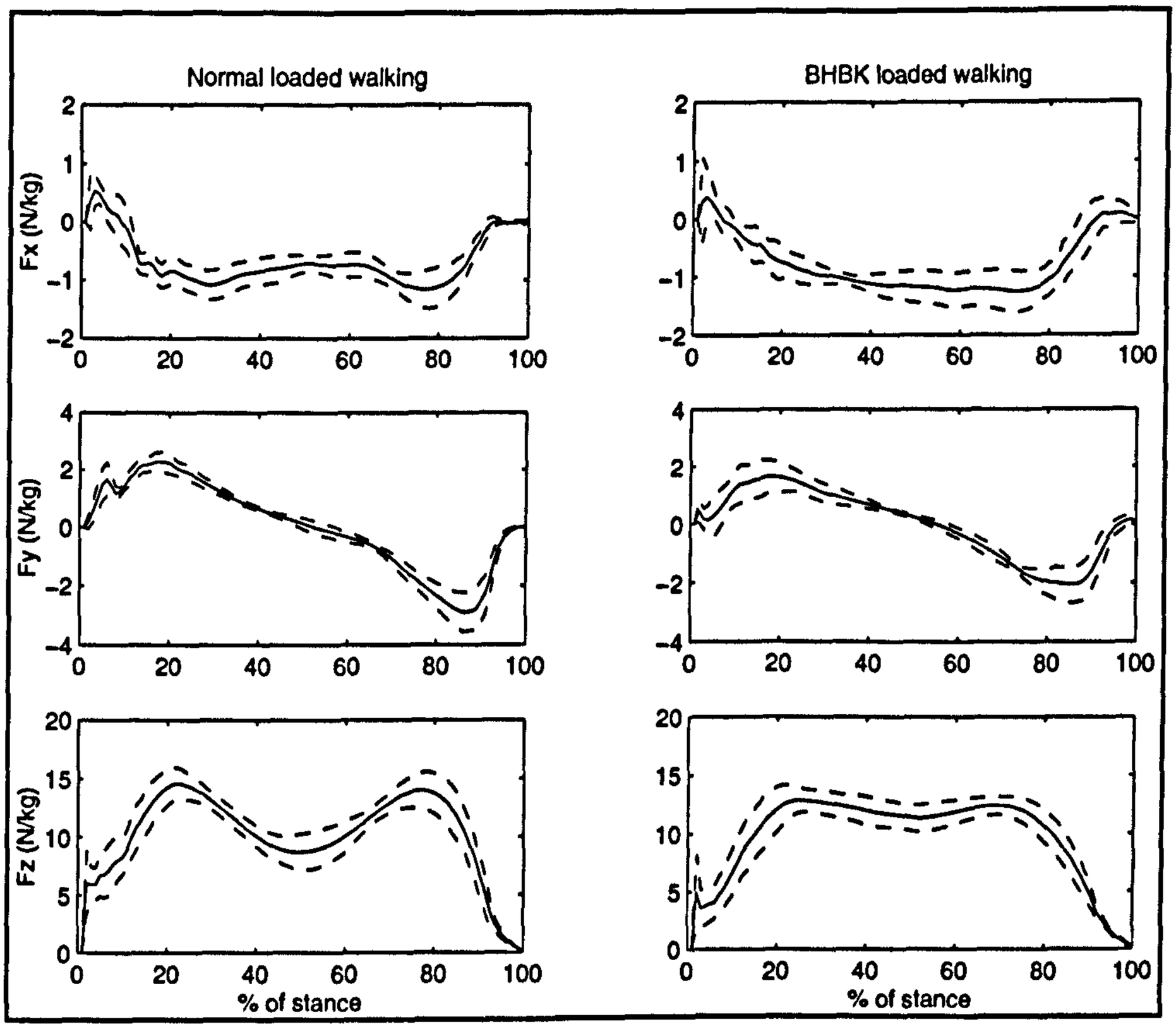

FIGURE 3.5 Comparison of ground reaction forces in bent-hip, bent-knee and normal loaded walking modes (Fx, Fy, Fz)

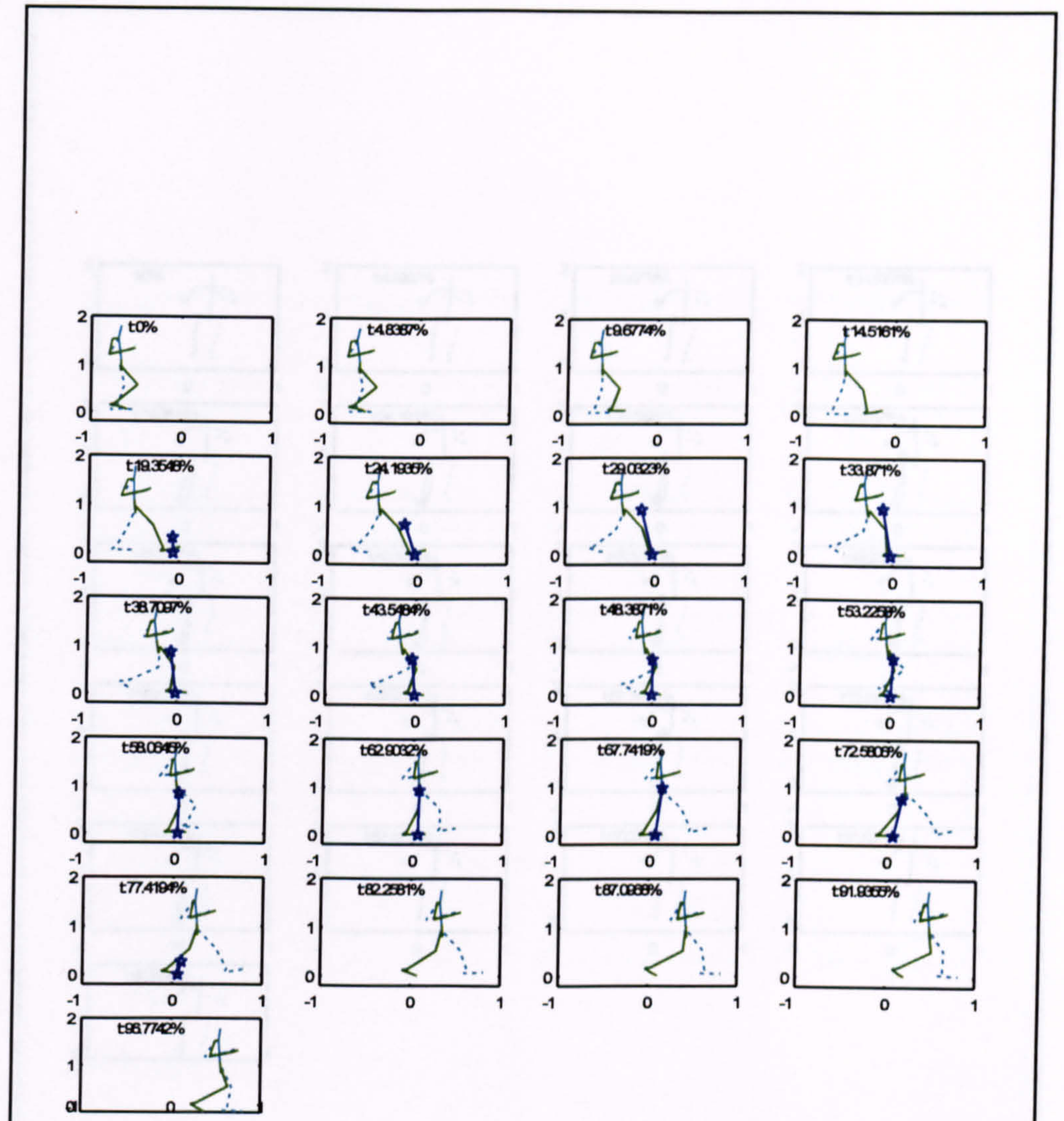

FIGURE 3.6.a Sagittal multiple view with superimposed GRF vectors in normal loaded walking.

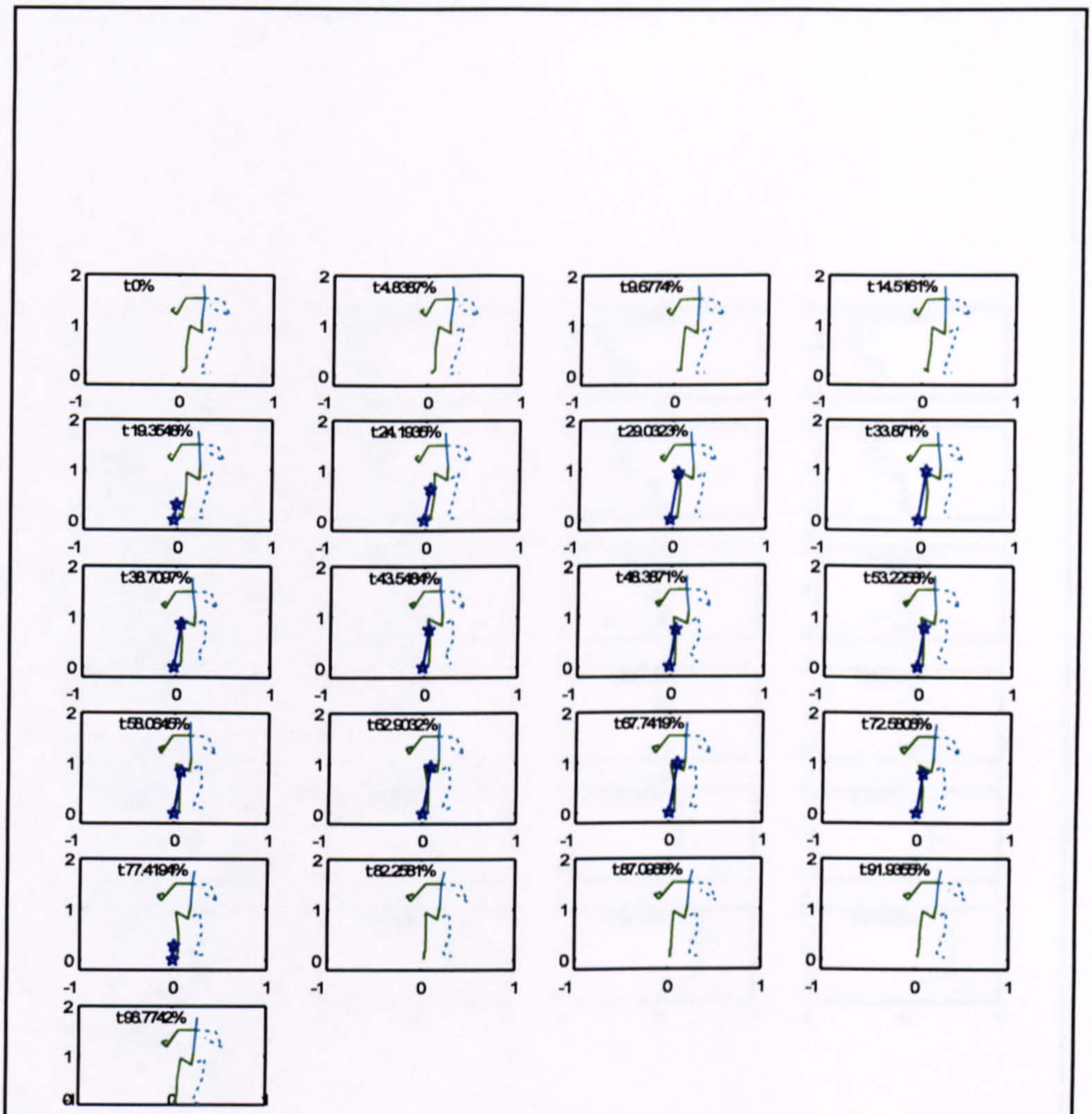

FIGURE 3.6.b Frontal multiple view of normal loaded walking, with superimposed GRF vectors.

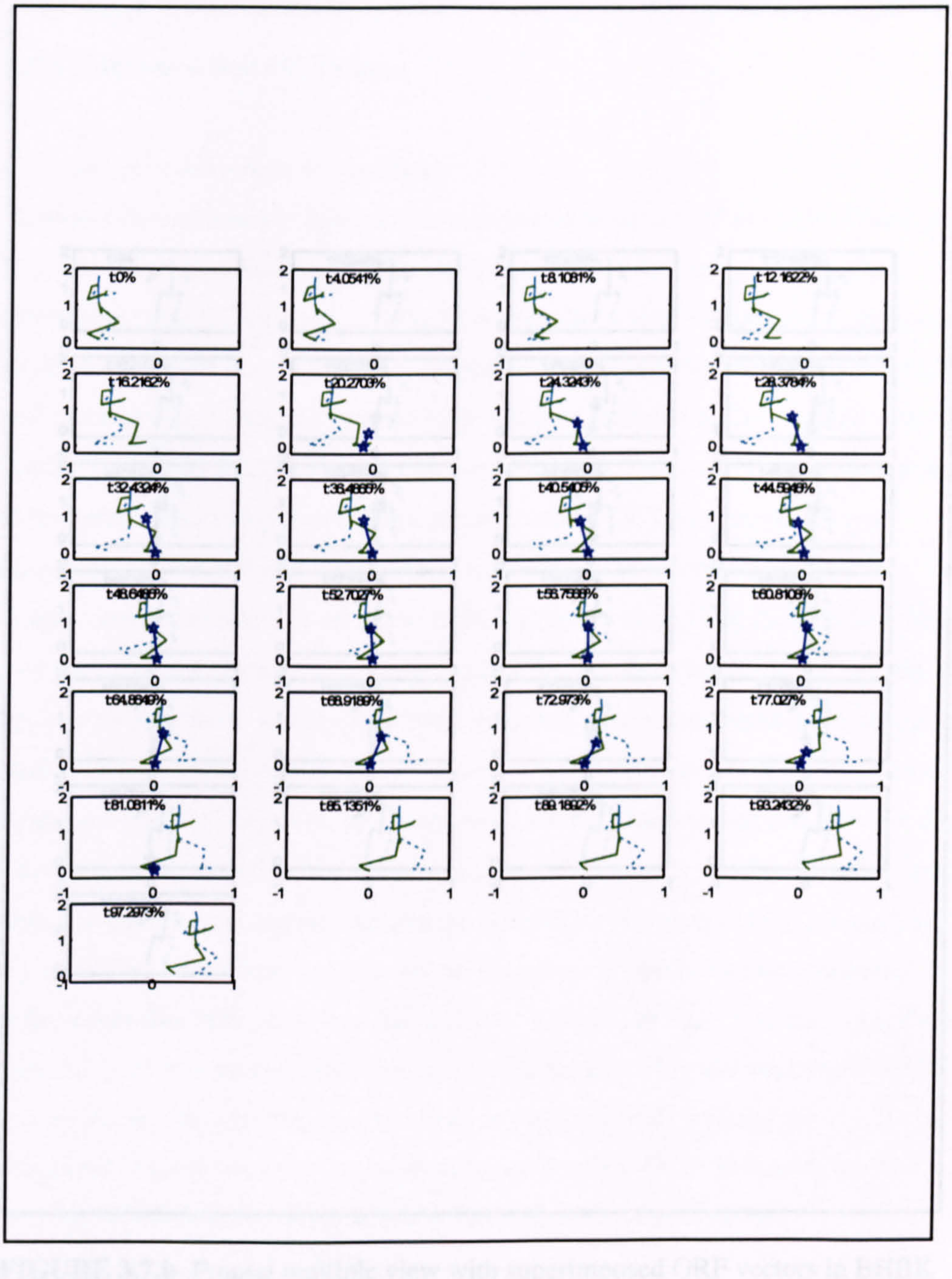

FIGURE 3.7.a Sagittal multiple view with superimposed GRF vectors in BHBK loaded walking.

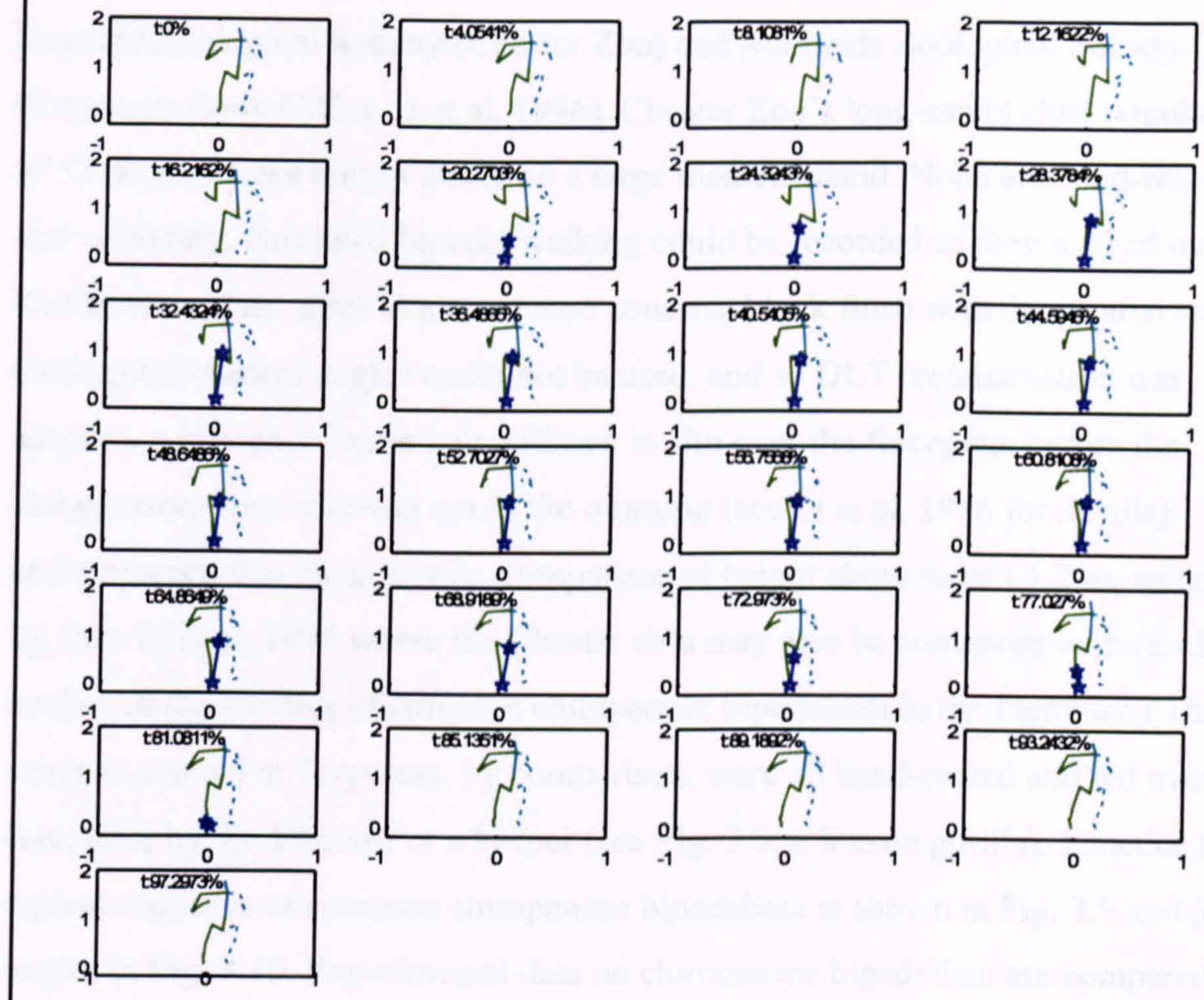

FIGURE 3.7.b Frontal multiple view with superimposed GRF vectors in BHBK loaded walking.

3.3 Chimpanzee bipedal walking

3.3.1 Subjects, Materials and methods

Experiments on common chimpanzee locomotion were carried out in the North of England Zoological Society (Chester Zoo) and Midlands Zoological Society (Twycross Zoo), U.K. (Li et al. 1996). Chester Zoo's long-established population of 32 chimpanzees ranges freely on a large moated island. None are hand-reared, and voluntary, untrained bipedal walking could be recorded as they walked over the Kistler forceplate, inset in a one-tonne concrete block flush with the ground surface. Orthogonal camera angles could not be used, and so DLT reconstruction was adopted, a reference frame being filmed in situ over the forceplate before the chimpanzees were allowed out in the morning (see Li et al. 1996 for details). The best sequence was for a female chimpanzee of height about height 1.2 m, weight 25 kg. (see Li et al. 1996 where the Chester data may also be compared with results for studies of the kinetics of common chimpanzee bipedalism in the literature.) The 4 subjects studied at Twycross, by comparison, were all hand-reared and led over the forceplate by the Director or a keeper (see Fig. 3.8, a female gorilla). Kinetics for a typical sequence of common chimpanzee bipedalism is shown in Fig. 3.9 and joint angles in Fig. 3.10. Experimental data on chimpanzee bipedalism are compared with human data previously reported in Li et al. (1996) in Figs. 3.11 and 3.12. From Figs. 3.8-3.11 it is immediately evident that chimpanzee bipedal walking is BHBK, and results in a smaller step length. GRFs in human BHBK walking are considerably more similar to those of chimpanzees than GRFs in human erect walking (NW). Detailed analysis will be carried out in later chapters.

3.4 Human NW and BHBK walking

Based on recordings made for other projects by our group (Li. et al 1996), some data about human walking NW and BHBK walking may be presented. The raw data includes video recordings and GRF measurements of erect walking at different

subject-determined cadences: slow, normal and fast, and in NW and BHBK walking.

Subjects' general parameters, including body weights, statures, and average velocities of the body CM, are listed in Table 3.4. Kinematic data, e.g. joint ranges of motion, are listed in Table 3.5. Detailed analysis of the experiments will be presented in Chapter 4.

TABLE 3.4 Subjects and Experimental Conditions for normal walking

	male (n=10)		female (n=12)		children (n=6)	
	mean	std	mean	std	mean	std
height(m)	1.7310	0.02	1.6625	0.06	1.29	0.10
weight(kg)	73.69	8.5	59.65	7.17	19.80	10.62
CM velocity(m/s)	1.450	0.38	1.525	0.41	1.405	0.26
cadence (steps/min)	54.69	9.45	57.65	10.15	66.79	12.41

Note: cadence here is equivalent to cycle time

TABLE 3.5 Human BHBK walking data (adults n=6)

mean weight	68.18 kg (± 11.15)
displacement	1.4725 m(± 0.1735)
average velocity	1.2929 m/s (±0.2148)
cycle_time	1.1500 s (±0.1108)
cadence	52.5756 steps/min (±)

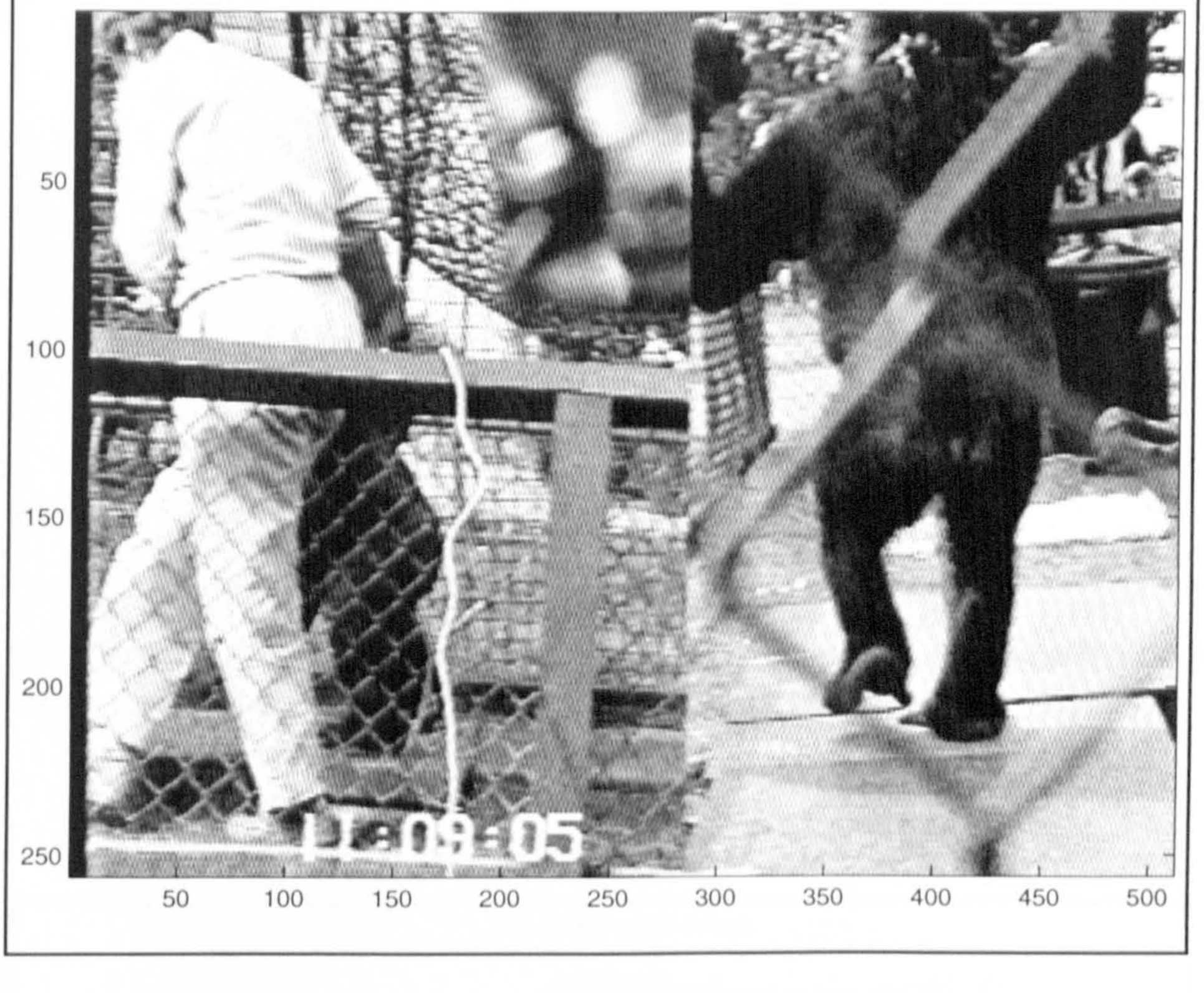

FIGURE 3.8 Guided bipedal walking of a lowland gorilla

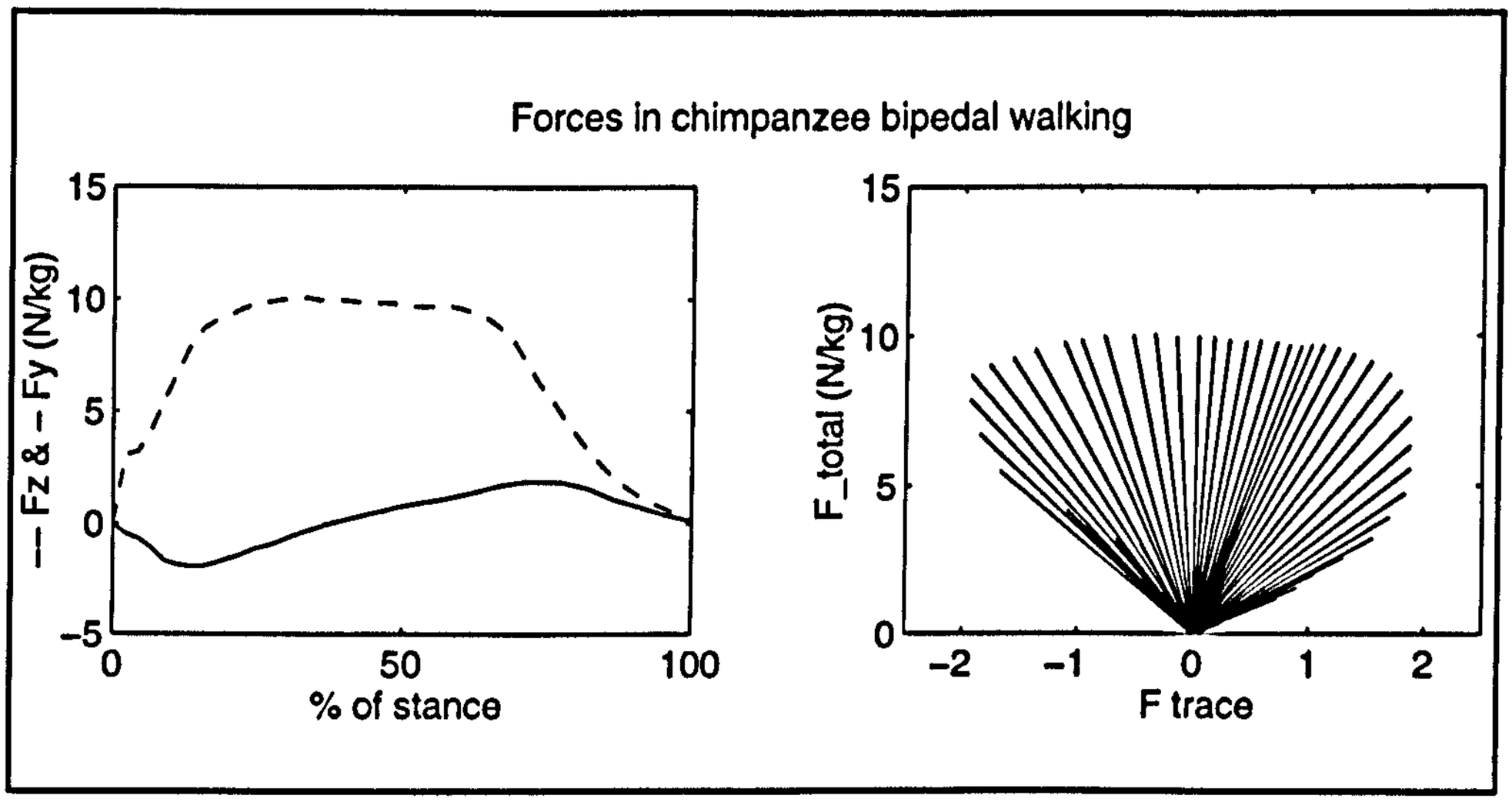

FIGURE 3.9. Ground reaction forces in chimpanzee bipedal walking; in right subfigure, the force trace is so short that it is looked as a point.

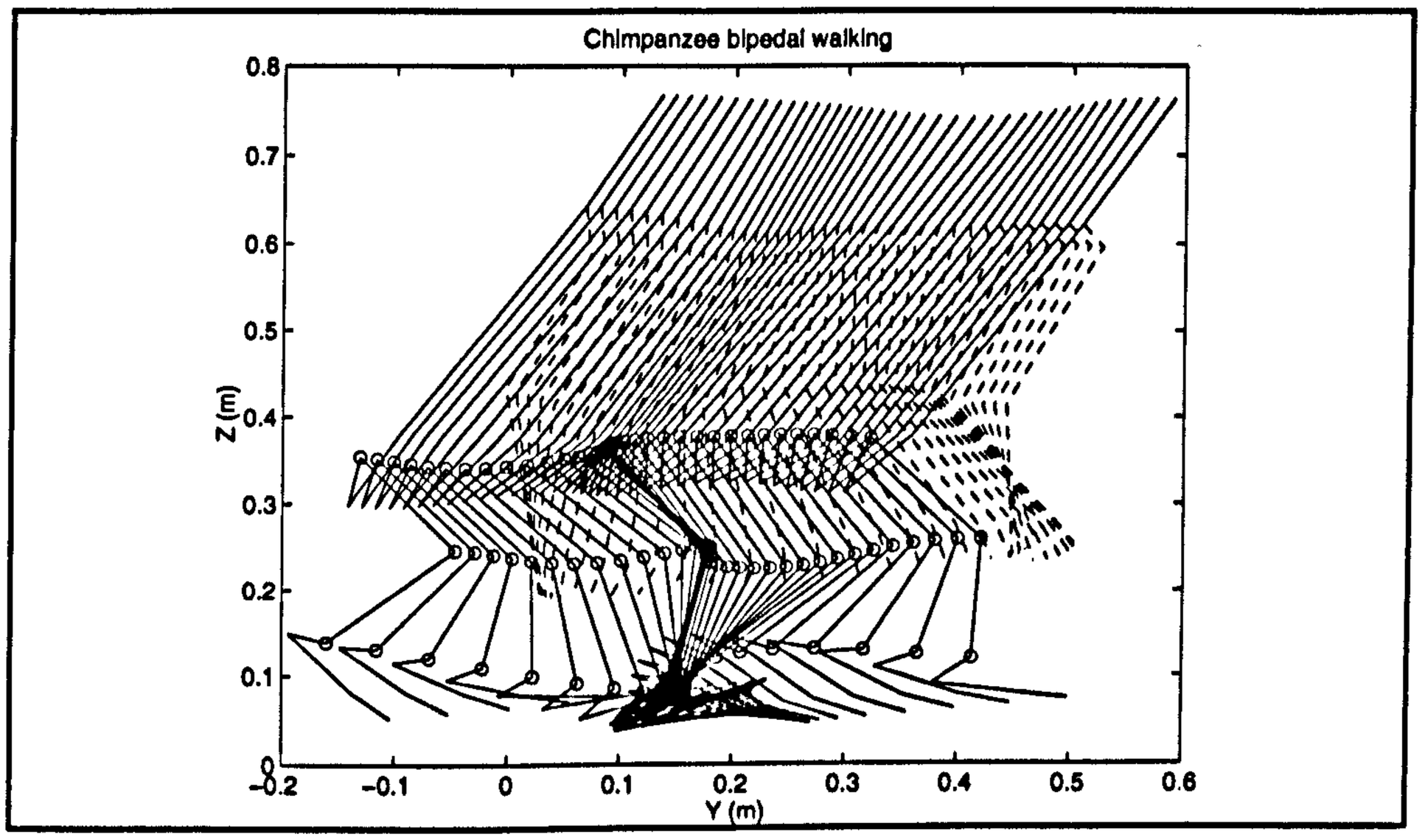

FIGURE 3.10 Stick figure representation of chimpanzee bipedalism

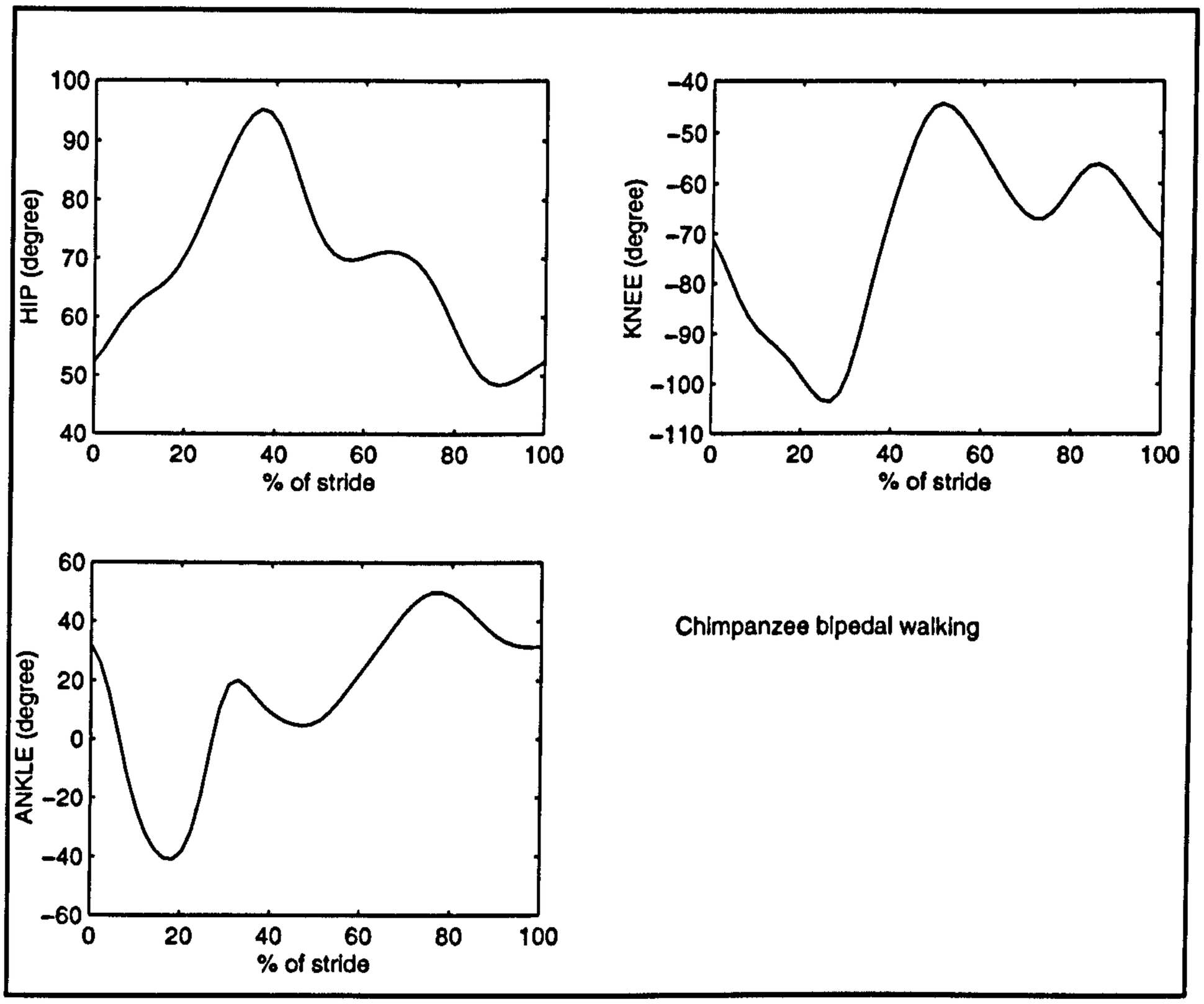

FIGURE 3.11 Joint angles during chimpanzee bipedal walking

CHAPTER 4.

JOINT DYNAMICS OF LOADED AND UNLOADED BIPEDAL WALKING

The lengths of ten fingers are different from each other.

Chinese proverb

Abstract

This chapter investigates whether there are any differences between erect walking and bent-hip, bent-knee walking, both unloaded and loaded, and includes a comparison between human and common chimpanzee gait. The primary method is known as joint dynamics, and involves calculation of joint parameters including angle and angular velocity, moment and power from experimental data. More specifically, we employed an inverse dynamics approach, where internal dynamic parameters such as joint forces and moments, are derived from known external conditions, such as kinematic data and ground reaction forces, GRFs. Although these parameters are calculated using rigid-body mechanics, the models represent biological entities. Results show that bent-hip, bent-knee (BHBK) walking has the lowest effectiveness whatever criterion is considered. Consideration of the requirement of larger muscles to sustain BHBK walking, resulting almost certainly in increased rotational inertia of the lower limb about the hip joint, suggests that selection would have favoured the early adoption of erect walking. As regards loaded walking, moments at the knee are larger and last longer in BHBK than erect loaded walking. In BHBK loaded walking, moments last almost through the whole stance phase. As a result of larger joint moments, the total power at the joints is almost 1.5 times greater in BHBK than erect loaded walking, and energy recovery is two times lower. Thus, results also indicate that selection against BHBK walking would be increased by load-carrying. Comparison of humans with common chimpanzees shows that kinematic and kinetic parameters of chimpanzee joints are less effective than those of humans. Larger peak moments act at the chimpanzee knee, and larger powers exist at the hip.

4.1 Comparison of Joint Parameters between Normal Erect Walking and BHBK Walking

4.1.1 Methods

Four self-determined modes of walking: fast, normal, slow and BHBK walking were performed by our subjects, walking loaded and unloaded. Data-collection methods were introduced in Chapter 2. The subjects were described in Chapter 3, and their basic statistics are listed in table 4.1. Parameters calculated for the lower limb are shown in Fig. 2.1.

TABLE 4.1 General Statistics of Different Modes of Walking
(N = 8, all subjects are adults)

Modes	SW	VCM (m/s)
BW	0.3900	1.2261±0.23
FW	0.4500	1.9329±0.14
SW	0.3950	1.0388±0.11
CW	0.4250	1.4703±0.13

Note:
SW- swing factor, swing time/cycle time in a stride;
VCM- average velocity of the centre of mass over a cycle;
BW = BHBK walking, FW = fast walking, SW = slow walking, CW = comfortable walking.

4.1.2 Results

4.1.2.1 Joint angles

TABLE 4.2 Comparison of joint angles (degrees) in different modes of walking (N = 6, all subjects are adults)

Gait	Abs Angle Mean	sd	Flex. max	Ext. min	Range
		Hip			
FW	19.0579	0.3031	15.8593	-39.7273	55.5866
NW	17.2225	0.2793	13.1139	-34.9322	48.0461
SW	16.9192	0.2721	12.2577	-34.3236	46.5813
BW	53.4964	0.3967	-26.8499	-73.8726	47.0227
		Knee			
FW	25.1315	0.3936	54.7692	4.3369	50.4323
NW	26.5274	0.4459	60.7141	7.7125	53.0016
SW	26.0427	0.4575	60.4801	6.5998	53.8803
BW	68.2180	0.3049	91.7959	46.3649	45.4310
		Ankle			
FW	61.7252	0.1484	72.3711	52.4037	19.9674
NW	61.1367	0.1709	72.6544	51.2370	21.4174
SW	63.9020	0.1840	76.6291	53.7257	22.9034
BW	49.0001	0.2591	67.6388	36.1250	31.5138

Notes:

Abs. Angle - average absolute angle;
FW - fast walking; NW - normal walking; SW - slow walking; BW- BHBK walking.

Joint angles in the lower limbs are listed in Table 4.2 and plotted in Fig.4.1.

4.1.2.2 Joint Angular Velocity

Joint angular velocities in the lower limbs are listed in Table 4.3 and plotted in Fig.4.2.

TABLE 4.3 Comparison of joint angular velocities (Deg./s) in different modes of walking.

Gait	Abs AV Mean	sd	Max	Min	Range
		Hip			
FW	133.3557	1.5062	185.5858	-224.9803	410.5661
NW	106.3883	1.3487	120.7235	-201.9687	322.6922
SW	75.8000	1.1645	84.9731	-166.4859	251.4590
BW	81.5458	1.1488	116.6531	-180.3236	296.9767
		Knee			
FW	130.2162	2.1748	311.3974	-194.6587	506.0561
NW	105.3097	1.8288	240.1511	-208.5700	448.7211
SW	85.7020	1.5361	176.1317	-224.2355	400.3672
BW	84.0022	1.5723	149.9408	-203.6716	353.6124
		Ankle			
FW	47.2443	1.0097	113.2141	-108.9467	222.1608
NW	45.6856	1.0955	116.1323	-112.6117	228.7440
SW	45.4696	1.0488	92.6973	-108.0074	200.7047
BW	45.9240	1.0156	94.0598	-98.6697	192.7295

Note:

Abs AV - Average absolute angular velocity over a cycle.
Other abbreviations as in previous tables

4.1.2.3 Joint Moments

Joint moments in the lower limbs are listed in Table 4.4 and plotted in Fig.4.3.

TABLE 4.4 Comparison of joint moments (Nm/kg) in different modes of walking.

Gait	Abs Moments Mean	sd	MAX	MIN	Range
		Hip			
FW	0.5928	0.0121	1.8313	-0.6518	2.4831
NW	0.5005	0.0109	1.5363	-0.5554	2.0917
SW	0.5425	0.0099	1.3372	-0.3314	1.6686
BW	0.6028	0.0123	1.6189	-0.4854	2.1043
		Knee			
FW	0.2149	0.0043	0.5882	-0.4979	1.0861
NW	0.2333	0.0055	0.6608	-0.1206	0.7814
SW	0.3087	0.0063	0.7393	-0.0324	0.7717
BW	0.4538	0.0100	0.2201	-1.2090	1.4291
		Ankle			
FW	0.3682	0.0103	1.2598	-0.0990	1.3588
NW	0.4088	0.0118	1.4598	-0.0972	1.5570
SW	0.4203	0.0120	1.4552	-0.0817	1.5369
BW	0.4516	0.0121	1.2723	-0.1260	1.3983

Note:

Abs Moments: average absolute moments over a cycle.

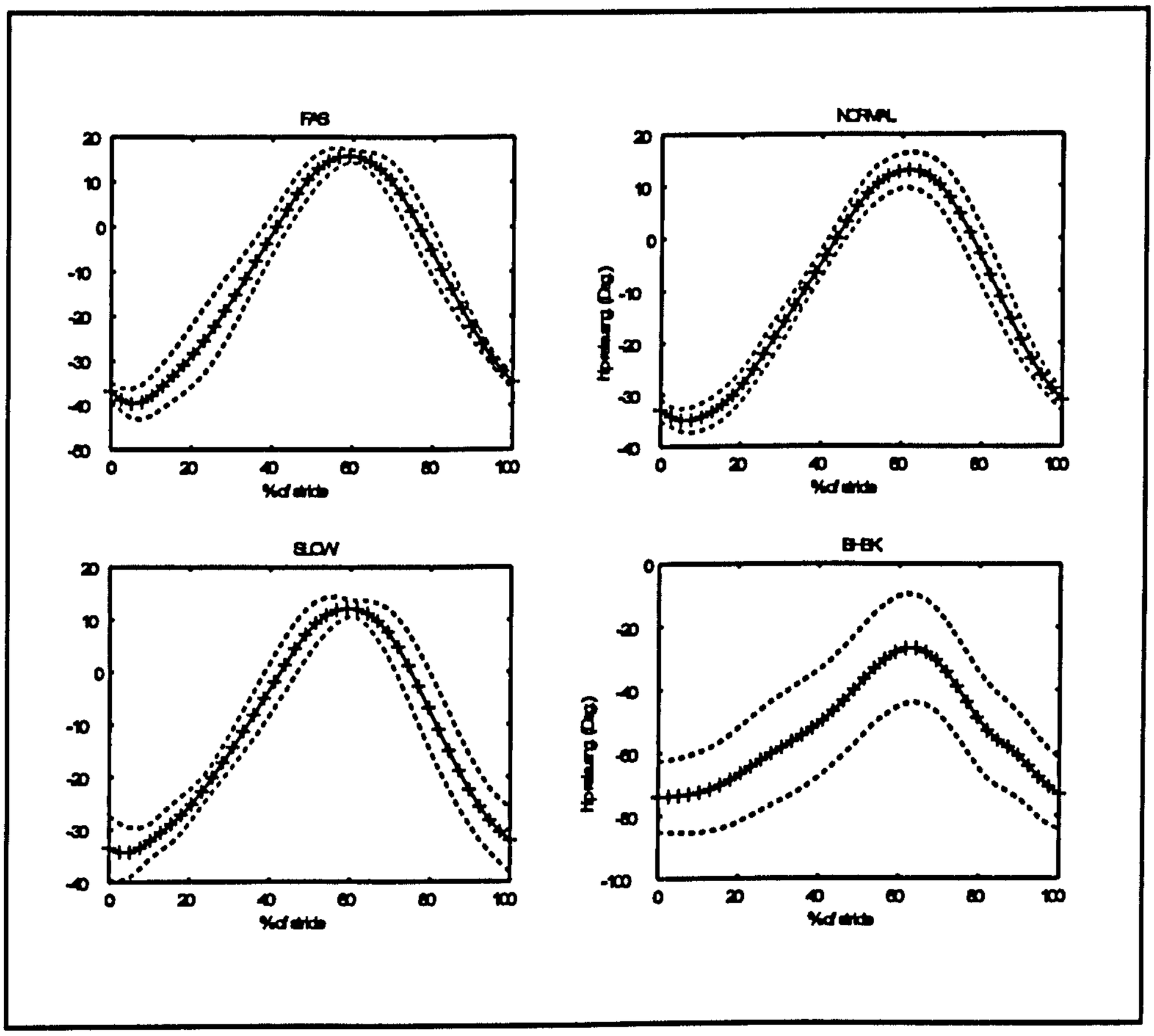

FIGURE 4.1.a Comparison of hip angles in different modes of walking; Stride begins at heel strike; + : mean, - : mean ± sd; rela.ang: relative angle.

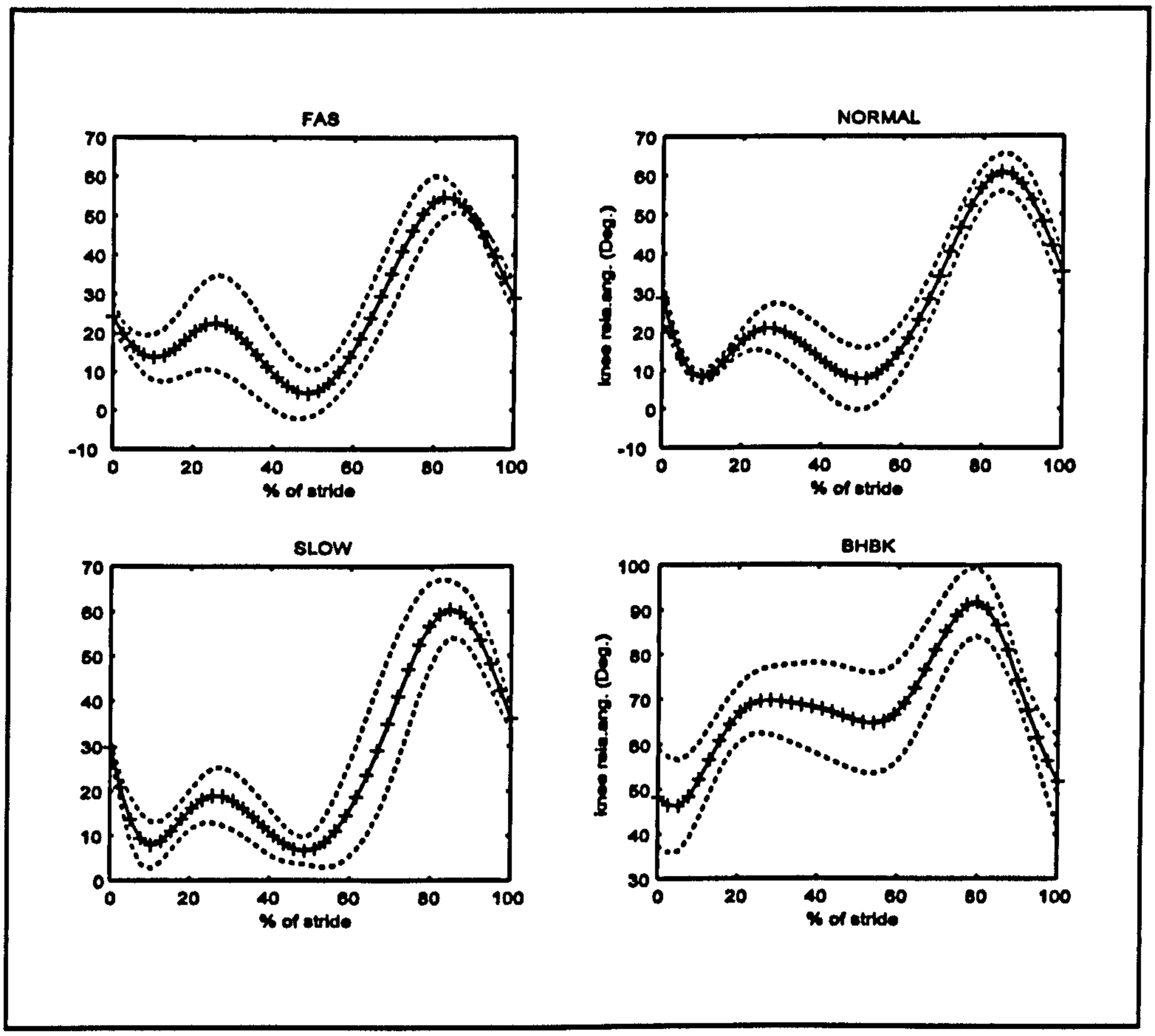

FIGURE 4.1.b Comparison of knee angles in different modes of walking. The explanation is similar to Figure 4.1.a.

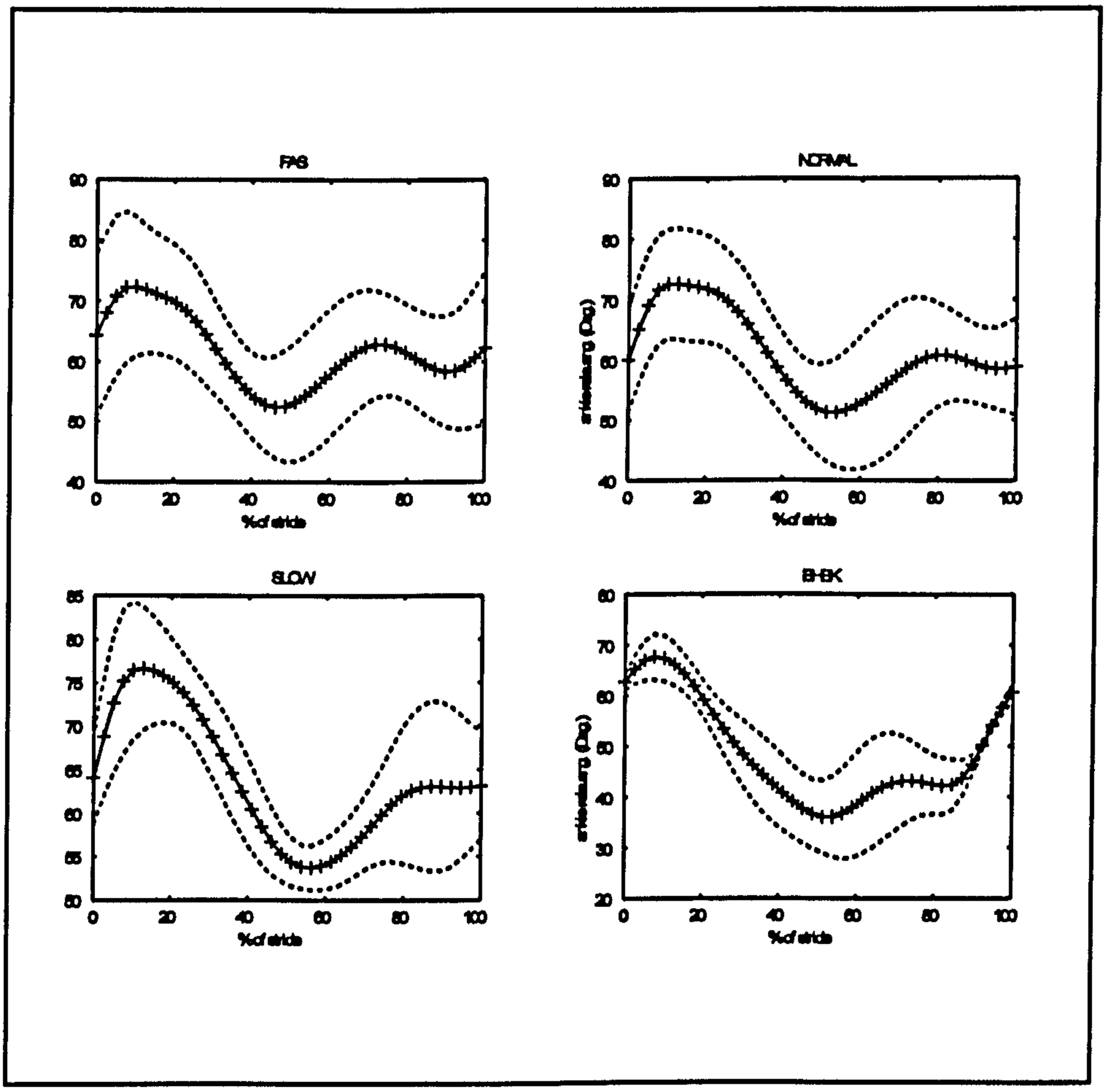

FIGURE 4.1.c Comparison of ankle angles in different modes of walking. The explanation for signs is similar to Figure 4.1.a.

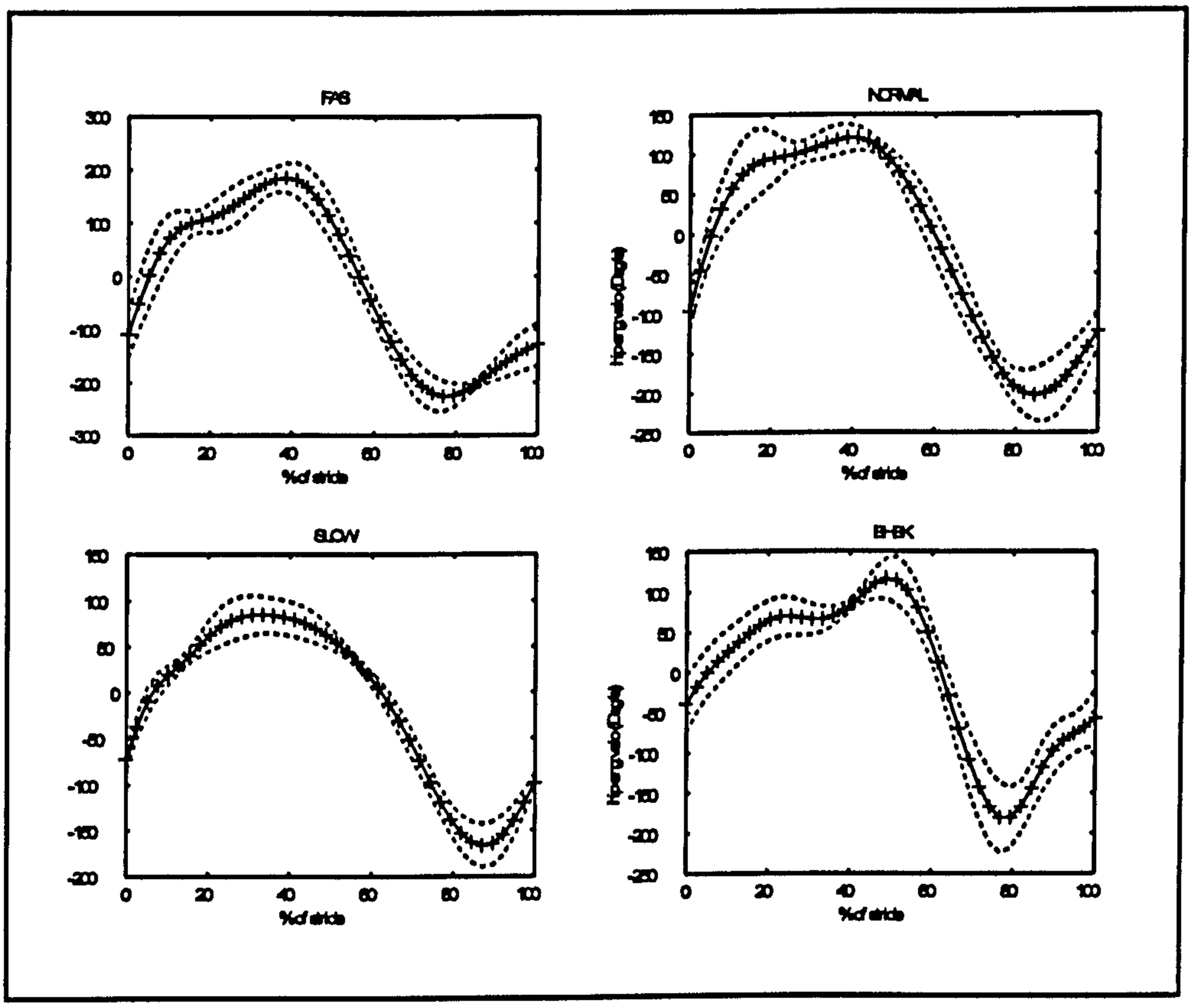

FIGURE 4.2.a Comparison of hip angular velocity in different modes of walking; rela.velo: relative velocity. The explanation for signs is similar to Figure 4.1.a.

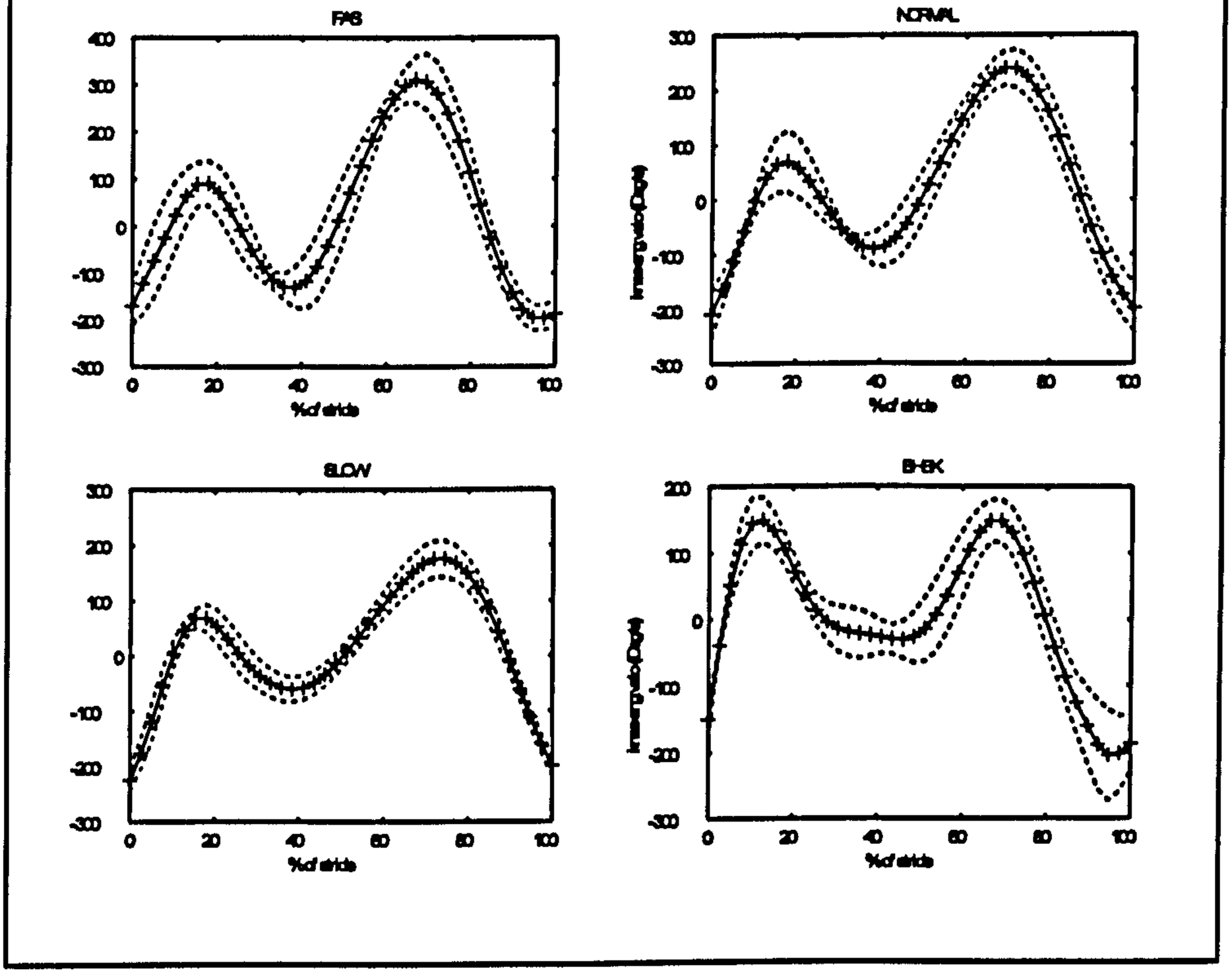

FIGURE 4.2.b Comparison of knee angular velocity in different modes of walking; rela.velo.: relative velocity; other signs similar to Figure 4.1.a.

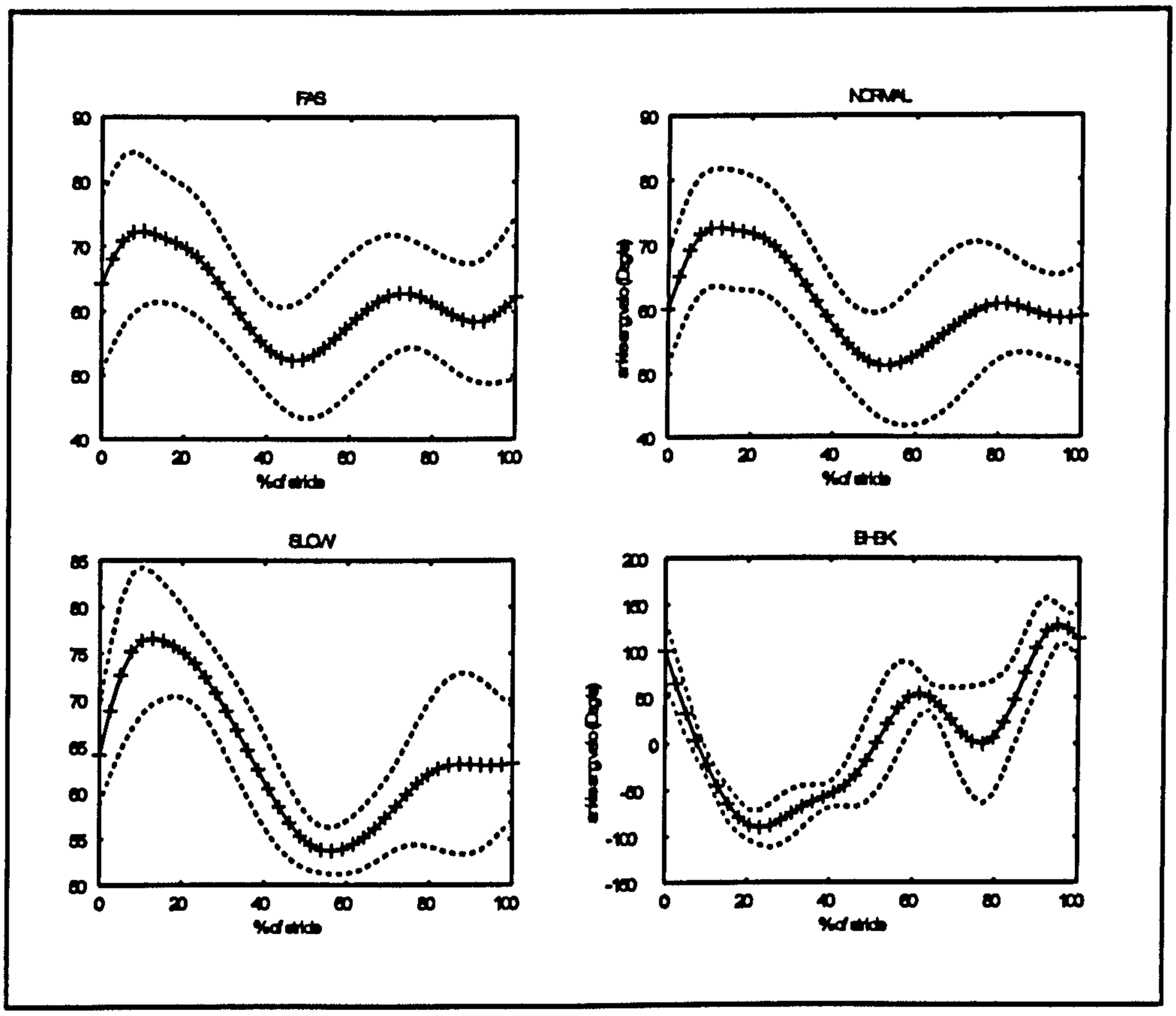

FIGURE 4.2.c Comparison of ankle angular velocity in different modes of walking; rela.velo. : relative velocity; other signs similar to Figure 4.1.a.

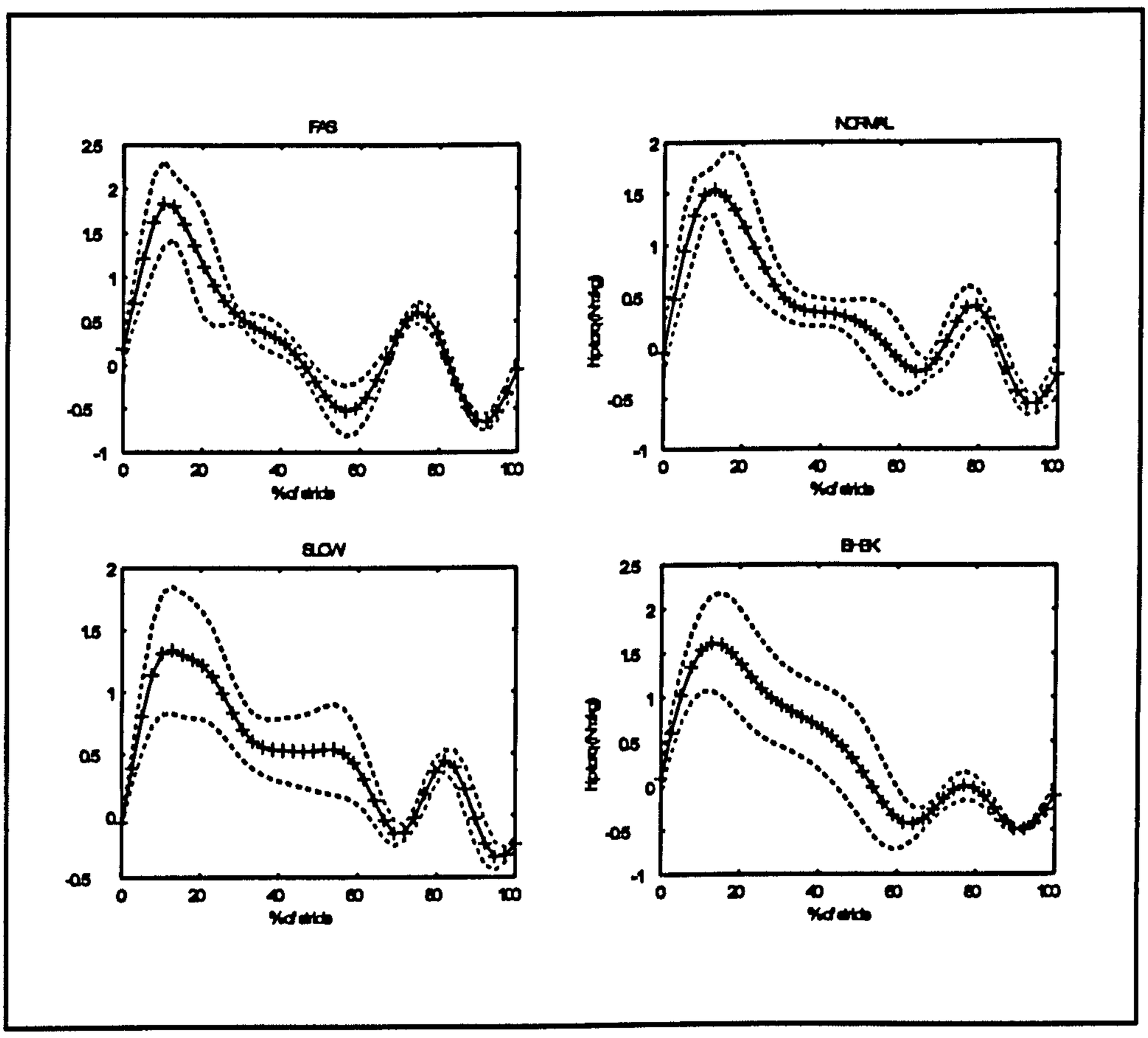

FIGURE 4.3.a Comparison of hip moments in different modes of walking; torq. : torque; symbols are as in Figure 4.1.a..

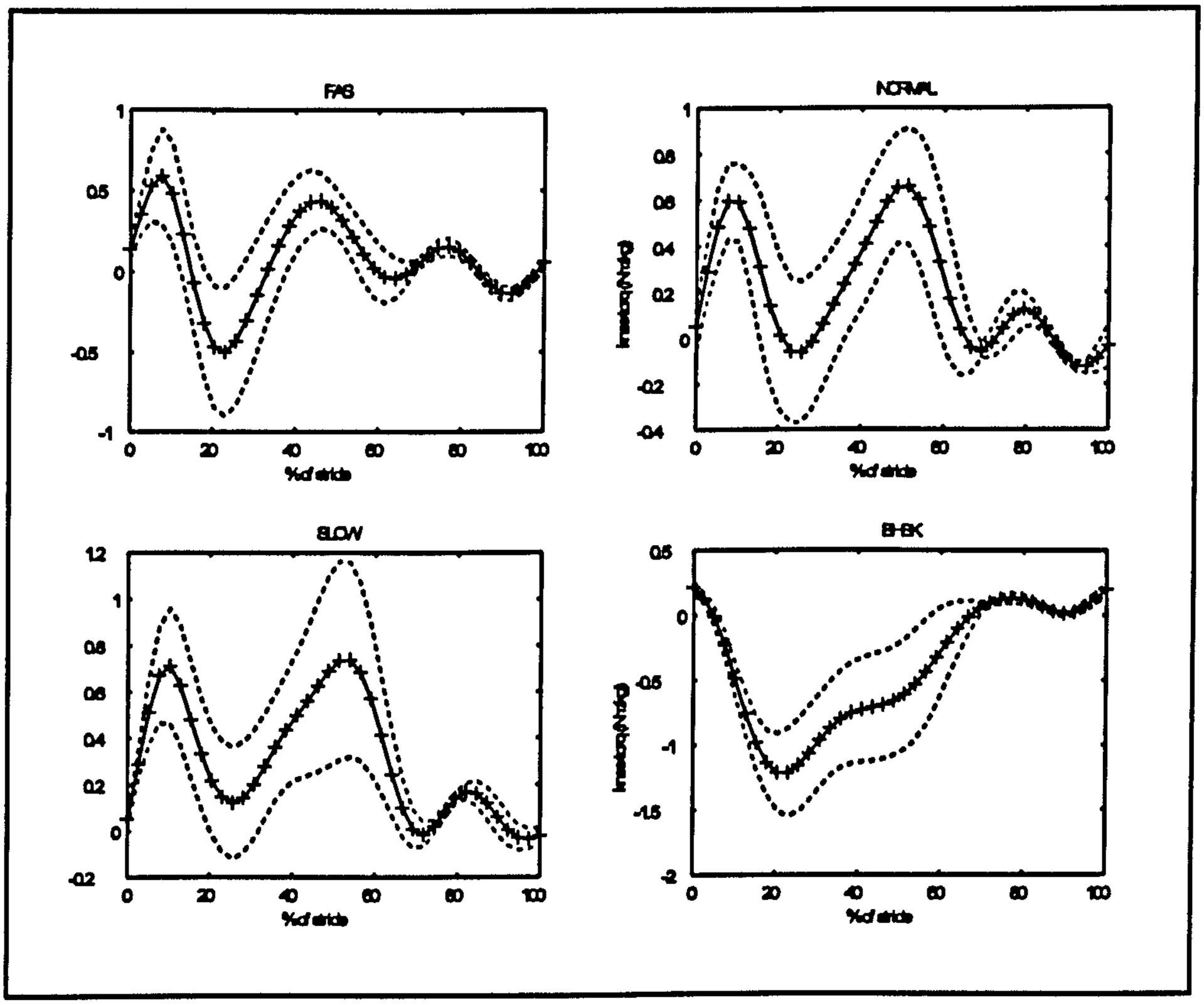

FIGURE 4.3.b Comparison of knee moments in different modes of walking; torq: torque; other symbols are as in Figure 4.1.a.

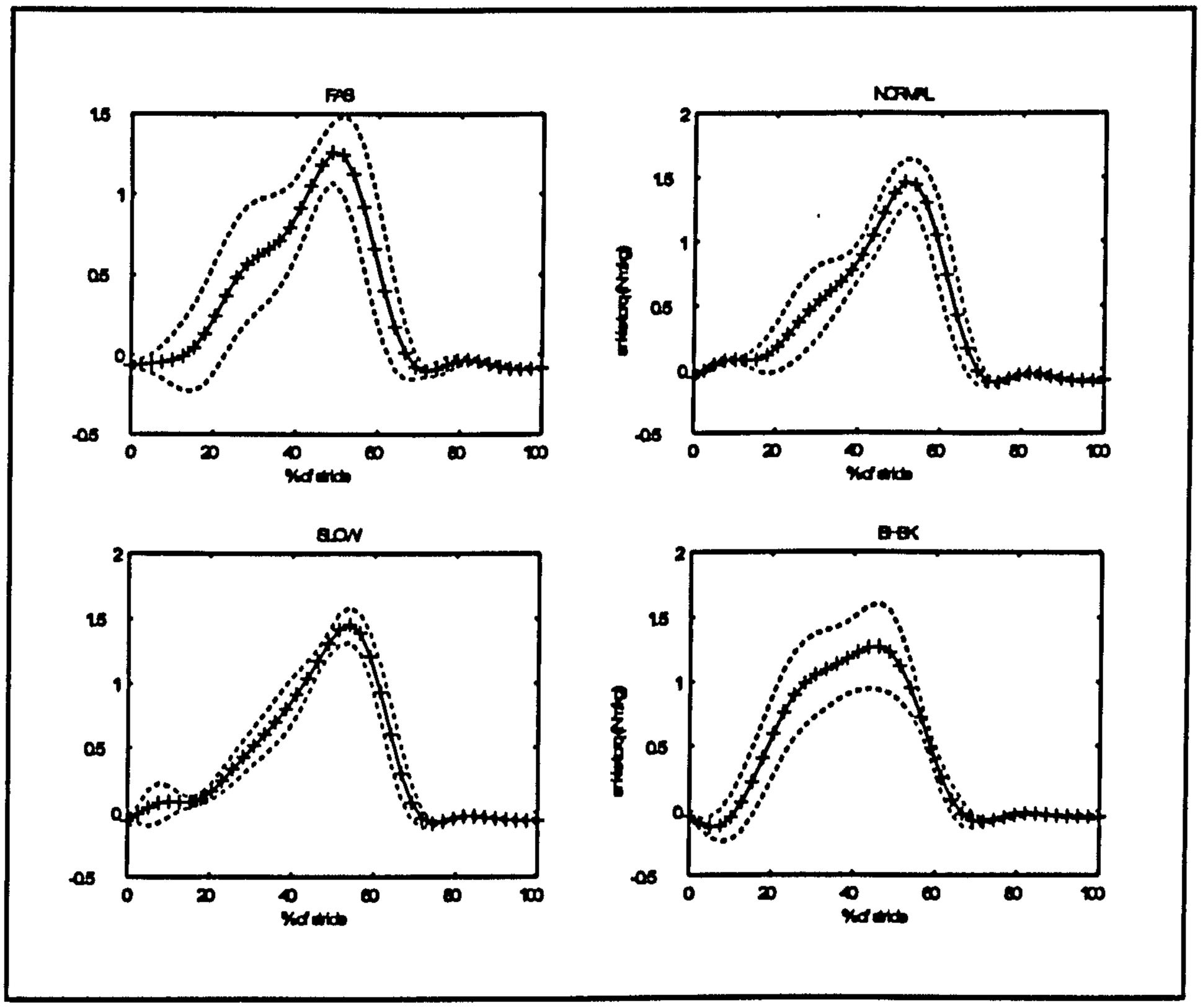

FIGURE 4.3.c Comparison of ankle moments in different modes of unloaded walking; torq : torque; other symbols are as in Figure 4.1.a.

4.1.3 Commentary

From Table 4.2 and Figs. 4.1 a-c, it is apparent that while in general, joint angles of the lower limbs in the three modes of erect walking are not significantly different from each other, those in BHBK walking are different from those in erect walking. The main differences are that 1) the hip and knee undergo much greater flexion in BHBK than in erect mode and 2) while the range of hip angles in BHBK walking is similar to that in erect walking, the range of knee angles is smaller and range of ankle angles larger in BHBK walking.

From Table 4.3 and Figs.4.2.a-c, it may be observed that BHBK and erect walking have similar angular velocities at the hip and ankle, but knee angular velocity is smaller in BHBK than in upright walking.

From comparison of joint moments (Table 4.4 and Figs.4.3.a-c), one of the most marked differences between BHBK and upright walking is that the knee moment has a very large flexor torque. The range of knee moments in BHBK walking is double that in normal and slow walking. In BHBK walking knee moments may reach twice their magnitude in fast walking and 10 times their magnitude in slow walking. The sign of the knee moments tells us that the muscles around the knee have to produce a very large extensor torque, to prevent collapse. However, in BHBK walking joint moments at the ankle and hip are similar to, or even slightly smaller than those in upright walking, though the hip has a rather larger flexion.

4.1.4 Discussion

BHBK walking requires a very large moment at the knee so to maintain balance. This moment appears to be so large that the angular velocity at the knee has to be decreased, implying that the . muscles around the knee are incapable of sustaining such moments while maintaining angular velocity at the levels seen in erect

walking. Thus, both the range of angles and angular velocity of the knee are smaller in BHBK. than in upright walking. From the viewpoint of the evolution of bipedalism, if early hominids indeed used to walk BHBK as often proposed, they would have required particularly powerful knee extensors. Even so, there may have been little net benefit, as the rotational inertia of the lower limb about hip would almost certainly have increased as a consequence. Therefore, assuming that selection would so operate on the locomotor system as to enable hominids to walk effectively, it is more likely that an upright mode of walking would have been selected for.

4.2 Comparison of erect and BHBK loaded walking

TABLE 4.5 Comparison of basic experimental conditions between normal loaded walking (NLW) and bent-hip, bent-knee loaded walking (BLW). (N = 8)

	NLW		BLW	
	mean	sd	mean	sd
Velocity CM (m/s)	1.3061	0.21	1.1418	0.20
Cadence(step/min)	53.56	4.03	50.43	8.30
DCM (m)	1.4588	0.17	1.3620	0.15

Note:
1.weight:77.5±6.60, height:1.785±0.06;
2. DCM - displacement of the centre of mass (m);

4.2.1 Methods

TABLE 4.6. Comparison of joint angle (R) between NLW and BLW
(N = 8)

	Hip		Knee		Ankle	
	mean	sd	mean	sd	mean	sd
Max (NLW)	0.4755*	0.10	1.1390*	0.12	-0.9035*	0.03
Max (BLW)	-0.1874*	0.41	1.4903*	0.11	-1.0608*	0.05
Min (NLW)	-0.6931	0.19	0.0906*	0.12	-1.3872*	0.19
Min (BLW)	-1.1436	0.59	0.7470*	0.13	-1.6839*	0.04
Max Range (NLW)	1.1686*	0.16	1.0484*	0.06	0.3854*	0.04
Max Range (BLW)	0.9562*	0.24	0.7433*	0.15	0.6232*	0.07

* $p<0.05$.

This section aims to investigate some aspects of loaded walking, contrasting erect and BHBK modes in terms of the kinematic and kinetic characteristics of the two modes. The experimental subjects were adult men. Kinematic and kinetic data were obtained as described in Chapters 2 and 3, and all required parameters: joint angle, angular velocity, moment, power at joints of the lower limb, and energy of the whole body, calculated using Newton's laws.

4.2.2 Subjects and Method

Details of method were as presented in Chapters 2 and 3. The subjects were 8 adult males who walked barefoot and wore tightly fitting swimming trunks, in NW and BHBK modes, while carrying 20 kg loads about the neck 16 sequences of video and kinetic data were available for this analysis. Digized data were filtered using a Butterworth filter (cut-off frequency 10 hz). The parameters of the experiment for subjects and speeds are listed in Table 4.5.

4.2.3 Results

4.2.3.1 Joint angles

The range of joint angles is listed in Table 4.6 and shown in Fig. 4.4. The range, R, at the hip in normal loaded walking (NLW) was larger than in bent-hip, bent-knee loaded walking (BLW). A similar situation occurred at the knee. In contrast, the range at the ankle was smaller in NLW than in BLW.. A phase shift was observed at the hip, where maximum flexion was in mid-cycle in NLW, but later, at about 60% of the cycle, in BLW (see fig. 4.4). Both maximum and minimum joint angles were significantly different, and the ranges also differ.

From Fig.4.4 and Table 4.6, it is apparent that not only were the maximum and minimum of the relative angles at the joints very different between the two modes of loaded walking, but also their time histories. The angular peak at hip in NLW occurred at mid-cycle (50%), but that for BLW later (60%). Since hip and knee ranges in BLW were smaller than those in NLW, ankle range was also larger, as required to maintain speed.

4.2.3.2 Angular velocities

A similar situation could be observed in angular velocities (Fig. 4.5): though the curves were similar, the magnitudes differ. The range of angular velocity at the knee was smaller in BLW than NLW, but the range of angular velocity at ankle was larger. This may result from a larger ankle angle. There was no significant difference at the hip. Phase shifting of angular velocities was not observed, which may indicate that joint angular velocity at the hip did not differ significantly.

4.2.3.3 Joint moments

It was discovered that the moments at the knee were very different in BLW and NLW. The latter moment changes from negative (from 0 - 30% cycle) to positive, but the former was always negative during stance (0-60% cycle). In addition, the magnitude of moments was much larger in BLW than NLW. Considering absolute moments, the value for BLW (0.8124) was almost 2.5 times larger than NLW (0.28), explaining why BLW is not normally employed. (Table 4.7 and Fig.4.6). Moreover, the knee moment was negative, or extensor, to support the heavy joint load. Secondly, though ankle moments were similar, both range and maximum value were somewhat largerin NLW. In contrast, the range at the hip was smaller in NLW. Thus, the ankle is more influential in NLW, but the hip in BLW.

4.2.3.4 Comparison of powers

Commentary

Powers differed greatly in the two modes of loaded walking modes (Fig 4.7 and Table 4.8). 1) almost every form of power is less in NLW than BLW. For example, absolute power at the hip was only 0.4451 w/kg for NLW, but for BLW it was 0.5903. At the knee, the absolute power was 0.7736 for BLW, but only 0.4984 for NLW. Power used for BLW was 0.5903 + 0.7736 + 0.8217 = 2.1856 w/kg, but the amount used for NLW was 0.4451 + 0.4984 + 0.5052 = 1.4487. If absolute power may be considered as an index of the work done by the body, work was 1.5 times more in BLW than NLW. In Table 4.5, a new index, pd, is

TABLE 4.7 Comparison of moments at lower limb joints (Nm/kg) between NLW and BLW
(N = 8)

	Hip	Knee	Ankle
	Mean sd	Mean sd	Mean sd
AM (NLW)	0.3972 0.15	0.2800* 0.07	0.4962 0.04
AM (NLW)	0.4997 0.17	0.8124* 0.13	0.5786 0.14
PM (NLW)	0.2996 0.18	0.1239 0.10	0.4807 0.04
PM (NLW)	0.3834 0.14	0.0448 0.00	0.5608 0.16
NM (NLW)	-0.0976 0.04	-0.1561* 0.12	-0.0155 0.00
NM (NLW)	-0.1163 0.03	-0.7676* 0.13	-0.0179 0.02
MRM (NLW)	1.7238 0.73	1.2765* 0.16	2.1536* 0.28
MRM (NLW)	1.9939 0.55	2.0459* 0.40	1.8649* 0.20
MAX (NLW)	1.1662 0.72	0.5181 0.32	2.0150* 0.25
MAX (NLW)	1.3439 0.40	0.3092 0.04	1.7059* 0.24
MIN (NLW)	-0.5577 0.05	-0.7584* 0.44	-0.1386 0.03
MIN (NLW)	-0.6499 0.17	-1.7366* 0.40	-0.1590 0.18

Note:
AM - average absolute moment; PM - average positive moment;
NM - average negative moment; MRM - maximum range of
moment; MAX - maximum moment; MIN - minimum moment)-BLW;
* $p<0.05$.

used to compare the two powers over the same distance. Pd is defined as absolute power divided by the distance travelled by the body centre of mass. Summing pd for all joints, we obtain 0.9898 for NLW but 1.6186 for BLW, so that the power spent per unit distance was only 60% of the value of BLW.

Though almost all forms of power were larger in BLW, the increments of power differ between joints. The ratio of absolute power in BLW to NLW was greatest at the ankle, 1.6264 (0.8217/0.5052), versus 1.552 (0.7736/0.4984) at the knee and 1.3250 (0.5903/0.4451) at the hip, so that the ankle and knee play more important roles in BLW than NLW.

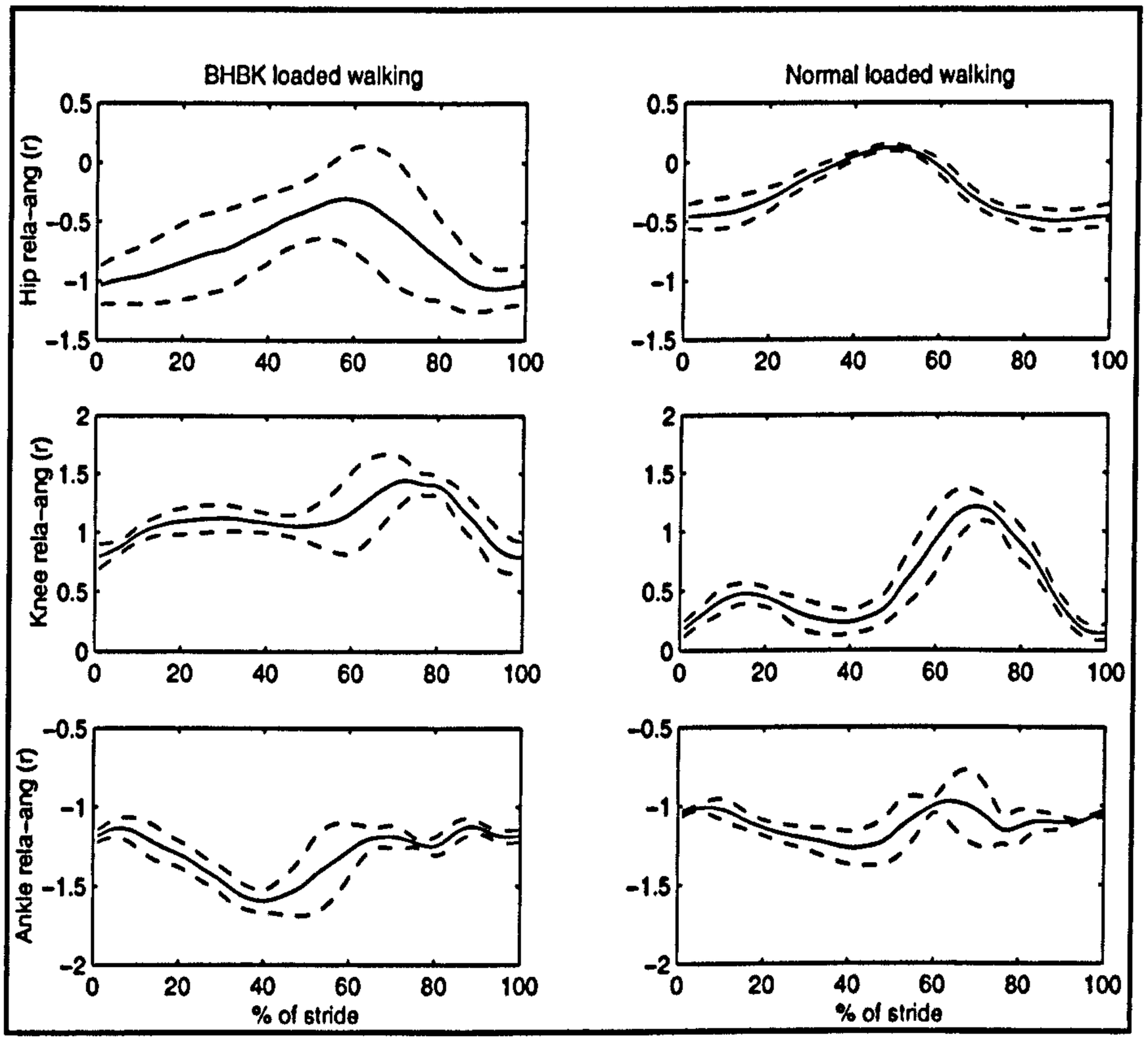

FIGURE 4.4 Comparison of relative joint angle (rela_ang) between normal and BHBK loaded walking

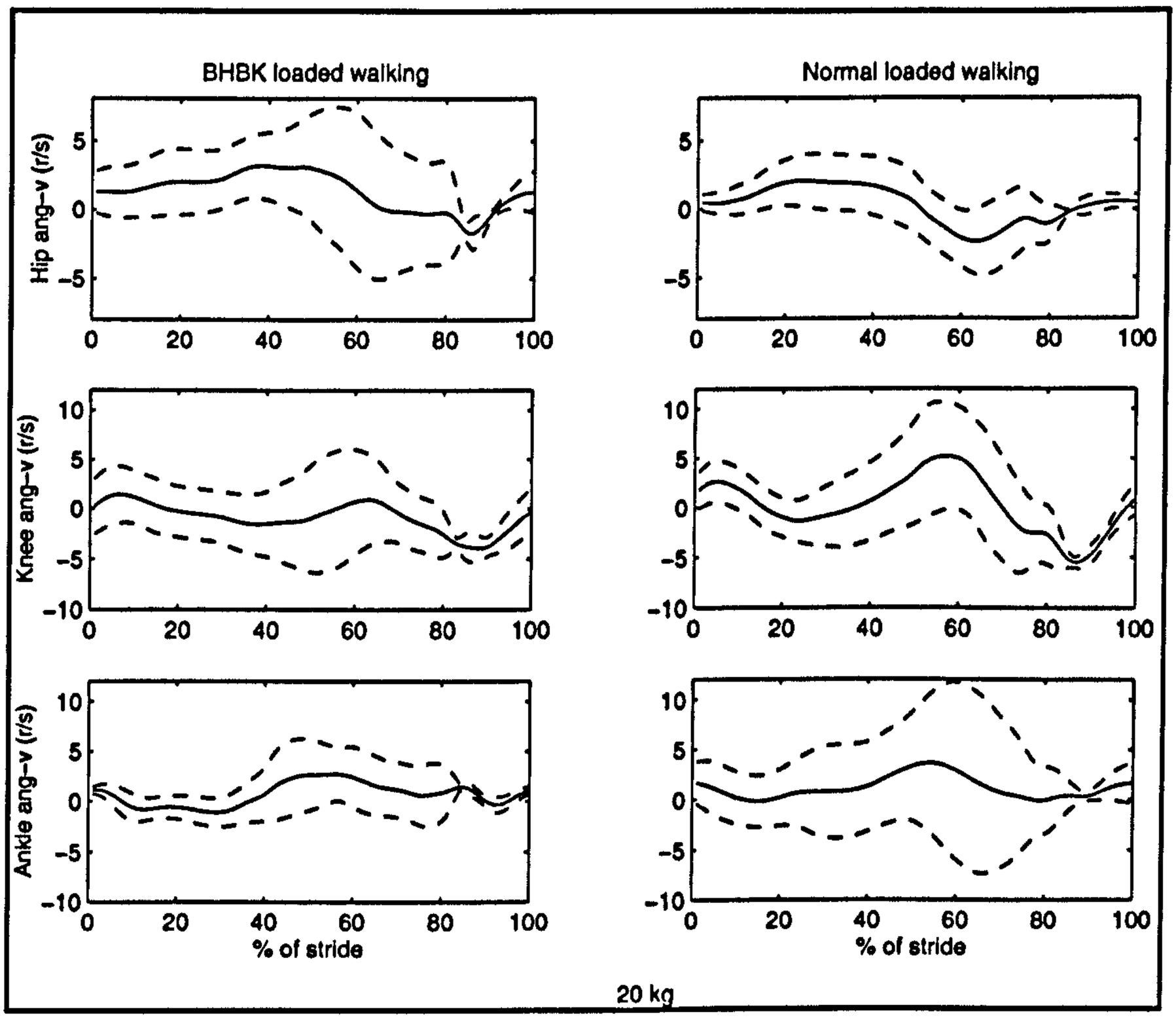

FIGURE 4.5 Comparison of angular velocities (ang_v) between the two modes of loaded walking

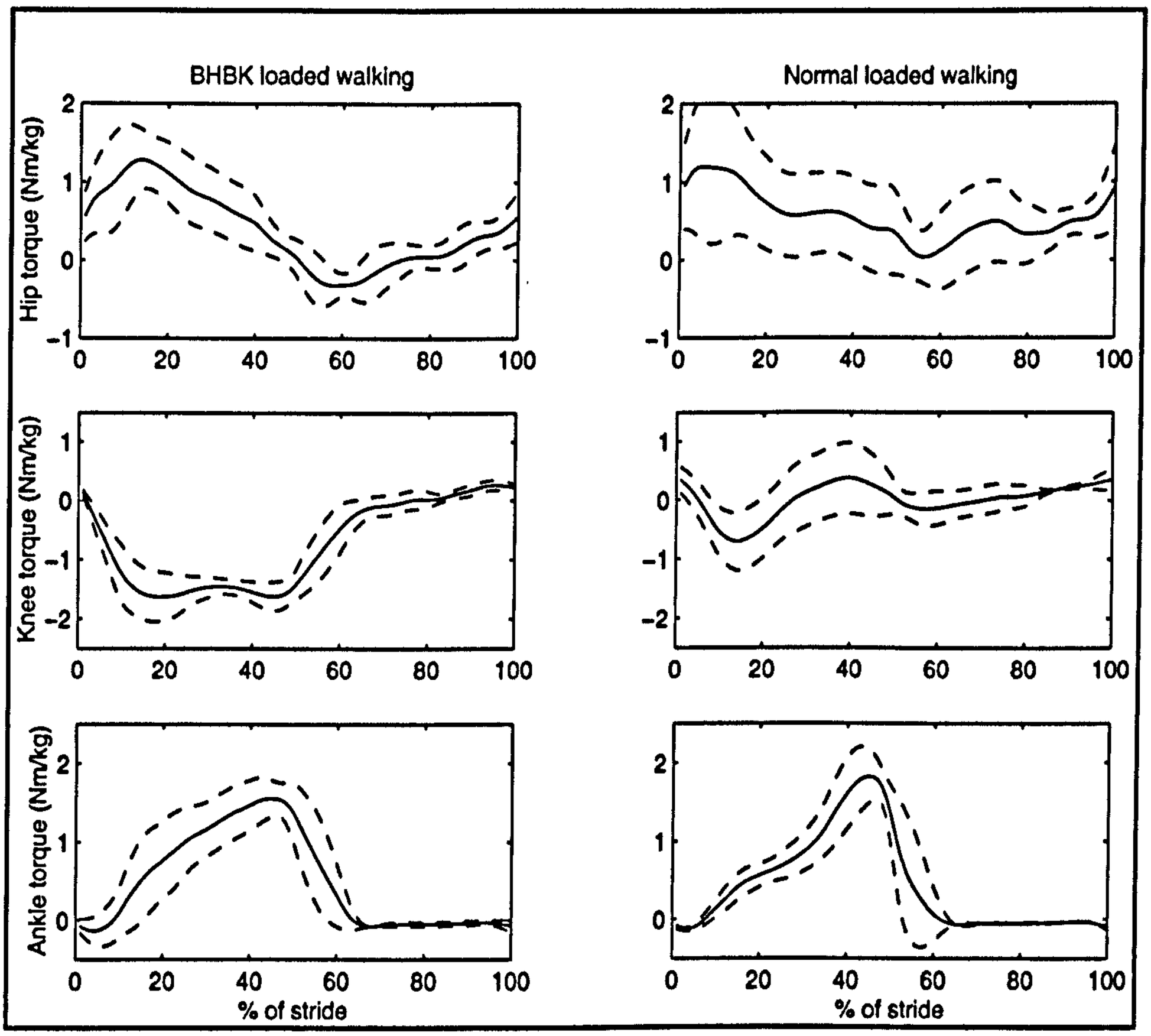

FIGURE 4.6 Comparison of torques between the two modes of loaded walking; torq : torque.

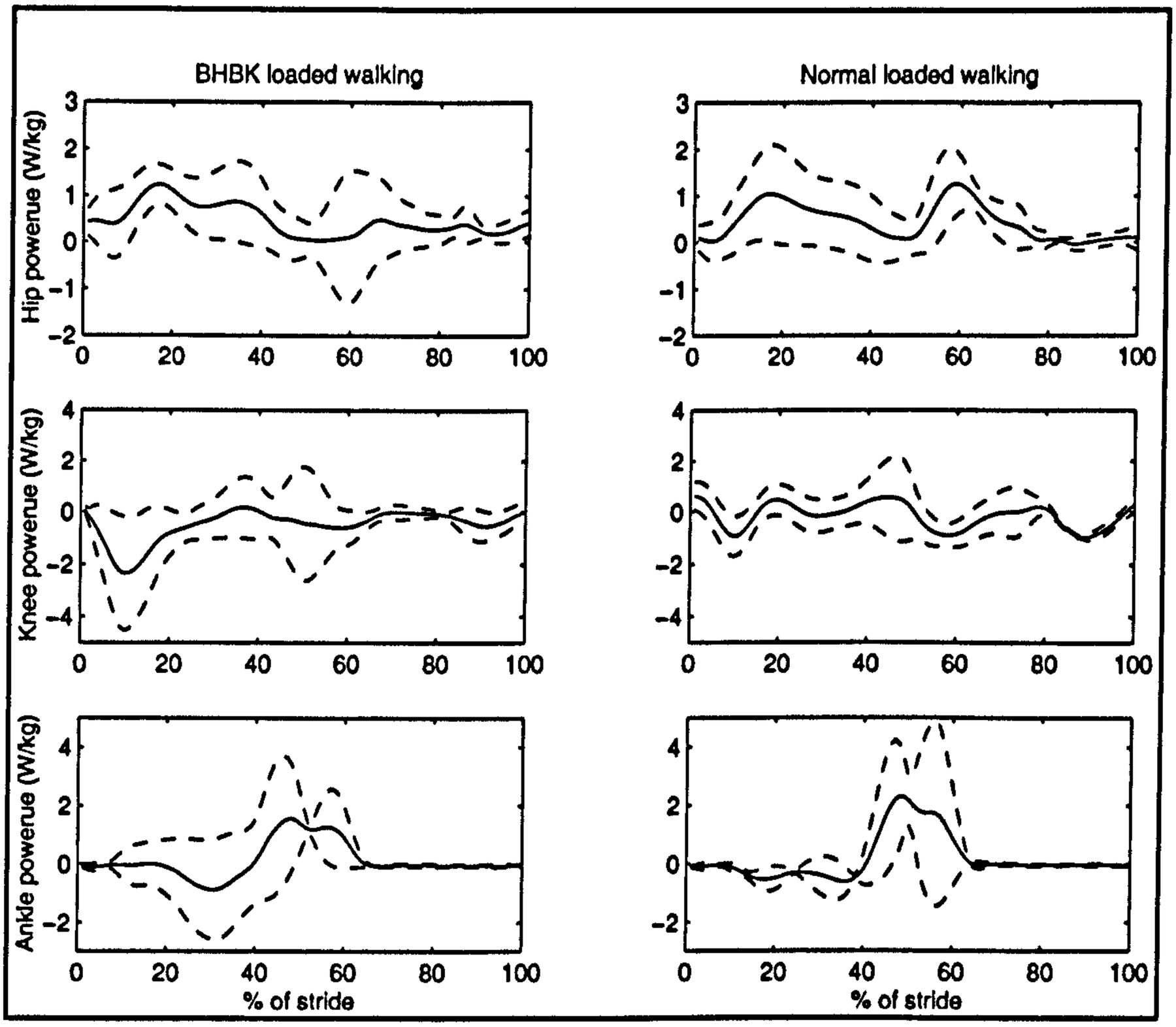

FIGURE 4.7 Comparison of powers between the two modes of loaded walking

4.2.4 Discussion

TABLE 4.8. Comparison of joint power (W/kg) between NLW and BLW (N = 8)

	Hip		Knee		Ankle			
	Mean	sd	Mean	sd	Mean	sd	Sum	sd
AP (NLW)	0.4451	0.22	0.4984	0.15	0.5052	0.23	1.4484*	0.20
AP (BLW)	0.5903	0.16	0.7736	0.40	0.8217	0.37	2.1856*	0.34
PP (NLW)	0.4153	0.22	0.1692	0.13	0.3572	0.24	0.9417	0.22
PP (BLW)	0.5556	0.17	0.1856	0.08	0.4247	0.25	1.1659	0.23
NP (NLW)	-0.0297	0.02	-0.3291*	0.03	-0.1480*	0.04	-0.5068*	0.12
NP (BLW)	-0.0347	0.01	-0.5880*	0.44	-0.3945*	0.14	-1.0172*	0.35
MAX (NLW)	1.5336	0.45	1.1581	0.79	3.9548	2.18	6.6465	1.84
MAX (BLW)	1.5769	0.22	1.5149	0.64	3.9256	1.82	7.0174	1.58
MIN (NLW)	-0.3201	0.20	-1.3462*	0.25	-0.9742*	0.50	-2.6405*	0.54
MIN (BLW)	-0.4900	0.22	-2.7618*	0.22	-2.3159*	0.93	-5.5677*	1.66
PD (NLW)	0.2949	0.11	0.3436*	0.10	0.3513*	0.18	0.9898*	0.13
PD (BLW)	0.4421	0.16	0.5525*	0.22	0.6239*	0.34	1.6185*	0.26
PBV (NLW)							0.7578*	
PBV (BLW)							1.4175*	

Notes:
1. AP - average absolute power; PP - average positive power; NP - average negative power; MAX -maximum power; MIN - minimum power.
2. PD - absolute power/distance travelled by the centre of mass.
3. PBV - absolute power/body weight and velocity of the centre of mass;
*p<0.05.

Further analysis of positive and negative powers indicates that positive powers are very similar in the two modes, and most differences relate to negative powers. During BLW, larger negative powers at the knee and ankle lead to an increase of absolute power. Thus, muscles may only be able to produce a limited positive

power for joint motion, or otherwise may only output limited maximum energy per unit time.

In textbooks, negative power is characteristically described as resulting from work done by external forces, such as gravity. The work done will be absorbed by biological tissues but may later be released, rather like a spring. But tissues may differ in that they cannot be assumed to be completely elastic, but rather act primarily plastically, but with a small elastic range. Within the elastic range, storage and release of energy may occur in succession. But outside this range, tissues may easily yield. As we have observed from comparison of joint moments (Table 4.6 and Fig.4.7), knee moments are not only larger in BLW but last longer. Thus, moments may take muscle groups acting at the knee out of their elastic range, leading to more rapid exhaustion.

In BLW, subjects automatically reduce their speed and cadence (see Table 4.5). While this suggests that BLW is more exhausting than NLW, lack of familiarity with the gait needs also to be taken into consideration.

The angle of flexion is smaller in all joints for NLW than BLW, and the angle of extension correspondingly larger (Table 4.6 and Fig.4.4): thus, joint ranges also differ. Thus, subjects adjust joint angles in order to maintain speed. However, despite differences in joint angle, differences in joint angular velocities were small.

The main difference between NLW and BLW is thus in joint moments. The knee moment in BLW is larger and lasts longer, so that total joint power is almost 1.5 times greater, or 40% more energy-expensive. Again, selection can be expected to have acted to eliminate BHBK walking.

4.3 Comparison between common chimpanzee and human bipedalism

4.3.1 Subjects and Method

Many sequences of voluntary bipedalism were obtained over a forceplate set in the chimpanzee enclosure at Chester Zoo, of which one was of particularly good quality. Previous comparisons with data in the literature showed that the kinetics of the sequence were entirely typical (Li et al. 1996). The subject was a female adult

TABLE 4.9 Comparison of joint angles (R) in chimpanzee and human walking

	Hip			Knee			Ankle		
	max	min	range	max	min	range	max	min	range
CW	-1.75	-2.15	0.4	1.8	0.6	1.2	1.3	0.7	06
BW	0.1	-1.0	1.1	1.2	0.6	0.6	1.2	0.7	0.5
NW	0.5	-0.5	1.0	0.8	0.0	0.8	1.2	0.7	0.5

Note:
CW: chimpanzee bipedal walking;
NW: human erect walking;
BW: human BHBK walking.

height 1.2 m, weight 25 kg, and age approximately 12 years. The data were compared with those for human subjects performing NW and BHBK walking in the laboratory, as described in Chapters 2 and 3. The statistics for human subjects were as follows: mean height 1.730 m (sd 0.02), mean weight 73.69 kg (sd 8.5), mean velocity 1.45 m/s (sd 0.38). Experimental data for chimpanzee bipedalism and that for two typical human subjects are given in Table 4.9 and Fig.4.8.

4.3.2 Results

From Figs.4.8 a-c, it is obvious that the chimpanzee used a form of BHBK gait, resulting in a smaller step length. Figs. 4.9 a-c indicate that GRFs in human BHBK

walking were generally similar to these of chimpanzees, although there were some small differences. However, GRFs during human NW are quite different from those in chimpanzee bipedalism.

4.3.2.1 Joint angles

Results for joint angles in different walking by subjects are given are given in Fig.4.8 and Table 4.9.

Commentary

When a chimpanzee walks bipedally, ranges of hip, knee and ankle angles differ from those observed in both types of human bipedal walking (Figs.4.8 - 4.9 and Table 4.9). The range of hip flexion in the chimpanzee was only half that in either human BHBK or NW (Table 4.10), but the range of motion of the knee joint is relatively large: however, it fails to compensate for the small range of flexion at the hip, resulting in shorter strides in relation to stature (see below). In addition, during chimpanzee walking, two peaks were observed in the curves for hip angle, while a single peak occurs in humans. Thus, the chimpanzee was not able to walk as fast as humans because of relatively small angular ranges at the hip joint. Although in compensation the chimpanzee's knee moved through a relatively large range, a smaller stride length (about 0.5 m) results. If we use a coefficient, ss, to evaluate the relationship between stature and stride length, where ss = stride_length/stature, ss was 0.4 (0.5/1.2) for the chimpanzee; 0.8571 (1.5/1.75) for human BHBK walking and 0.9714 (1.7/1.75) for human NW. If ss may be used as an indication of the efficiency of bipedal walking, human walking is clearly more efficient.

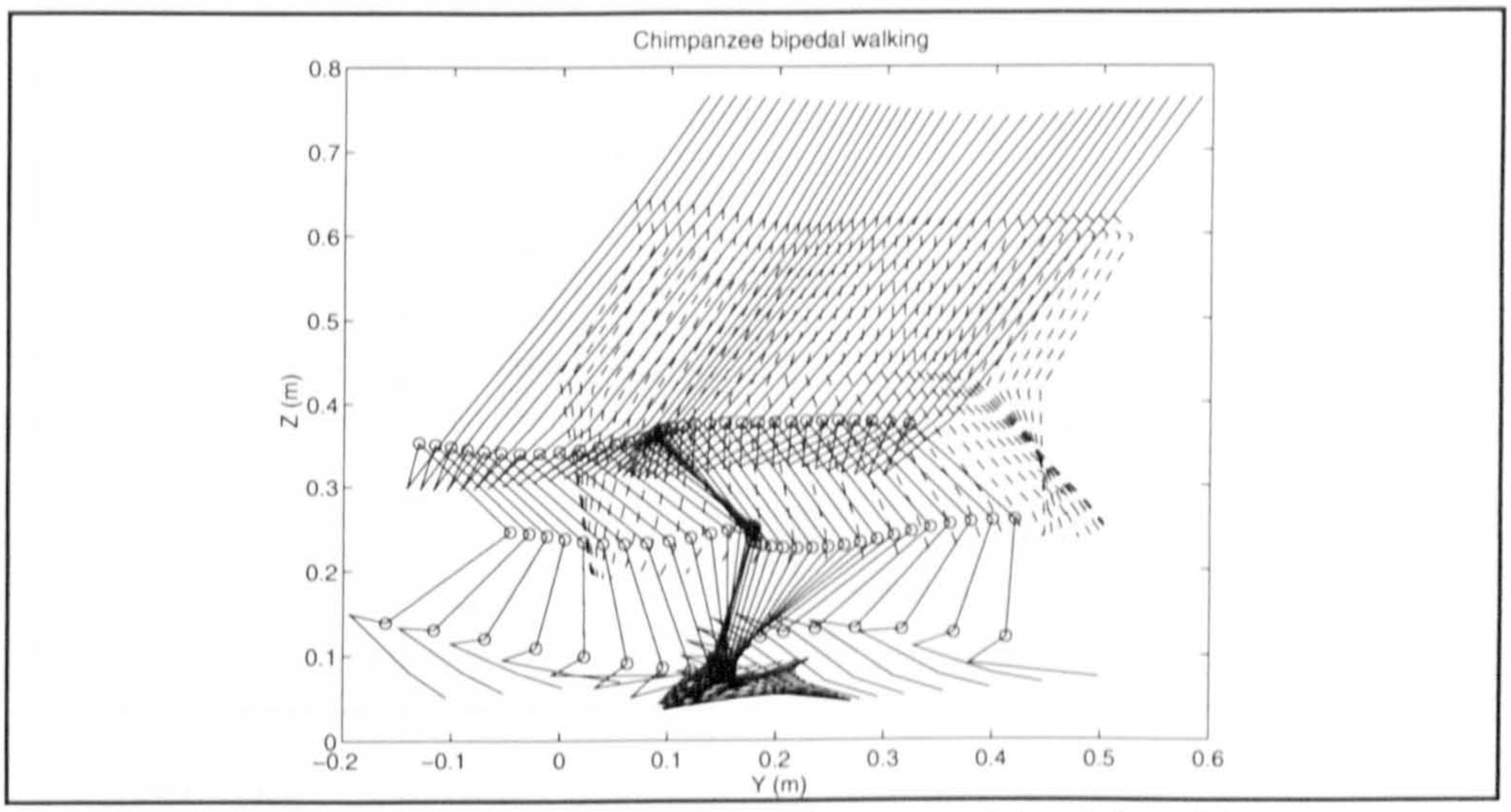

FIGURE 4.8.a An example sequence of chimpanzee bipedal walking

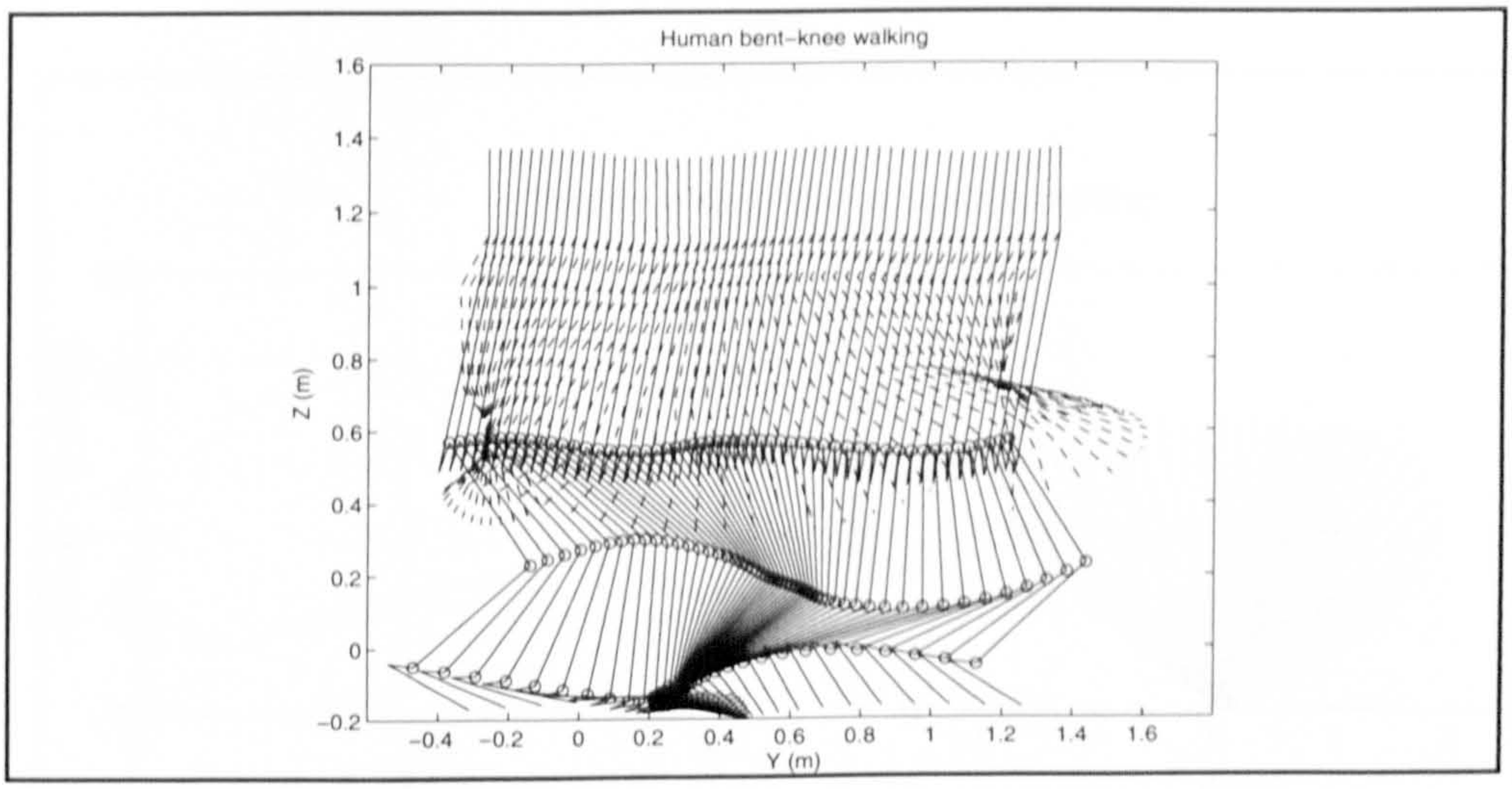

FIGURE 4.8.b An example sequence of human BHBK walking

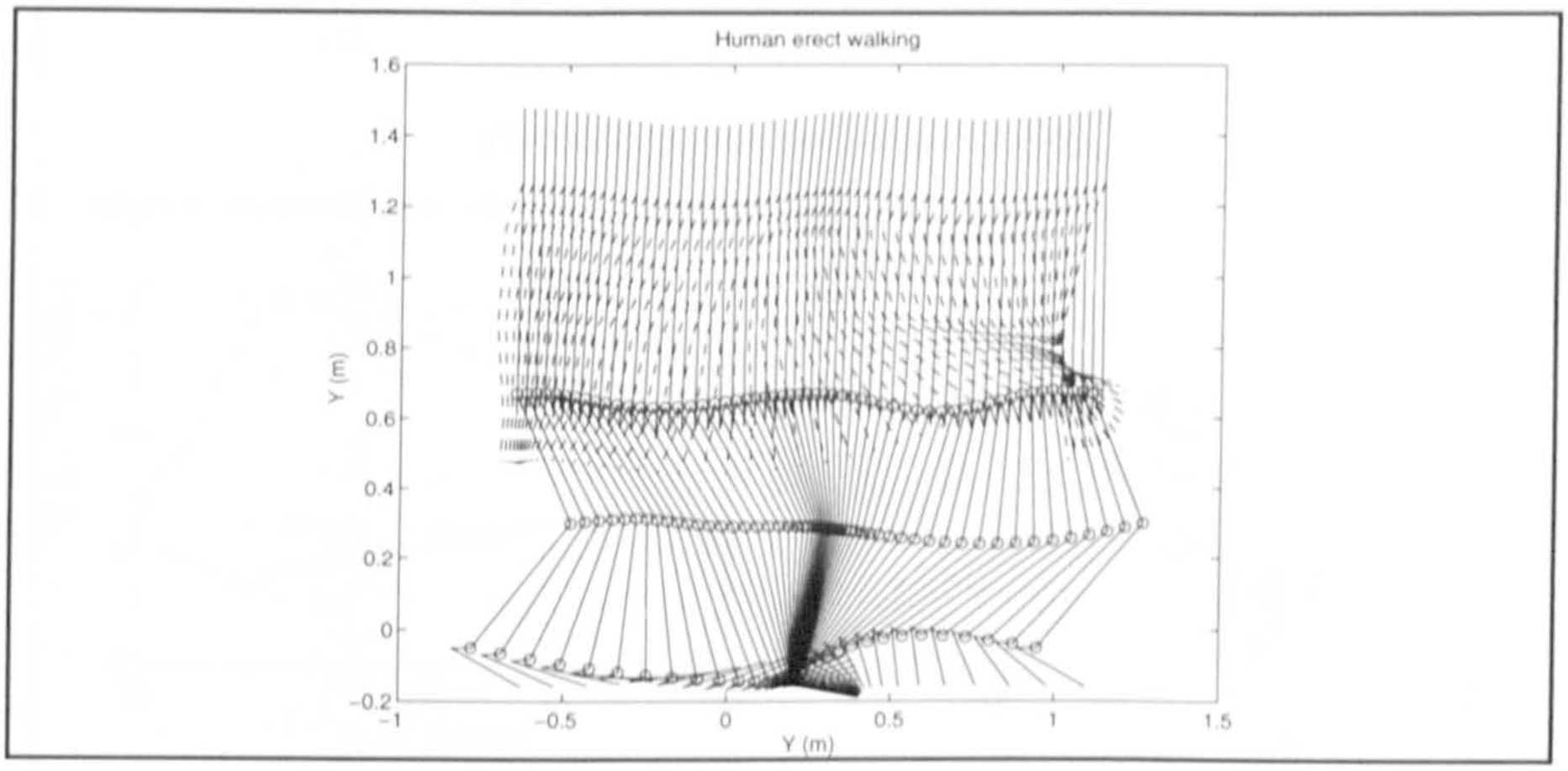

FIGURE 4.8.c An example sequence of human erect walking

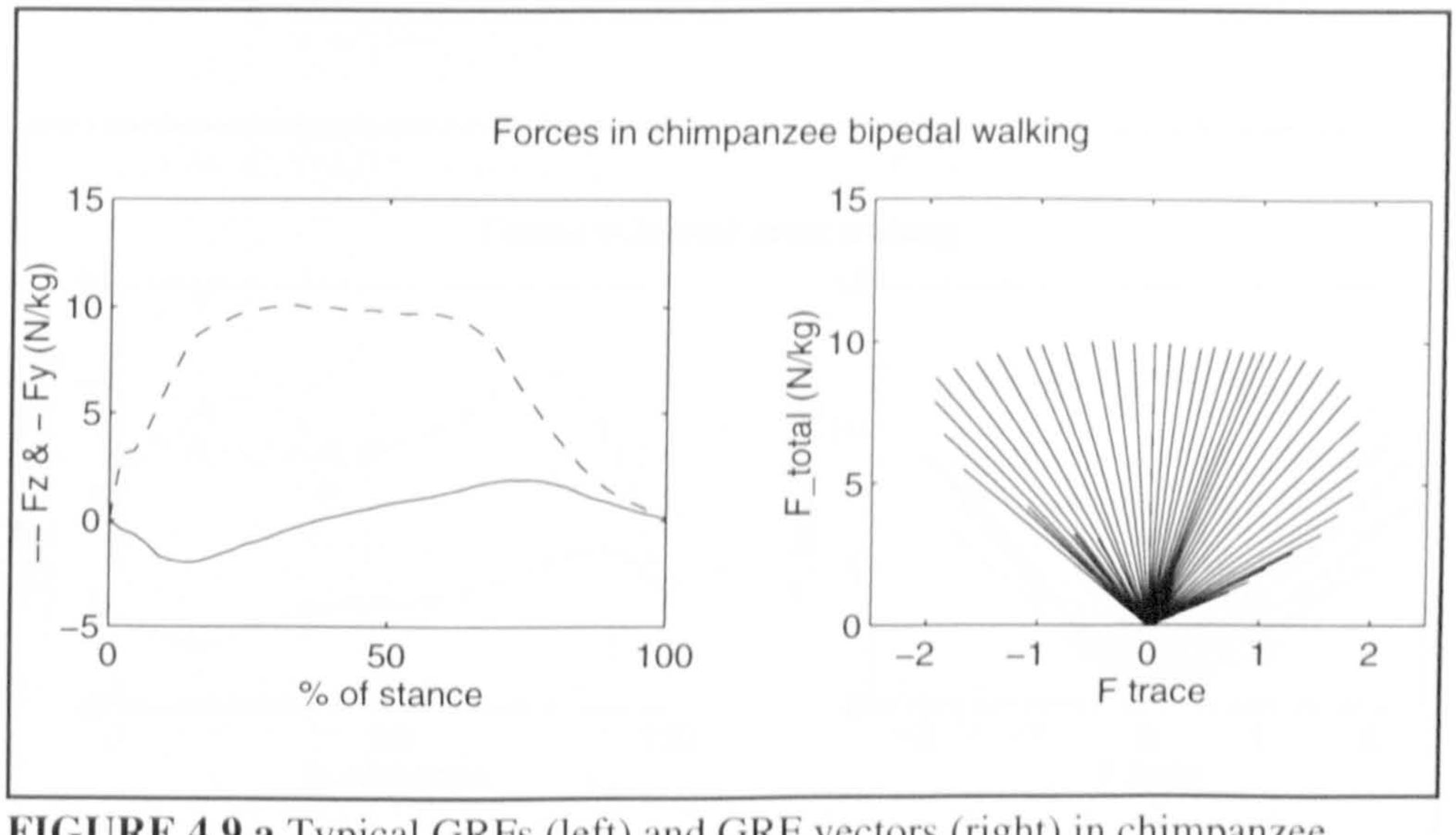

FIGURE 4.9.a Typical GRFs (left) and GRF vectors (right) in chimpanzee bipedal walking; in right sub-figure, the force trace is so short that it is looked as a point.

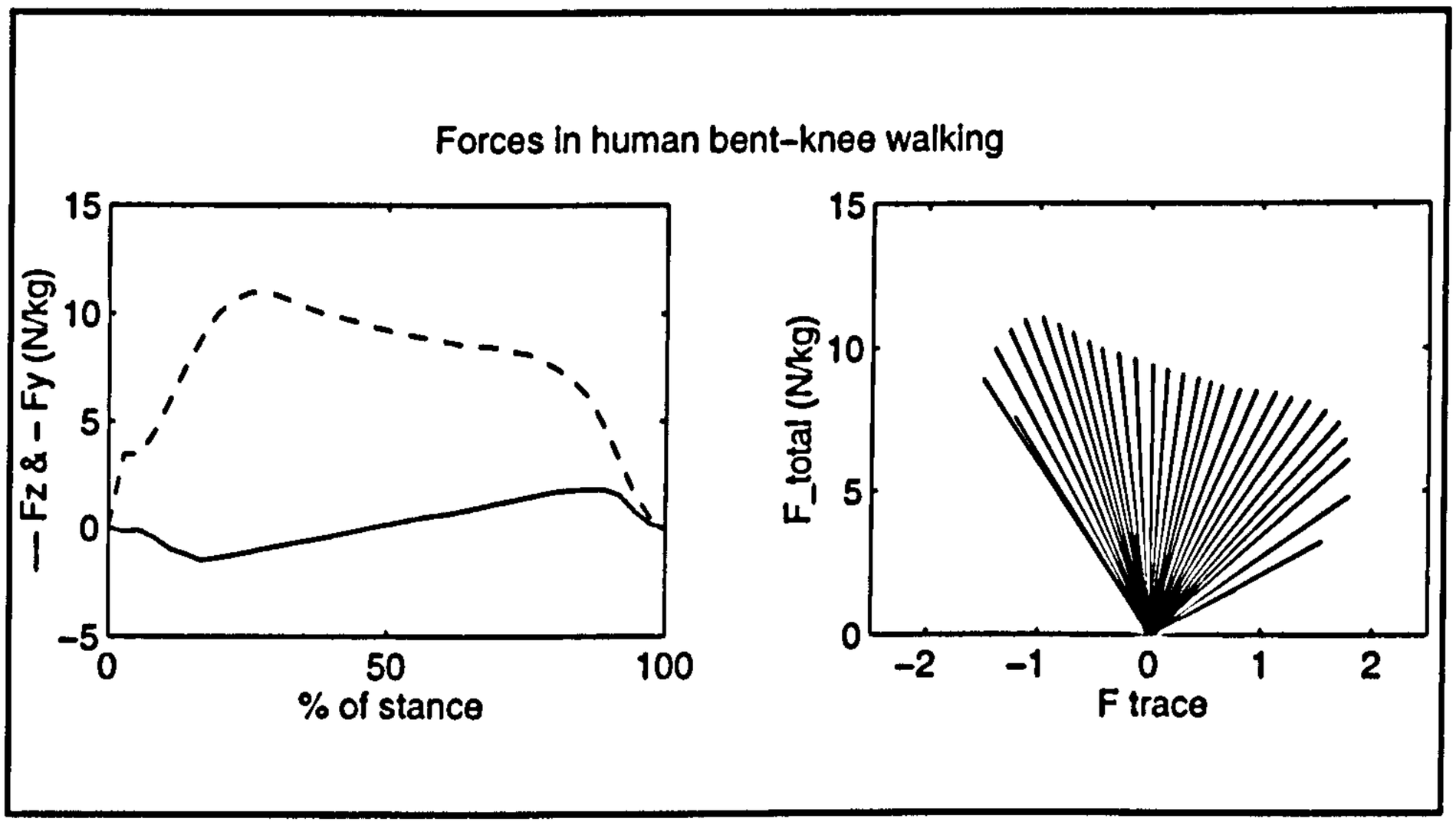

FIGURE 4.9.b Typical GRFs (left) and GRF vectors (right) in human BHBK walking; in right sub-figure, the force trace is so short that it is looked as a point.

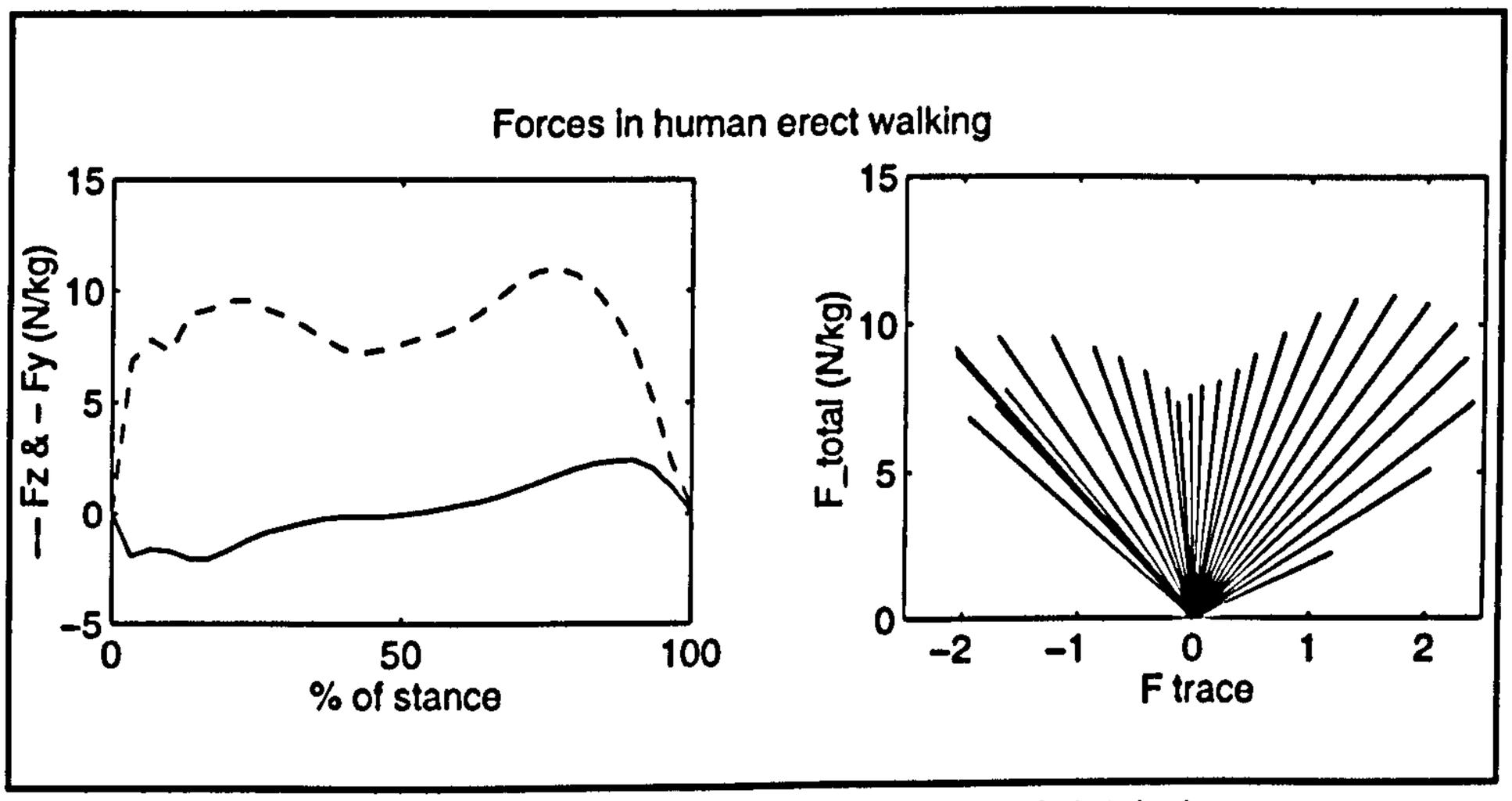

FIGURE 4.9.c Typical GRFs (left) and GRF vectors (right) in human erect walking; in right sub-figure, the force trace is so short that it is looked as a point.

4.3.2.2 Angular velocities

Angular velocities at the chimpanzee hip were smaller than for humans, although angular velocities of the knee and ankle joints were similar to those seen in humans (Fig.4.10-4.12 and Table 4.10.).

TABLE 4.10 Comparison of joint velocities (r/s) in chimpanzee and human walking

	Hip			Knee			Ankle		
	max	min	range	max	min	range	max	min	range
CW	1.5	-2.2	3.7	2.5	-6	8.5	3.2	-2.2	5.4
BW	3	-3	6	5	-4	9	3	-2	5
NW	3	-3	6	5	-3	8	2.5	-2.5	5

abbreviations as Table 4.9

Thus, the chimpanzee hip is less effective in bipedal walking than that of humans.

4.3.2.3 Moments

Table 4.11 shows that knee moments in the chimpanzee were relatively larger than those in human BHBK or NW (see also Figs.4.10 - 4.12). The strong flexion of the knee is sufficient to account for this finding. In human upright walking, hip and ankle moments play the major roles in propulsion, while the knee only assists the other joints. In human BHBK walking, moment distributions were similar, but hip

and ankle moments are relatively large.

TABLE 4.11 Comparison of joint moments (Nm/kg) in chimpanzee and human walking

	Hip			Knee			Ankle		
	max	min	range	max	min	range	max	min	range
CW	3	-0.2	3	1.4	-0.5	1.9	1.2	-0.5	1.7
BW	1.8	-1.8	3.6	0.2	-0.5	0.7	2.2	0	2.2
NW	1.2	-1	2.2	0.8	-0.2	1.0	1.8	0	1.8

abbreviations as Table 4.9

4.3.2.4 Joint powers

Almost all forms of powers at the chimpanzee's joints were larger than those in human NW or BHBK walking (Table 4.12 and Figs.4.10 - 4.12), and absolute, positive and negative powers were all larger than in either human walking mode, so that the chimpanzee unquestionably did more work than did our human subjects during bipedal walking.

4.3.3 Conclusions

Thus, for the chimpanzee investigated, almost all joint parameters were worse than either human NW or BHBK walking, resulting mainly from smaller angular range at the hip, but a bigger range at the knee. Secondly, the chimpanzee hip and knee were so flexed that the two joints are acted upon by larger peak moments, resulting

in greater joint power. Thus, an even stronger selective pressure can be expected to have operated against chimpanzee-like than human BHBK-like bipedalism in early hominids.

TABLE 4.12 Comparison of power (W/kg) between chimpanzee and human BHBK and upright walking

	Hip	Knee	Ankle	sum
AP(CW)	0.945	0.524	0.411	1.880
AP(BW)	0.546	0.425	0.451	1.421
AP(NW)	0.590	0.219	0.540	1.351
PP(CW)	0.329	0.458	0.034	0.828
PP(BW)	0.530	0.116	0.101	0.747
PP(NW)	0.475	0.133	0.125	0.733
NP(CW)	0.615	0.066	0.378	1.059
NP(BW)	0.016	0.309	0.349	0.674
NP(NW)	0.115	0.087	0.416	0.617
MAX(CW)	1.964	2.954	0.442	
MAX(BW)	1.039	0.572	1.049	
MAX(NW)	1.828	0.836	1.524	
MIN(CW)	-5.142	-0.481	-2.360	
MIN(BW)	-0.234	-2.399	-1.210	
MIN(NW)	-0.900	-0.589	-2.802	

Note:
1. AP:average absolute power; PP: average positive power; NP: average negative power; MAX: maximum power; MIN: minimum power.

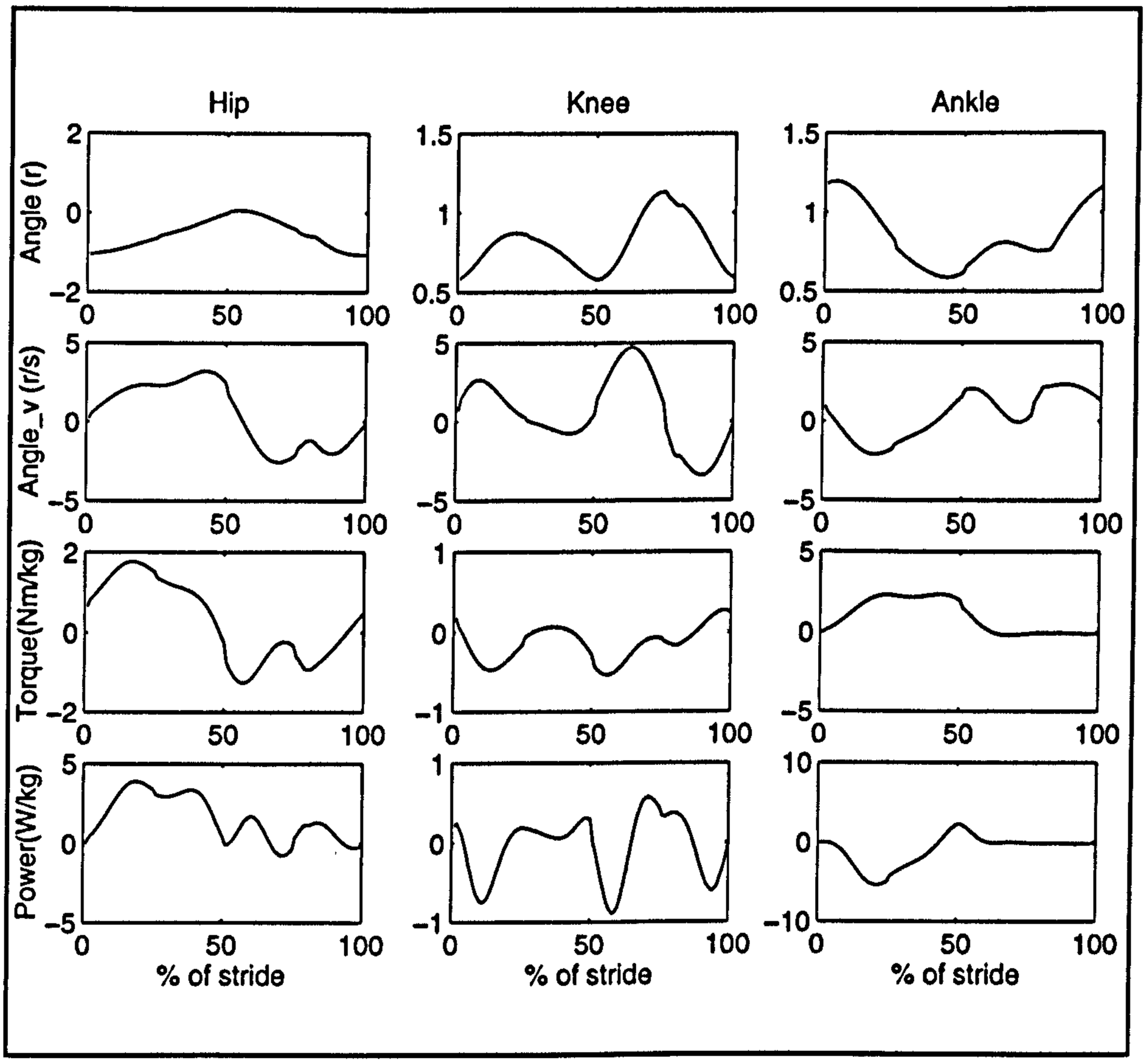

FIGURE 4.11 All results for human BHBK walking
Angle_v - Angular velocity

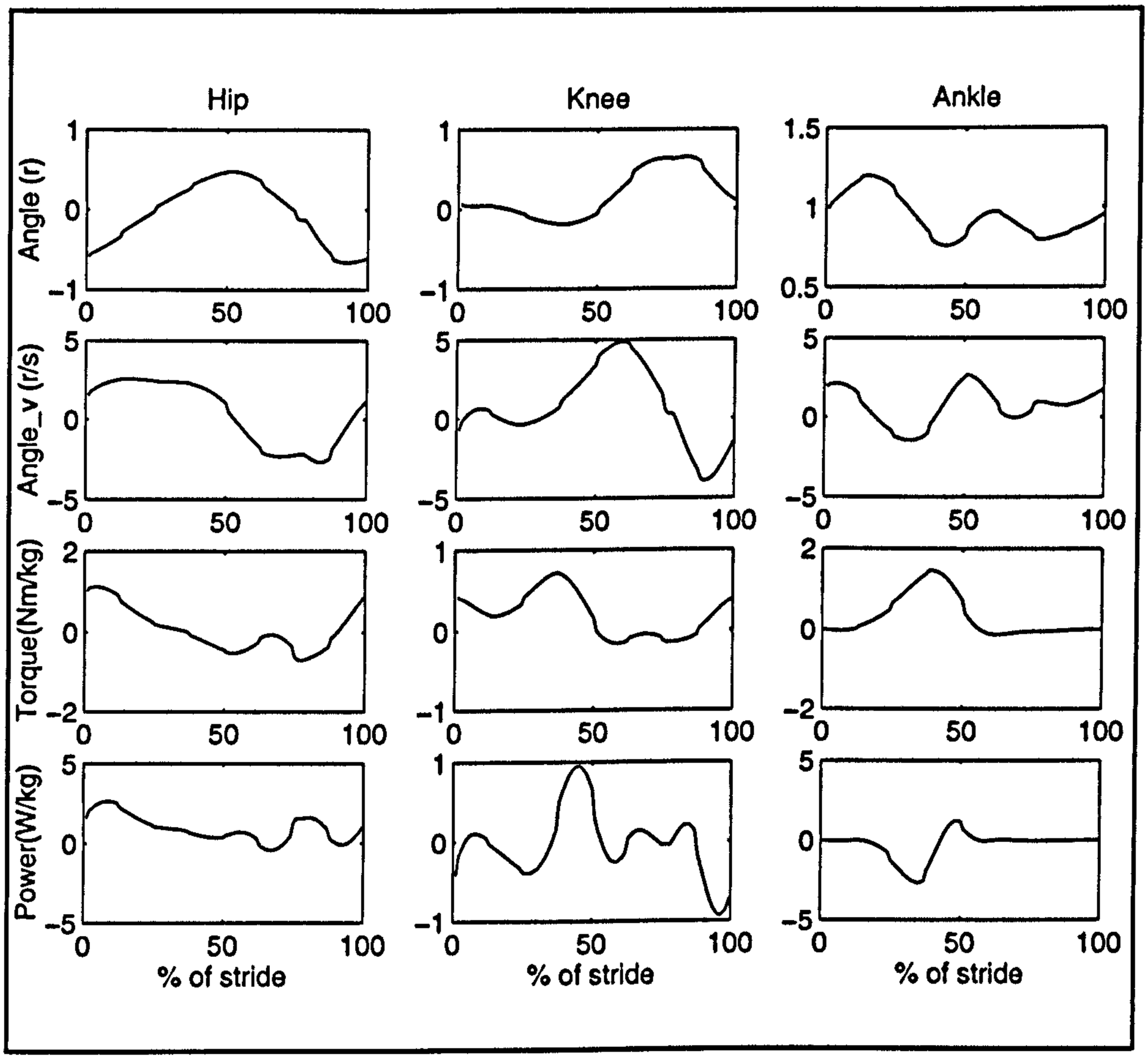

FIGURE 4.12 All results for human normal walking
Angle_v - Angular velocity

CHAPTER 5. ENERGY TRANSFORMATION IN BIPEDALISM

It is a very light feeling to see someone carrying a very heavy load.

Chinese Proverb

Abstract

This chapter aims to investigate 1) whether there are different patterns of energy transformation in different gaits; 2) which gait may be better from the viewpoint of saving energy, and 3) what relationship may exist between the evolution of bipedalism and energy exchange. Human subjects were required to walk using different gaits, including BHBK walking and normal walking, and a recorded sequence of bipedalism by a common chimpanzee was used as a comparison. It was found that among various modes of human walking, comfortable walking has the best effect on energy transformation and BHBK walking the worst, on the same criterion. The chimpanzee had the least effective energy transformation. The results imply that if early hominids walked in the commonly-hypothesized BHBK mode, selection would have acted to eliminate it.

5.1 Energy transformation in various gaits

5.1.1 Gait selection

As discussed in Chapter 1, energy consumption may have been an influence on the evolution of bipedalism. A particularly interesting aspect of energy consumption is the manner in which energy changes when humans walk bipedally. Whether a gait is, or is not, effective generally depends on whether, and to what extent it conserves the energy spent during motion. A similar problem is why, in everyday life, people select a particular, self-determined 'comfortable' velocity, not a slower or faster speed.

It is known that the work done by muscles increases with the velocity of the centre of mass. Based on this point, it would be expected that a slower velocity should be better than any more rapid speed in conserving energy. But, in fact, people nearly always walk at a particular, 'comfortable' speed, which is not their slowest pace.

Here we are concerned with two particular types of mechanical energy: kinetic and potential energies. When humans move, these two forms of energies are known to exchange during a gait cycle. The energy fluctuation represents the work done by the muscles and the body.

This element of my thesis provides, and applies, a simple method by which to assess which mode of walking and which velocity might be optimal in terms of mechanical energy cost. The method is based on particle mechanics, and considers the effect of energy transformation between kinetic and potential forms as an assessable condition.

5.1.2 Materials and methods

5.1.2.1 General method

The methods used here to appraise a given walking procedure are mainly of two kinds. One is based on the centre of mass (CM) and the other on the segments. Zarrugh (1981) applied a relatively complete approach when he measured a subject 's mechanical efficiency in treadmill walking. He considered the total work done by the body to consist of all segment rotational and translational energy; measured metabolic power as body output, and obtained an efficiency by comparing the two. The approach satisfies mechanical theory. But in general, it is not very easy to do such complex work under simple experimental conditions, since some important parameters, such as the rotation of segments and the coefficient of mass, cannot be obtained easily and accurately. Furthermore, the measurement of metabolic power of a subject moving on a treadmill may interfere with normal motion. In addition, as Zarrugh himself indicated (1981, p.158) his method only considers work done in terms of positive power, so that calculated efficiency may be less than is the case.

Cavagna and colleagues (1976, 1977) defined a parameter "recovery" and investigated this parameter in the motion of many subjects. Their approach was based mainly on particle mechanics, where the whole system is considered as a particle with mass. The kinetic energy and potential energy in the body's CM can be obtained by integrating recorded ground reaction forces (GRFs), and then, 'work recovery' can be estimated. But the approach ignores the role of negative power, since all work done was computed absolutely (see Winter 1983; and Williams and Cavanagh 1983). In addition, under their definition, recovery at 'comfortable' speed reached nearly double that in slow or fast walking (Cavagna et al. 1976), which seems to be contrary to findings in physiological experiments. Nevertheless, as the method is very simple and requires fewer assumptions, it has been widely used to analyze different subjects, including humans (Winter 1990) and chimpanzees (Kimura 1996).

Cavagna and colleagues (1976) found that human comfortable walking has high 'recovery', but some animal motion has comparatively low 'recovery': for example, Kimura (1996) studied the trends in displacement of the body centre of gravity during the ontogeny of chimpanzee bipedal walking and found that the energy recovery of younger chimpanzees is smaller than that of adults.

5.1.2.2 Subjects and methods

Subjects and general experimental methods are as described in section 3.1 of Chapter 3. A total of 280 trials were retained for analysis. The method used in this chapter (also see Chapter 2) is similar to Cavagna's (1977), being based on particle mechanics.

In general, change of energies in a system is produced by the work done by internal and external forces. When work done is positive, biological tissues (e.g. muscles) output energy to make the body move. When work done is negative, biological

tissues may absorb and store some energy. Because it is still unclear how muscles absorb and store energy (Winter 1983; Williams and Cavanagh 1983), we have to estimate work done by calculating the range of changes in system energy: in kinetic energy (KE) in potential energy (PE) and their influence on each other. We define the range of change in KE and PE as the work done for maintaining the movement of the body CM, and the range of change in the sum of KE and PE as the work produced by biological tissues. By integrating forceplate data, we readily obtain the curves of KE and PE. Thus, we can investigate the dynamic trend of the two energies during walking. The method is described in detail in Chapter 2, and we can calculate the kinetic and potential energies of CM. according to equations 2.1 - 2.11 in section 2.3, Chapter 2.

5.1.3 Results

Energy fluctuations in different modes of walking are presented in Figs 5.1 - 5.4. In Figs.5.1-5.4, the curves start at the left heel strike (LHS), then proceed through right toe takeoff (RTO), right heel strike (RHS) and left toe takeoff (LTO), finishing at the second left heel strike. Because the double support factor differs between modes of walking, the duty factor may also differ. On average, RHS is always at 50% of the cycle, as the right and left sides of the body can be taken to act symmetrically. In comfortable walking, RTO falls at a mean 7.5% and LTO 57.5% of a stride. In fast walking, RTO falls at 5% and LTO 55% of a stride. In slow and BHBK walking, RTO falls at a mean 10%, and LTO 60% of a stride (see also Swing factor [SF] in Table 5.1). Note that in Fig. 5.1.b. - 5.4.b., in order to compare changes in the two energies, the curves of KE, and PE have been moved to the coordinate system of the sum of the kinetic and potential energy, KE+PE.

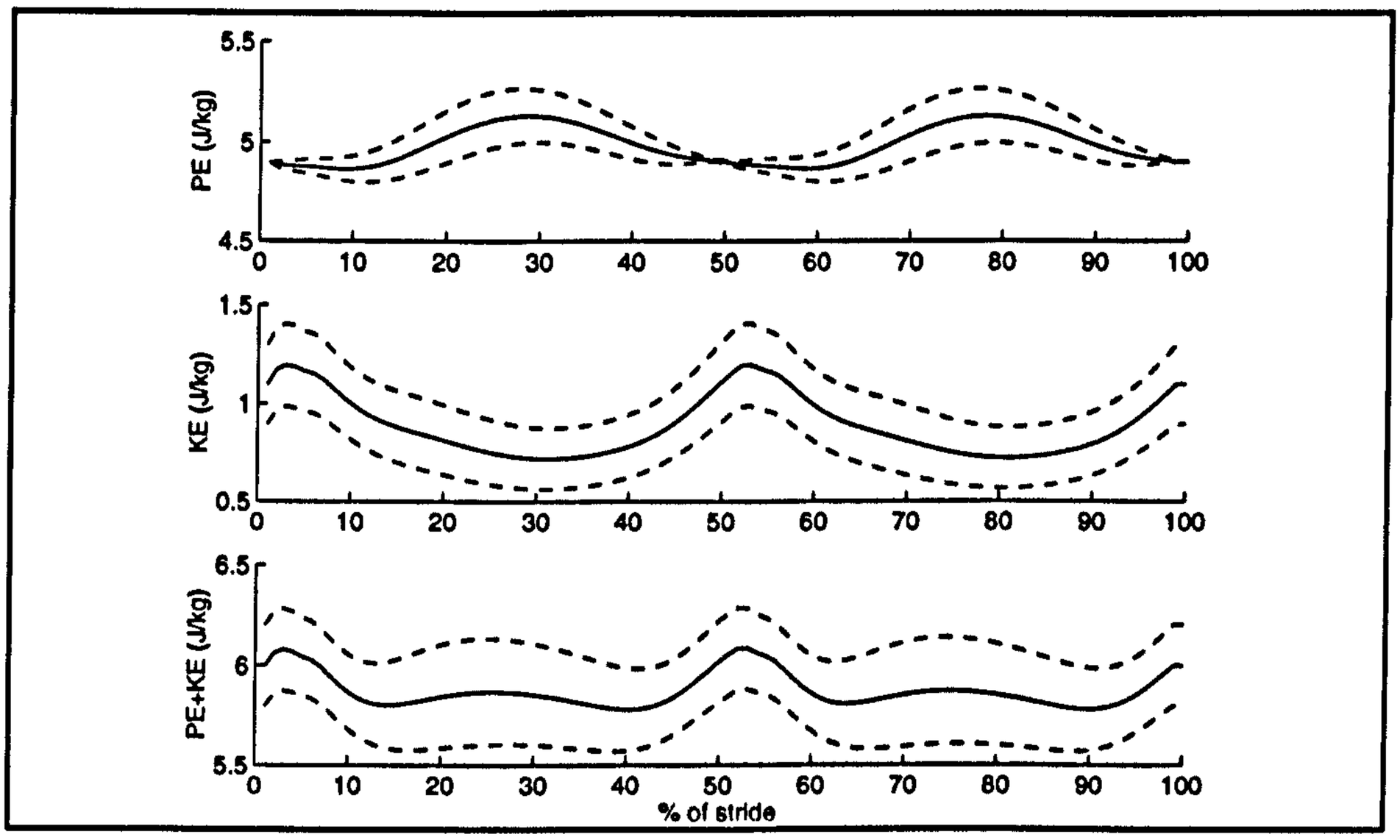

FIGURE 5.1.a Energy fluctuation in comfortable walking (N = 70 trials,- mean, -- mean ± sd)

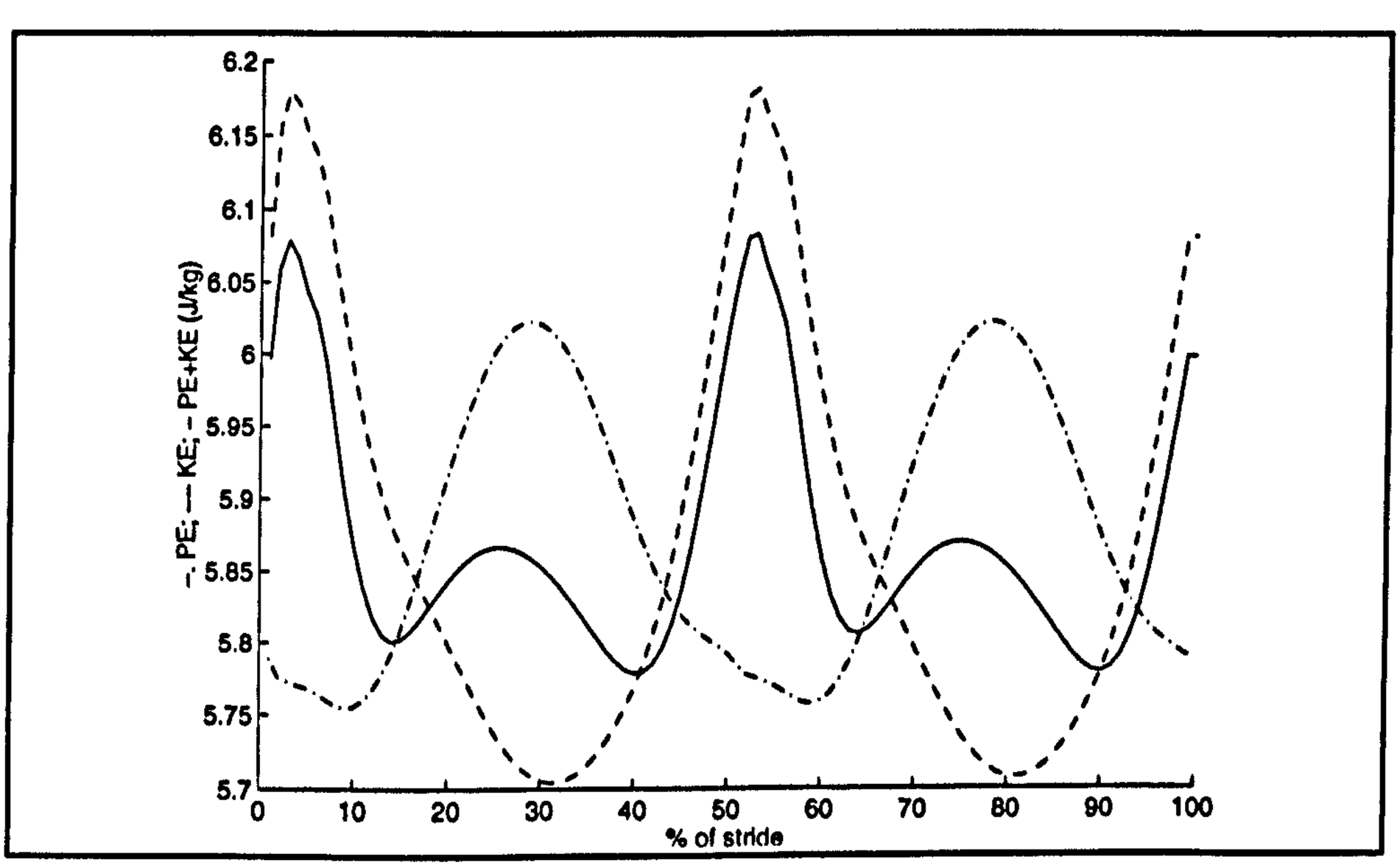

FIGURE 5.1.b The changes in KE, PE and the sum of PE+KE during comfortable walking. To compare three energies, PE and KE have been moved to PE+KE's coordination system.

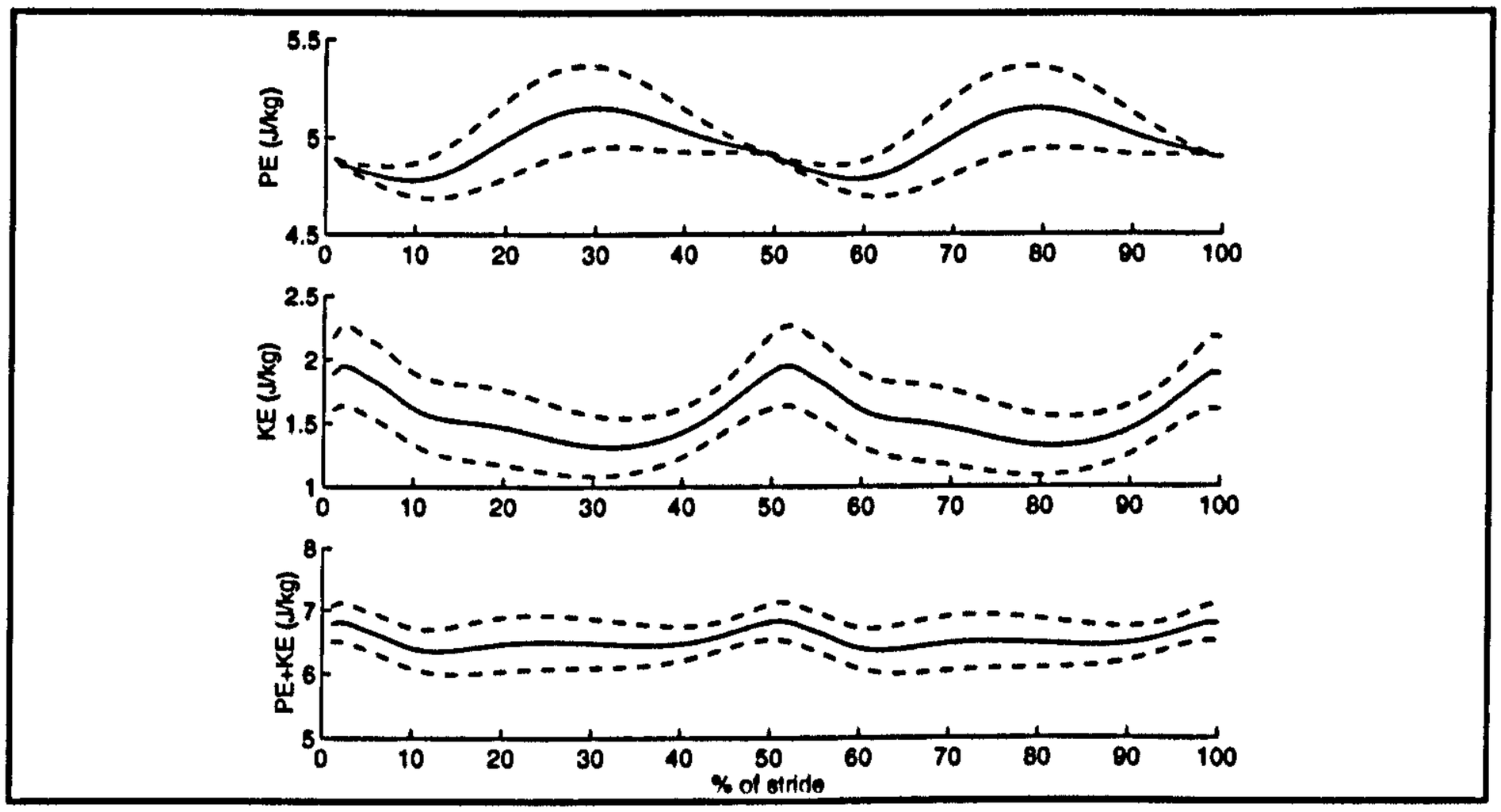

FIGURE 5.2.a Energy fluctuation in fast walking (N = 70, - mean, -- mean ± sd)

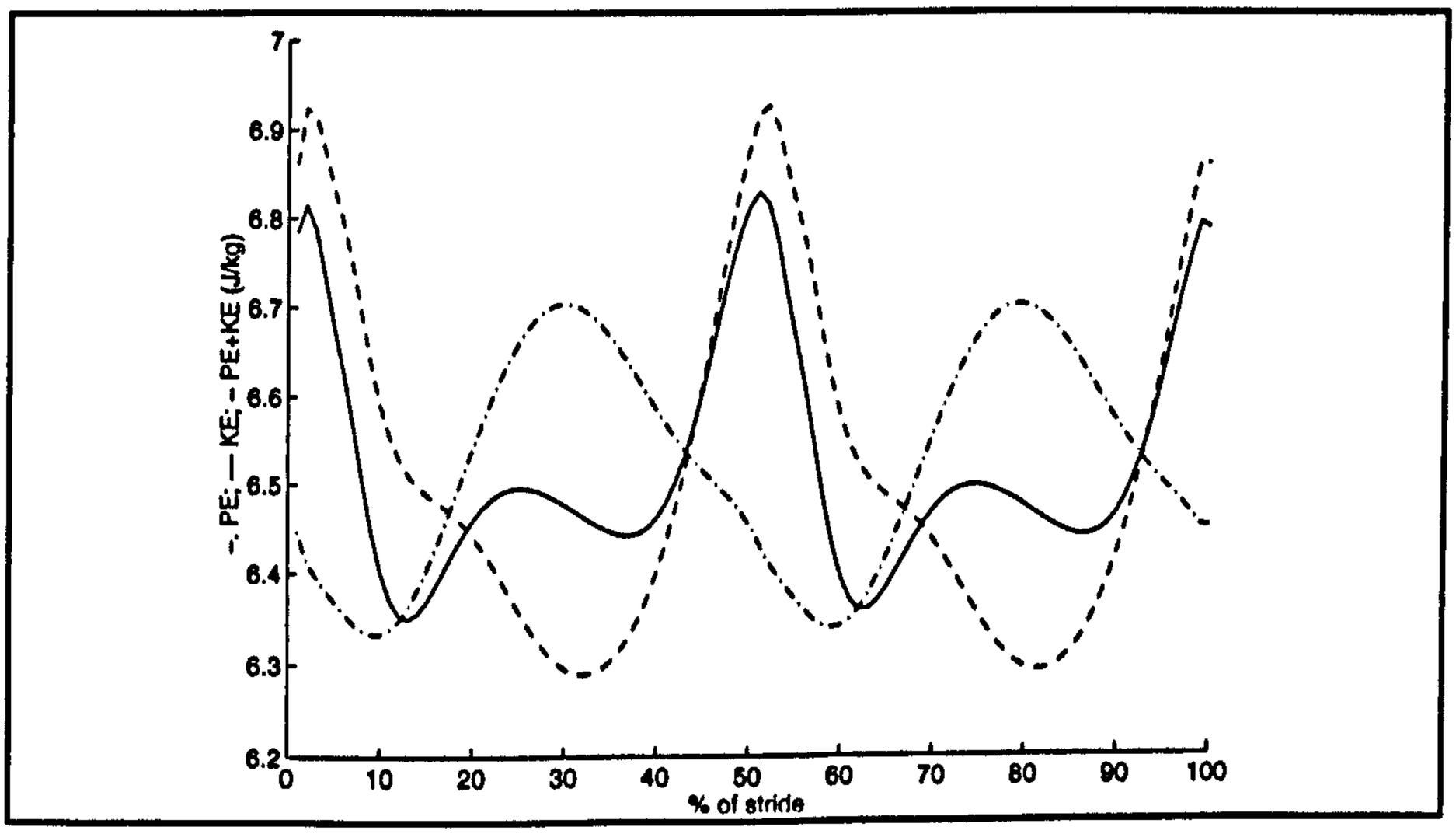

FIGURE 5.2.b The changes in KE, PE and the sum of PE+KE in fast walking. To compare three energies, PE and KE have been moved to PE+KE's coordination system.

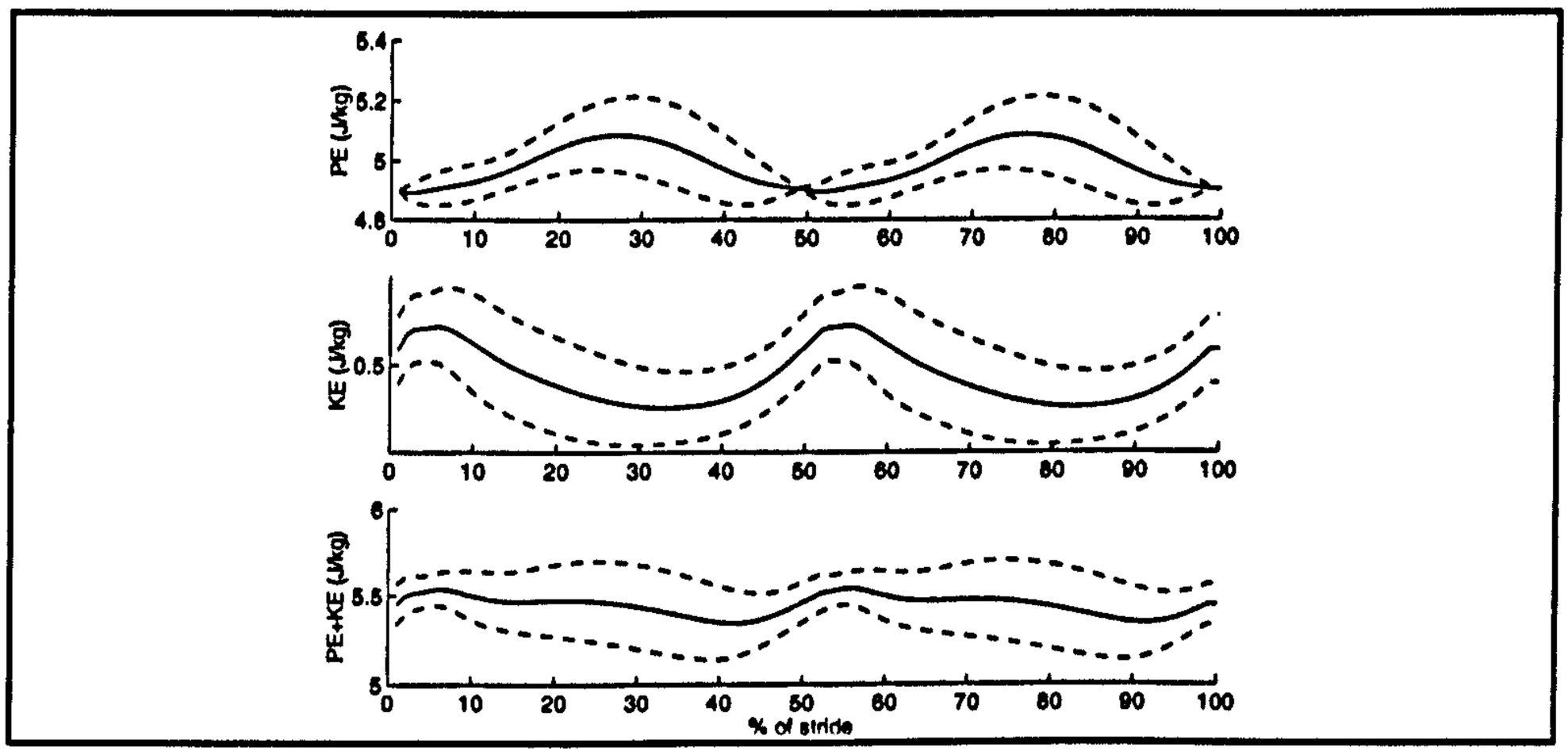

FIGURE 5.3.a Energy fluctuation in slow walking (N = 70,- mean, -- mean ± sd)

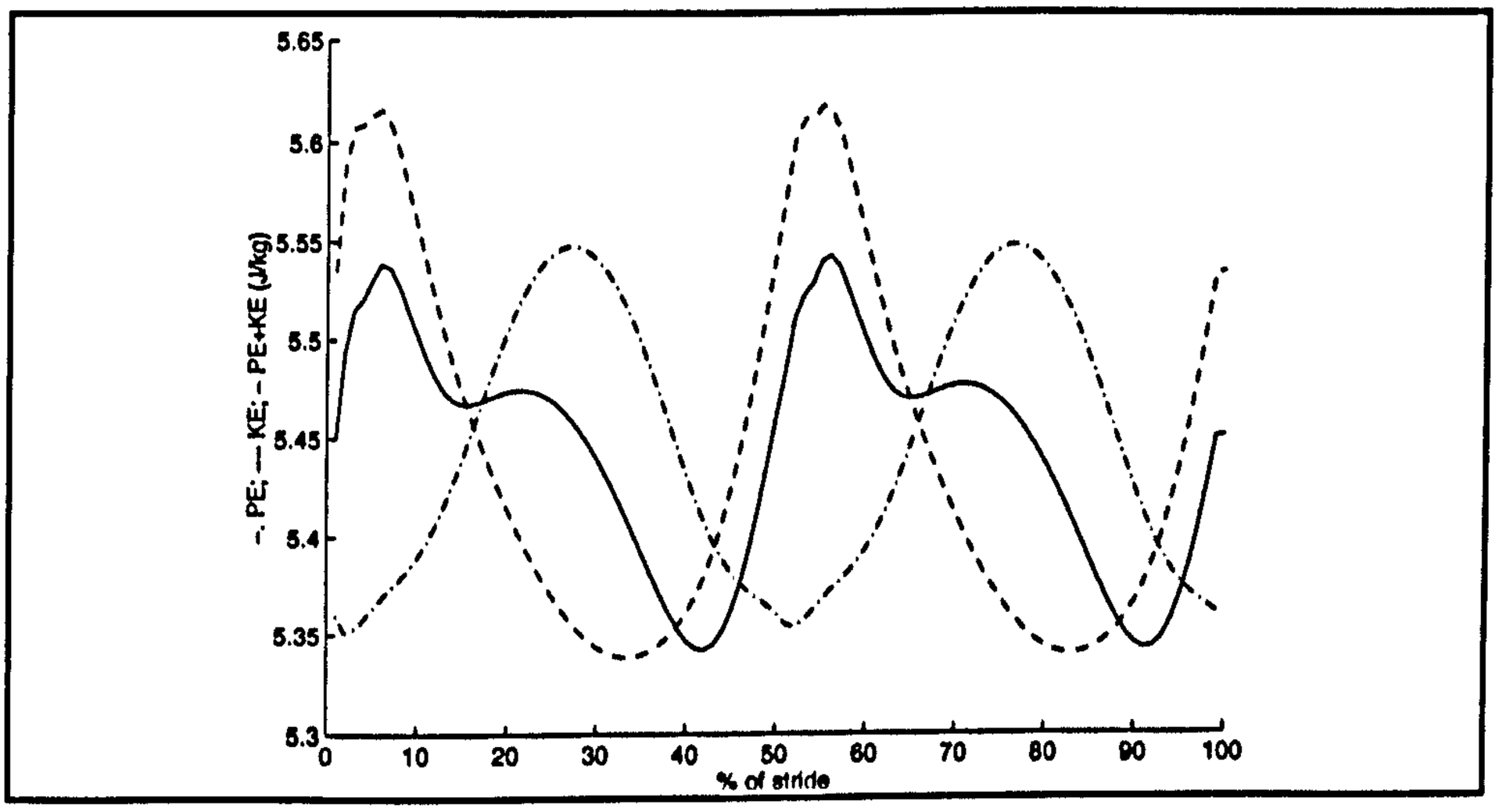

FIGURE 5.3.b The changes in KE , PE and the sum of PE+KE during slow walking. To compare three energies, PE and KE have been moved to PE+KE's coordination system.

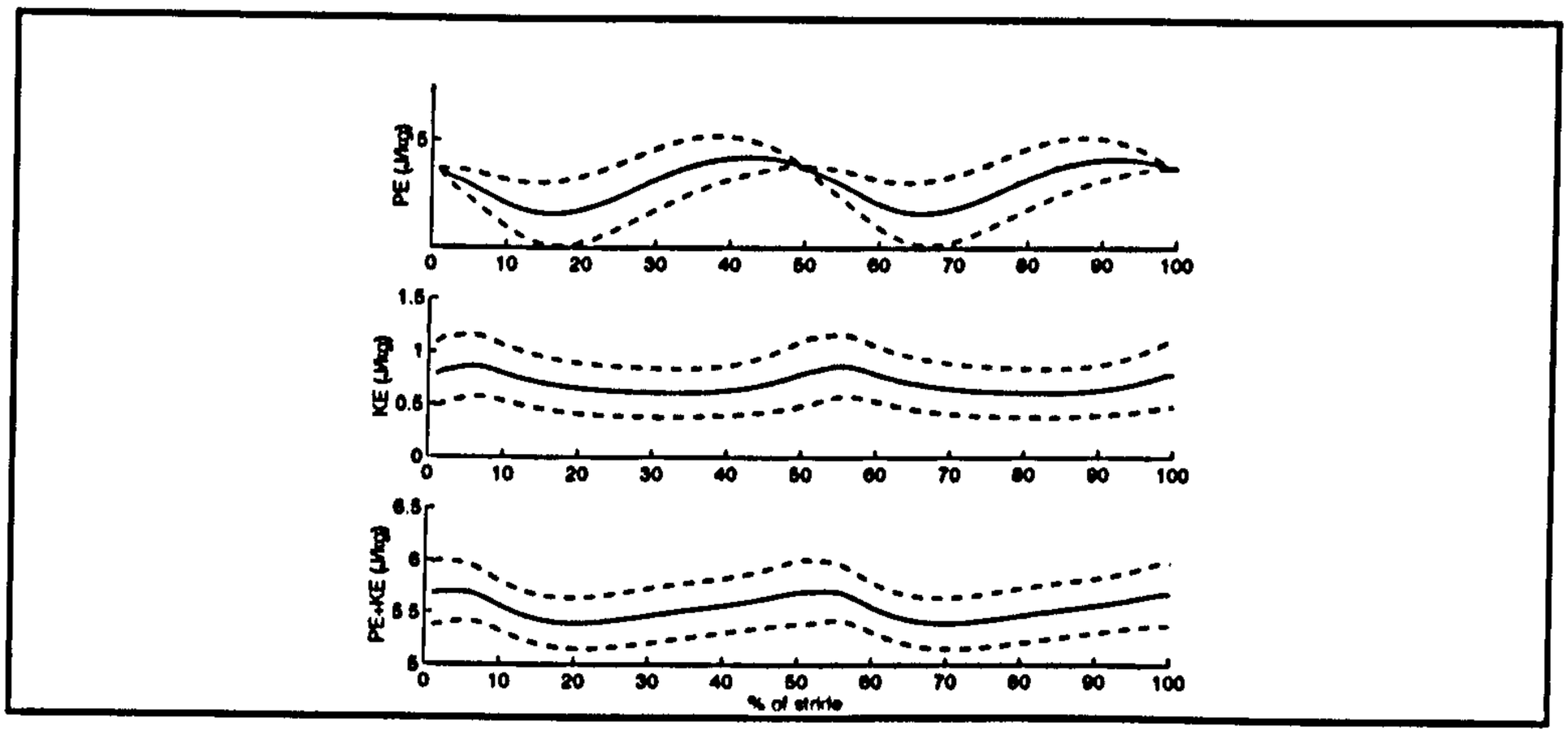

FIGURE 5.4.a Energy fluctuation during BHBK walking (N = 70,- mean, -- mean ± sd)

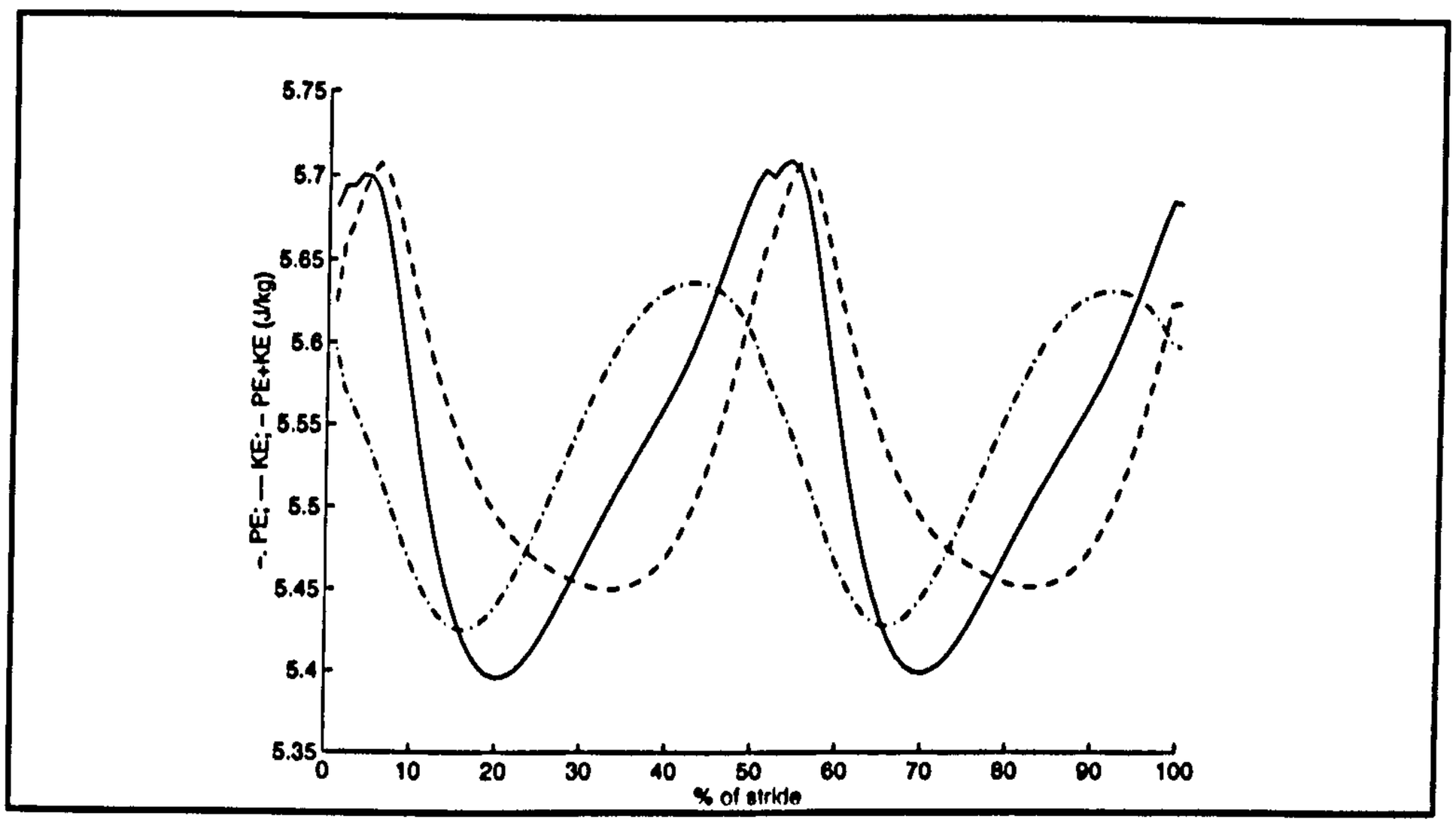

FIGURE 5.4.b The changes in KE, PE and the sum of KE+PE during BHBK walking. To compare three energies, PE and KE have been moved to PE+KE's coordination system.

At a glance, it is apparent that KE and PE in normal human walking tend to change alternately. In other words, KE increases while PE decreases and vice-versa. This condition may be described as energy transformation or energy exchange. In normal walking, the sum of the kinetic and potential energy, PE+KE, oscillates within a relatively smaller range than KE and PE (see Fig. 5.1.b-Fig. 5.3.b). But in BHBK walking, the range of KE+PE is similar to that of KE and PE (see Fig. 5.4.b).

Range of fluctuation of energy

To analyze the work done by the whole system (the body) for maintaining motion, the range of changes in energies, ΔE, was computed as follows.

$$\Delta E = \max(E) - \min(E) \qquad (5.1)$$

ΔE represents the work done by the body to maintain the motion of the whole body. E may represent KE, PE or KE+PE. The larger ΔE, the greater the work done.

Each form of ΔE has a different meaning. ΔKE, kinetic energy and ΔPE, potential energy, indicate the energy for maintaining motion. However, Δ(KE+PE) signifies the energy output by the body, in other words, Δ(KE+PE) is the work done by the body tissues.

A total of 280 trials were analyzed. The results are shown in Fig.5.1 - Fig.5.4 and listed in Table 5.1 and 5.2. Analysis of variance (ANOVA) for the above tables shows that the significance of all terms is $p<0.05$. The statistical results in detail are F_{VCM} 406.46,$F_{\Delta PE}$ 192.18,$F_{\Delta KE}$ 30.96, $F_{\Delta(PE+KE)}$ 41.77,F_{ϵ} 3.94 and F_{η} 16.80, $F_{0.05;(3,276)}$= 2.65.

5.1.4 Discussion

5.1.4.1 Calculated results for different modes of gait

It is obvious from Table 5-1 and figs.5-1.b - 5-3.b that there is energy transformation during human normal, slow, comfortable and fast walking. In other words, KE increases while PE decreases, and vice-versa. Because energy exchange exists, human expend less total energy Δ(KE+PE) (the range of change of the sum of the kinetic and potential energies) to produce greater energetic effectiveness, ΔKE and ΔPE. This result is completely in agreement with Cavagna et.al (1976), though our approach is different from theirs. It is also very clear that there is little energy exchange in human BHBK walking (Fig 5-4.b). Since energy exchange is so small, human BHBK walking must expend more energy Δ(KE+PE) for less effectiveness in motion, ΔKE and ΔPE (see Table 5.1).

It may be meaningless to compare directly the change of the kinetic and potential energies, ΔKE and ΔPE in different modes of walking, since ΔKE and ΔPE of any subject vary proportionally with the velocity of CM. Moreover, as the velocity of CM in BHBK walking is relatively smaller, so ΔKE, and ΔPE are also smaller than others (see Fig.5.5 and Fig.5.6). However, Δ(KE+PE) seems to be different from ΔKE and ΔPE.(Fig.5.7) . From Fig.5.7, although the VCM is not high in BHBK walking, Δ(KE+PE) is rather large (also see Table 5.1).

To compare the effects of the energy transformation of different walking, we define two coefficients. One is

$$\epsilon = \frac{\Delta KE + \Delta PE}{\Delta(PE+KE)} \qquad (5.2)$$

where, ΔKE and ΔPE are the range of changes in kinetic energy and the range of changes in potential energy respectively, and Δ(KE+PE) is the range of changes of

TABLE 5.1 Comparison of the effects of the energy transformation in different modes of walking

	SF	VCM(m/s)	ΔKE(J/kg)	ΔPE(J/kg)	Δ(KE+PE)(J/kg)
BW	0.3900	1.2261±0.23	0.2801±0.10	0.2548±0.12	0.3883±0.16
FW	0.4500	1.9329±0.14	0.6475±0.15	0.4175±0.13	0.5204±0.13
SW	0.3950	1.0388±0.11	0.3130±0.05	0.2650±0.09	0.2944±0.10
CW	0.4250	1.4703±0.13	0.4850 ±0.08	0.3075±0.10	0.3529±0.09

Note:

1.BW - BHBK walking; FW - fast walking;, SW - slow walking; CW - comfortable walking

(N = 70 trials each)

2.SF - swing factor, the proportion of swing time and total cycle time;

the sum of the kinetic and potential energies.

ϵ is a dimensionless parameter representing the effect of energy transformation. The larger it is, the greater the energy exchange. From the function (Tables 5.1 and 5.2), ϵ for comfortable walking is largest, 2.4790 and therefore comfortable walking is optimal. ϵ for fast and slow walking is almost the same, at about 2.2. In contrast ϵ is smallest in BHBK walking, 1.5241 (Table 5.2). It can be observed that the ϵ parameter for BHBK walking is rather smaller than for other modes (Fig. 5.8).

To evaluate the effect of energy exchange on the velocity of the centre of mass, we have defined another coefficient as follows.

$$\eta=\frac{VCM}{\Delta E} \qquad (5.3)$$

where VCM is the average velocity of CM and ∆E is the range of change the

TABLE 5.2 Comparison of effects in different modes of walking (N = 70 trials each)

	VCM	∆KE	∆PE	∆(PE+KE)	η	ϵ
BW	1.2261±0.23	0.2801±0.10	0.2548±0.12	0.3883±0.16	3.7638±1.70	1.5241±0.58
FW	1.9329±0.14	0.6475±0.15	0.4175±0.13	0.5204±0.13	4.0075±1.23	2.2014±0.80
SW	1.0388±0.11	0.3130±0.05	0.2650±0.09	0.2944±0.10	3.9041±1.24	2.2002±0.87
CW	1.4700±0.13	0.4850±0.08	0.3075±0.10	0.3529±0.09	4.5449±1.49	2.4790±0.99

(Abbreviations as for Table 5.1)

Note:

1.BW,FW,SW,CW: bent-knee walking,fast walking,slow walking and comfortable walking;

2.VCM:velocity of the centre of mass ;

3.∆KE,∆PE and ∆(KE+PE):the changed ranges of the kinetic energy, the potential energy and the sum of the kinetic and potential energy.

4. η=VCM/∆(PE+KE);

5. ϵ=(∆KE+∆PE)/∆(PE+KE).

energy.

In this investigation, VCM is calculated from the length of a stride divided by its time duration, and ΔE is the range of change of the sum of the kinetic and potential energy, Δ(KE+PE). η expresses the per unit energy effects on the velocity of CM. In fact, as E is calculated from the energy per unit mass, η has similar meaning to the general expression E/(mass*g*v) (Alexander and Goldspink 1975). Therefore η is comparable among different modes of walking. The larger η, the better the effect. Among all modes of walking the largest value, 4.5449, is for comfortable walking, and the smallest, 3.7638, is for BHBK walking (Table 5.2 and Fig. 5.9). The η for comfortable walking is more than 1.2 times that for BHBK walking.

5.1.4.3 Influence of positive or negative energy

TABLE 5.3 Analysis of variance (ANOVA) of data from Tables 5.1 and 5.2

	F	k	P
VCM	406.46	0.077	<0.05
ΔPE	192.18	0.049	<0.05
ΔKE	30.96	0.054	<0.05
Δ(PE+KE)	41.77	0.060	<0.05
ϵ	3.94	0.696	<0.05
η	16.80	0.401	<0.05
new_recovery	19.90	0.096	<0.05

Note:
1.$F=s1^2/s2^2$(see general statistics texts)
1.$F_{0\,05;(3,276)}=2.65$;
2.$k=k*(s2^2/n)^{0.5}$ used to decide the distance between groups (see Bowker,1959 p.298)

If we explore the meaning of the two coefficients ϵ and η something interesting may be found. Firstly, if we consider the change of negative energy (regarded as the absorption and storage of energy in biological tissues, e.g., muscles), we may introduce a proportional coefficient k ($0<k<1$), so that ΔE may be redefined as $\Delta E(1-k)$. When all negative energy is absorbed, k reaches a maximum and $\Delta E(1-k)$ a minimum. If we assume that all biological organisms have the same function of absorption and storage, k should be a constant for all forms of energy at a given time, including KE, PE and KE+PE. Under this assumption, ϵ in the function (5.3) is still correct:

$$\epsilon = \frac{\Delta KE(1-k)+\Delta PE(1-k)}{\Delta(PE+KE)(1-k)} = \frac{\Delta KE+\Delta PE}{\Delta(PE+KE)} \qquad (5.4)$$

Therefore, the function (5.3) cannot be influenced by the positive or negative signs of the energies.

Coefficient η has a special physical meaning. Its unit is 1/(mass*velocity). In other words, it expresses the degree of the change of mv (mass x velocity). The larger it is, the smaller mv. The body obtains a maximum forward velocity for the minimum mv change in 'comfortable' walking. This would explain why humans choose 'comfortable' walking as their usual mode.

We may conclude that 1) human normal walking is energetically better than human BHBK walking; 2) comfortable walking is, energetically, the best of the three speeds.

What are the main reasons which lead to the differences in the various modes of walking? We can usefully seek them in the GRFs exerted during gaits of normal subjects.

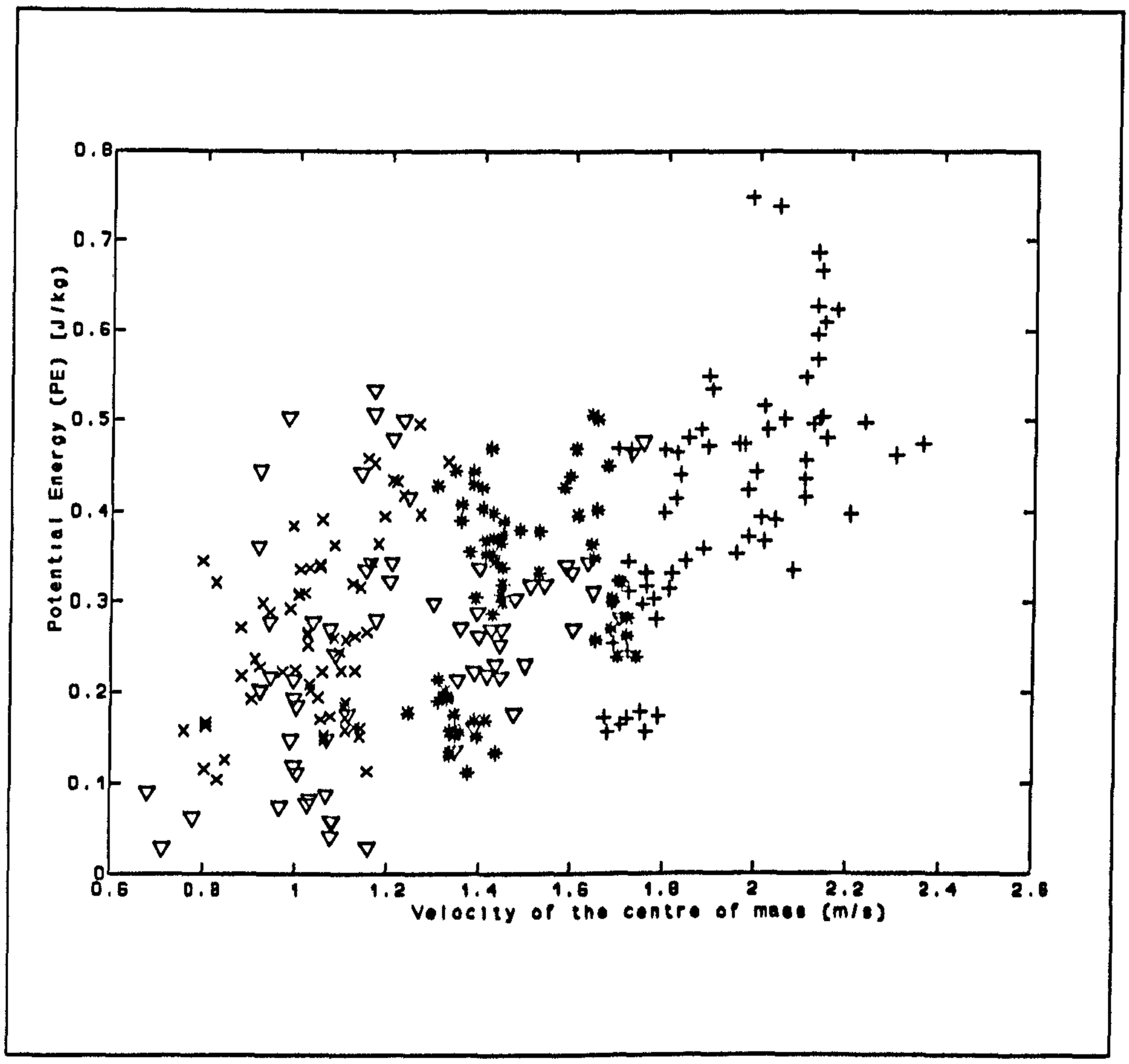

FIGURE 5.5 Comparison of the Δ(PE) of different modes of walking, where x - slow, * - comfortable, + - fast and ∇- BHBK.

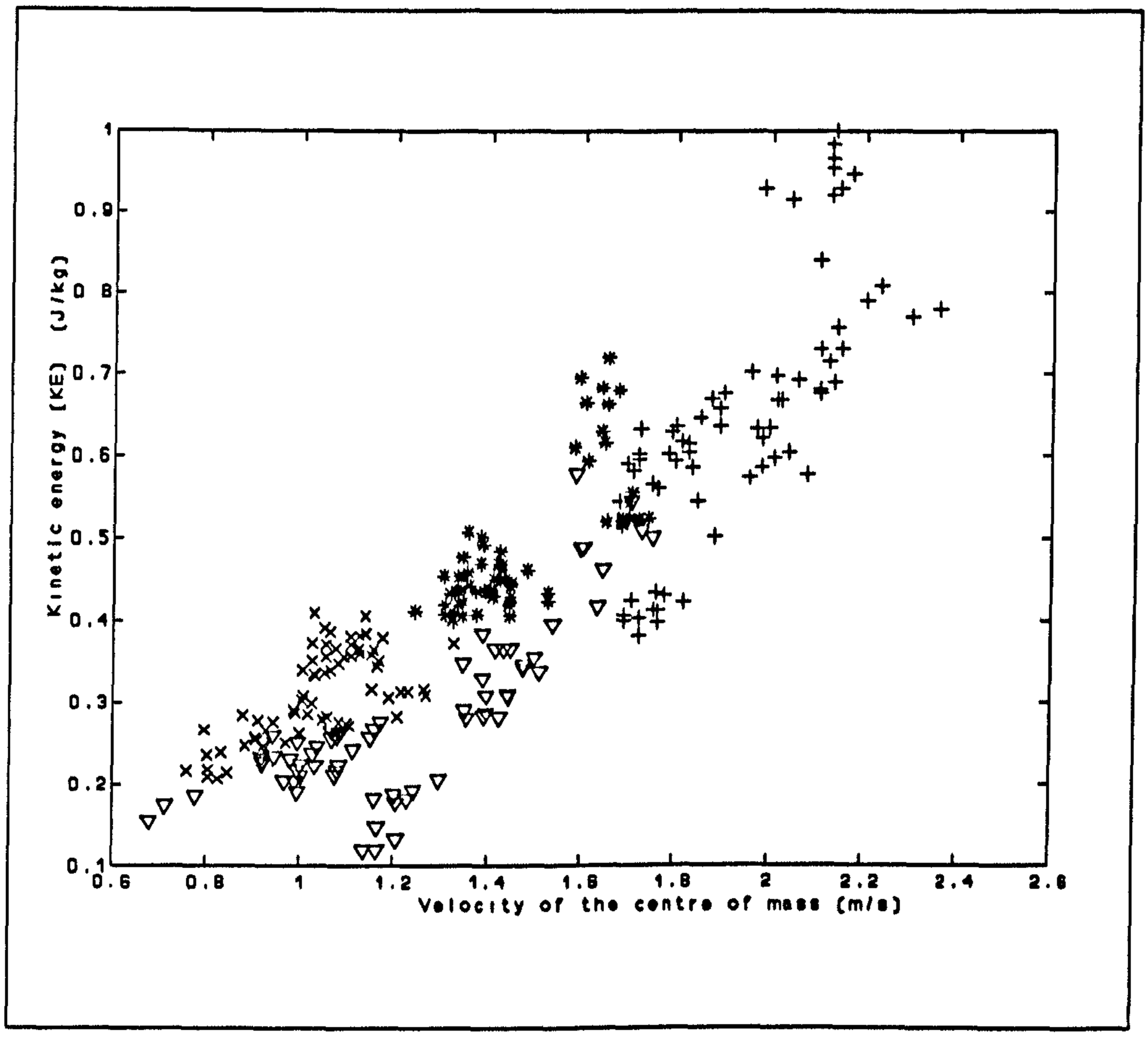

FIGURE 5.6 Comparison of the Δ(KE) of different modes of walking, where x - slow, * - comfortable, + - fast and ∇- BHBK.

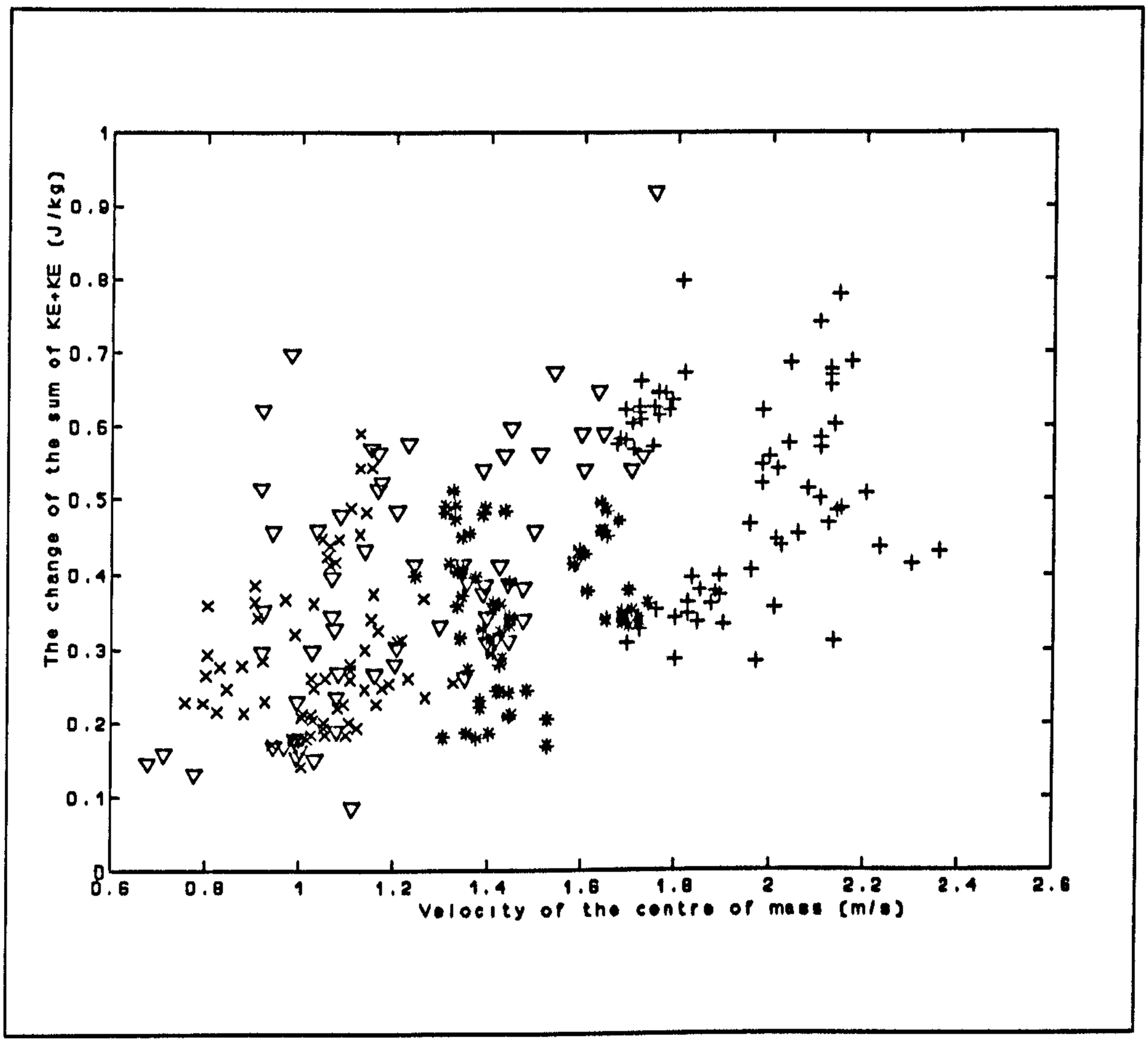

FIGURE 5.7 Comparison of the Δ(PE+KE) of different modes of walking, where **x** - slow, ***** - comfortable, **+** - fast and ∇- BHBK.

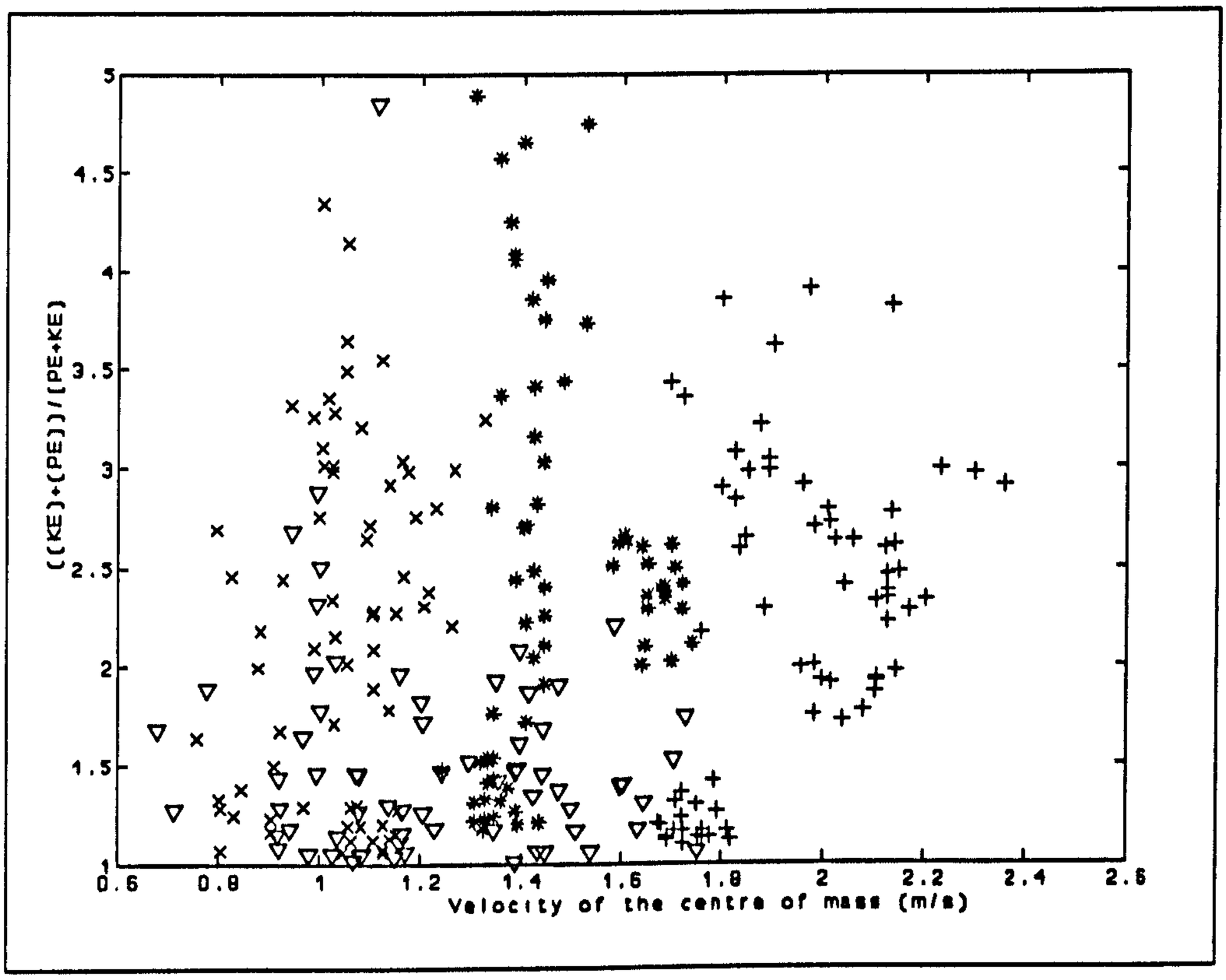

FIGURE 5.8 Comparison of the ε of different modes of walking, where x - slow, * - comfortable, + - fast and ∇- BIIBK.

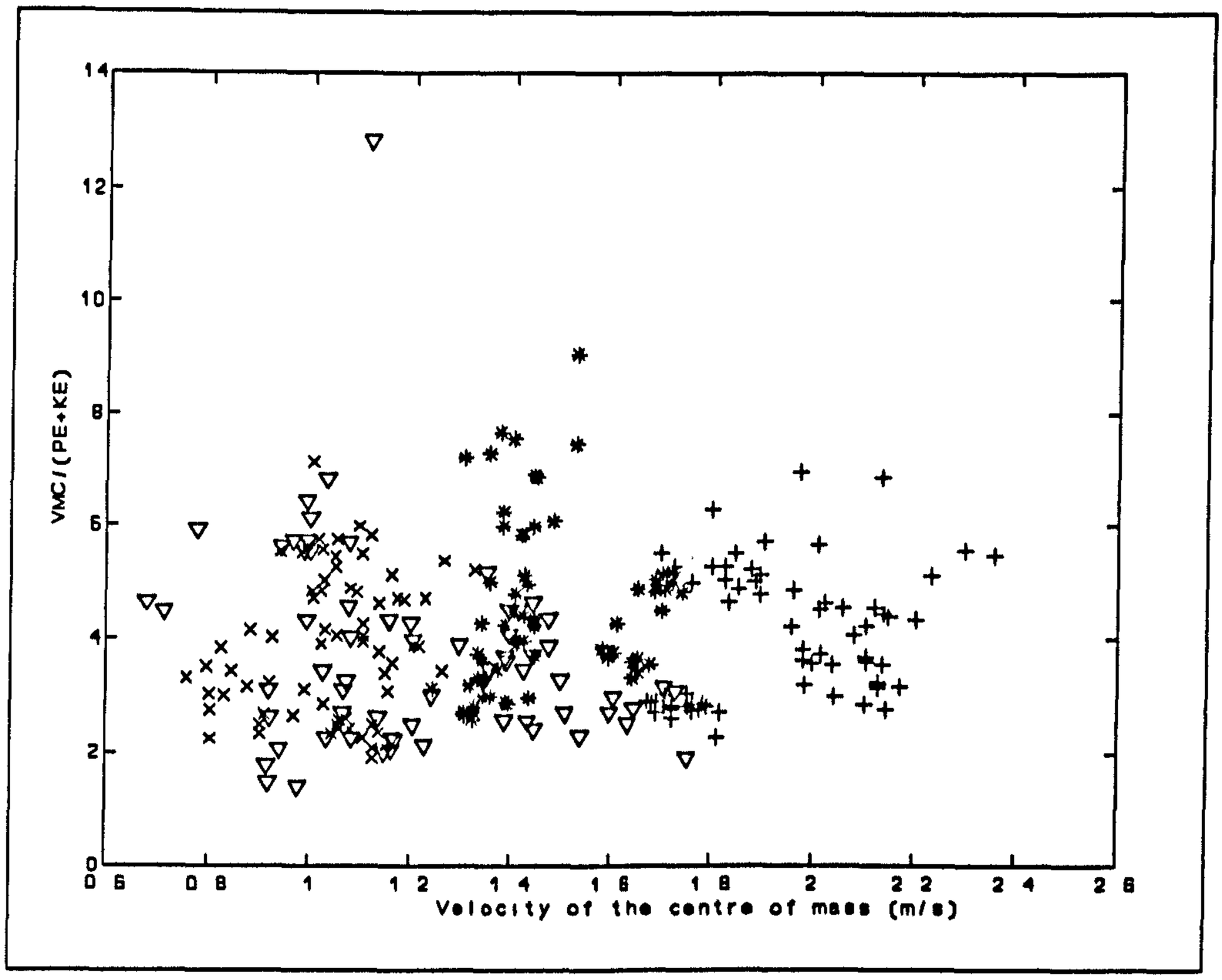

FIGURE 5.9 Comparison of the η of different modes of walking, where **x** - slow, * - comfortable, + - fast and ∇- BHBK.

5.1.4.4 Possible reasons for differences in energy transformation

There are two factors which may influence energy transformation during walking. One is the shape of the vertical force curves. With the depression in mid-stance portion of the vertical forces, the whole body acceleration in the vertical direction decreases to make the body CM rise, which may transfer kinetic energy into gravitic potential energy (see Fz for comfortable and fast walking in Fig.5.10). But this may not be the main factor, since the shape change in vertical force is the greatest in fast walking, but the energy transformation in fast walking is not optimal.

Another important factor is the phase relationship between KE and PE. When the sagittal force changes from negative to positive, the forward acceleration changes from negative to positive (see Fy GRFs in Fig. 5.10). Thus, the velocity of the body CM always reaches a minimum at mid-stance. On the other hand, when the vertical force reaches a minimum, the displacement of the body CM reaches its maximum. In normal (erect) walking, the kinetic energy reaches a minimum and the potential energy reaches a maximum at the same time (see Figs. 5.1.b to 5.3.b). Therefore energy transformation is rather good in normal walking. But in BHBK walking, the change in the two energies does not occur at a suitable phase. Since in BHBK walking the minimum vertical force occurs in the later part of stance, not at mid-stance, the maximum potential energy also occurs in the later part of stance (see BHBK walking in Figs. 5.4.b and 5.10).

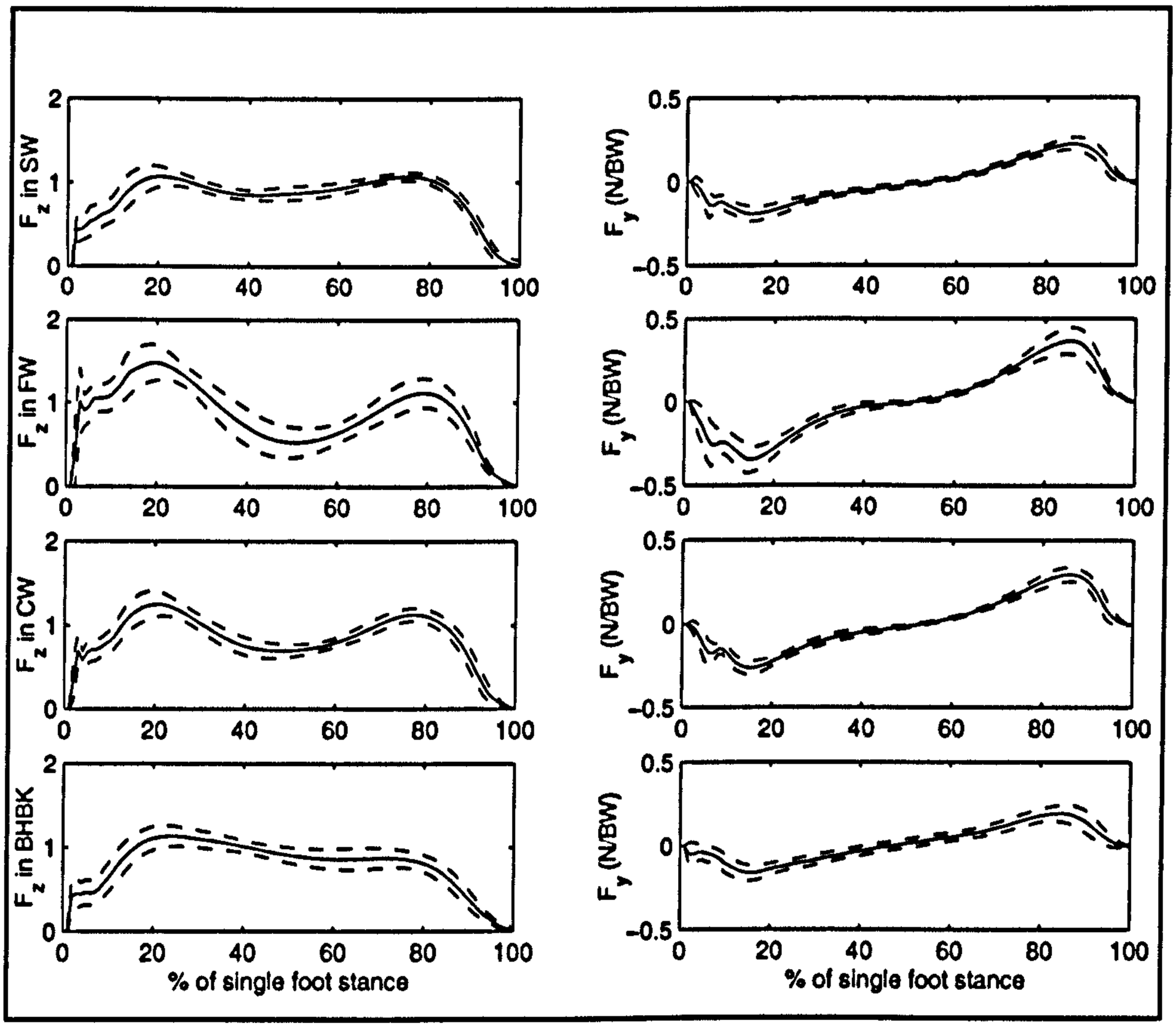

FIGURE 5.10 Comparison of the GRFs in different modes of walking (N = 70 for each mode, - mean,-- mean ± sd), where BW- body weight.

5.1.4.5 Comparisons with the literature

Let us compare the results of this paper with those of other authors. Zarrugh (1981) found that 1.7 m/s is the most effective velocity for a subject, while Cavagna et al. (1976) determined the most effective velocity to be 1.1 m/s in terms of recovery of work. This chapter reports an optimum velocity of 1.47 m/s, if 'comfortable' velocities are averaged. It is difficult to say which of the three alternatives is most correct, since every method has its special characteristics. Considering that the subjects in this research were normal people in general life roles, we feel that 1.5 m/s might be a suitable value.

Kimura (1996) found that 'recovery' in common chimpanzees increases with maturation: adult chimpanzees (> 5 year olds) have better recovery than infants. His calculations gave recoveries in the range 10-60%, commonly 30%, close to those of humans (as in Cavagna et al. 1976). If recovery in quadrupedal running was not greater than that in bipedal walking, chimpanzees might have been expected to select the latter motion a long time ago, given the same ecological needs as hominids. However, the recovery decreases with the velocity of the CM, e.g., 40% at 0.5 m/s to 20% at 1 m/s, so that chimpanzees only walk effectively at lower speeds. Kimura stresses the ability to maintain extended hindlimbs as a vital basis for energy economy in bipedal walking. From our results, and in my opinion, the mode of walking may be a more dominant factor. Although humans have strong hindlimbs which can be maintained in extension more or less indefinitely, they get little better energy transformation in BHBK walking than do chimpanzees.

5.1.4.6 A new 'recovery'

In order to compare our results with those of Cavagna and other authors, we may define

'recovery ' as:

$$recovery_n = \frac{(\Delta PE + \Delta KE) - \Delta(PE + KE)}{(\Delta PE + \Delta KE)} \quad (5.5)$$

where all components are defined as previously.

With data from Table 5-1, we obtain recovery$_n$ of 55.47% for comfortable walking; 51% for fast walking; 49% for slow walking and 27.41 for BHBK walking, in agreement with Cavagna (1976) and Kimura (1996).

5.2 Comparison of chimpanzee bipedalism and human walking

Using the chimpanzee GRFs presented in Chapter 3 and the above method, it appears that energy transformation of the CM is nearly absent in our chimpanzee (Table 5.5. and Fig. 5.11). On the other hand, energy transformation in both human erect and BHBK walking are better than that of our chimpanzee (Figs. 5.1.b - 5.3.b). To compare the effect of energy transformation, we modified the method of Cavagna et al. (1976) to compute energy recovery as equation 5.5. The results (Table 5.4) show that human upright walking is the best of the modes of walking examined.

Kimura (1996) observed that chimpanzees do obtain partial energy transformation in bipedal walking, at least as adults and at slow speeds. But in general, upright walking has better energy exchange than does BHBK walking. We may surmise

TABLE 5.4 Comparison of energy transformation in chimpanzee and human walking

	VCM (m/sH)	DCM (m/H)	ΔPE (J/kg)	ΔKE (J/kg)	ΔPKE (J/kg)	RC %
CW	1	0.816	0.172	0.559	0.726	8
BW	0.625	0.800	0.254	0.280	0.388	37
NW	0.850	0.918	0.417	0.647	0.520	51

Note:

CW: N=1; NW: N = 20; BW: N=20.

VCM: velocity of the centre of mass /H;

DCM:distance of the centre of mass /H;

H: stature;

RC:recovery = ((ΔPE+ΔKE)- ΔPKE)/ (ΔPE+ΔKE);

that our chimpanzee was less effective in bipedal walking than Kimura's because she was not trained to walk upright, and therefore uses a BHBK mode, which limits joint motion range and results in worse biomechanical effects.

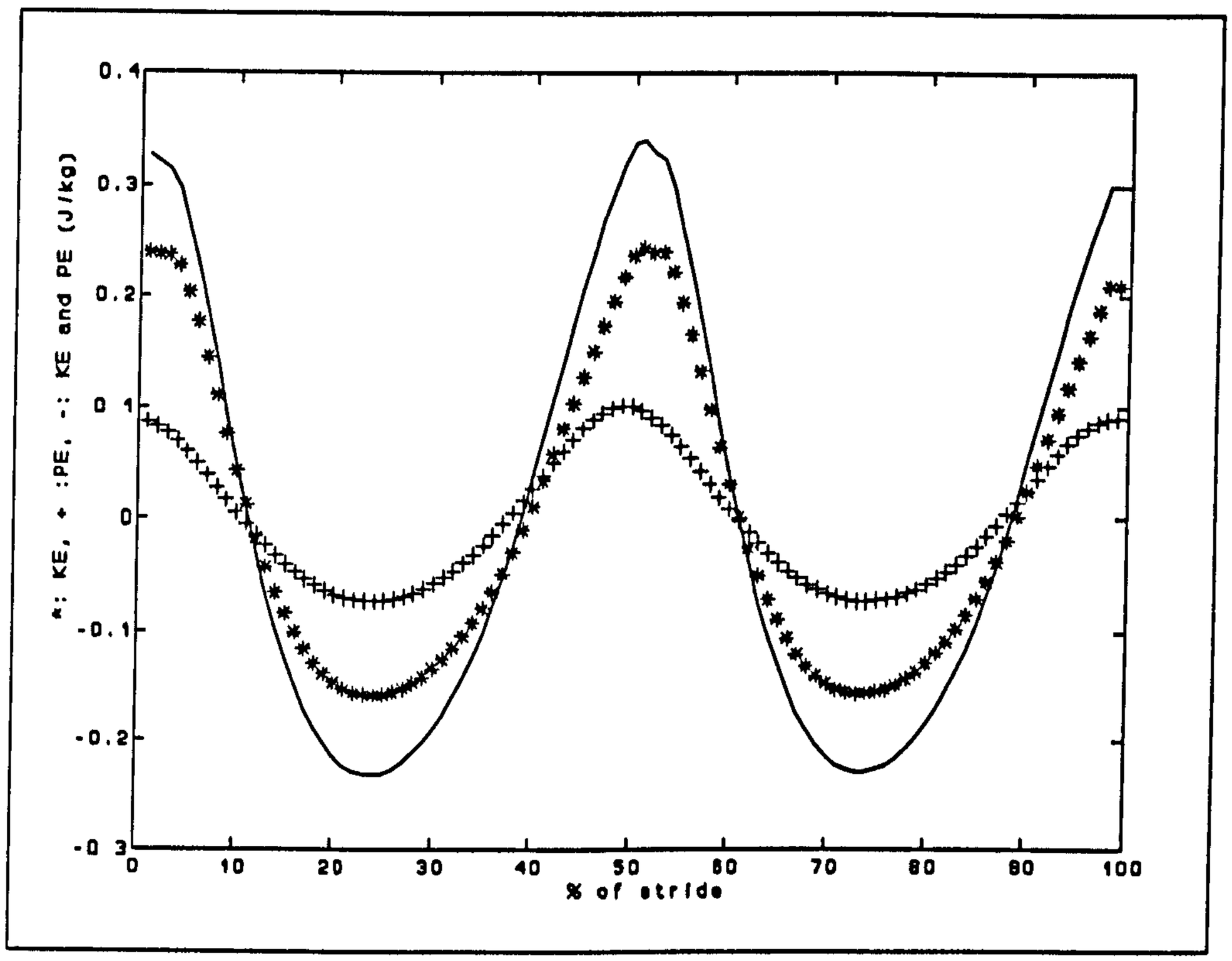

FIGURE 5.11 Energy transformation in chimpanzee bipedal walking, where * : KE, +- : PE, and - : the sum of KE and PE.

5.3 Conclusions

We may confidently conclude that human erect walking is considerably more effective in terms of energy transformation than BHBK walking, while comfortable walking is the best of all erect modes of walking. Finally, according to the method of this paper, the optimal walking velocity may be about 1.5 m/s.

The results of this section support the proposition that if early hominids used to walk BHBK, selection would act strongly in favour of its replacement by erect walking, to decrease energy expenditure. From the perspective of energy transformation, dynamic effects in chimpanzee walking are far worse than in both human upright walking and human BHBK walking. Thus, we would expect that if there was a stage in which human ancestors walked like modern chimpanzees, selection would favour adoption of more human-like BHBK walking or upright walking.

CHAPTER 6. WORK DONE DURING BIPEDALISM

Moderation is a virtue

Confucius

6.1 ABSTRACT

The goals of this section were twofold: 1) to compute work done in different modes of walking, and 2) to investigate a fundamental concept in biomechanics: the meaning of positive and negative signs for work, power and energy. I calculated different forms of work and power using two different approaches: particle mechanics and joint dynamics. In BHBK walking, positive work done was always larger than negative work done. If positive work done is considered as the effort output from the body to power walking, it may be concluded that BHBK walking expends more work done than does normal upright walking. It is suggested that positive and negative work may play a different functional role in both modes of walking.

6.1 Introduction

Work, power and energy are so important that they are often used as criteria for evaluation of motion and for building principles of motion. Thus the meaning of their signs has considerable significance for the interpretation of results of calculations. Taking the case of level bipedal walking (or any cyclical/endurance motion, such as running, cycling or rowing), if total work is assessed by the sum of positive work (PW) and negative work (NW), such total work may be small or nil. Should we conclude from this that the human body has done no work ? Of course not. But how then should we interpret sign in biomechanics?

Many authors (eg. Cappozzo, 1975; Alexander 1977, 1980, 1984; Apkarian 1989;

Winter 1979, 1983, 1988 and 1990; Williams and Cavanagh 1983; Schenau and Cavanagh 1990) have argued that in biomechanics both positive work and negative work should be considered as work done by the body, and have therefore calculated work and power in terms of absolute values. Whatever activity is being performed, energy will always be expended: when a man walks down stairs, consumption of oxygen can still be recorded. This concept has been widely employed in explanations of different effects of motion. Some authors (Zarrugh 1981; Cavagna et al. 1976 and 1977) consider only the positive component of energy changes. Others (such as Eng and Winter 1990) divided work done into two components: generated and absorbed. Various definitions of positive work and negative work are available (McMahon 1984 and 1985), and physiological studies (Taylor et al. 1980, 1985; Cavagna et al. 1976 and 1977) have determined the relationship of velocity and metabolic work. Whatever definition of positive and negative sign is used, calculated mechanical work and powers are never completely in agreement with physiological data.

If we consider positive and negative work or powers to have the same sign, their physical meaning should be the same. In fact, positive and negative work express completely different phenomena, at least in terms of the direction of effect of forces. As some authors have put it, negative power indicates absorption and storage of energy (Winter 1983; Eng and Winter 1995) and negative work done includes phenomena similar to the braking of a car (Alexander 1980). Moreover, when positive and negative powers are considered in terms of absolute values, their total may be rather too large. Sometimes it may be even larger than metabolic values, which latter should reflect the real energetic expenditure of organisms.

This section endeavours to review the problems outlined above, with reference to data from a large series of experiments, mainly concerning humans walking in different modes. We calculate different forms of work and power from two alternative perspectives: considering the entire body as a particle; or considering the joints as the source of drive.

6.2.1 Subjects and methods

The subjects and experiments were described in Chapter 3. Methods for calculation of work done was shown in section 2.3, Chapter 2.

To determine the meaning of the sign of power and work, we calculated each in different forms. Firstly, particle mechanics is used in computation of work done on the centre of mass (CM). In this approach, the whole body is treated as a system, the composition of which is unknown, and to investigate which we can only observe its external responses. Thus, we estimate work done about the system according to equations 2.3- 2.9. In other words, once we obtain GRFs, we can calculate accelerations, velocities, displacements and work done using particle mechanics.

Calculations of joint power were described in 2.2, Chapter 2 and Chapter 4. Joint powers were calculated for the lower limb joints since their sign will influence our understanding of mechanical effects in walking. Joints, forces and directions for the sagittal plane are shown in Fig. 2.1.

The method of calculation of powers is that in Winter (1990) and standard engineering texts book (see equations 2.1-2.3).

To facilitate interpretation of the meaning of positive and negative signs, all forms of work done and powers were then calculated and compared.

6.2.2 Results

Results for work done during different modes of walking are shown in Fig. 6.1- 6.2 and Table 6.1.

TABLE 6.1 Comparison of work done in forward direction in different modes of walking.

	Work done (J/kg)							
modes	ch	sl	no	fa	b	e	bb	be
PW	0.721	0.515	0.965	1.659	0.996	0.357	1.025	0.326
NW	-0.438	-0.446	-0.897	-1.360	-0.089	-0.612	-0.001	-0.548

ch = walking like chimpanzee; sl = slow normal walking; no = normal walking at a comfortable speed; fa = fast normal walking; b = acceleration from standing; e = deceleration to standing; bb = flexed-knee acceleration from standing; be = flexed-knee deceleration to standing; PW = positive work done; NW = Negative work done.

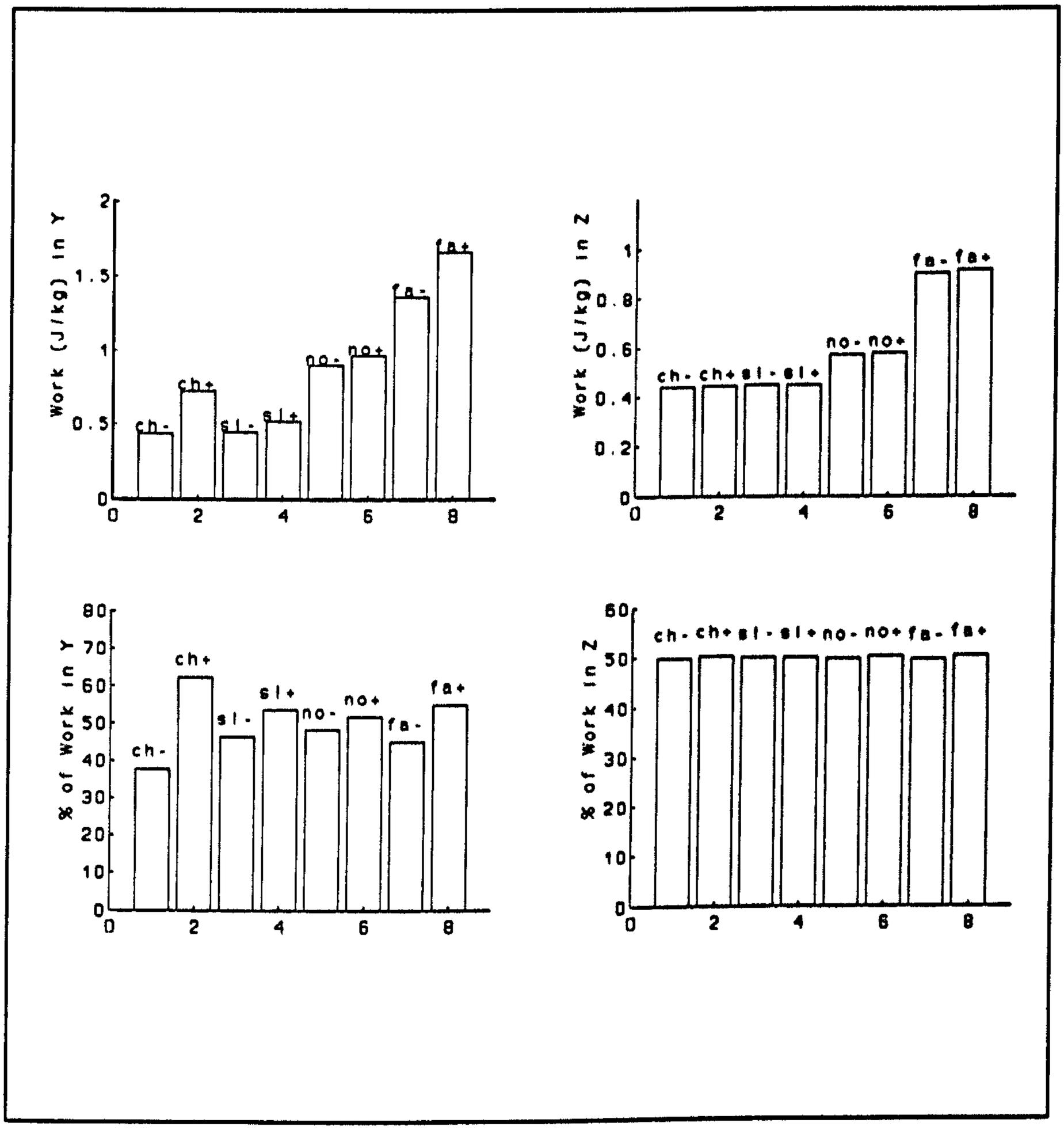

FIGURE 6.1 Comparison of work done in different modes of walking.

FIG. 6.1 Note: ch = walking like a chimpanzee; sl = slow normal walking; no = normal walking at a comfortable speed; fa = fast normal walking. + or - = positive or negative work done.

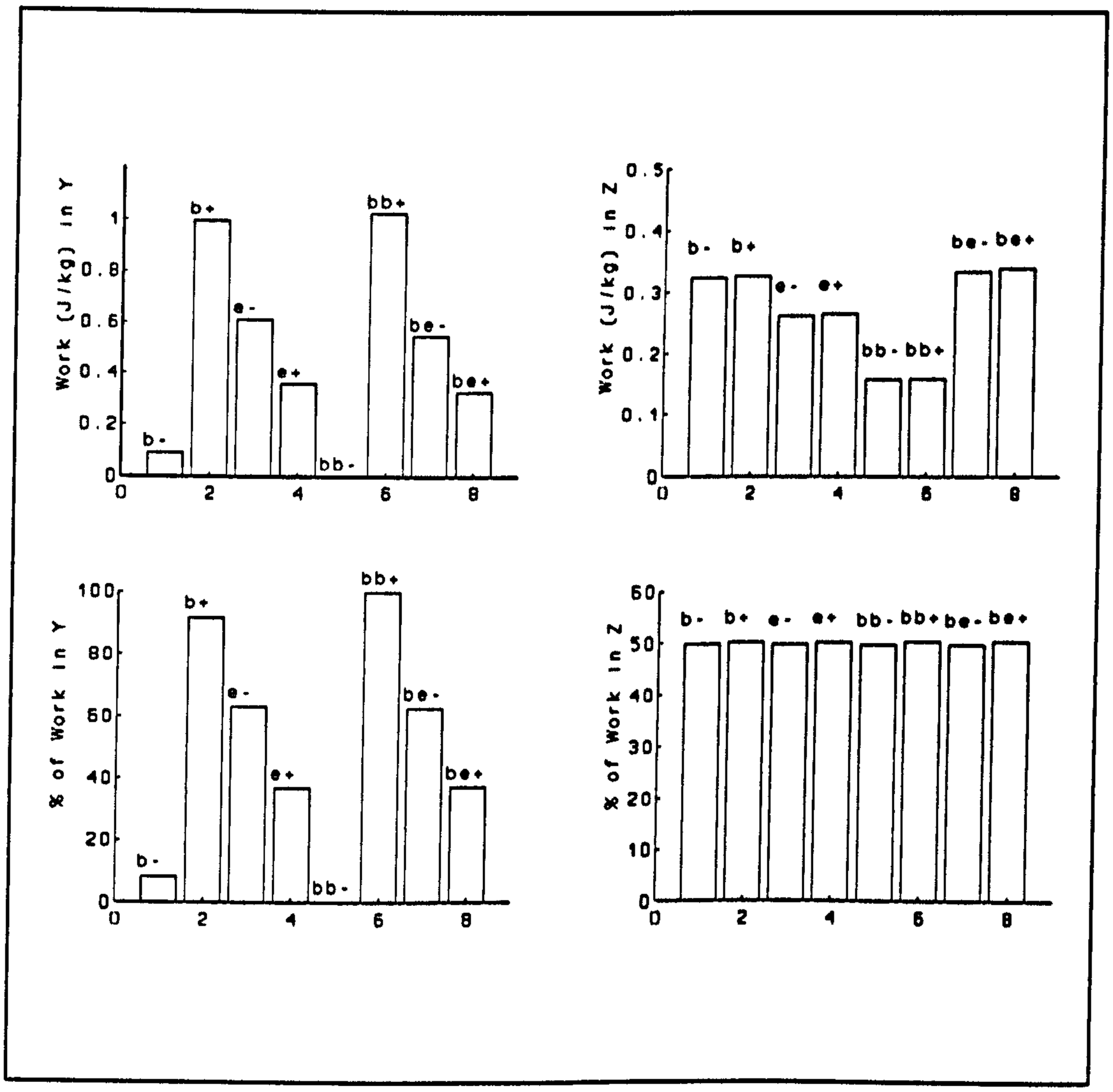

FIGURE 6.2 Comparison of work done in different modes of starting and finishing procedure.

FIG 6.2 Note: Comparison of work done in different modes of starting and stopping. Note: b = acceleration from standing; e = deceleration to standing; bb = flexed-knee acceleration from standing; be = flexed-knee deceleration to standing;

6.2.3 Discussion

From Fig 6.1 and 6.2, it is apparent that chimpanzee-like walking has very large values for positive work done in comparison to negative work. A similar case is found in fast normal walking. Of all modes of walking, normal walking at a comfortable speed has the smallest difference between positive and negative work done.

As indicated above, since ground reaction forces (GRFs) before and in the middle of a gait cycle are negative and displacement always positive, negative work is done in the half-cycle when the body receives resistance from ground, that is 'braking'. On the other hand, positive work done expresses 'propulsion'. The results of experiments on starting and stopping are shown in Fig. 6.2, where it is very apparent that starting needs much positive work and stopping much negative work. In a physical sense, if a person begins walking from a standing start, he needs to expend much energy in order to accelerate himself. Thus, positive work done is generally accepted to mean that the body is outputting energy. However, the meaning of negative work in this case is debatable.

Some might argue that negative work done means that the body is absorbing, or storing energy; others simply that less energy is being expended. Whatever viewpoint we take, we can agree that negative work done can be beneficial, since either energy expenditure is being reduced or energy can be returned to the body. From this viewpoint, normal walking, among all modes, is most mechanically effective, as it has the smallest difference between the two forms of work. So far, we seem to be reaching the conclusion that the more the negative work, the more effective is walking. For a moment, let us consider a related problem: joint power, which is another form of work done, expressing work done per unit time. Joint power was calculated according to general text books and Winter (1988), and is shown in Table 6.2.

TABLE 6.2. Comparison of power (W/kg) at joints between loaded normal walking and loaded flexed-knee walking. (N = 8, male adults only.)

	Hip		Knee		Ankle			
	mean	sd	mean	sd	mean	sd	sum	sd
AP(n)	0.4451	0.22	0.4984	0.15	0.5052	0.23	1.4484*	0.20
AP(b)	0.5903	0.16	0.7736	0.40	0.8217	0.37	2.1856*	0.34
PP(n)	0.4153	0.22	0.1692	0.13	0.3572	0.24	0.9417	0.22
PP(b)	0.5556	0.17	0.1856	0.08	0.4247	0.25	1.1659	0.23
NP(n)	-0.0297	0.02	-0.3291*	0.03	-0.1480*	0.04	-0.5068*	0.12
NP(b)	-0.0347	0.01	-0.5880*	0.44	-0.3945*	0.14	-1.0172*	0.35
MAX(n)	1.5336	0.45	1.1581	0.79	3.9548	2.18	6.6465	1.84
MAX(b)	1.5769	0.22	1.5149	0.64	3.9256	1.82	7.0174	1.58
MIN(n)	-0.3201	0.20	-1.3462*	0.25	-0.9742*	0.50	-2.6405*	0.54
MIN(b)	-0.4900	0.22	-2.7618*	0.22	-2.3159*	0.93	-5.5677*	1.66
PD(n)	0.2949	0.11	0.3436*	0.10	0.3513*	0.18	0.9898*	0.13
PD(b)	0.4421	0.16	0.5525*	0.22	0.6239*	0.34	1.6185*	0.26

AP = absolute power; PP = positive power; NP = negative power; Max = maximum power; MIN = minimum power; PD = absolute power/ distance travelled by the centre of mass; n = loaded normal walking ; b = loaded bent-knee walking * = $p<0.05$

From Table 6.2, focussing on the sign of powers, negative power at the knee seems rather large in bent-knee walking. This results mainly from large moments at the joints. The large negative power may indicate that much energy is being absorbed and stored around the knee. On the other hand, lower positive power at knee indicates that the knee plays a smaller propulsive role. According to our conclusions from analysis of the whole body in the last section, the muscles around the knee may play only a 'braking' role during flexed-knee walking. However,

during normal walking (Table 6.2), both the amount and the sign of power about the knee show that muscle function partly in propulsion, and partly in braking.

Up to now, if we ignore whether muscles are actually shortening or contracting isometrically it appears that it is the proportion of positive and negative work or power that plays an important role in energy consumption. When the ratio of positive and negative values approximate 1 (although positive power should always remain larger than negative power), walking may be optimal. 'Comfortable' walking is a good example of this. When the ratio is far greater than 1, the body will output much energy but not absorb or store adequate energy. When the ratio is far less than 1 negative work (or power) greatly exceeds positive work (or power) the body may absorb too much energy and locomotion cannot continue, or tissues may even fail. Therefore, an ideal motion may be defined by an optimum ratio of positive to negative work, slightly larger than 1, such as our 'comfortable' normal walking.

6.2.4 Conclusions

From the above experiments, calculation of work and power, and analysis of results, three conclusions may be reached:

(1) whatever we understand by sign, positive work done is always larger in BHBK walking than that in normal walking. This suggests that BHBK may need more energy output from the body than does normal walking.

(2) in general, positive and negative signs do express different physical meanings in biomechanics. Positive signs of work and power often indicate that the body is producing or outputting energy. This often takes the form of propulsion of the body. Negative signs of work and power indicate that the body may be absorbing or storing energy. The energy may be released in the next demi-cycle, as in walking, or may not be completely released, as in flexed-knee walking or stopping

(3) in general cyclical motion, e.g. level walking or loaded walking, an optimum ratio of positive and negative work, viewed from the perspective of particle mechanics, may be near to 1. Even when considering individual joints, a similar case may be observed.

6.3 Dynamic analysis of stability in human loaded walking

6.3.1 Introduction

While the biomechanics of unloaded walking have been extensively addressed (eg. Alexander 1980; Winter 1990; Cappozzo 1975; Williams and Cavanagh 1983) few authors have addressed the effects of loading. Taylor et al. (1970, 1980) investigated the loaded walking of animals, but have done so only by by physiological methods.

During loaded walking, we would expect both the velocity and height of the body centre of mass (CM) to be important factors influencing the stability of the whole body. If loads are placed on the shoulder or fastened about the lumbar spine, there will be an upwards or downwards shift, respectively, in the whole body CM: an upwards shift is obviously likely, at some point, to lead to instability. Similarly, we might expect greater velocities, at some point, to lead to instability. However, where would the onset of instability occur?

If we take as our whole body system a subject bearing a load, GRFs acting on the body will result in angular accelerations at the CM. The product of the angular acceleration and the moment of inertia of the whole body can be used as a suitable criterion of the stability of loaded walking, where stability of the whole body will decrease with the increase in that product.

6.3.2 Methods and Procedures

The method was as follows:

1) We represented the whole body (subject and load) by a simple three-segment model, made up of two lower limbs (leg-foot) and one upper body (head-trunk-arm, HTA);

2) Subjects, loaded in one of three different ways, were required to walk along the experimental pathway at self-determined 'slow', 'comfortable', 'fast' speeds as described in Chapters 2 and 3.

3) We applied dynamic equations to the models. According to Newton's Laws, the system (three-segment-model) and external forces acting on the system have the relationship:

$$\sum F = ma_c \qquad (6.1)$$

$$\sum M = I\beta \qquad (6.2)$$

where m - mass, including subject's own weight and the load carried; I - the moment of inertia of the whole system; a_c - acceleration of CM; β - angular acceleration about CM. Using GRFs from forceplate records, we can then calculate the velocity and displacement of the CM. As different known loads were applied at different known heights, different heights of the CM are also known.

4) Obtaining joint motion from the analysis of motion sequences allowed us to input both kinematics and GRFs and thus calculate the angular acceleration and moments about the CM. In these calculations, reaction forces from both feet were taken into consideration, by introducing a suitable duty factor.

5) Force curves were divided into those associated with slow , comfortable and fast modes of walking according to the general shape of the GRF curves, and stability calculated under the three situations.

6) From the above, I established possible optimal areas at different velocities and heights of the CM.

6.3.3 Results

Results (see Figure 6.3-6.5) show that there are different dynamic responses for different modes of walking.

In general, taking the stability of the centre of mass as our criterion, stability in loaded walking decreases with an increase in the height and velocity of the CM. However, a lower height of the CM does not always satisfy the criterion of stability. Neither does a greater height of CM always lead to reduced stability. If CM is low but velocity is higher, a decrease in stability will also result (see Fig. 6.3-6.5). Rather, it is apparent that different modes of loaded walking each have a characteristic height/velocity area, beyond which stability decreases. From Fig. 6.3-6.5, comfortable walking provides a larger stability area and fast walking has a smaller stability area. The differences of stability areas result from the differences of GRFs: thus, modes of walking tend to have their own characteristic areas of stability.

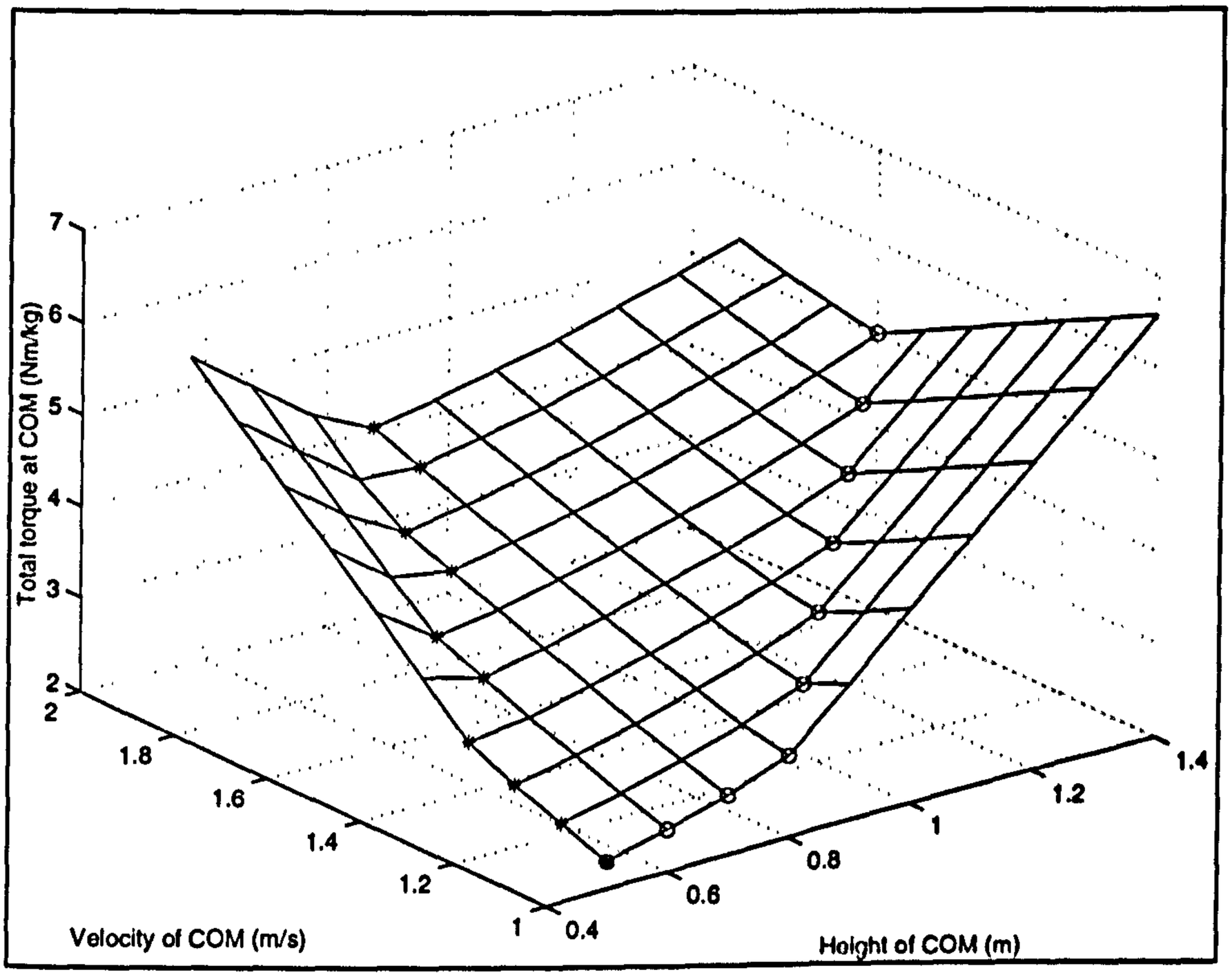

FIGURE 6.3. Simulation of the stability zone of loaded comfortable walking

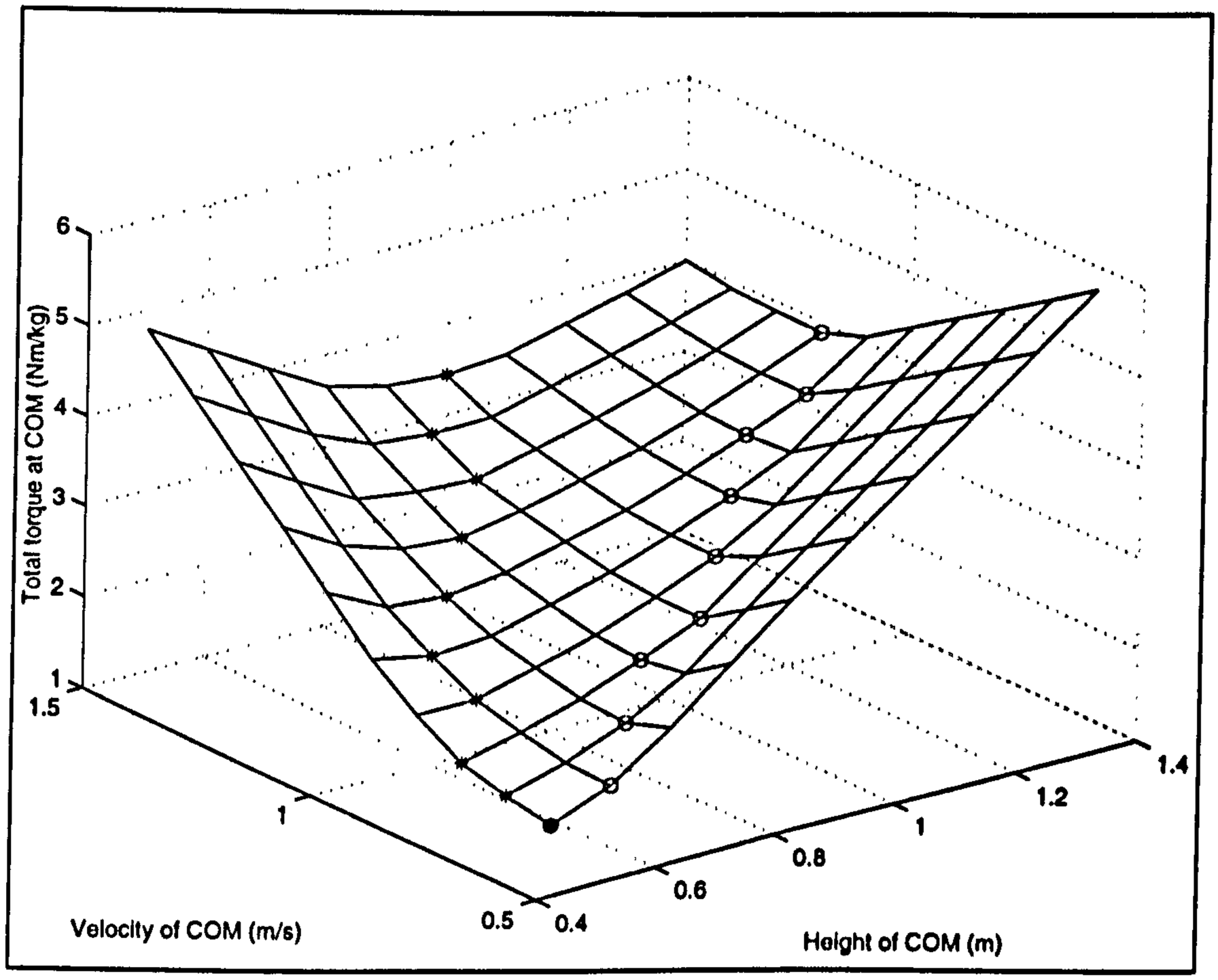

FIGURE 6.4. Simulation of the stability zone of loaded slow walking

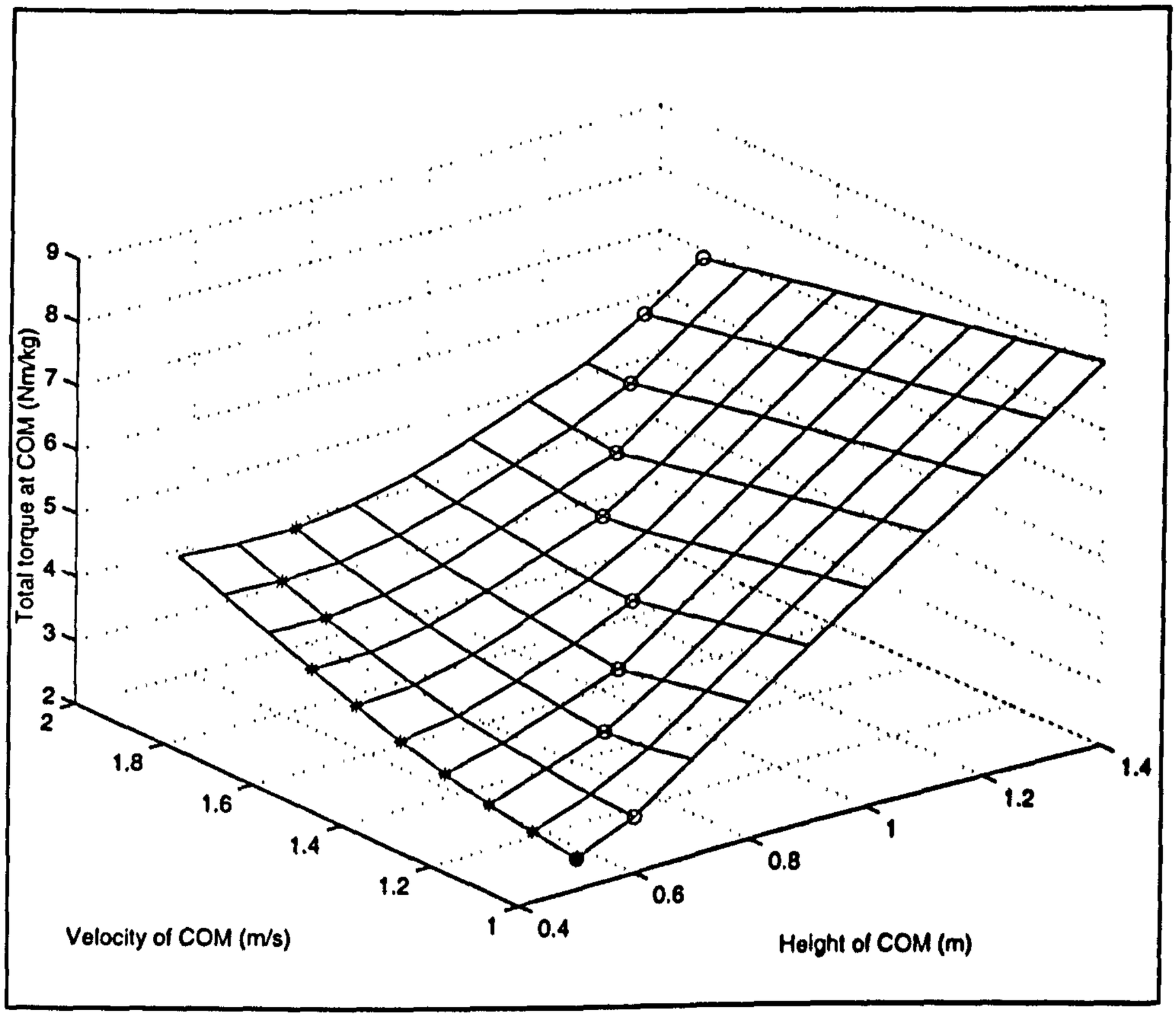

FIGURE 6.5. Simulation of the stability zone of loaded fast walking

6.3.4 Conclusions

For different modes of loaded walking, there are characteristic areas wherein optimum stability may be obtained and beyond which the stability of human walking may decrease.

CHAPTER 7.
RECONSTRUCTION OF THE BIPEDALITY OF EARLY HOMINIDS

A desire to know nature is the source of research.

ABSTRACT

The acquisition of bipedalism is one of the definitive characteristics in the evolution of early hominids. Using ADAMS-Android (MDI, 1995) I built androids of the early hominids *Australopithecus afarensis* AL-288-1 'Lucy' (c. 3.6 Mya) and *Homo erectus* WT-15000, the Nariokotome youth (c.1.8 Mya), simulated their walking and evaluated its biomechanical features. Model segment lengths were taken from the literature for AL-288-1 but measured from a cast of WT-15000 and values for segment mass distribution were estimated by reference to living humans. Joint motion functions derived from real subjects were applied to the models. An optimization method was developed to make the androids walk as perfectly as possible. Results show that simulated ground reaction forces (GRFs) are very similar to GRFs measured for living adults. WT-15000 has smaller joint powers and moments than AL-288, and it was generally the case that androids with a relatively short trunk, such as WT-15000 tend to walk with higher mechanical effectiveness. This suggests that selection may have operated to increase the length of the lower limb, or decrease that of the trunk, during the period of interest (c. 4 Mya - 1.5 Mya).

7.1 Introduction

The fossil record shows that hominid body proportions vary at different periods of human evolution (Schultz 1937 and later). This would imply that their bipedal walking may also have been different at different periods. So far no direct evidence of the manner of walking of early hominids has been discovered: even the Laetoli footprints (Leakey, 1979) tell us little as they may have been made by any of three or even four possible contemporaneous hominid species. To investigate the locomotion of extinct species, we can however reconstruct their body parameters, such as proportions, as physical systems and then examine the behaviour of these physical systems under various alternative hypotheses of behaviour. By a process of

elimination, we may ultimately determine which behaviours are possible, and which the most likely.

In this chapter, I reconstruct early hominids as mechanical multi-rigid-body models, place the models in an environment and let the models walk, driven by motion files representing alternative hypotheses of behaviour. The simulated walking is evaluated on the basis of the criterion of mechanical parameters including joint moments and powers. By comparing the walking of various alternative models, we examine the relationship between gaits and the change in body proportions between *Australopithecus afarensis* and early African *Homo erectus*.

7.2. Simulation experiments

7.2.1 Reconstruction of models of fossil species and construction of human models

When subjects are early hominid fossils, it is, of course, difficult to get accurate data on weight, limb lengths and mass distribution. Estimated segment parameters vary according to authors' methods (see, eg. Jungers 1982, 1988; McHenry 1988; and Feldesman and Lundy, 1988).

To obtain the segment lengths of WT-15000, all available elements of a cast made by the Kenya National Museum were scanned accurately using a Cyberware 3030 HiREZ Laser Scanner and the skeleton reconstructed with reference to estimates in the literature (McHenry 1988, 1992; Jungers, 1988, 1982; and Ohman et al., submitted ms.). For AL-288-1, I followed the quite consistent estimates of segment lengths, etc. in Jungers et al (1988) and Johanson et al. (1982). The model parameters are listed in Tables 7.1 and 7.2, but in summary were: AL-288-1 stature 1.05 m, body weight 30 kg. Because the mass distribution of early hominids is probably impossible to reconstruct precisely, mass distributions have been

TABLE 7.1 Models' size and mass

model	time (mya)	weight (kg)	stature (m)	leg length (m)
al-288	3.6	30.3	1.05	0.500
al-333	3.6	77.9	1.60	0.732
wt15k_a	1.8	48.0	1.60	0.812
wt15k_d	1.8	49.8	1.40	0.812
male_w	0	76.0	1.75	0.885
male_jt	0	82.2	1.80	0.900
male_di	0	29.6	1.40	0.680

calculated based on human data from Chandler (1975) (see Table 7.2). After body proportions and total mass have been determined, mass distribution may be worked out from the relative mass and relative moments of rotation of segments (Chandler et al., 1975 and Jensen 1989). In spite of arguments about the stature, weight and sex of the fossils, it is generally accepted that AL-288-1 had a relatively long trunk and short lower limbs, although the significance of (Jungers 1982; Jungers and Stern 1983; Schmid, 1983).

A single model of AL-288-1 was available from previous work (Crompton et al. 1998) and a similar model of the more fragmentary putative male *Australopithecus afarensis* skeleton AL-333 was also constructed.We also built an inertial model of the best known skeleton of early *Homo*, the Nariokotome skeleton, KNM WT-15000. This proved to be less straightforward, although (or perhaps because!) a cast of the complete skeleton was available to us. Some discussion of the procedure is therefore necessary here, although the work was a collaboration outside the immediate scope of this thesis (Ohman et al. submitted ms.).

We laser-scanned each skeletal element individually, and proceeded to

reconstruction of the skeleton from the resulting individual solid models. As part of this process, we compared the elements of the skeleton with those from an age-and sex-matched human skeleton of known stature at time of death, for which vertebral body heights were virtually identical to WT-15000. It was apparent from the comparison that the published reconstruction of the WT-15000 skeleton (Model A in Figure 7.1.a) was internally inconsistent: when the distance between superior and inferior articular facets were used to estimate vertebral column length, and the latter added to the other bony elements, the error of our estimate for the stature of the human skeleton was <0.2%. However, when we applied the same method to WT-15000 we obtained an estimated stature (Figure 7.1.a Model D) some 15 cm shorter than those in previous reconstructions (Ruff and Walker 1993) based on long bone regressions alone. As part of a collaborative study, the original fossil specimens were then examined at Kenya National Museum, confirming these findings. However, these studies also indicated that the individual suffered from degenerative disease of the vertebral column. Nevertheless, as this is the only known specimen of this species, we currently have no way of knowing to what extent the shortness of the trunk in both the old (Model A), and even more the new (Model D) reconstruction of WT-15000 is typical of the species, or an artifact of disease.

All four models of fossil species were then compared to two models of two modern male adults, one the author, a Chinese of normal fitness (male_w), the other a European athlete (male_jt), and to a model of a 12 year old modern human Chinese male (male_di) (see Table 7.1).

A simple environment, a horizontal plane was selected, to load the androids' walking and produce GRFs. Reconstructed androids look like in Fig.7.1.b.

7.2.2 Joint functions

To drive the models, joint motion functions were derived from kiniesiological

experiments on real subjects as in previous chapters (Chapter 2 - 3). The lower limb joint functions used are shown in Fig. 7.2.

FFIGURE 7.1.a: Models 'a' (left) and 'd'(right) of the Nariokotome youth, WT 15000 from Ohman et al. (Submitted ms.)

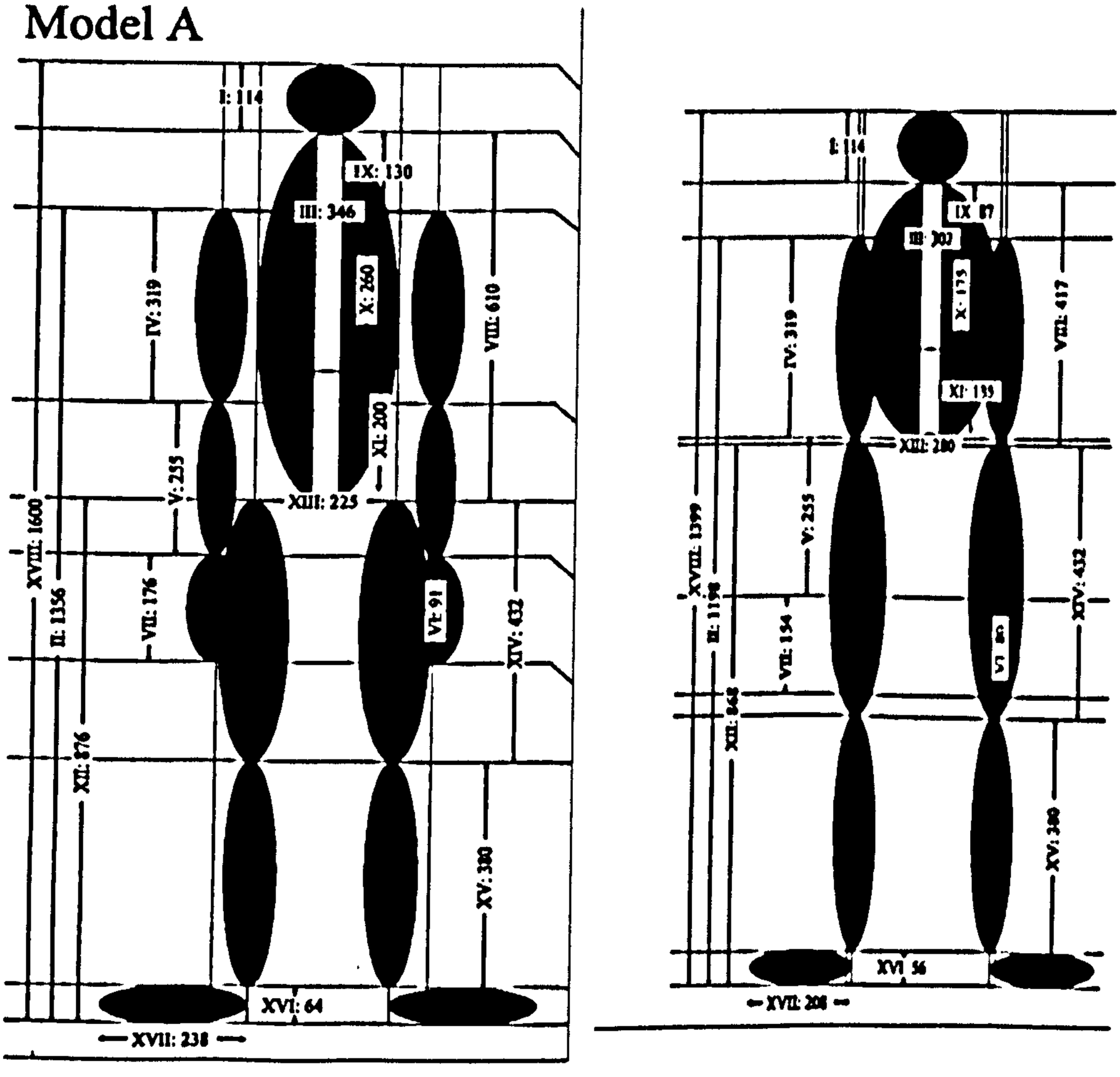

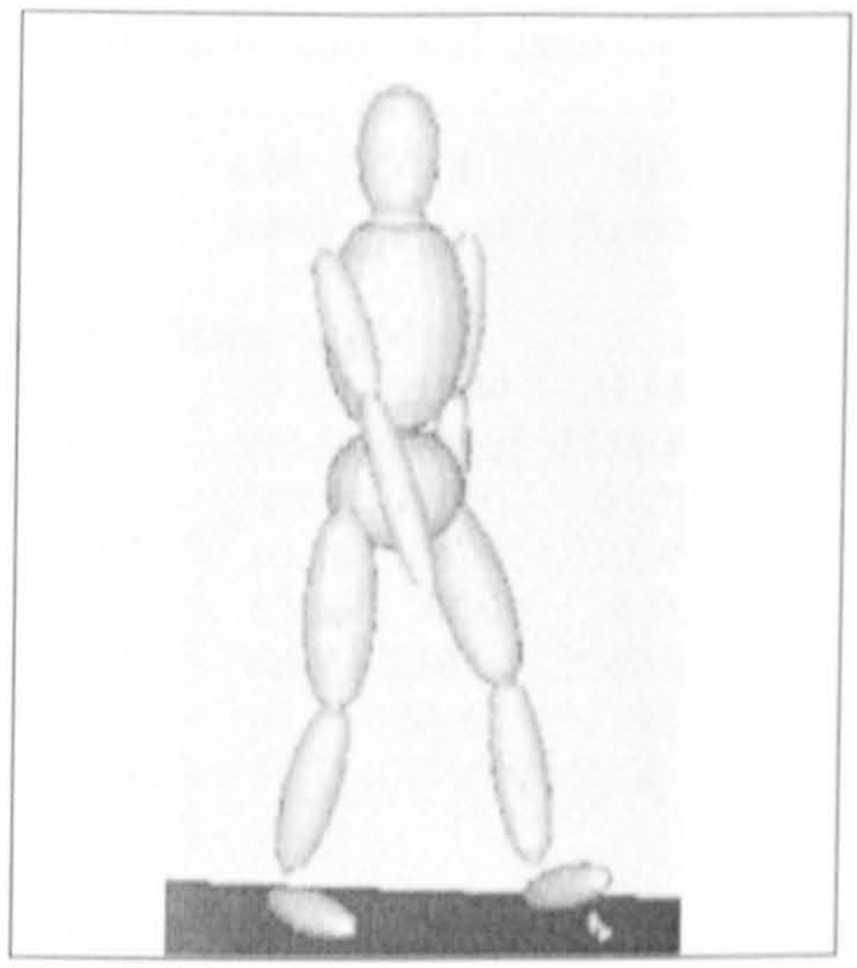

Fig. 7.1.b.c Modern human

Fig.7.1.b.a AL-288-1

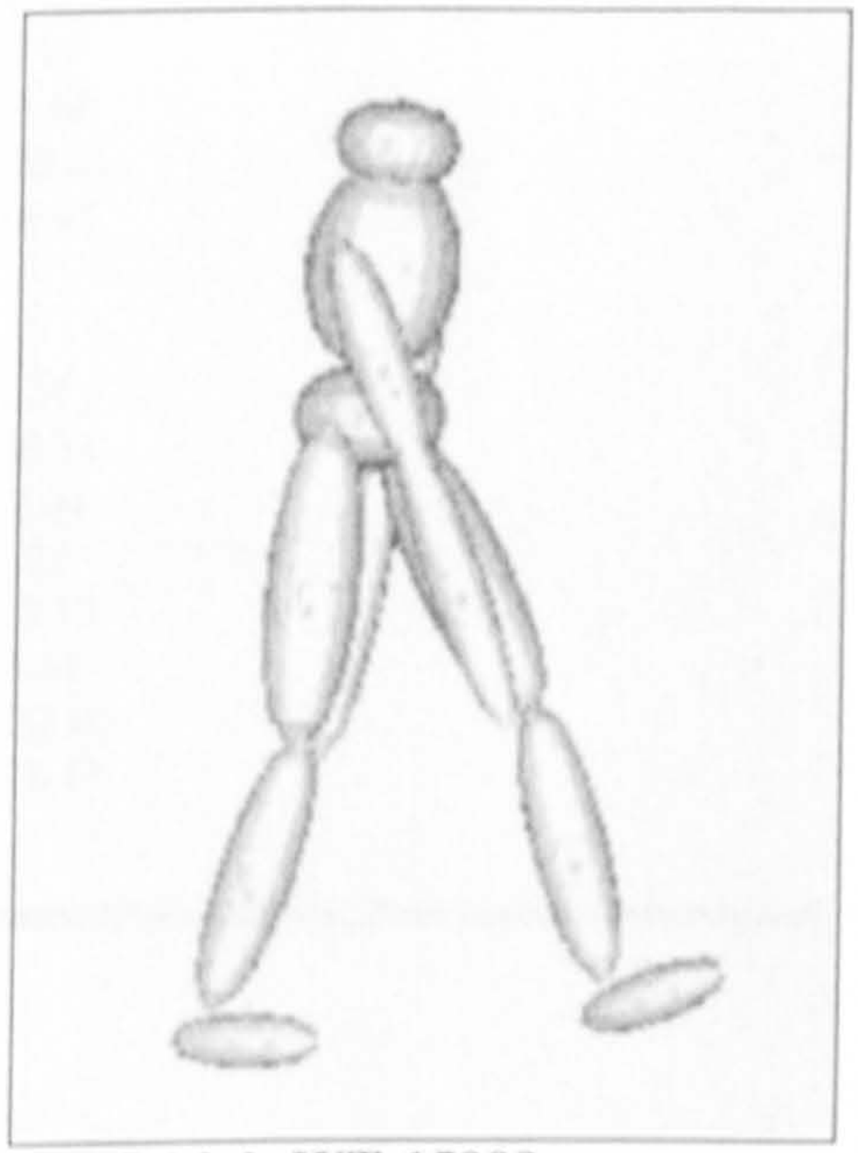

Fig. 7.1.b.b WT 15000

TABLE 7.2 Segment lengths and mass distributions

	length (mm)	mass (kg)	CM (mm)	Ixx (kg.cm^2)	Iyy (kgcm^2)
AL 288-1					
Body weight	30.2999	height 1.05			
head	125	2.121	63.00	31.44	31.44
trunk	380	13.51	205.96	1756.25	1756.25
upper arm	239	1.090	105.63	55.70	55.70
forearm	224	0.575	93.18	22.49	22.49
hand	170	0.273	69.36	4.50	4.50
thigh	281	3.454	129.54	230.96	230.96
calf	235	1.454	95.41	63.42	63.42
foot	200	0.244	51.51	12.27	12.27
KNM-WT 15000					
Body weight	49.8	height 1.40			
D					
head	114	3.11	75.69	73.33	70.24
trunk	417	25.95	218.24	3695.28	2398.34
upper arm	319	1.44	162.58	138.38	132.04
forearm	255	0.84	105.61	46.78	45.21
hand	154	0.29	78.64	8.88	7.17
thigh	432	5.08	169.20	977.98	1013.44
calf	380	2.06	157.62	252.04	252.05
foot	208	0.65	116.63	20.26	18.43
A 48 kg	1.60 m				
head	114	3.11	75.69	73.33	70.24
trunk	610	25.95	218.24	7621.28	4946.34
upper arm	319	1.38	162.58	138.38	132.04
forearm	255	0.81	105.61	46.78	45.21
hand	154	0.29	78.64	8.88	7.17
thigh	432	5.03	169.20	977.98	1013.44
calf	380	1.98	157.62	252.04	252.05
foot	238	0.62	116.63	25.26	23.43

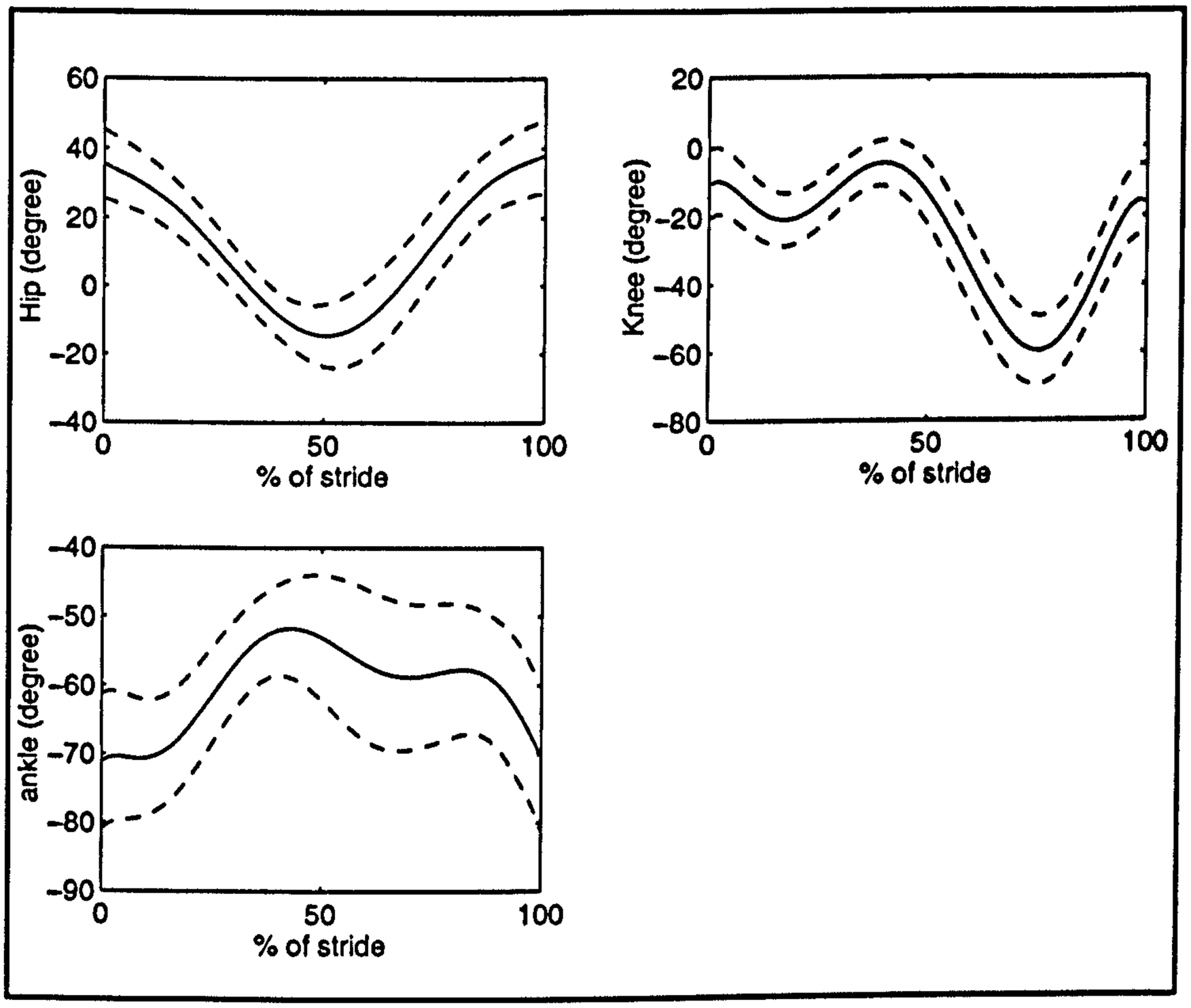

FIGURE 7.2 Joint motion (N = 28); - mean, -- mean ± sd

7.2.3 Dynamic simulation

The androids' walking was analyzed dynamically to produce simulated kinetic data. If an android could walk, which means that it satisfied the dynamic equilibrium conditions of multi-rigid-body mechanics, and if the GRFs between the android and ground were similar to the forces measured by forceplate from real subjects' during the experiments from which the motion functions were derived, I considered the experiment successful. For successful experiments, the simulated data were used to compute all mechanical parameters, including joint moments and powers by multi-rigid-body mechanics, mainly based on Langrange equations.

In fact, as many sources of error exist in the whole procedure of reconstruction, success in the first simulation was very difficult to achieve. To obtain success reliably, we had to consider additional.methods.

7.3 A Computational Method for Complex Simulations

7.3.1 A general complex problem

When building any model of a whole body, we often face and have to solve the problem of complexity. Such a model includes many essential data: body weight, stature, segment lengths and mass distribution. Since many parameters existed in the segments and joints of a model, many coefficients needed to be adjusted so that the model might walk similarly to a real human. Such multi-variable problems may not permit simple solution. To address this problem, I defined a object function which expresses the level displacement over which a model can walk. The object value is influenced by given joint motion and segment parameters.

In mathematical terms, the problem may be described as below.

object function f(**X**,**G**) (7.1)

subject to $\mathbf{X_a}<\mathbf{X}<\mathbf{X_b}$

$\mathbf{G_a}<\mathbf{G}<\mathbf{G_b}$

where **X** are segment parameters and **G** motion functions, and $\mathbf{X_a}$, $\mathbf{X_b}$, $\mathbf{G_a}$, $\mathbf{G_b}$ are constraint conditions or boundary conditions.

This problem is the same as that which I need to solve when building an android to simulate human motion. The model may include many variables **X**, such as limb length, mass distribution and joint rotation. Sometimes we cannot obtain the exact value of the variables, but we can know their range ($\mathbf{X_a}$ and $\mathbf{X_b}$). Similarly, the model may include many functions **G**, for example, joint motion. As there are always experimental errors, we cannot obtain exact joint functions. But a range of joint motion may be determined.

An hypothetical distribution of an object function is shown in Fig.7.3, where the object function is multi-peak and has two variables. We need to search for a pair of finite points, or coordinates where the object function obtains the best value, i.e. the highest peak. How can we find them?

7.3.2 The Finite Points Method

The basic idea of The Finite Point Method (FPM) is that in a complex mechanical model meaningful solutions may exist in some finite areas or at finite points (coordinates, see peaks in Fig. 7.3). Though the points may be not the best ones, they make the model physically 'sensible' and may be used to interpret an actual experiment. (Some might consider using optimization methods, but as an object function is generally not single-peak [or convex-domain], see Fig.7.3, optimization methods cannot be used directly in this situation).

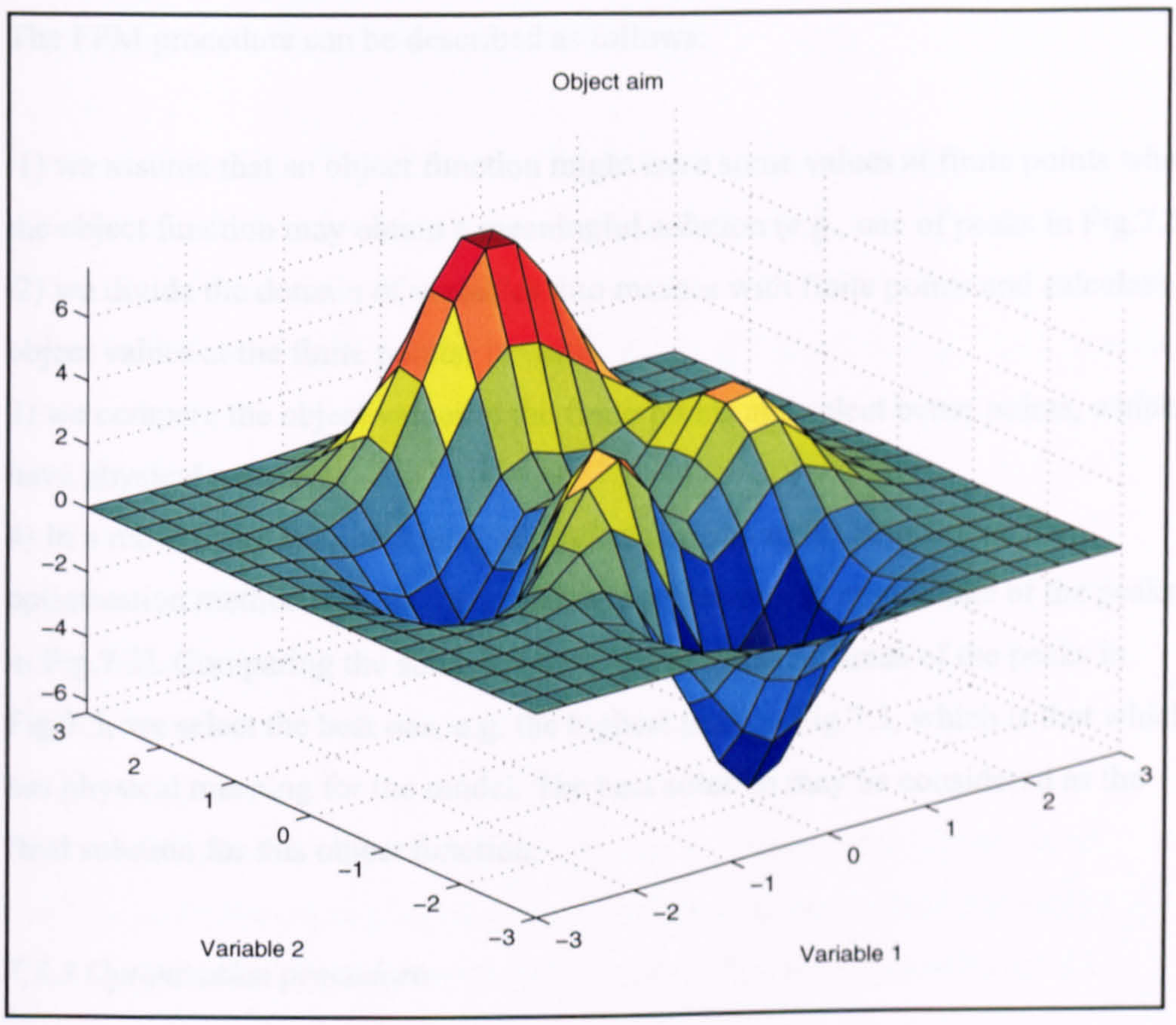

FIGURE 7.3 Explanation of the Finite Point Method.

The FPM procedure can be described as follows:

1) we assume that an object function might have some values at finite points where the object function may obtain a meaningful solution (e.g., one of peaks in Fig.7.3);
2) we divide the domain of variables into meshes with finite points and calculate object values at the finite points;
3) we compare the object values at the finite points and select better points, which have physical meaning;
4) In a much more restricted area, around such meaningful points, I use an optimization method and obtain an accurate solution (e.g. around one of the peaks in Fig.7.3). Comparing the solutions, e.g., the meaningful areas of the peaks in Fig.7.3, we select the best one, e.g. the highest peak in Fig.7.3, which is that which has physical meaning for the model. The best solution may be considered as the final solution for this object function.

7.3.3 Optimization procedure

I designed an optimization method as follows.

In order to obtain a successful result f, we have to adjust many variables: x_i,i=1..m,and g_j, j=1..n where x_i are segment parameters and g_j are joint function data. We express the problem mathematically as follows:

$$\max \ f(x_1..x_m, g_1..g_n) \qquad (7.1)$$
$$\text{subject to } x_{ia}<x_i<x_{bi} \ \ i=1..m$$
$$g_{ja}<g_j<g_{jb} \ \ j=1..n$$

where x_{ia}, x_{ib}, g_{ja} and g_{jb} are constraint conditions.

In mathematics, this an optimization problem. To solve equation 7.1, the

optimization procedure was performed as below.

1) Given a possible $x_i^{(0)}$ i=1..m and $g_j^{(0)}$ j=1..n, and an assessment value δ;
2) Simulate calculation with dynamic analysis to get a $f^{(0)}$;
3) Calculate $\partial f/\partial x_i$, i=1..m or $\partial f/\partial g_j$, j=1..n
   if $\partial f/\partial x_i^{(0)}>0$ or $\partial f/\partial g_j^{(0)}>0$, then progress $x_i^{(0)}$ or $g_j^{(0)}$ to $x_i^{(1)}$ and $g_j^{(1)}$ in a suitable direction;
   if $\partial f/\partial x_i^{(0)}<0$ or $\partial f/\partial gj^{(0)}<0$, then keep $x_i^{(0)}$ or $g_j^{(0)}$ to $x_i^{(1)}$ or $g_j^{(1)}$;
4) Simulate calculation by dynamic analysis to get a $f^{(1)}$;
5) Compare $f^{(1)}$ and $f^{(0)}$
   if absolute ($f^{(1)}$-$f^{(0)}$)> δ; $x_i^{(0)}<=x_i^{(1)}$,$g_j^{(0)}<=g_j^{(1)}$and $f^{(0)}<=f^{(1)}$; return to 3)
   else if absolute ($f^{(1)}$-$f^{(0)}$) < δ; end.

FPM cannot guarantee that we always get correct solution, because an object function is not always as good as is Fig.7.3. However, the method is powerful enough that we can always know whether a problem can or cannot be solved.

7.4 Results

7.4.1 Simulated Ground Reaction Forces (GRF)

Simulated GRFs (Fig. 7.4) were obtained and in general the patterns were all very similar to forces measured by forceplate during real normal human adult bipedalism, suggesting that the gait of AL-288 and KNM WT-15000 was indeed likely to have resembled that of modern humans.

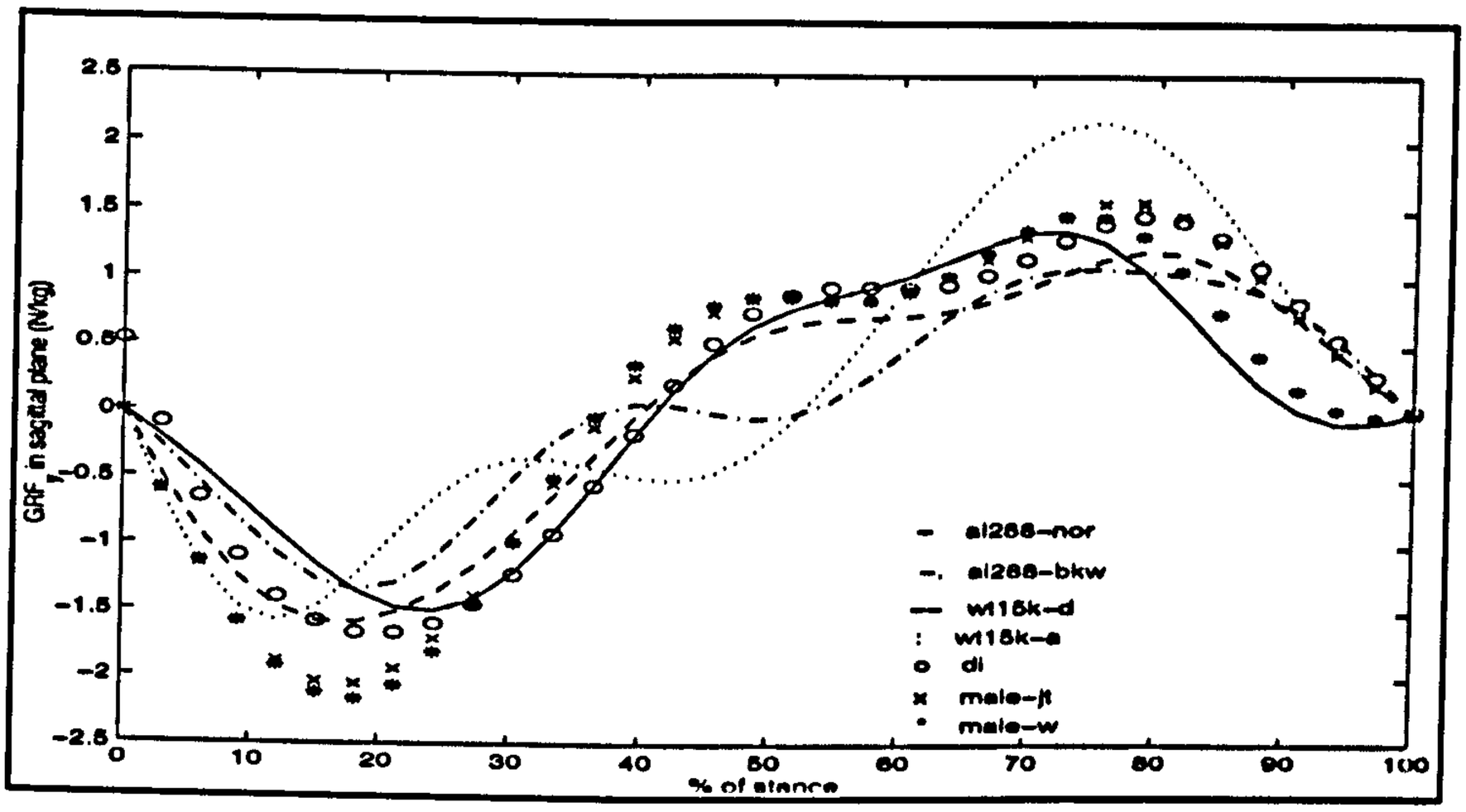

FIGURE 7.4.a GRFs in the sagittal direction in different simulations

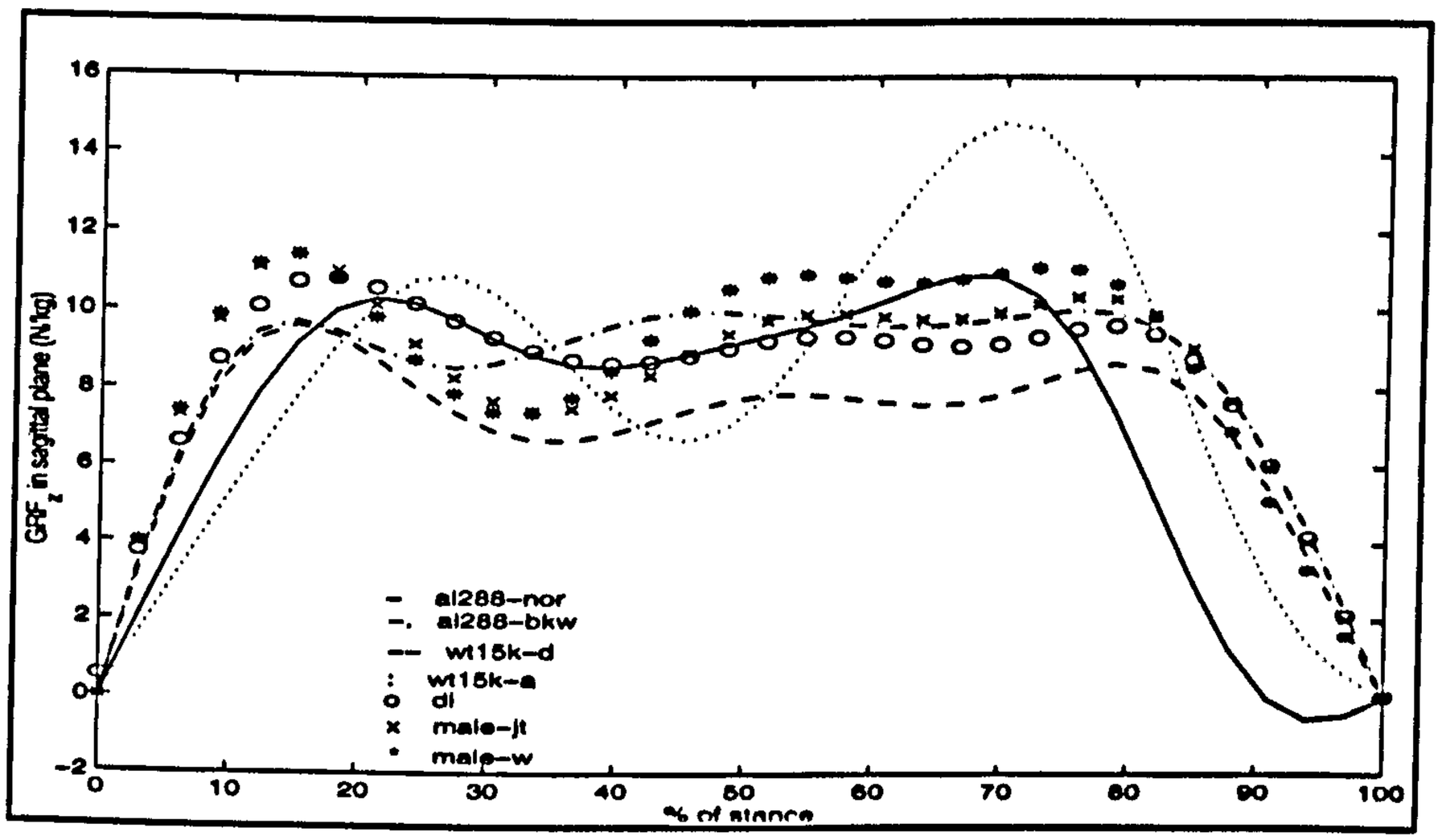

FIGURE 7.4.b GRFs in the vertical direction in different simulations

7.4.2 Joint parameters

Joint moments and powers were used as the means of evaluating which simulations were 'better'. They seem to be a reasonable criterion, since joint moments may indeed be involved in our subjective assessment of "saving" or "wasting" energy, since humans, in general, choose a form of motion which spends as little energy as possible while obtaining as great a displacement possible; while joint power is related to work and energy consumed by walking. According to biomechanical theory (see, eg. Winter, 1990), joint power shows how much work biological tissues have to do (ie, how much energy they have to produce per unit time) to maintain a form of gait. How much power a form of motion expends determines whether it is or is not an energy-saving form of motion.

All forms of powers were calculated and are compared in Tables 7.3 and 7.4, taking into consideration the special biomechanical meaning of positive and negative work (Alexander, 1980; Zarrugh, 1981; and Winter, 1990). Joint moments and powers of AL-288, WT-15000 and the other models are shown in Figs.7.5-7.6.

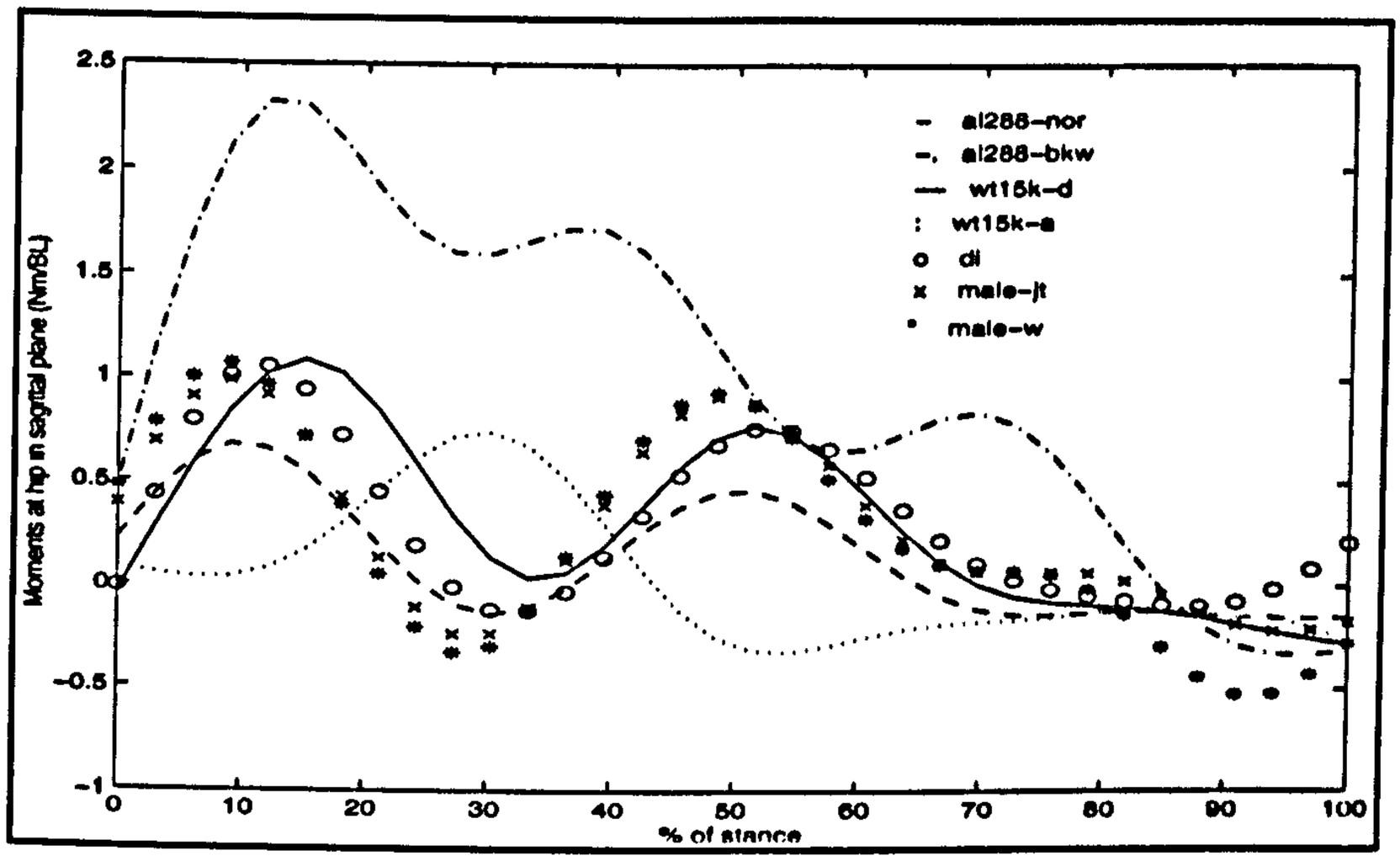

FIGURE 7.5.a Hip moments in different simulations

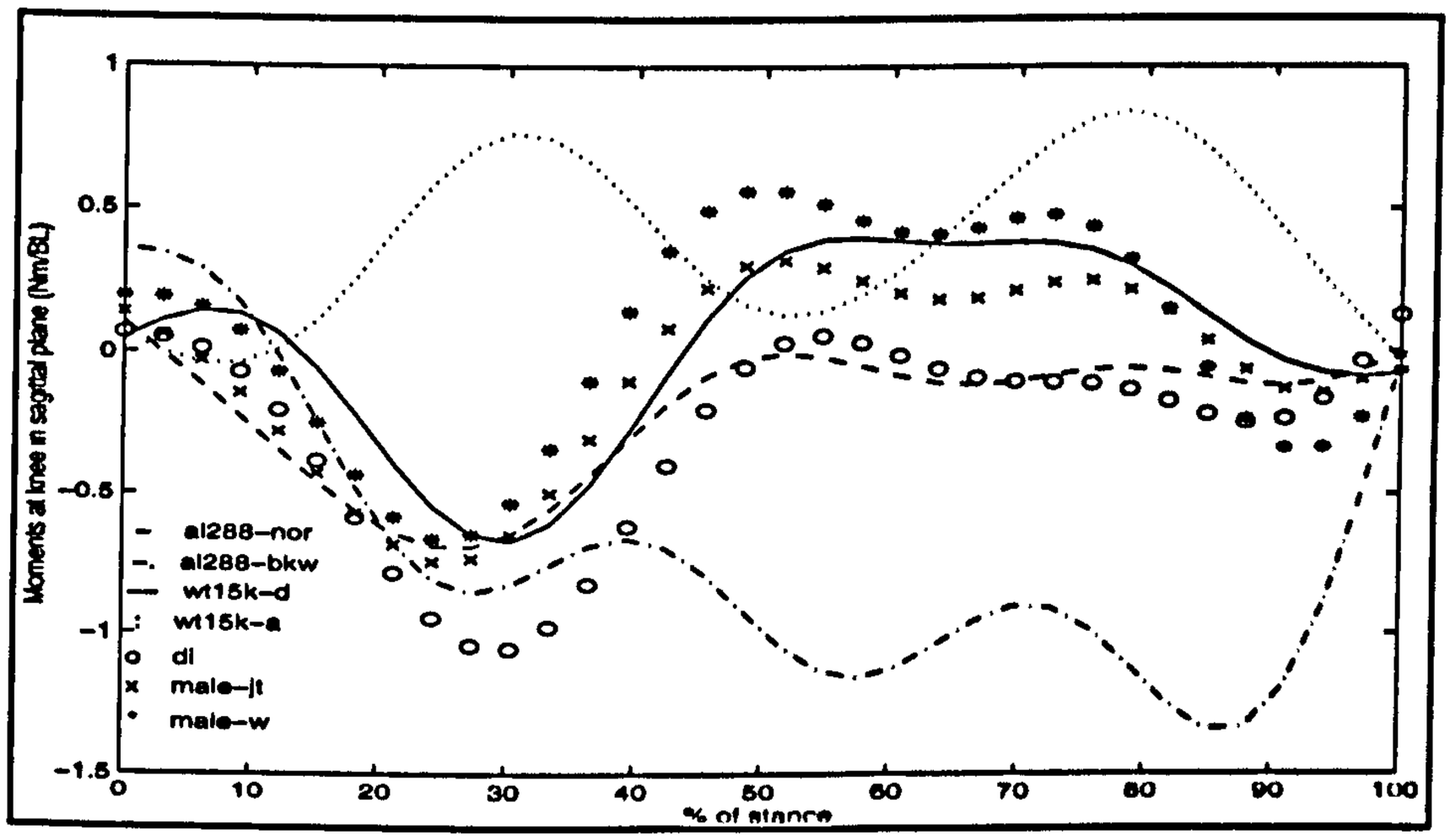

FIGURE 7.5.b Knee moments in different simulations

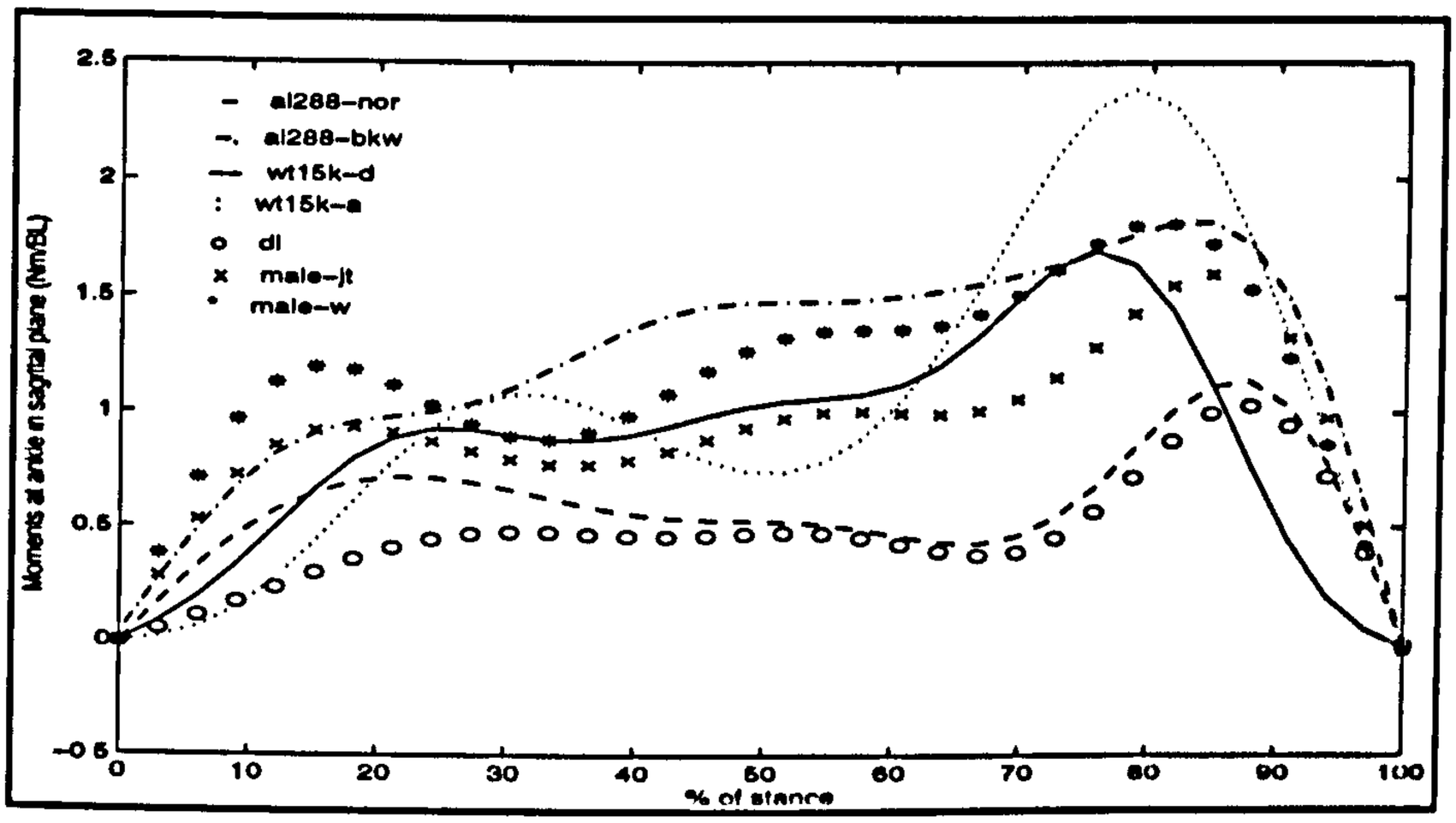

FIGURE 7.5.c Ankle moments in different simulations

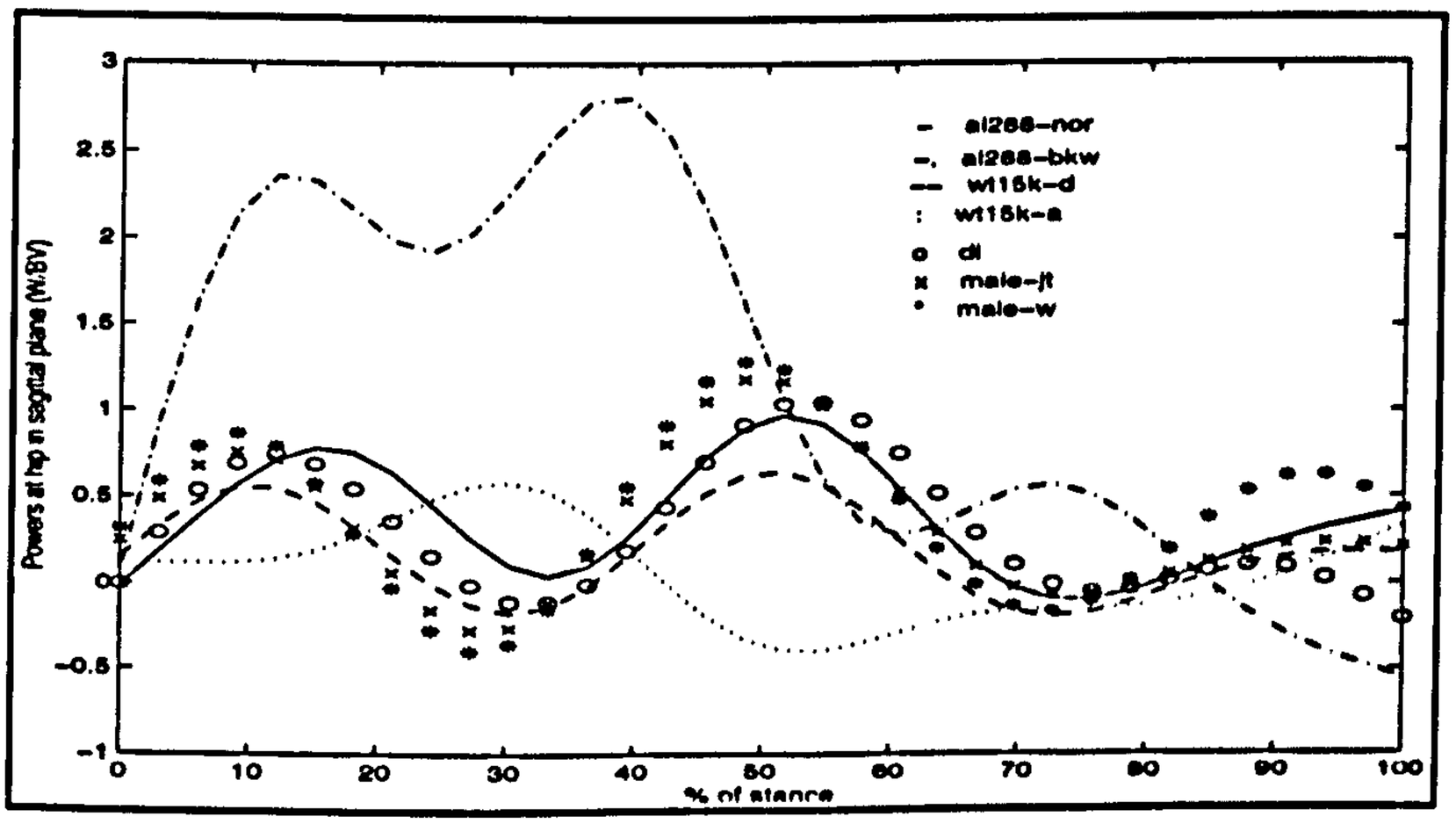

FIGURE 7.6.a Hip power in different simulations

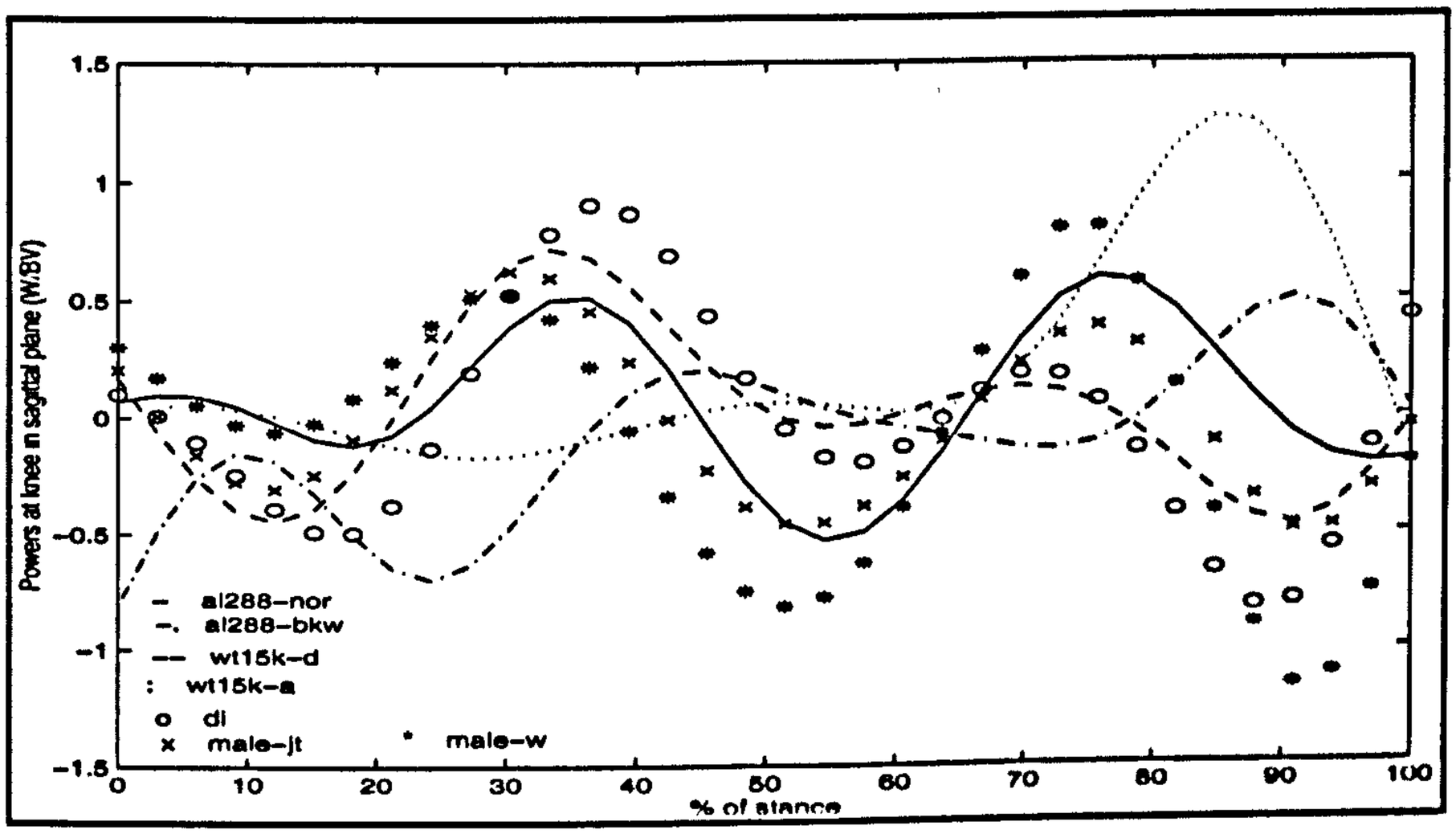

FIGURE 7.6.b Knee power in different simulations

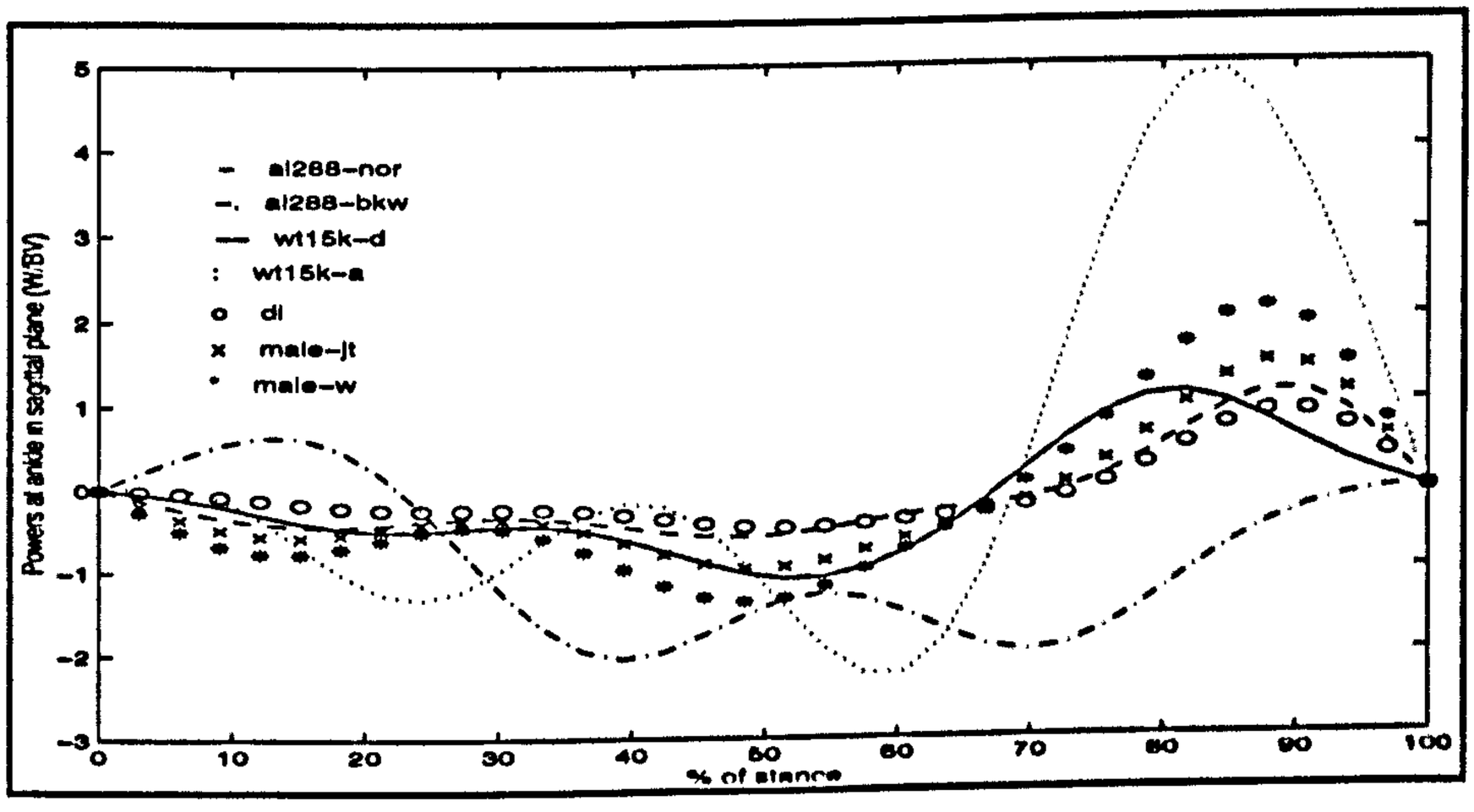

FIGURE 7.6.c Ankle power in different simulations

TABLE 7.3 Comparison of average absolute powers (W/BV) in various models

	al-288	wt15k-d2	male-jt	di	male-w
ankle	0.6007	0.4300	0.6054	0.3167	0.8626
Knee	0.3105	0.2561	0.2867	0.3514	0.4453
hip	0.3809	0.2558	0.4024	0.3511	0.5019
sum	1.2921	0.9419	1.2945	1.0192	1.8098

Note: W/BV: Watts/ (Body Weight and Velocity).

TABLE 7.4 Comparison of Joint Peak Moments (Nm/BL) in different models

	al-288		wt15k-d2		male-jt		di		male-w	
hip	1.21	-0.26	0.68	-0.15	0.99	-0.24	1.05	-0.12	1.14	-0.56
knee	0.41	-0.70	0.11	-0.70	0.32	-0.74	0.13	-1.05	0.60	-0.71
ankle	1.73	-0.01	1.14	-0.02	1.60	-0.02	1.03	-0.01	1.93	-0.04
sum	3.35	-0.97	1.93	-0.87	2.91	-1.00	2.21	-1.18	3.67	-1.31

7.5 Discussion

7.5.1 Comparison of various models

In general, WT-15000 has smaller moments and powers than AL-288 (see Table 7.3 and 7.4).

Although a typical value for the weight of a modern male is 80 kg, much heavier than any likely values for AL-288-1 and KNM WT-15000, both the joint moments and powers for the male humans are relatively small. This suggests that humans have reached a better adjustment of body segment proportions than did their ancestors. Although humans have become taller and heavier, they need to spend little more energy per unit weight and per unit velocity for moving their body. Moreover, as modern man is taller than was *Homo erectus*, s/he can walk more quickly than could that early hominid.

7.5.2 A possible explanation for the differences among models

Why are there such differences among the models? One reason may be the ratio of the upper body to the lower limb lengths (RUL). The increase in trunk length results in the increase of the segment's principal moments of inertia. According to the theorems of moments of momentum, if lower limb lengths remain constant while the trunk increases in length, moments at hip have to increase to maintain the stability of the upper body. Thus, a relatively small proportion of the upper body (head and trunk) to lower limb length may be beneficial for bipedalism. This observation is in agreement with Jungers and Stern (1983) and Preuschoft and Witte (1991).

During the earlier evolution of hominid bipedalism there seems to have been a tendency to decreasing RUL. If common chimpanzees can be taken to represent the ancestral condition, where occasional BHBK walking occurs, they indeed have longer and bulkier trunks, RUL approximately 1.4 ~ 1.6. AL-288 (c. 3.6 Mya) has a relatively long trunk, compared to her short lower limbs; her RUL may be approximately 1.1 ~ 1.2. Either upright or BHBK walking on the ground may have

accompanied arboreal quadrupedalism in her repertoire. Considering the four models of WT-15000 compared in Ohman et al. (submitted ms.), the RULs are 0.8916, 0.8091, 0.6539 and 0.6539, clearly smaller than AL-288's. WT-15000 (1.8 Mya) might thus have evolved relatively longer lower limbs, or a smaller RUL, than AL-288-1, in order to obtain high mechanical effectiveness during walking. For modern humans, however, the RULs are approximately 1 (adults) and 1.2 ~ 1.4 (children). From the above, it may be suggested that there was a tendency of decreasing RUL from 4 Mya to 1.8 Mya, to enhance effectiveness in walking. Since 1.5 Mya the tendency might have changed to an increase in RUL, perhaps as an effect of brain size increase, or a change in selective pressures. From the biomechanical viewpoint, a relatively large upper body is disadvantageous for bipedal walking, as our analysis of WT-15000 and AL-288-1 shows. It is possible therefore that an optimum RUL might be selected for, unless selection for other qualities acted more strongly.

While, according to Witte et al. (1991) a longer trunk may act to compensate for accelerations and decelerations of the lower limb which might reduce stability of the whole body, in this study we have not examined the fate of the model at the level of individual segments, and we cannot, therefore evaluate this possibility without further experiments.

7.6 Conclusions

From a comparison of energy expenditure at the lower limb joints, we may thus conclude that KNM WT-15000 walked more effectively than did AL 288-1. A smaller ratio of the upper body to the lower limb is a major factor in this difference in performance. However, in view of the much greater absolute body size the relatively larger RUL of modern humans is not associated with a marked deficit, perhaps as the result of a better match of limb proportions to the joint motion patterns employed in these simulations.

CHAPTER 8. RECONSTRUCTION OF THE LOADED WALKING ABILITIES OF EARLY HOMINIDS

Working changed man.

Chinese Proverb

8.1 Fossil limb lengths, swing frequency and load carrying

ABSTRACT

This section analyzes the relationship between the intermembral index and hand-carrying. Using as dual criteria match between upper and lower limb swing time, and ability to carry loads in the hand, AL-288 could only have carried loads of 15%-50% the weight of the upper limb while maintaining swing symmetry, but WT-15000 and modern humans weights 3 times heavier than the upper limb. The carrying ability of chimpanzees is worse than that of AL-288-1. The intermembral index of modern humans, at 68-70, is around the smallest, and is optimal for hand-carrying under our criterion. Under reduced selection pressure for hand-carrying, we might expect humans to evolve a longer upper limb, to improve unloaded swing symmetry.

8.1.1 Proportions of upper limbs in fossils

The intermembral index, (humerus + radius length) x 100/(femur + tibia length), is different in different hominid fossils: it is 88 (80-90) for AL-288-1 (3.6 Mya), 70 for WT-15000, 68-70 for modern humans, all of these having shorter forelimbs than other living hominoids (the index is 100-110 for chimpanzees (bonobos around 102, common chimpanzees around 107), around 120 for gorillas and 140-145 for orangutans (Coolidge, 1933; Zihlman and Cramer, 1978, Napier and Napier, 1967 and Aiello and Dean, 1990). This phenomenon suggests that changes in the intermembral index (IMI) may be implicated in human evolution, particularly in the evolution of bipedalism.

What selective pressures could have lead to changes in IMI during human evolution, and how do changes in IMI affect mechanical performance? As shown by Preuschoft

and Witte (1991) possible answers may be sought in mechanical principles relating to the symmetry of motion, since swing times or frequencies of the upper and lower limbs should be equal to each other for optimal efficiency in walking, although slight differences would be tolerable. However, Preuschoft and Witte (1991) did not fully consider the effects of load-carrying, and I therefore give this aspect particular attention.

8.1.2 Method: similarity of frequencies

8.1.2.1 Frequency of a free limb

Ignoring the constraints of joint shape and musculoligamentous attachments, a limb hanging freely at a joint should act like a pendulum. If raised from its position of rest and then released, a limb of given proportions will swing with a given natural frequency. This effect is well understood and may be exploited, for example, to measure the rotational inertia of a limb (see, eg. Crompton et al. 1993). This pendulum-like motion is of course a vital energy-saving mechanism, since little muscle activity is needed to sustain it. In real life, the swing frequency of a limb may be adapted for a given special behaviour and may therefore differ from the frequency of a free pendulum. Experimental results for human bipedal walking, for example, indicate that there is a tendency for departure from the natural frequency of the upper limb near the transition between slow and normal walking rates (Webb et al. 1994). Webb et al. (1994) investigated the relationship between the stride frequency (SF) and the natural pendular frequency (NPF) of the upper limbs, and found that the relative stride frequency (RSF, the ratio of SF to NPF) is in the neighbourhood of 1: in single-swing, slightly larger 1 (average 1.1, see Webb [1994] Fig. 9.a), and in double swing smaller than 1 (average 0.7). This may mean that in most cases, where single swing occurs, humans prefer a slightly higher stride frequency than the NPF.

This is understandable, since theoretically, the stride frequency in NPF (RSF =1) should be optimal for the upper limbs. But human limbs, as biological structures, cannot be equivalent to ideal pendulums; further, stride frequencies in human walking are determined by many factors, including physiological and psychological ones. From the experiments of Webb et al. (1994), RSF in single swing is close to 1, which suggests that in some situations, humans prefer a RSF near the NPF.

While humans might, theoretically, be expected to walk at a particular speed, which is both fast and efficient, in practise, we tend to walk slower or faster than this theoretical optimum. The statistical average speed may be either higher or lower than the theoretically optimal value, but this does not, of course, imply that the theoretical value is not actually optimal.

Here, however, I am concerned only with the coordination of the upper and lower limbs. Whatever the value of SF, in single swing (which predominates in normal life) efficiency requires that upper limb frequency matches that of the lower limbs. When analyzing the models of fossil species, I assume that carrying a light object in the hands may contribute to this matching of the frequency of the upper and lower limbs. I select the NPF value for our analysis because of its general importance and to simplify the dynamic equations expressing the motion of the swing limb. I do not, however, imply that humans only walk at NPF.

With respect to "double swing", my function actually gives a similar tendency to that seen in single swing (see Fig.1), but double swing is really outside of the scope of this thesis.

Thus, notwithstanding the work of Webb et al. (1994), in order to save energy the swing frequency of a limb should remain as close as possible to its natural frequency,

and this chapter is based on this assumption, pending verification and clarification of the finding of Webb et. al. (1994)

In general, the natural swing time (1/frequency) of a limb is determined by

$$T\sqrt{\frac{mgZ}{I}}=2\pi \qquad (8.0)$$

$$f=\frac{1}{2\pi}\sqrt{\frac{mgZ}{I}} \qquad (8.1)$$

$$also \quad T=2\pi\sqrt{\frac{cL^2}{gZ}} \qquad (8.2)$$

Where T - swing time for a complete ycle (s); f - frequency, (Hz) or 1/s; L - limb length (m); I - rotational inertia about the centre of rotation; c - a parameter related to limb shape; m - mass of the limb; g - the gravity constant; Z - the distance from the centre of mass to the centre of rotation. From equation (8.1), we can see that swing time is proportional to rotational inertia. From (8.2), it is apparent that swing time will be primarily mainly decided by the length of the limb.

8.1.2.2 Why humans have small intermembral indices

From the viewpoint of the symmetry of motion, a IMI of 100, where upper and lower limbs have the same length, should therefore be the most beneficial for bipedal walking. The upper and lower limbs will move in completely reverse phase. Is the IMI of chimpanzees then actually nearly ideal, and why is the IMI of modern humans smaller than 100?

When the IMI is larger than 100, the swing time of the upper limb will be greater than that of the lower limb. As Preuschoft and Witte (1991) show, this is not beneficial for bipedal walking. The larger the IMI, the worse the effect on motion. Equally, if the IMI is smaller than 100 (the length of upper limb is shorter than the lower limb), the swing time of the upper limb may be less than that of the lower limb, neither is this beneficial for bipedal walking. If, however, we consider the consequences of holding an object in the hand, we may, in fact, then benefit from a smaller IMI. Holding something in the hand increases the rotational inertia of the upper limb, and therefore the swing time of the upper limb may come to approximate that of the lower limb. Thus, the upper limb may move symmetrically but in opposite phase to the lower limb. If there is selection in favour of an ability to hand-carry, an IMI less than 100 is likely to be evolved.

This may explain why human IMIs are smaller than those of other hominoids. Human IMIs, and by extension, those of some early hominids, may have become adapted for carrying, while the IMI of other hominoids may be adapted to the symmetry of motion (and/or, to a greater or lesser extent, to a longer reach in arboreal grasping and climbing). If symmetry of motion is considered as a criterion, however, it is also true that striding quadrupedal mammals would be expected to have a IMI around 100. From this viewpoint, chimpanzees (IMI 102-107) are better adapted for quadrupedalism than gorillas (around 120) or orang-utans (around 140).

If we agree that a smaller IMI will benefit loaded bipedal walking, how heavy loads are the most suitable for AL-288-1, WT-15000, chimpanzees and modern humans ? Let us calculate swing time for different IMIs.

8.1.2.3 Carrying weight and frequency

To simulate an IMI close to 100, we may let the hands hold a weight such that swing

time of the upper limb will be equal to that of the lower limb. From (8.1) and (8.2), we have the relationships, when $T_1=T_2$

$$\frac{I_1+I_c}{(m_1+m_c)gZ_n}=\frac{I_2}{m_2gZ_2} \quad (8.3)$$

where m_1 and m_2 - masses of upper limb and lower limb, respectively and m_c - the mass held by the hand; Z_1, Z_2, Z_n - the distances of the centre of mass (CM) to the centre of rotation, such as the shoulder or hip; I_1, I_2, I_c - the rotational inertia of the upper limb, the lower limb and the object carried. For a loaded upper limb, CM should be:

$$Z_n=\frac{m_1Z_1+m_cL_1}{m_1+m_c} \quad (8.3.1)$$

If we treat limbs as simple bars, the rotational inertia will be 1/3 mass x square of length, thus (8.3) will be:

$$\frac{\frac{1}{3}m_1L_1^2+m_cL_1^2}{(m_1+m_c)gZ_n}=\frac{\frac{1}{3}m_2L_2^2}{m_2gZ_2} \quad (8.4)$$

where L_1, L_2: upper and lower limb lengths.

From (8.3) and (8.4), we get (8.5):

$$\frac{\frac{1}{3}m_1L_1^2+m_cL_1^2}{\frac{1}{2}m_1L_1+m_cL_1}=\frac{\frac{1}{3}m_2L_2^2}{\frac{1}{2}m_2L_2} \qquad (8.5)$$

Simplifying (8.5), we get (8.6):

$$L_1\frac{\frac{1}{3}m_1+m_c}{\frac{1}{2}m_1+m_c}=\frac{2}{3}L_2 \qquad (8.6)$$

Letting $L_1/L_2=L_p$, $m_c/m_1=M_p$, we obtain (8.7) and (8.8).

$$L_p=\frac{1+2M_p}{1+3M_p} \qquad (8.7)$$

$$M_p=\frac{L_p-1}{2-3L_p} \qquad (8.8)$$

M_p is, as above, the ratio of the mass held by a hand to the mass of the upper limb, and L_p is the proportion of the length of the upper limb to that of the lower limb, that is, the IMI /100. Since M_p must be larger or equal to zero, thus L_p has to be larger to or equal to 2/3 (0.6667) and smaller or equal to 1, that is, $2/3<L_p<1$.

8.1.3 Calculated results

Given L_p from 0.67 ~ 1, we obtain a plot of L_p, IMI against weight carried with hands (see Fig. 8.1).

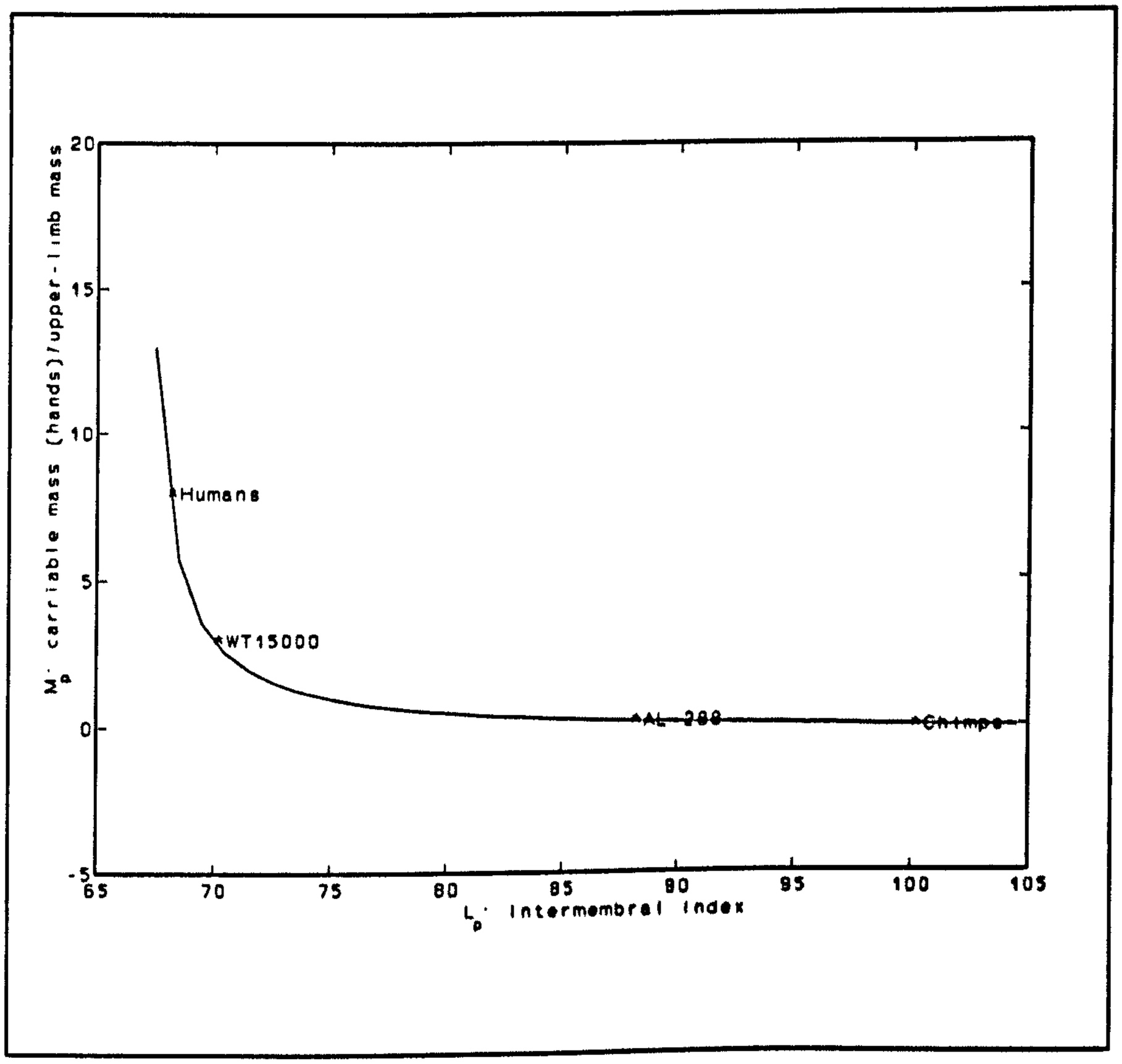

FIGURE 8.1 Relationship between the intermembral index and carrying weight by hands

8.1.4 Discussion

Given data for fossils, modern humans and other living hominoids, we can obtain different suitable carrying weights for different subjects (see Fig. 8.1). It is obvious that if the IMI of AL-288-1 is between 80-90, s/he could only carry a weight of 50%-15% of the weight of the upper limb, while maintaining swing symmetry between upper and lower limbs, but WT-15000 (IMI 70) and modern humans (IMIs 68-70) could carry 3-8 times the weight of the upper limb. Chimpanzees have an IMI about 100-108 and their carrying ability is the worst: theoretically able to carry nothing without disturbing swing symmetry in bipedal walking. Newborn humans, incidentally have a similar IMI to chimpanzees (Aiello and Dean, 1990) and would thus have similar problems with loaded bipedal walking.

If we require similarity of swing time of the upper and lower limbs, and maintain hand-carrying ability as the second criterion, from equation (8.8), it is clear that the IMI of modern humans has obtained an optimum, 68-70, which could not be reduced without detriment to either performance criterion. Freed from selection to hand-carry, but under continued selection for swing time symmetry, the IMI should increase towards 100, that is, the length of the upper limb should increase in length: reduction in hindlimb length would of course reduce maximum stride length.

8.2 Loaded gait of fossil species AL-288-1 and KNM WT-15000

ABSTRACT

In this section, I compare several modes of loading: static loading, hand carrying, and carrying over the shoulder in AL-288-1, WT-15000 and modern humans. Research methods differ according to mode. Results indicate that 1) AL-288-1 would have had

the best static loading stability and modern humans the worst; 2) in contrast modern humans have the best hand-carrying ability while that of AL-288-1 would have been the worst and finally 3) WT-15000 would have had the best capabilities for over-the-shoulder carrying of light loads, while the abilities of AL-288-1 and modern humans for over-the-shoulder carrying are similar. From simulated dynamic parameters, such as moment and power at joints, it is discovered that AL-288-1 would perform loaded bipedal walking with the lowest mechanical effectiveness of all models. AL-288-1 spends nearly more 1.4 times power than KNM WT-15000 and modern humans. On the other hand, KNM-WT 15000's performance is excellent during loaded walking, having similar or better dynamic response than that of modern humans. In other words, a shorter trunk and longer leg may be advantageous for lightly loaded bipedal walking. Maximum loads for AL-288-1 might be about 10 kg and for KNM WT-15000 up to 20 kg.

8.2.1 Method

The method applied in this section is similar to that in Chapter 7. I constructed representations of AL-288-1, KNM WT-15000 and modern humans as androids, multi-rigid-body mechanical models under ADAMS (MDI, 1995), and simulated loaded bipedal walking for different gaits, including loaded upright walking (NLW) and loaded BHBK walking (LBW). A computational method was used to make the androids walk as well as possible (see Chapter 7). However, joint functions (see Fig. 8.2) used to drive models are of course derived from experiments on loaded walking of real subjects. Calculated results are normalized by models' body weight rather than the sum of body weight and load. We then evaluated its biomechanical features as in Chapter 7.

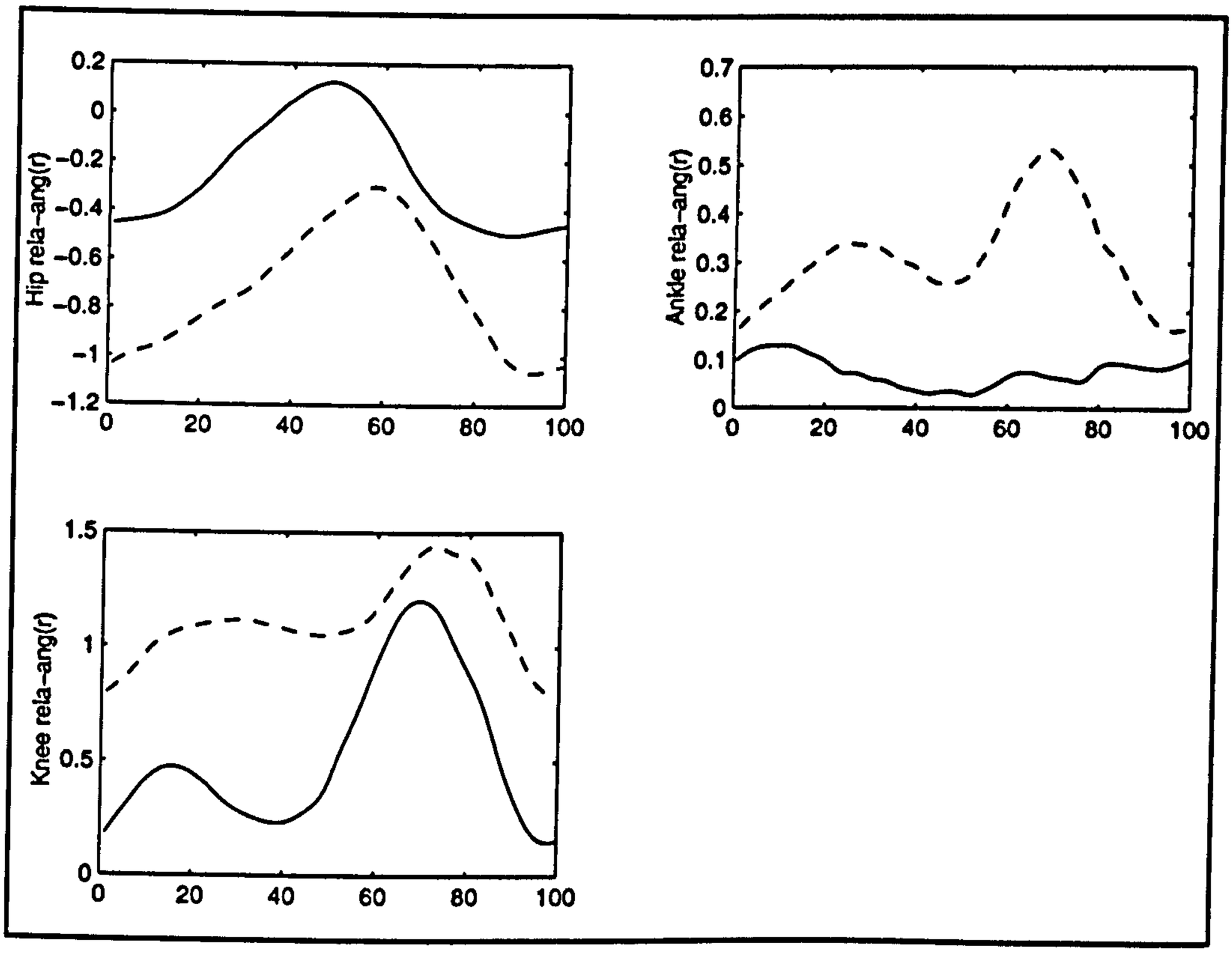

FIGURE 8.2 Comparison of joint angles in two modes of loaded walking
Load carried - 20 kg; rela_ang - relative joint angle

8.2.2 Results

8.2.2.1 Simulated ground reaction forces

Simulated GRFs (Fig. 8.3) were derived, and in their general pattern were very similar to the forces measured by forceplate studies of real human adults in loaded walking, suggesting that the gait of AL-288-1 and KNM WT-15000 was indeed similar that of modern humans.

As previously, joint moments and powers were considered as criteria for evaluating whether models were effective during loaded walking. Joint power, work done per unit time, is related to energy consumed by gait, and shows how much work biological tissues have to do to maintain a form of gait. The amount of power required indicates whether the form of gait is energy-effective. Joint moments and powers of all models are shown in Figs. 8.4 - 8.5, and all forms of powers are compared in Tables 8.3 and 8.4. Power normalized by weight and velocity, or weight and displacement is presented in Figs. 8.6 a - c.

Different values for joint moments and powers were derived for different models, despite the use of identical motion functions (Fig. 8.6 a - c). Considering joint moments and powers alone, KNM WT-15000 requires the least joint power, and is thus the most mechanically effective on this criterion. AL-288-1 however spends almost 1.4 times more joint power than either KNM WT-15000 or modern humans.

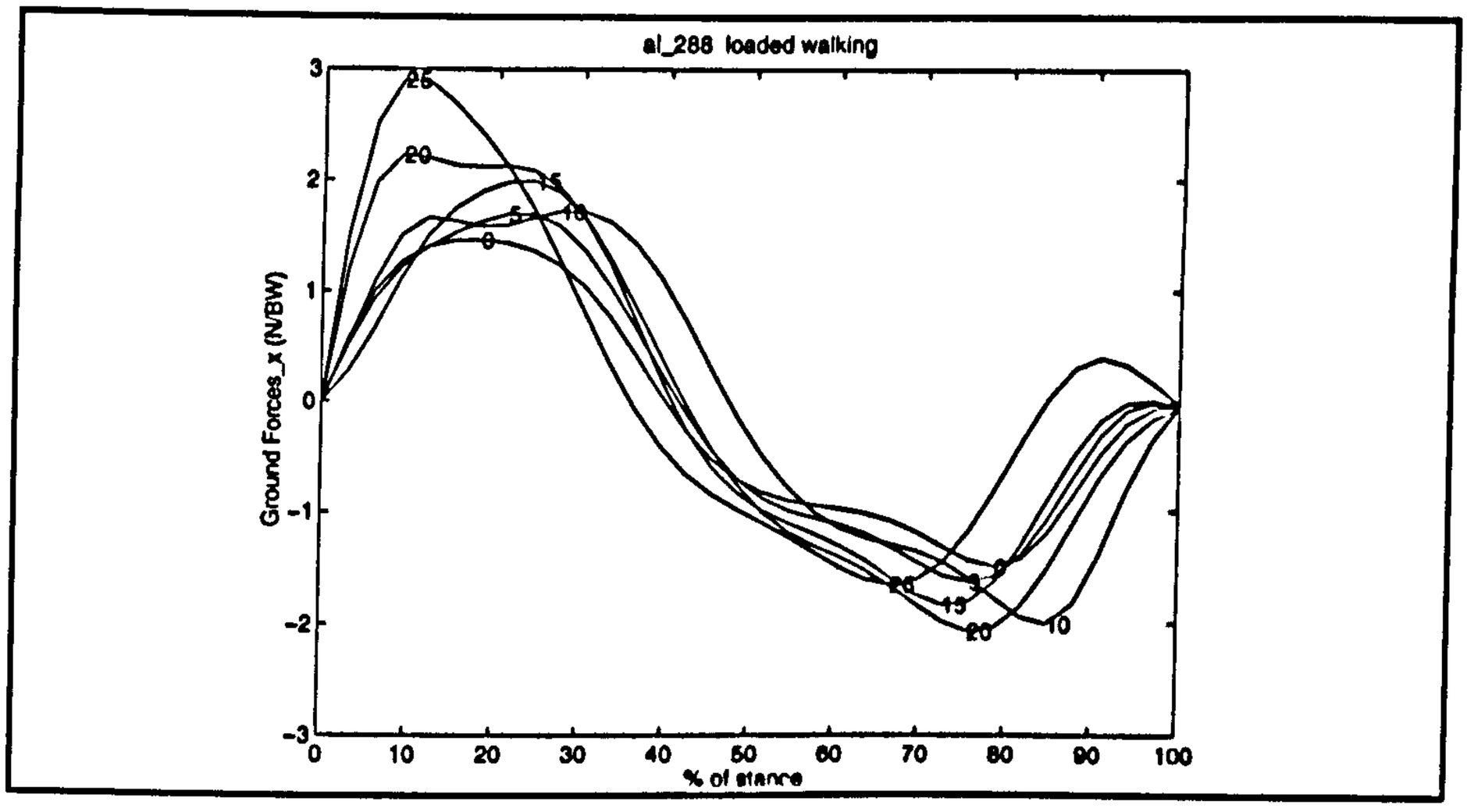

FIGURE 8.3.a. Simulated ground reaction forces, Fx: AL 288-1 under different loads. BW: body weight.

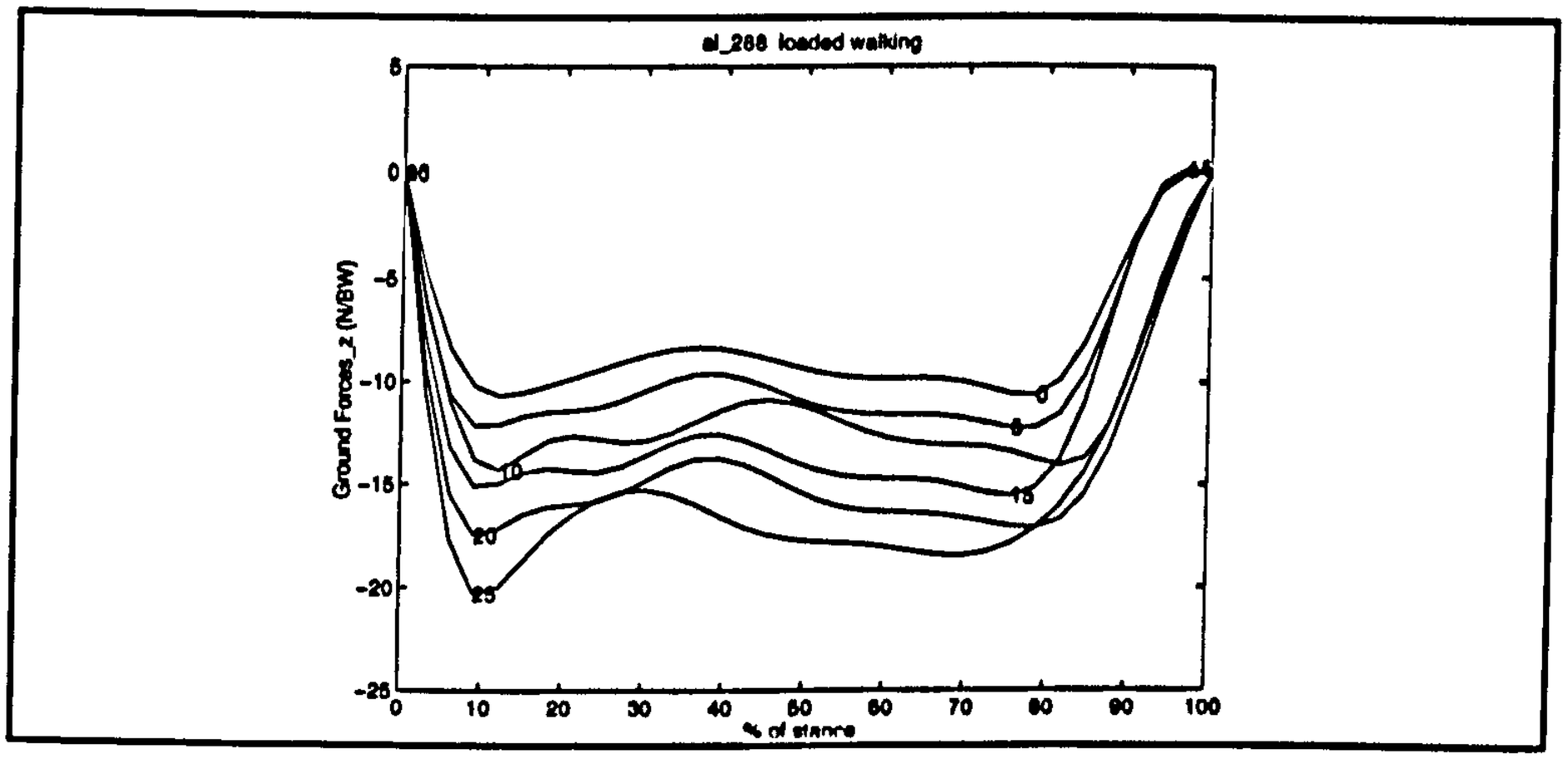

FIGURE 8.3.b Simulated ground reaction forces Fz: AL 288-1.

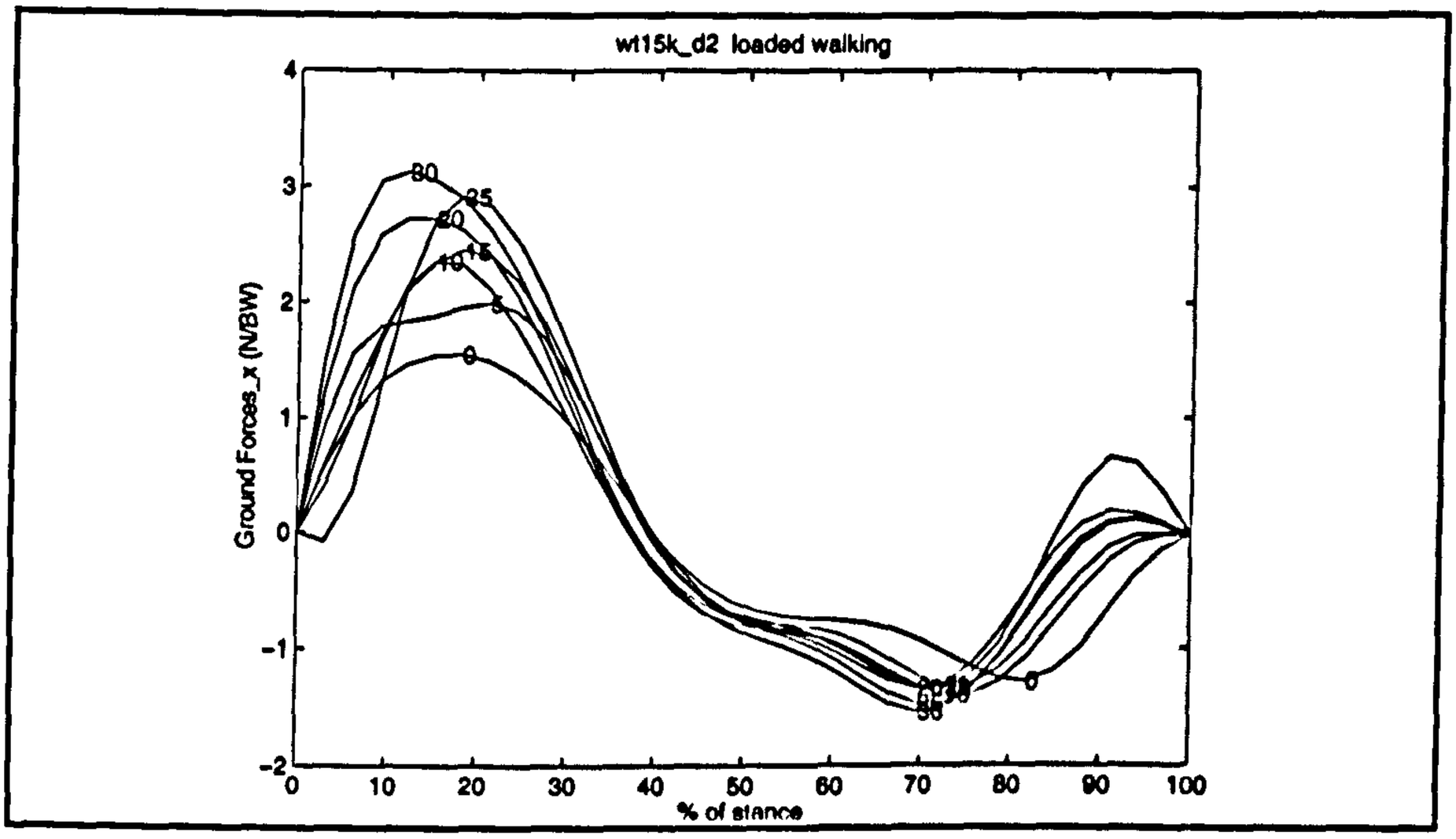

FIGURE 8.3.c Simulated ground reaction forces Fy, for KNM-WT 15000

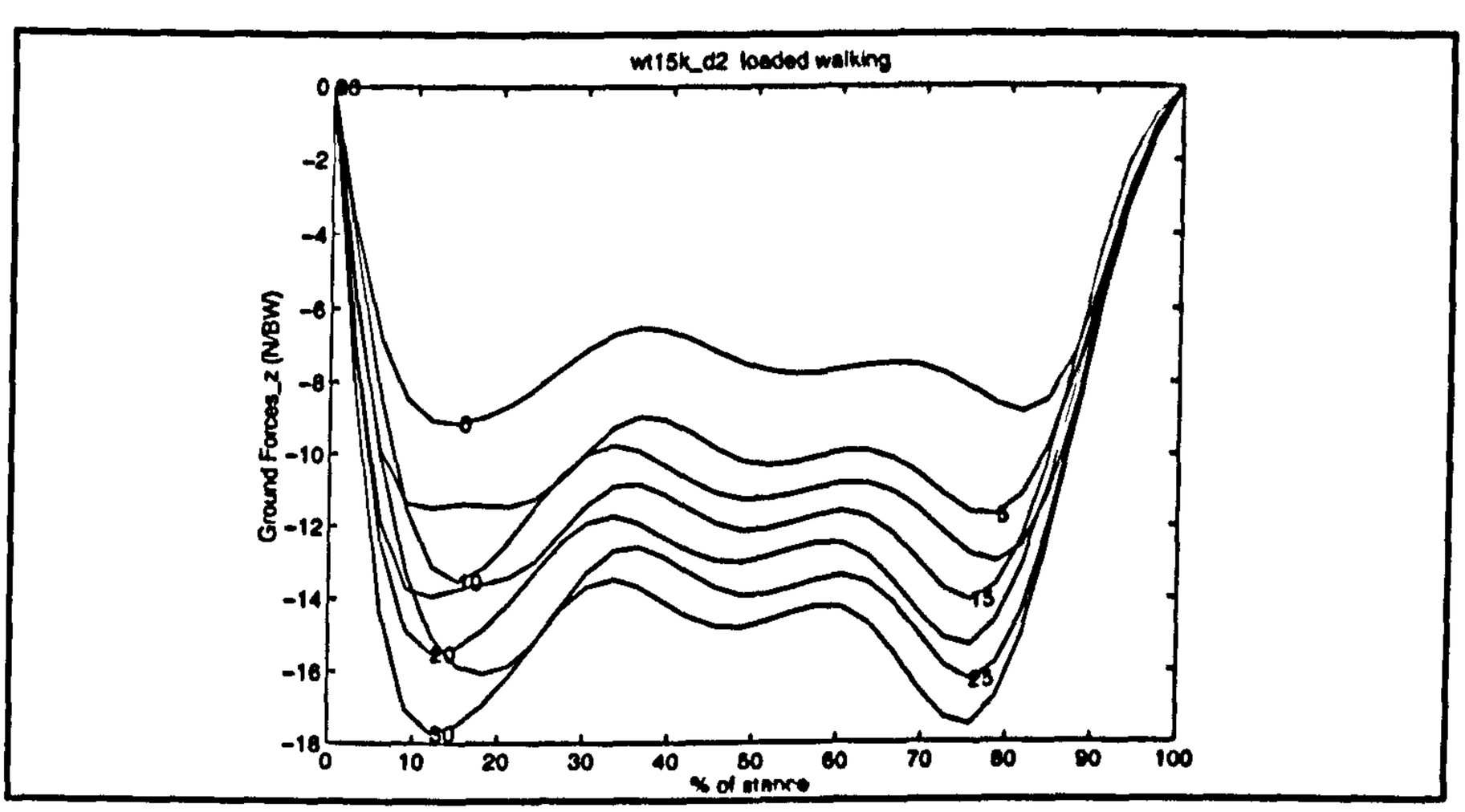

FIGURE 8.3.d Simulated ground reaction forces Fz, for KNM-WT 15000

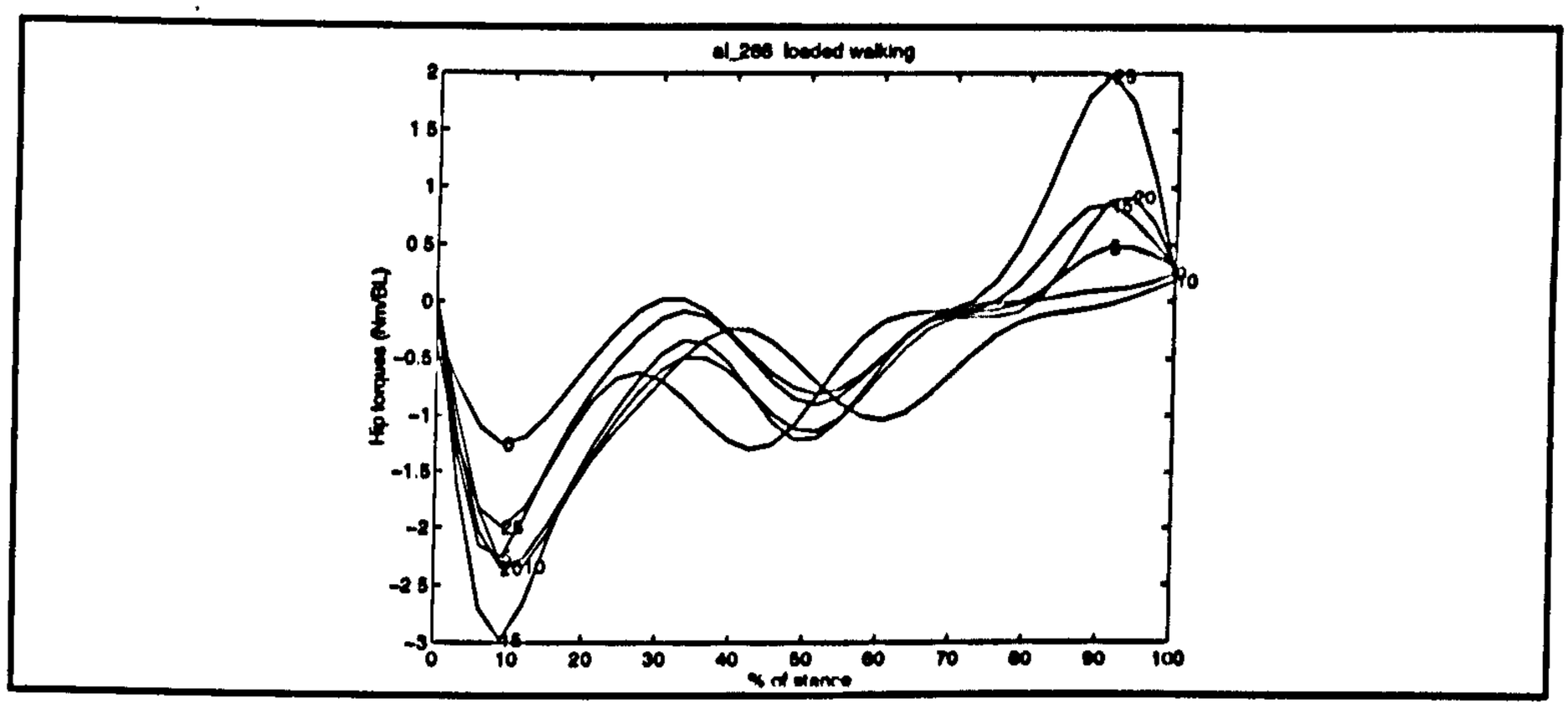

FIGURE 8.4.a Simulated joint moments at hip for AL 288-1
Nm: Newton x m, BL: body weight x leg length.

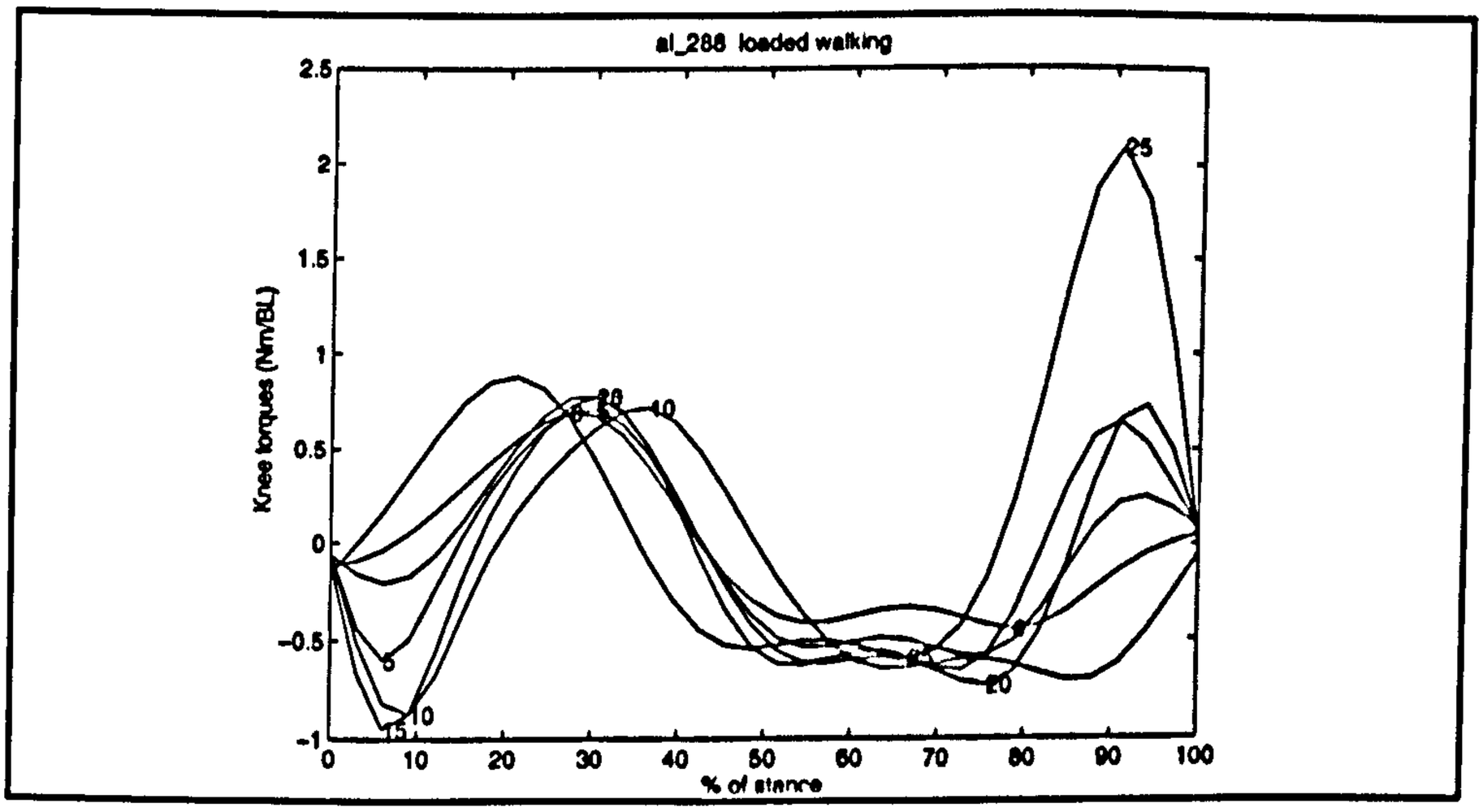

FIGURE 8.4.b Simulated joint moments: AL 288-1, at knee

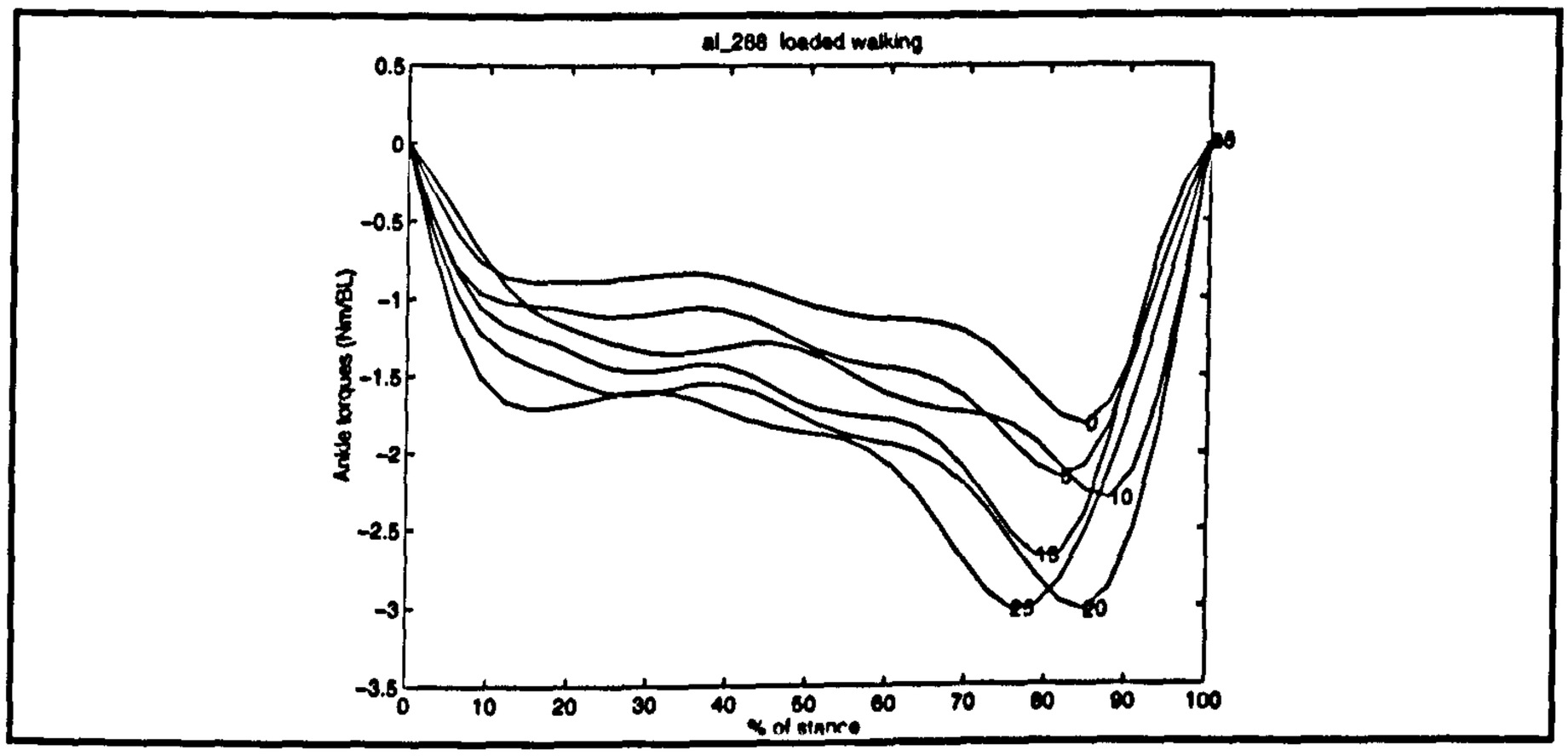

FIGURE 8.4.c Simulated joint moments: AL 288-1, at ankle

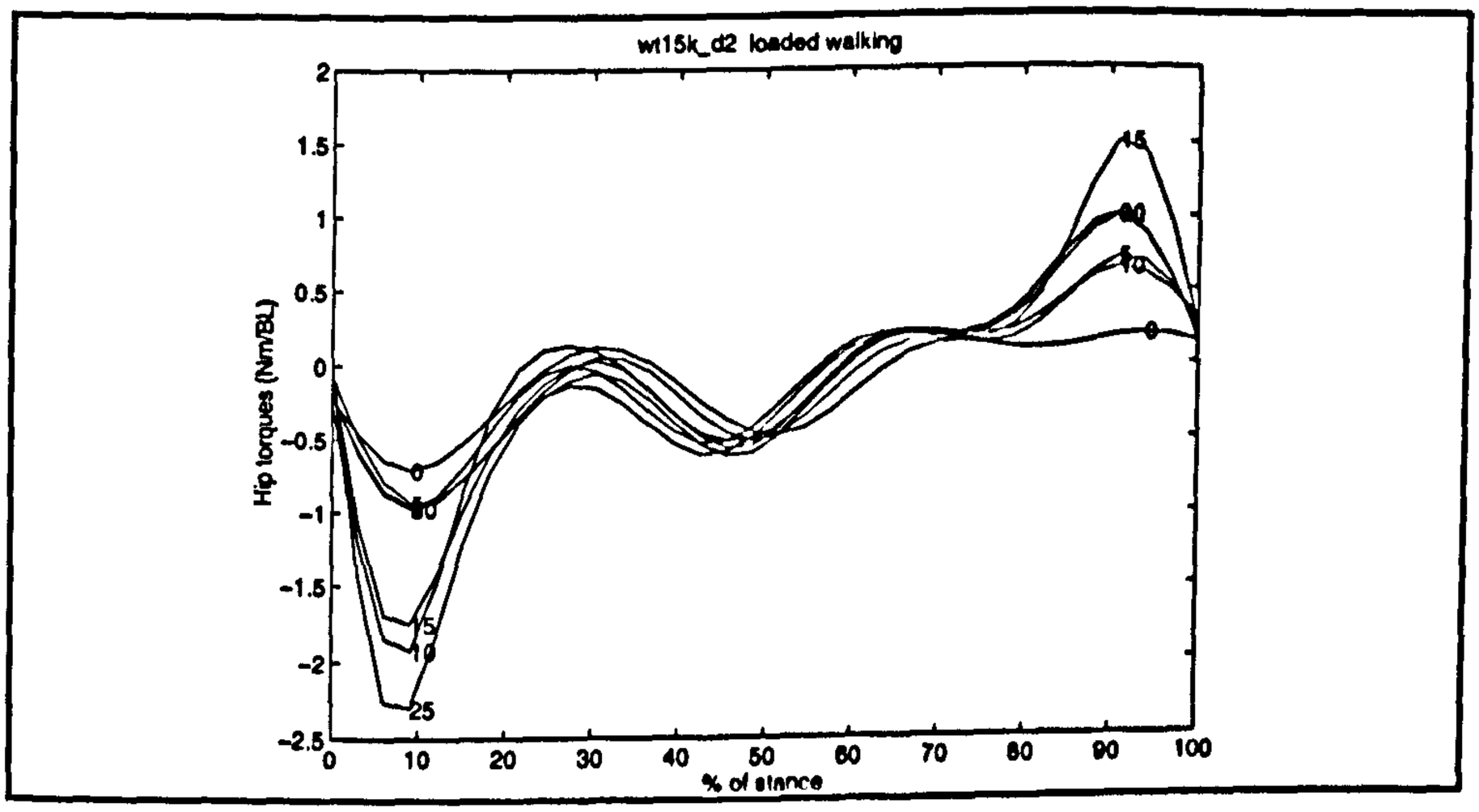

FIGURE 8.4.d Simulated joint moments: KNM-WT 15000, at hip

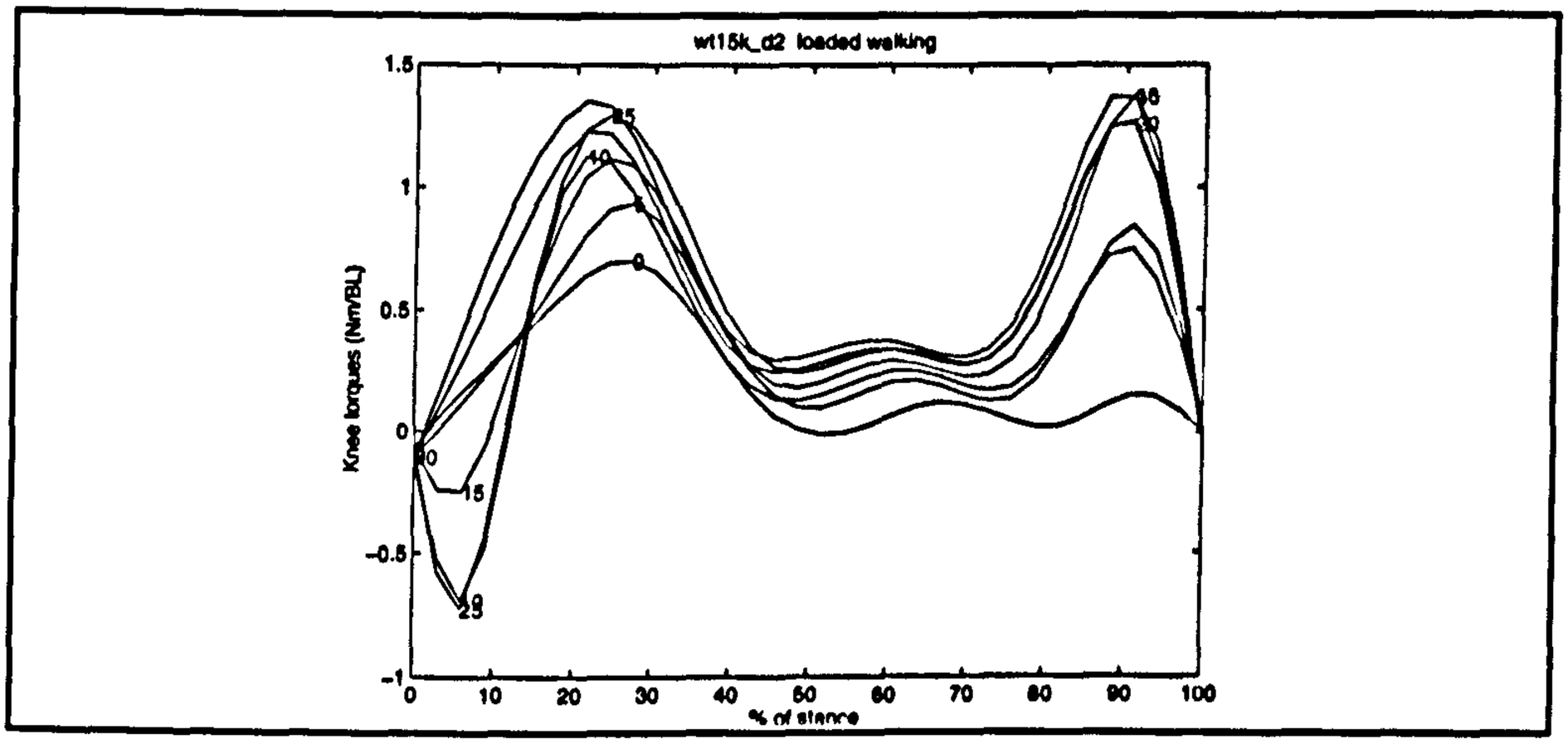

FIGURE 8.4.e. Simulated joint moments: KNM-WT 15000, at knee

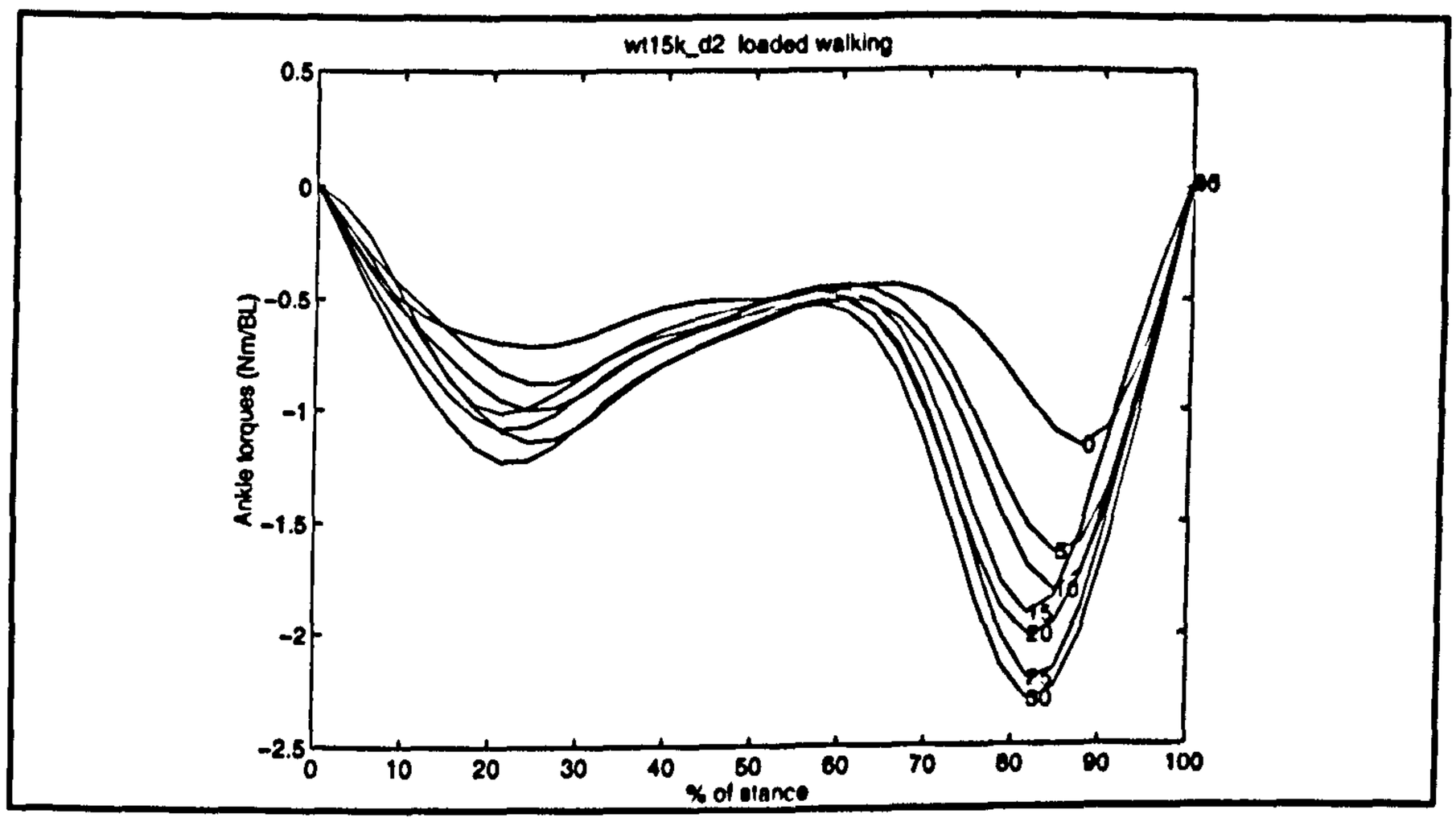

FIGURE 8.4.f. Simulated joint moments : KNM-WT 15000, at ankle

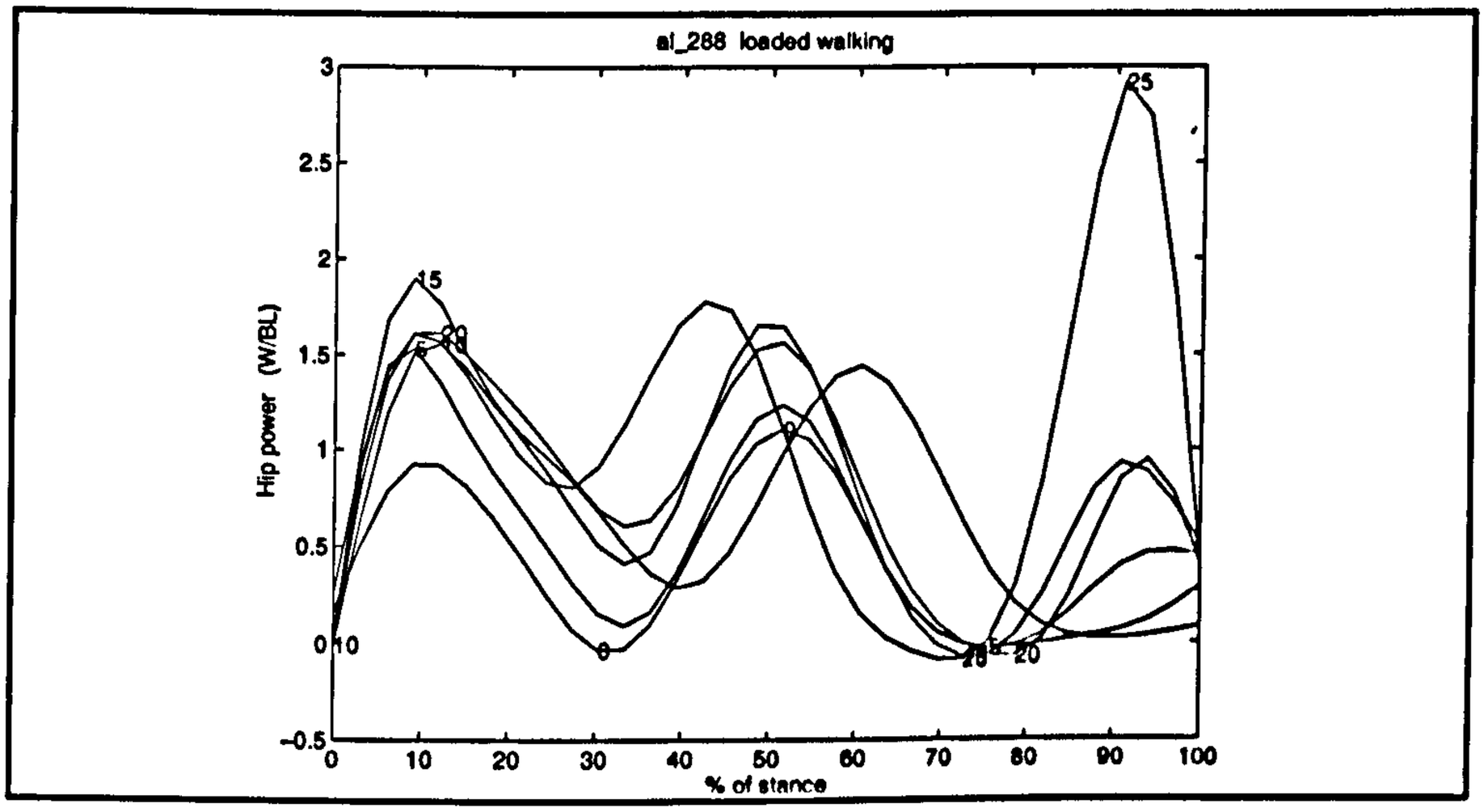

FIGURE 8.5.a Simulated joint powers: AL 288-1, at hip

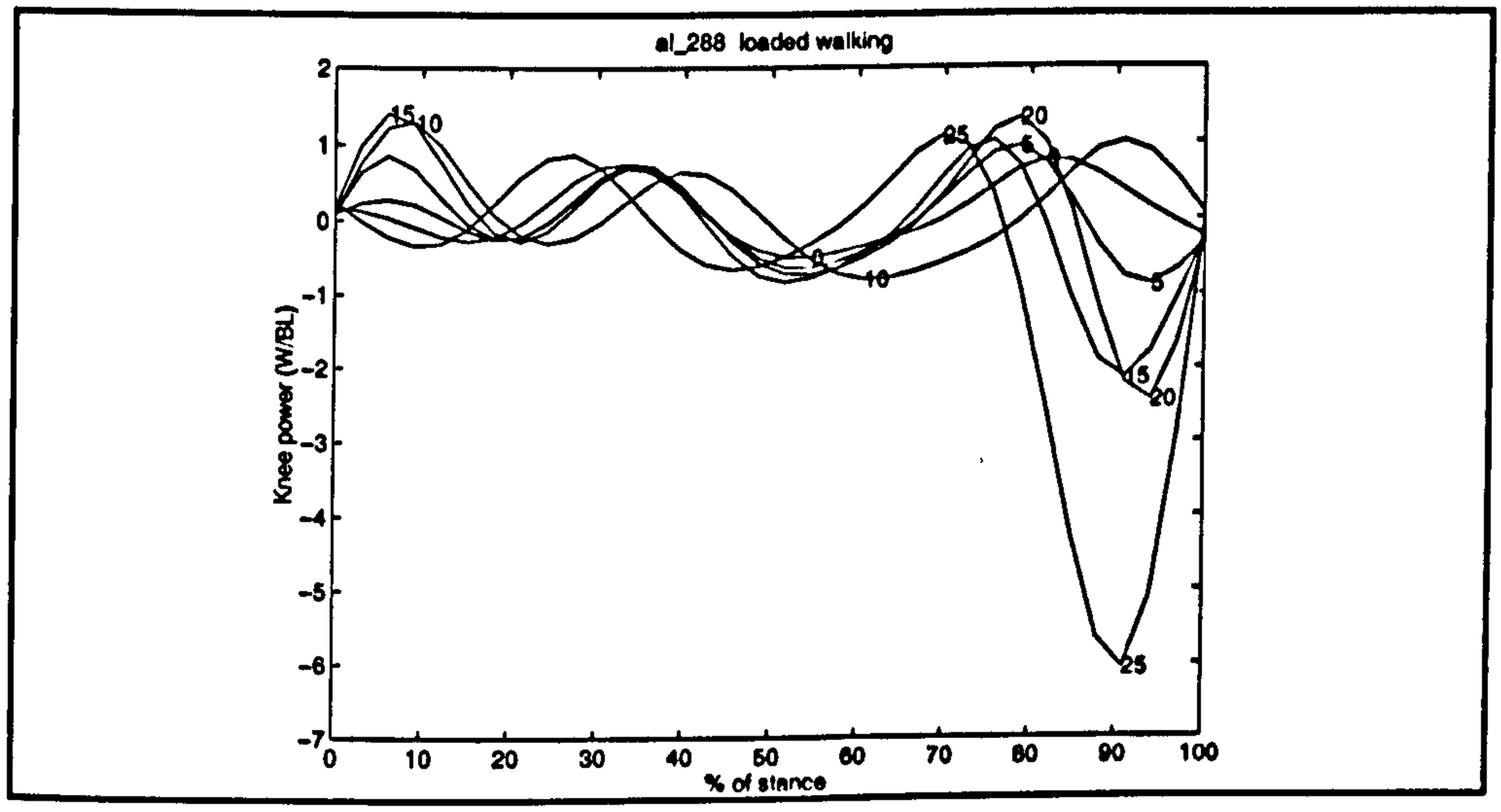

FIGURE 8.5.b Simulated joint powers: AL 288-1, at knee

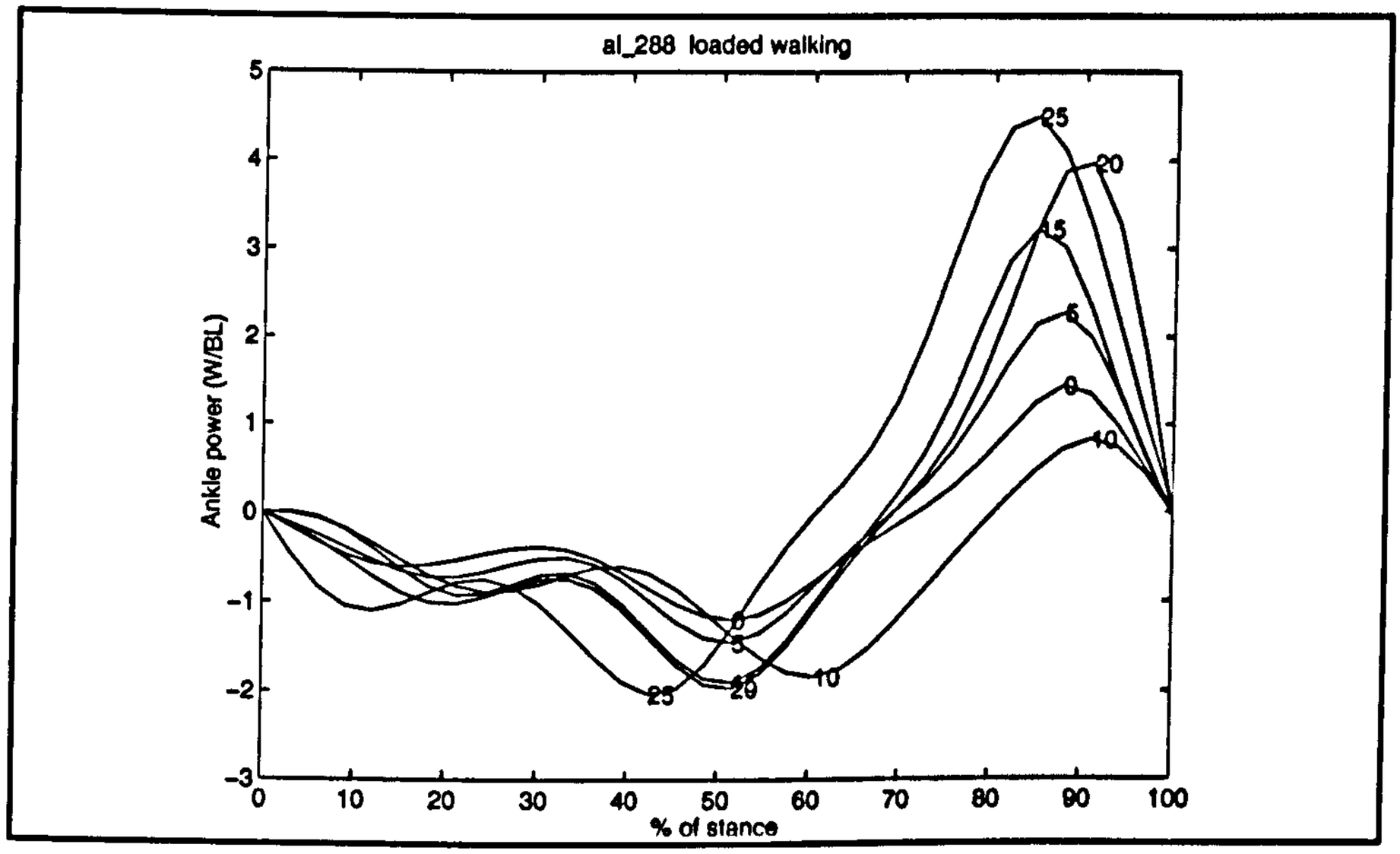

FIGURE 8.5.c Simulated joint powers for AL 288-1, at ankle

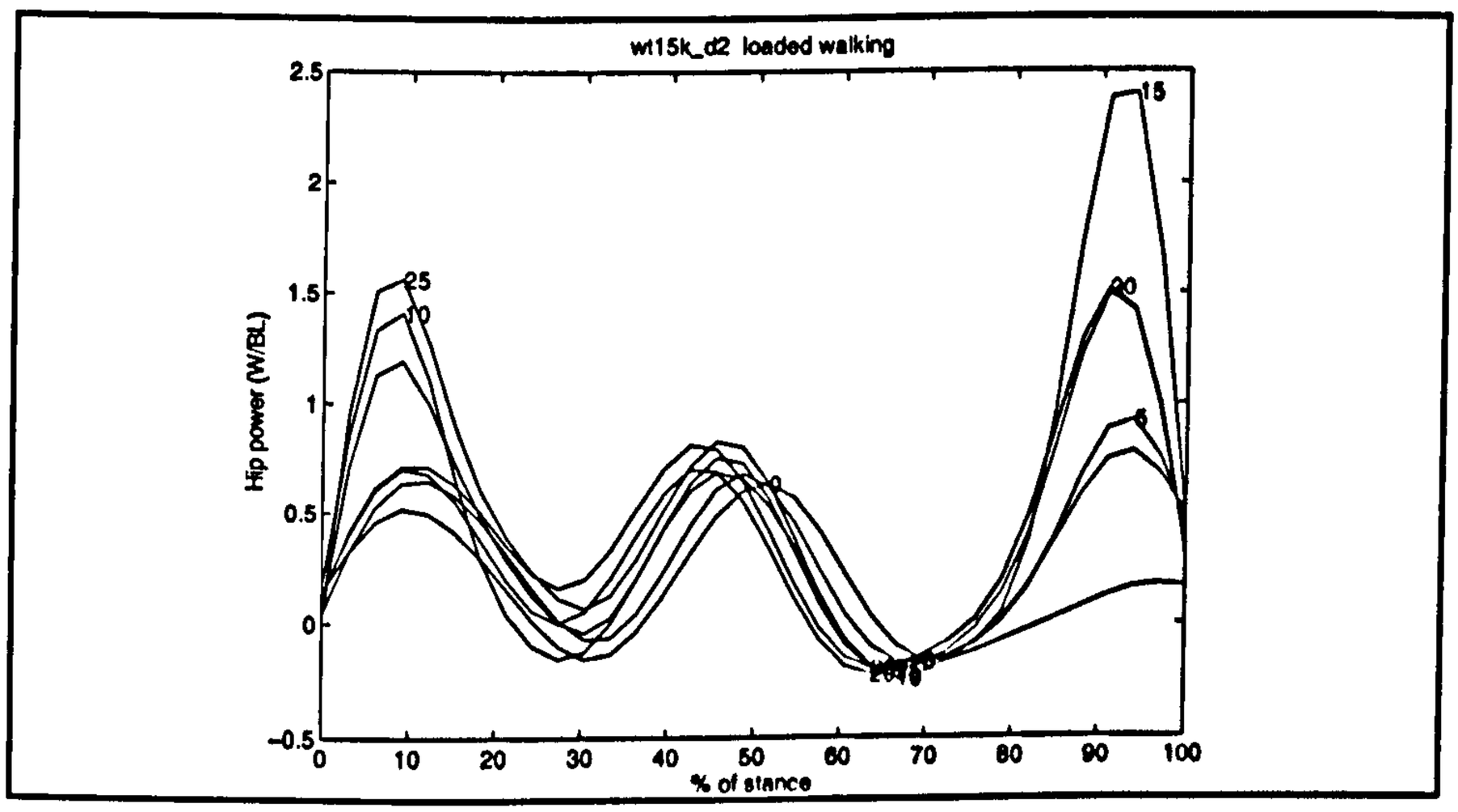

FIGURE 8.5.d. Simulated joint powers for KNM-WT 15000, at hip

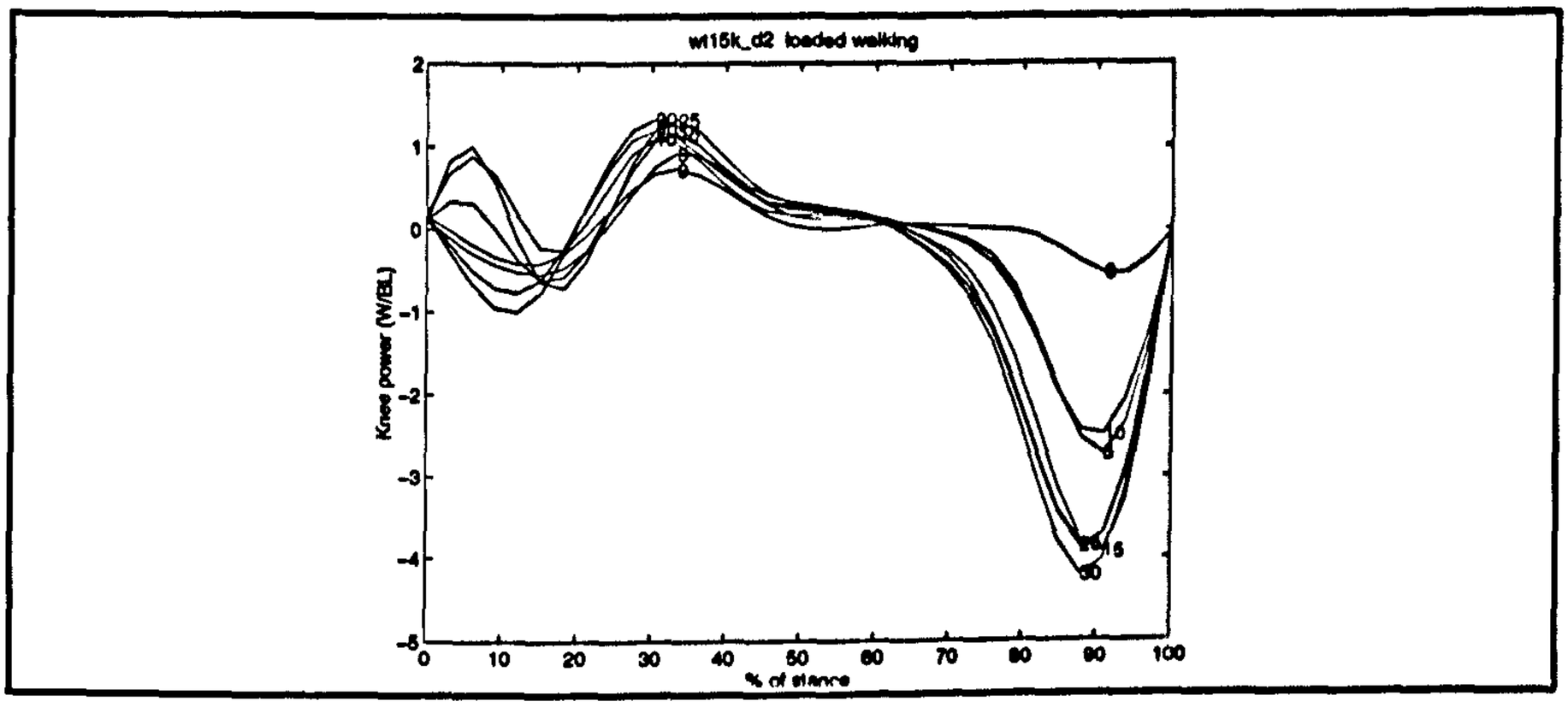

FIGURE 8.5.e. Simulated joint powers for KNM-WT 15000, at knee

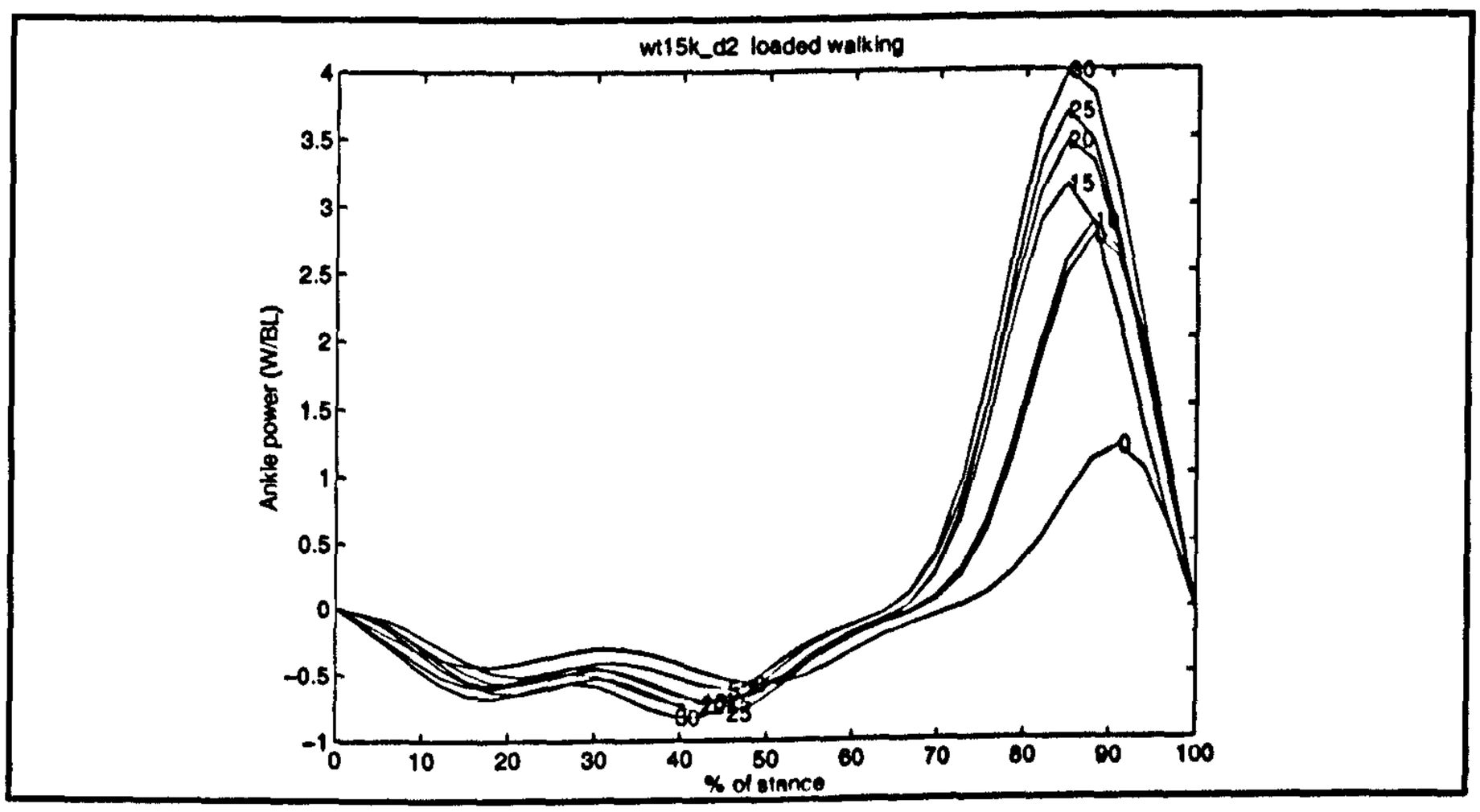

FIGURE 8.5.f. Simulated joint powers for KNM-WT 15000, at ankle

To facilitate comparison of the different models, we needed to normalize joint powers to create dimensionless parameters. Various approaches exist: 1) normalization by body mass (kg), speed (m/s) of CM and forward acceleration (m/s^2) (see Fig.8.6.a); 2) normalization by body weight (kg and gravity) and speed of CM in m/s (Alexander, 1992) (see Fig. 8.6.b). This is a classical method, but it uses the gravity constant, g, to replace horizontal acceleration; and 3) normalization by body mass (kg) and displacement (m) of CM (Taylor et al. 1980; and Cavagna et al. 1976) (see Fig. 8.6.c). This method is easily understood and widely used, but it does not provide a dimensionless measure of power. I favour instead method 1, which does provide a dimensionless measure of power, and as the acceleration due to gravity acts only in a vertical direction, replaces it by the horizontal acceleration of the CM. The figures show that the three methods may lead to different results., but whatever the method used, the WT 15000 model uses less power than other models, when carrying light loads (less than 15% body weight), although its curve converges with those of modern humans at loads of 20-30% body weight and exceeds them above 35% body weight. A curious finding is that AL-333 uses less power than all other models with the exception of the modern human athlete: this is however a fragmentary fossil and the reconstruction is relatively unreliable.

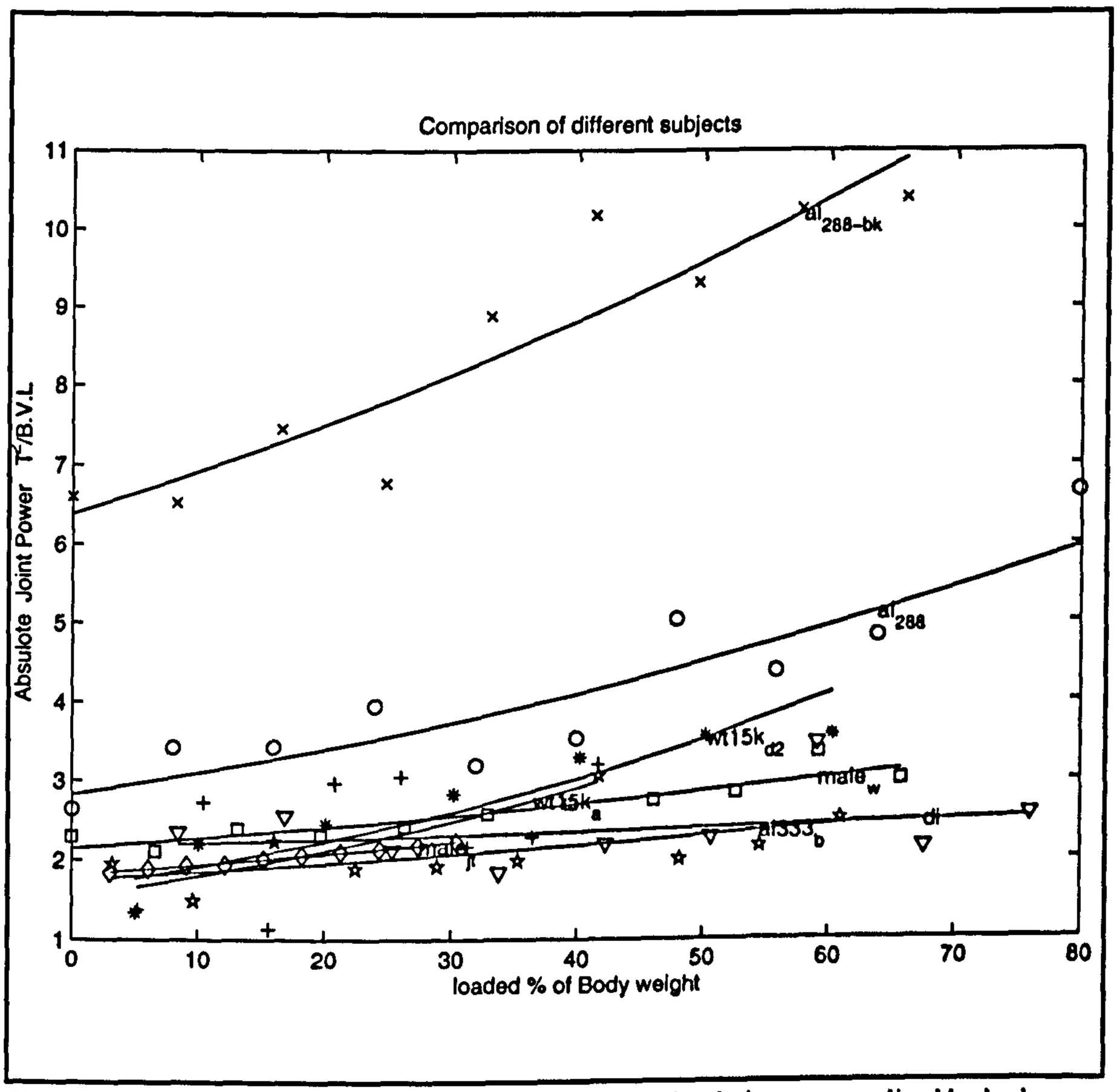

FIGURE 8.6.a Comparison of power between different simulations, normalised by body mass (kg), speed (m/s) of CM and forward acceleration (m/s^2).

Al288-bk: AL-288-1 in BHBK walking; al333-b: AL-333-1, a male *Australopithecus afarensis*, 1.5 m height and 80 kg weight; wt15k-d2: WT 15000 short-stature model; wt15k-a: WT 15000 tall-stature model; male_w: male human adult height 1.75 m, weight 76 kg weight; di: male child, 12 years old, 30 kg, 1.4 m height; male_jt: male adult human athlete, 1.8 m height, 80 kg weight.

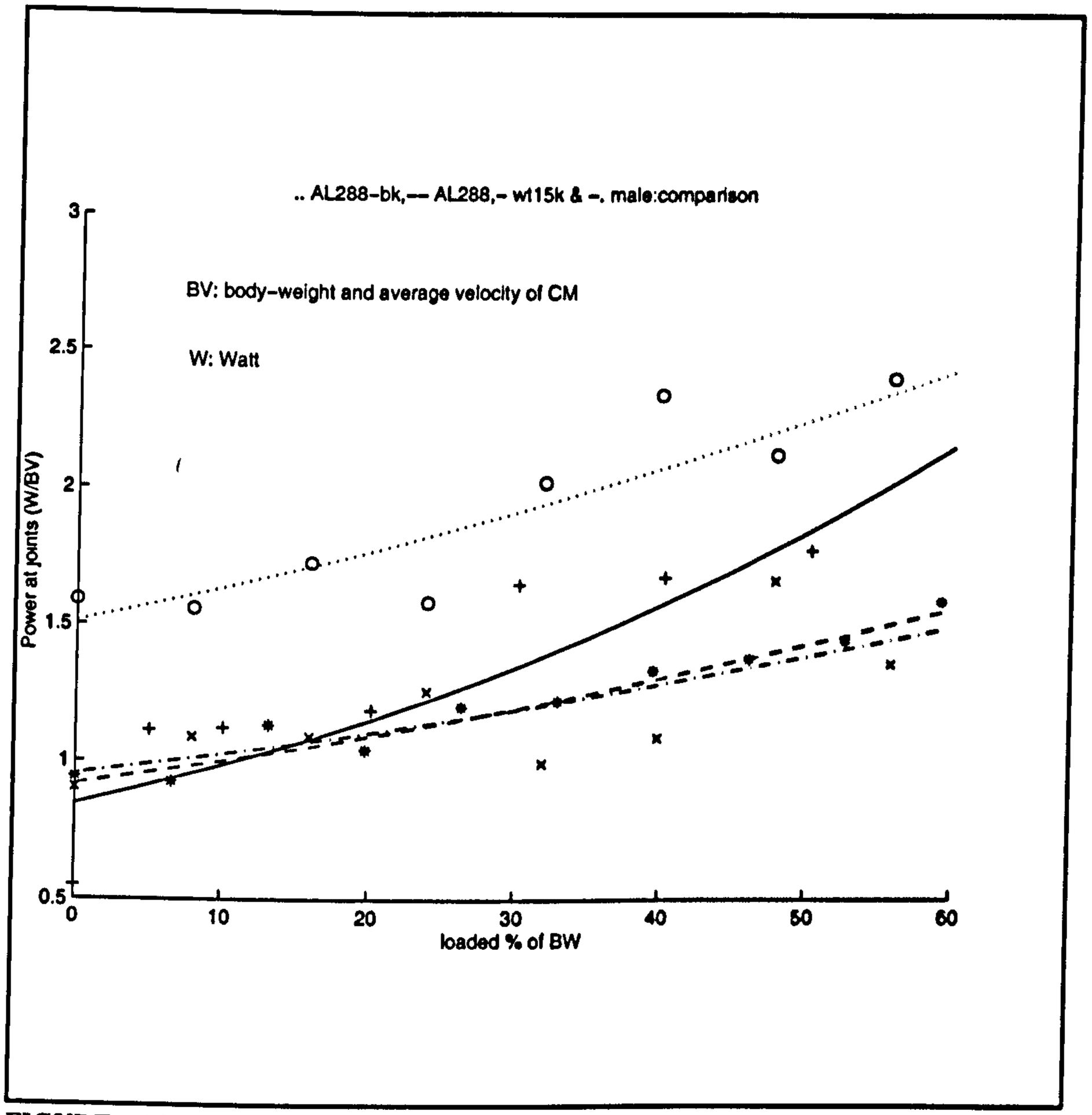

FIGURE 8.6.b Comparison of power between different simulations, normalization by body weight (kg and gravity) and speed of CM in m/s (Alexander and Goldspink 1977) Abbreviations as Fig. 8.6.a.

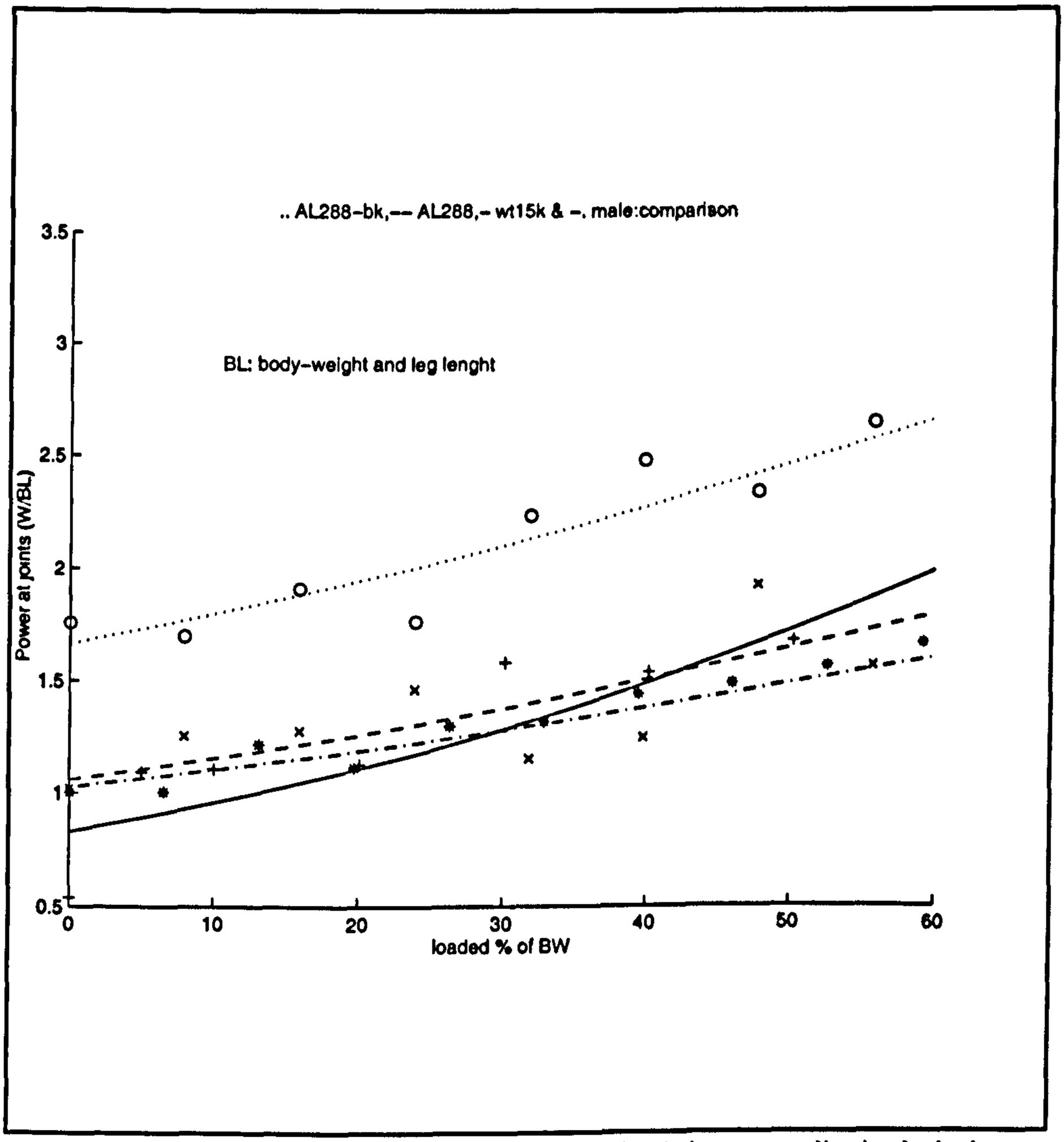

FIGURE 8.6.c Comparison of power between different simulations, normalization by body mass (kg) and displacement (m) of CM (Taylor et al. 1980 and Cavagna et al. 1976) Abbreviations as Fig. 8.6.a.

8.2.2 Reasons for differences between models

One of main reasons for the differences may be the ratio of the upper body to lower limb length. A longer trunk will increase the segment principal moments of inertia, and according to the theory of the moment of momentum, when lower limb lengths remain constant, but the trunk increases in length, moments at hip have to increase to maintain upper body stability. This possibility is in agreement with the discussion in Preuschoft and Witte (1991).

8.2.3 Conclusions

The results show clearly that WT-15000's proportions offer a strong advantage over AL-288-1 in load carrying, while the disadvantages of BHBK walking for AL-288-1 reported by Crompton et al. (1998) are greatly increased when loads are carried.

CHAPTER 9. MUSCULOSKELETAL MODELS OF FOSSIL SPECIES AND THE EVOLUTION OF BIPEDALISM

If a load is increased the optimum frequency remains the same: if the load is too great for that frequency to be kept up it is better to change gear.

A. V. Hill (1950)

Abstract

This chapter attempts to predict the pattern of muscle forces in erect and BHBK walking in modern adults, and the early hominids AL-288-1 and WT-15000 based on a simplified model of the musculoskeletal geometry of the lower limb. Despite its preliminary nature, the model predicts the general pattern of muscular activity in human erect and BHBK walking as revealed by EMG, quite well, and it may therefore be regarded as a reasonable representation of biological reality. The model shows that muscle forces are larger in BHBK walking than in erect walking, and have to output more power. Muscle moment arms and velocities will be smaller in BHBK than in erect walking, and muscle length ranges will also be relatively small.

9.1 Introduction

So far, we have investigated the bipedalism of early hominids using particle mechanics or multi-rigid-body models. A study of the biomechanics of the locomotor system cannot however be complete without an attempt to study the motive source of the locomotor system, the muscles. At this stage, such a study, which is attempted in this chapter, can only be tentative and exploratory.

Many have tried to calculate muscle forces, using a variety of techniques including mathematical optimization (Morrison 1970; Seireg and Arvikar 1973; Khalil et al. 1976; Hatze 1977; Crowninshield 1978; Hardt 1978, 1978a and Hase 1996) or from EMG data (Hof and Berg 1981; Patriarco et al. 1981; Olney and Winter 1985; Jacobs et al. 1996).

A range of studies of nonhuman primate muscle mechanics also exist (eg. Kumakura 1989; Hirasaki et al. 1996) but few if any have investigated the relationship between muscle force and gaits for early hominids. In this chapter, I attempt to reconstruct muscle forces and powers in early hominids during bipedal walking.

My approach is as follows.

1) We apply data on muscle attachments in modern humans to the available data on lengths of bones in early hominid skeletons, and use the resulting geometry to build musculoskeletal models of the early hominids AL-288-1 and WT-15000. In this study, we confine our attention to the lower limb.

2) Joint motion and joint moments from different gaits are input to the models, and using mathematical optimization, muscle forces are calculated.

3) Calculated muscle forces are verified by comparison with EMG data measured from living human subjects during bipedal walking. If the calculated muscle forces have similar activity patterns to EMG data, the calculated muscle forces are treated as realistic.

4) We compare muscle parameters, including forces and powers calculated for musculoskeletal models for AL-288-1, WT-15000 and modern humans walking in different gaits.

Table 9-1 Skeletal dimensions of early hominid fossils and a small modern human sample

	Measurements (cm)										
Subject	PW	PH	FL	FHW	FKW	TL	TKW	TAW	FOL	HA	PKW
AL288	8.53	17.47	28.1	2.7	2.4?	23.0?	3.1	2.4	?	2.6?	2.0?
Wt15k	11.5	20.1	42.8	4.4	5.8	34.8	4.8	3.7	?	3.0?	2.0?
A/W	0.74	0.87	0.66	0.61	0.41	0.80	0.66	0.65	?		
Modern Adults:											
male	11.0	19.0	42.0	4.3	6.0	35.0	4.5	3.5	23.0	3.25	2.0
Female1	10.5	19.0	41.0	4.0	5.5	35.5	5.0	3.5	21.0	3.0	2.0?
Female2	10.0	19.5	41.0	4.1	5.5	36.5	4.5	3.5	21.0	3.5	2.0

Definitions of measurements are graphically defined in Figure 9.1
Question marks indicate estimated measurements. A/W: ratio of data in AL-288 and WT15k.

9.2 Musculoskeletal models of fossil species

9.2.1 Assumptions

For the purposes of this exploratory study, we have not attempted to measure muscle attachments directly from fossil specimens, as high-resolution measurements of the original specimens would be necessary. We assume instead not only that the internal geometry of muscles of fossil species (which we can never know) would have been similar to that of modern humans, but that the attachments to bones would have been at the same locations and proportions of the bone lengths as it is in living humans. We further assume point origins, and measurements for our models were made only in the sagittal plane.

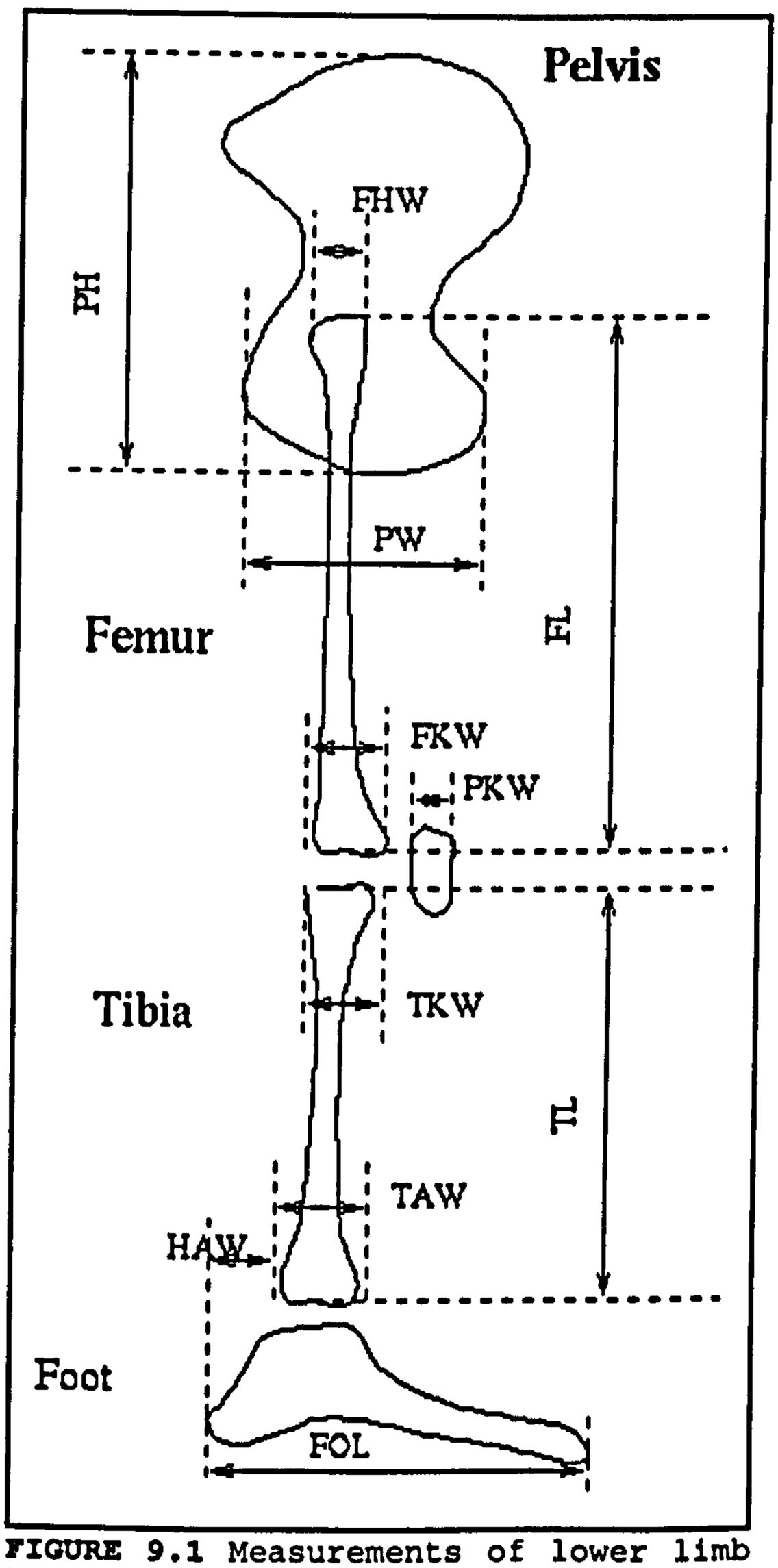

FIGURE 9.1 Measurements of lower limb bones in the sagittal plane. See Table 9-1 for abbreviations.

9.2.2 Measurements used

The measurements made on bones are shown and graphically defined in Fig. 9.1 and tabulated in Table 9.1. Data from the literature (Johanson et al. 1982) was used almost exclusively for

AL-288-1, but a complete cast was available for WT-15000 in our laboratory, and direct measurements could be made. Data was also obtained by measurement of modern adult human and chimpanzee skeletons in the Departmental museum. Where bones are missing in the fossils, estimates were made by reference to modern humans and chimpanzees. Where there is a large difference between the two, the human case was adopted.

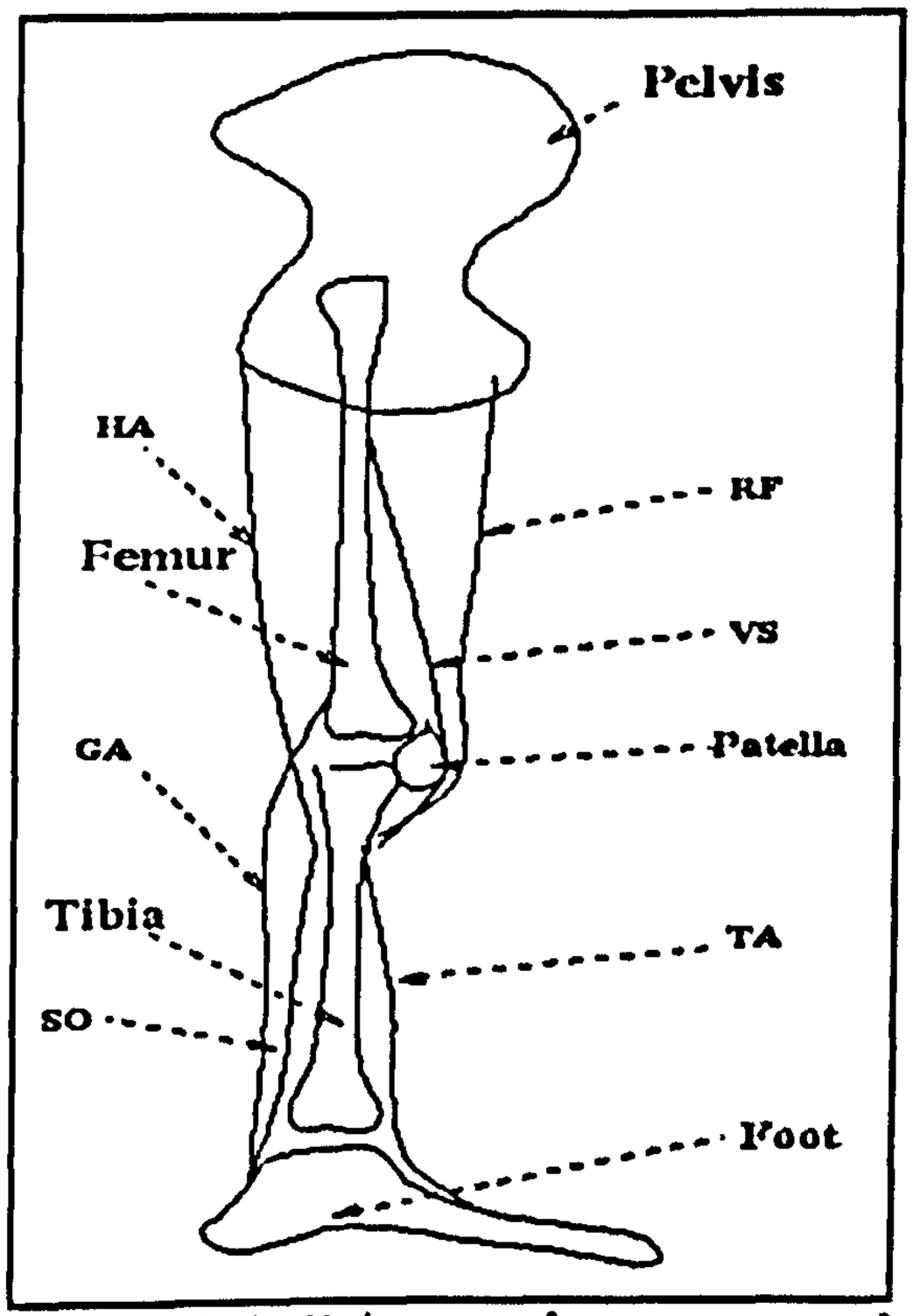

FIGURE 9.2 Main muscle groups and attachments in musculoskeletal models.

9.2.3 Muscle attachments

To simply our model, only seven main muscles and muscle group were considered : rectus femoris (RF), vastus lateralis/medialis (VS), Biceps femoris/semitendinosus/semimembranosus (HA), gastrocnemius (GA), gluteus maximus (GU), tibialis anterior (TA) and soleus (SO) (see Fig.9.2). The muscles/muscle groups were chosen as among those which play major roles during bipedal walking. Names of muscles/muscle groups represent only broad functional units, which reduces the error resulting from inaccurate attachments.

9.3 Calculation of muscle parameters

9.3.1 Local reference frames

To compute muscle force and power, kinematic parameters of muscles including length, velocity and moment arms, must first be calculated. To do so, we have defined reference frames at the hip, knee and ankle joints, with two reference frames at each joint: a proximal frame, fixed at the proximal segment, and a distal frame fixed at the distal segment (see Fig. 9.3). For example, at the hip there is a reference frame fixed at the pelvis, and another at the femur. In this way, we may conveniently calculate muscle motion as a joint rotates a given relative angle.

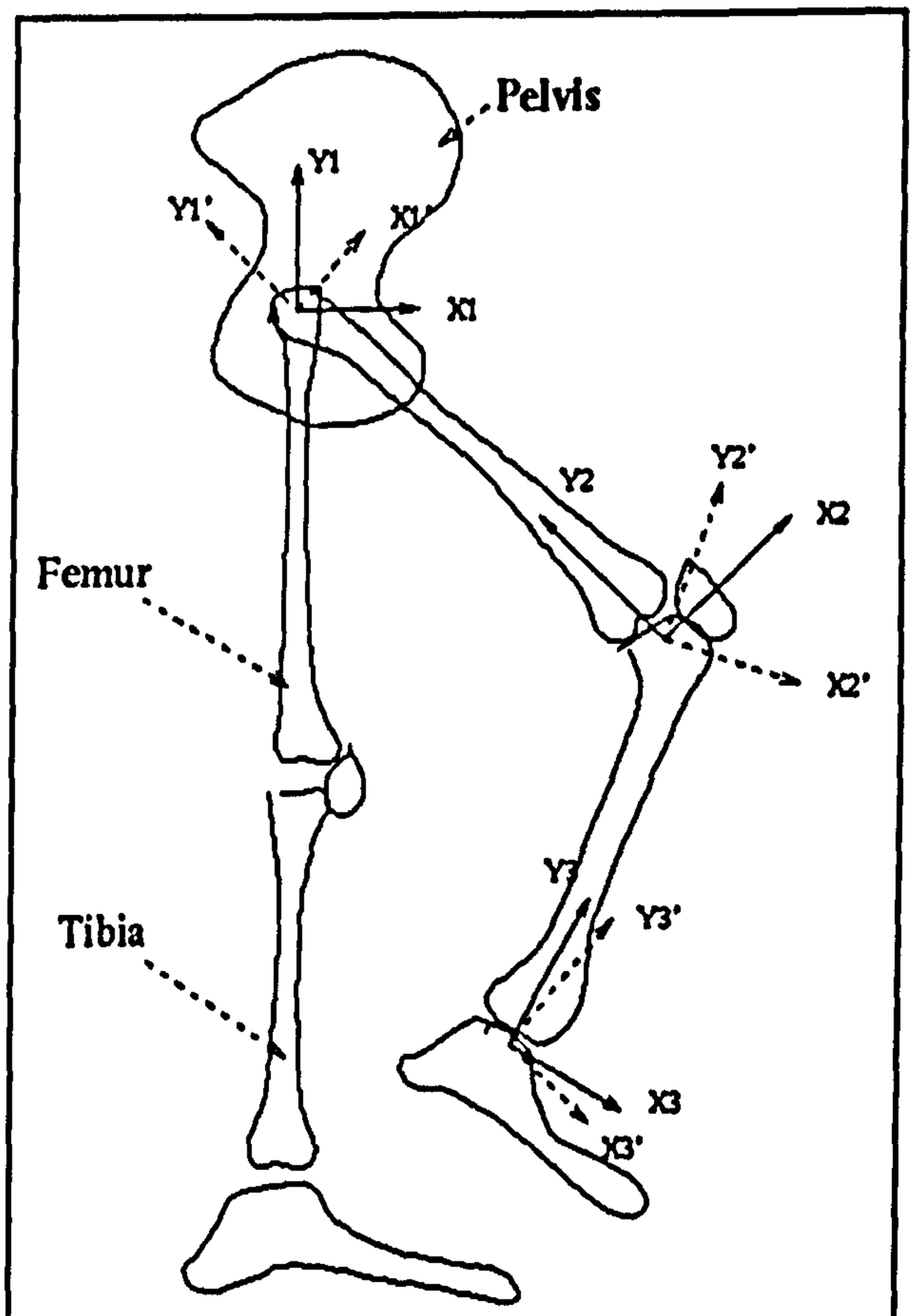

FIGURE 9.3 Explanation of the relationship between the proximal and distal frames.

9.3.2 Muscle length and velocity

The distal frame enables us to utilize relative joint angles between segments, which are relatively easy to obtain in actual experiments on walking. In the distal frame, muscle attachments of course maintain unchanged attachments. The whole distal frame rotates about the same centre as the proximal frame (see Fig. 9.3). Under these conditions, coordinates in the two frames have a relationship as follows:

$$p_1 = R \cdot p_2 \qquad (9.1)$$

where p_1 and p_2 are coordinates in the proximal and distal reference frames respectively, and; R is the rotation matrix;

$$R = \begin{matrix} \cos() & \sin() \\ -\sin() & \cos() \end{matrix} \qquad (9.2)$$

where () - relative joint angle between two reference frames;

If we define a muscle attachments in a frame (segment), we can easily calculate the attachments' coordinates from the other reference frame. However a segment rotates, we can calculate muscle lengths in either the proximal system or the distal system.

For example, if a muscle, such as VS, originates on point p_1 on femur, passes through point p_2 on the patella (which we have assumed to be fixed on the femur) and inserts on point P_3 on the tibia, the muscle length should be the sum of the distance of p_1 - p_2 and p_2 - p_3.

$$L_m = D(p_1, p_2) + D(p_2, R \cdot p_3) \qquad (9.3)$$

where L_m - muscle length; D - distance between two points; R - rotation matrix, decided by the relative angle between the two frames;

The method is very convenient for calculating muscle parameters. If the local coordinates of each muscle and the relative joint angle are given, a multi-joint muscle's length can easily be calculated. For a biarticular muscle, over both joints, we apply (9.3) twice to calculate total muscle length.

Once the muscle lengths in each time interval of a sequence of walking are worked out, muscle contraction or stretching velocity can be computed:

$$v_m = \frac{dL_m}{dt} \qquad (9.4)$$

where v_m - muscle velocity (m/s) and dt - time interval.

Contraction is defined as positive muscle force, and eccentric action of a muscle as negative muscle force. Similarly, contractive muscle velocity is defined as positive and eccentric velocity as negative. When a muscle force and a velocity have same direction, positive power is produced, otherwise, negative power.

where P_m - muscle power (W); F_m -

$$P_m = F_m \cdot v_m \qquad (9.5)$$

muscle force (N) and v_m - muscle velocity (m/s);

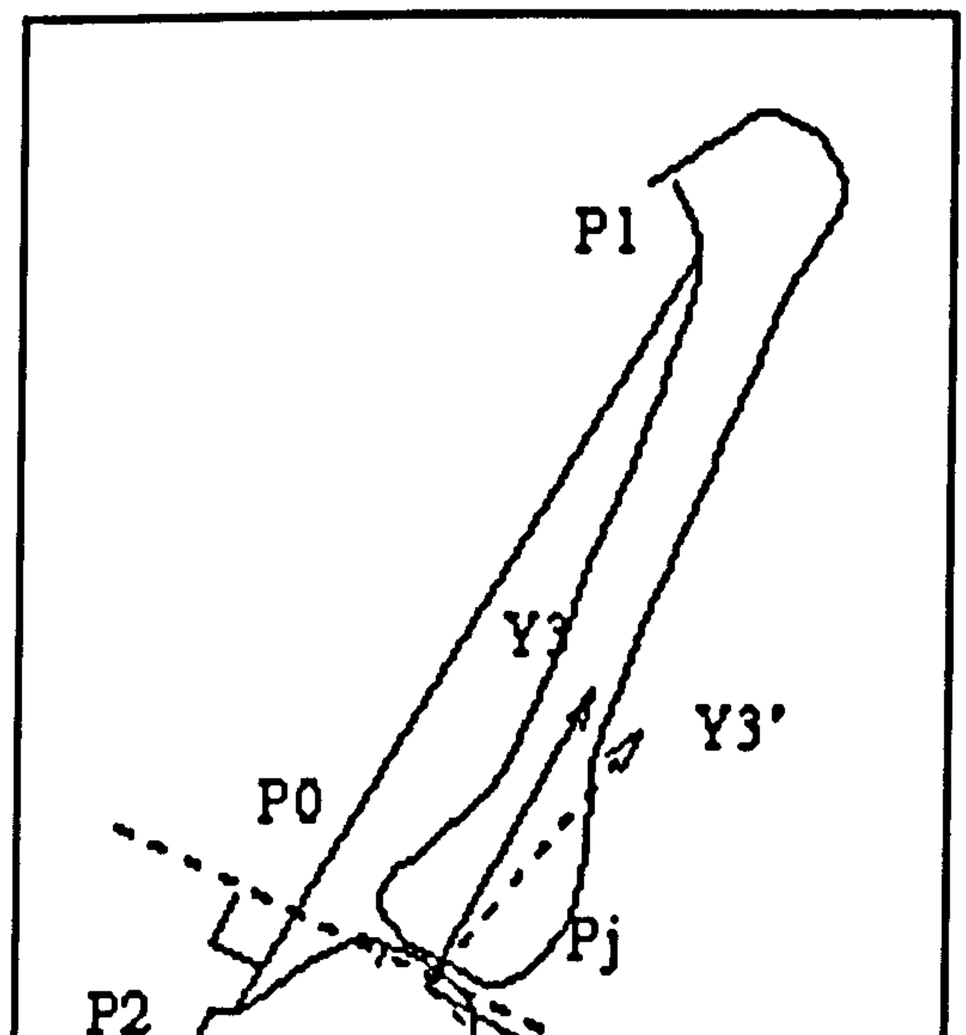

FIGURE 9.4 Measurement and calculation of muscle moment arms.

9.3.3 Moment arm of muscles

If the muscle's local coordinates (on bones) and relative joint angle are given, the overall 'muscle fibre direction' (line of action) may be calculated. Thus, the muscle's moment arm about a joint can be worked out. Firstly, we have two vectors $v_1(p_1, p_2)$ and $v_2(p_0, p_j)$. (Fig. 9.4) When the two vectors come to lie at right angle, their dot-product should be 0. Secondly, p_0 must be on the same line as p_1 and p_2. Thus, we have condition functions 9.6.1 and 9.6.2.

$$0 = v_1(p_1, p_2) \cdot v_2(p_j, p_0) \qquad (9.6.1)$$

$$f_L(p_0) = f_L(p_1) = f_L(p_2) \qquad (9.6.2)$$

$$a_m = D(p_j, p_0) \qquad (9.6)$$

where, p_1 and p_2 are two points on a muscle; p_j is the instant centre of the joint; p_0 is a point shared by vectors v_1 and v_2; f_L is a line function decided by p_1 and p_2; a_m - muscle moment arm (m); v_1 - a vector between two points on the muscle; v_2 - a vector between p_0 and p_j.

Generally, p_1, p_2 and p_j are given, then p_0 can be calculated by 9.6.1 and 9.6.2. Thus, a moment arm can be calculated according to equation 9.6.

9.4 Calculation of Muscle Force

9.4.1 Mathematical Optimization

While muscle forces are undoubtedly responsible for producing joint moments to drive segment motion, it is less clear how many muscles work together to produce joint moments. Various authors (Hardt 1978; Cowninshield 1978; Jacobs and Bobbert, 1996; Patriarco 1981; Seireg and Arvikar 1973) have tried to solve the problem using optimization approaches, and the present study takes a similar approach to the problem as in these papers, building on their achievements.

I assume that in order to produce joint moments, the muscles around a joint work optimally to distribute their forces so that the total muscle force reaches the minimum necessary. With the help of mathematical optimization, we can express the problem as follows.

$$\begin{aligned} &\textit{Object: minimum} \quad \Sigma(c_i \cdot F_{mi}(t)) \\ &\textit{subject: } F_m(t)\cdot A_m(t)=M(t),\ F_{mi}(t)\geq 0,\ i=1..n \end{aligned} \qquad (9.7)$$

where, F_m - a vector of muscle forces; A_m - matrix of muscle moment-arms; M - a vector of joint moments; c - coefficients

Equation (9.7) implies that the joint moments at three joints will be distributed among muscles in order to produce a minimum total of muscle forces.

Or:

$$\begin{aligned} &\textit{Object: minimum} \quad \Sigma(v_{mi}(t)\cdot F_{mi}(t)) \\ &\textit{subject: } F_m(t)\cdot A_m(t)=M(t),\ F_{mi}(t)\geq 0,\ i=1..n \end{aligned} \qquad (9.8)$$

Where F_m- vector of muscle force; A_m - matrix of muscle moment arms; M - a vector of joint moments; v_{mi}- muscle velocity in muscle i; n - total number of muscles. Equation (9.8) indicates that the joint moments at three joints will be distributed among muscles in order to produce the minimum total of muscle powers. Because of its physiological meaning, equation (9.8) may be a better expression of the relationship than equation (9.7).

In this chapter, there are 7 muscles and three joints under consideration. Therefore, M (in 9.7 and 9.8) includes hip, knee and ankle moments. Matrix Am includes the seven muscles' moment arms about the three joints. From the above, muscle moment-arms can be calculated. Further, the earlier chapters provide us with abundant joint moment data.

To solve equations 9.7 and 9.8, the Linear Program, a method of mathematical optimization (see general mathematical textbooks), is applied. Results for an example case are given in the next section.

9.5 Calculated Example Results

9.5.1 Normalisation of parameters

We assume that AL-288 and WT 15000 walked in several modes for which we have obtained numerous experimental recordings from real subjects. In previous chapters, we have calculated joint functions from video data, and joint moments from video data and forceplate data combined. To make our calculations more reliable, we input average joint functions obtained from 6 subjects to our musculoskeletal models.

To input 'actual' joint moment to a model, we transfer a real subject's joint moments to the model's moments as follows:

$$M = M_r \frac{mL}{m_r L_r} \qquad (9.9)$$

where M - model's joint moment; m - model's body weight; L - model's leg length; m_r - real subject's body weight; L_r - real subject's leg length; M_r - real subject's joint moment.

Joint angles are of course dimensionless. Therefore when we input M and joint angles to a model, we will obtain the model's 'actual muscle forces'.

9.5.2 Results for AL-288-1

Fig. 9.5 and 9.6 give example results for erect (NOR) and BHBK (BKW) walking

for AL-288-1 respectively.

We have further analyzed responses in other modes of gait, including normal walking (NOR), slow walking (SLO), fast walking (FAS), bent-knee walking (BKW), normal loaded walking (NLW) and bent-knee loaded walking (BLW). Since this chapter is only a tentative trial of our technique, we provide merely a summary of the main findings so far.

9.5.3 Summary of calculated results

1) muscle forces during BHBK unloaded and loaded walking are much larger (up to 4 times larger) than in during erect unloaded walking, at any speed, or for loaded erect walking.

2) muscle velocities during BHBK walking are less (30%-50% less) than during erect walking;

3) the moment arms of the major muscles/muscle groups are less (by 20- 30%) in BHBK gait than in erect walking;

4) the length ranges of major muscles/muscle groups during BHBK walking are shorter (by 10%-20%) than those during erect walking;

5) the powers required of the main muscles/muscle groups are larger during BHBK walking than during erect walking (by 40%-50%).

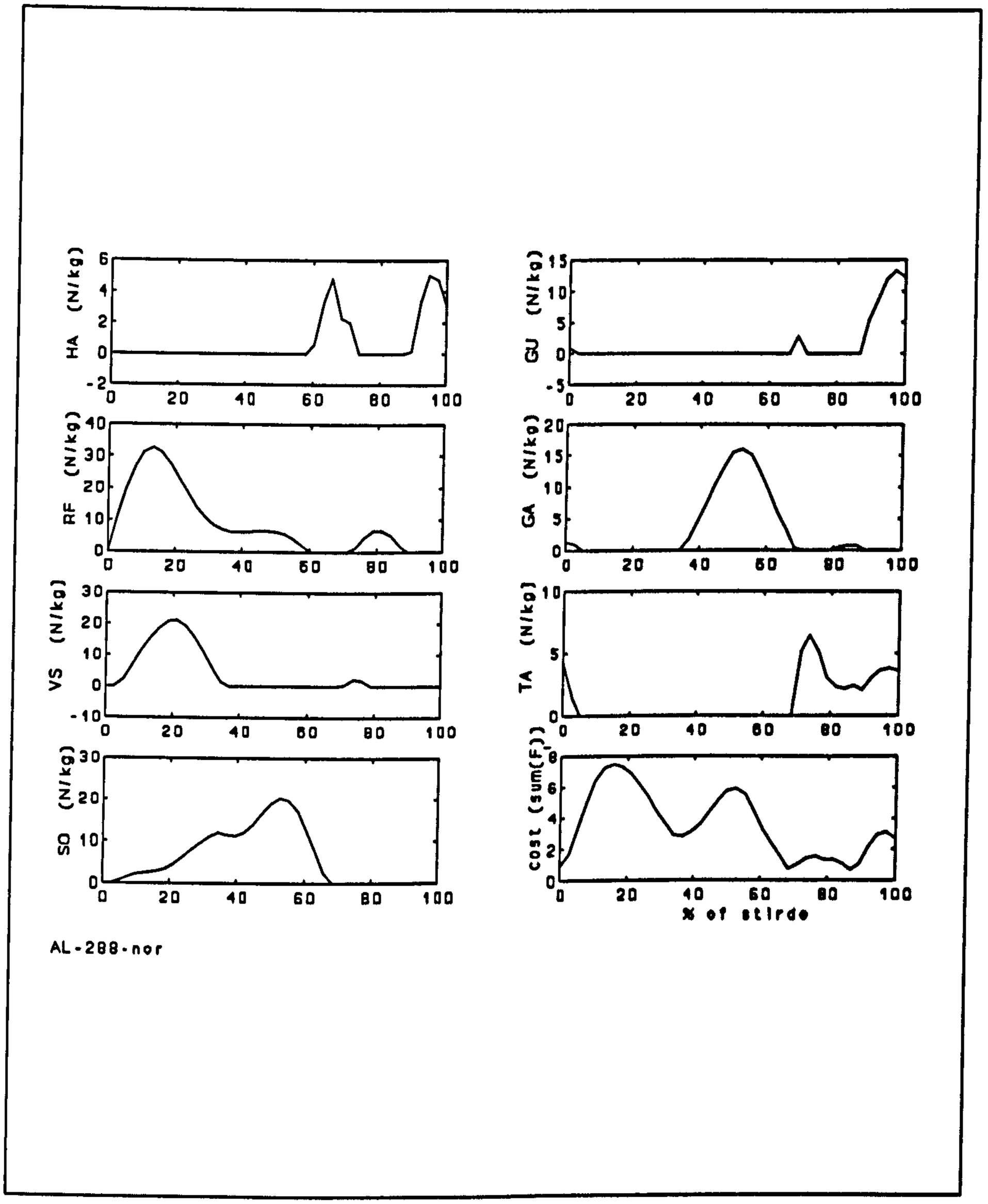

FIGURE 9.5.a Muscle forces in AL 288-1 in erect walking.

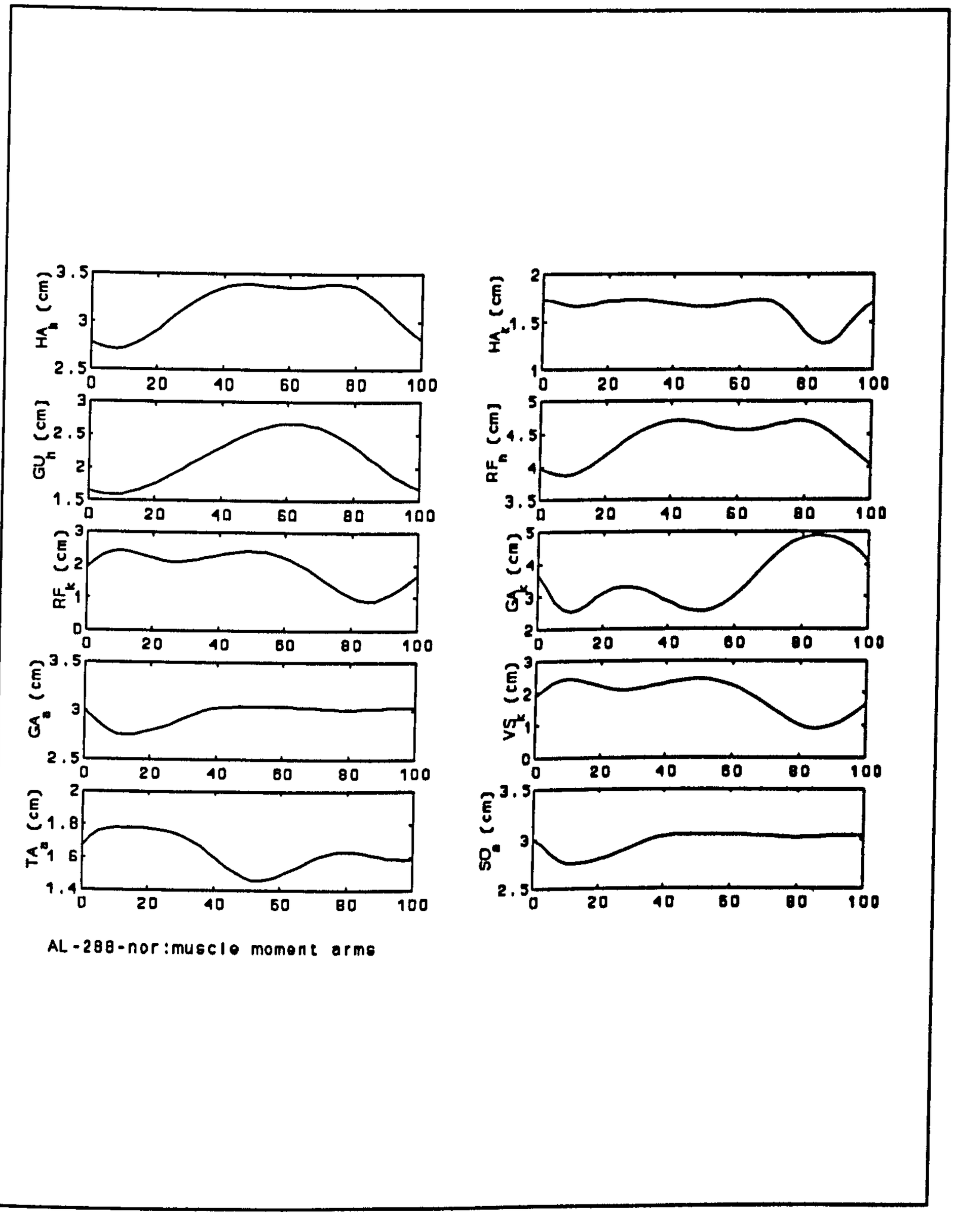

FIGURE 9.5.b Muscle moment arms in AL-288 at erect walking.

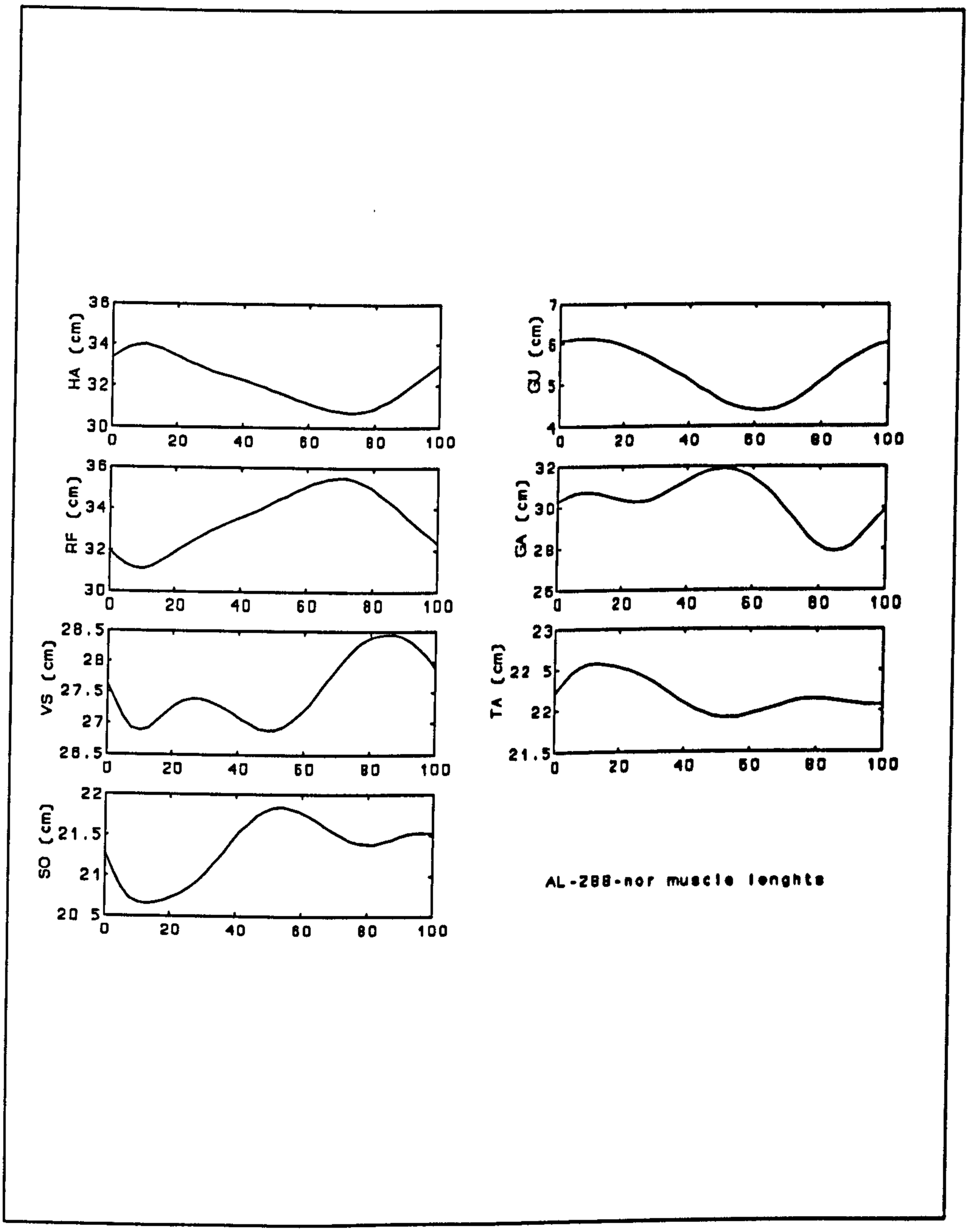

FIGURE 9.5.c Muscle length ranges in AL 288 in erect walking.

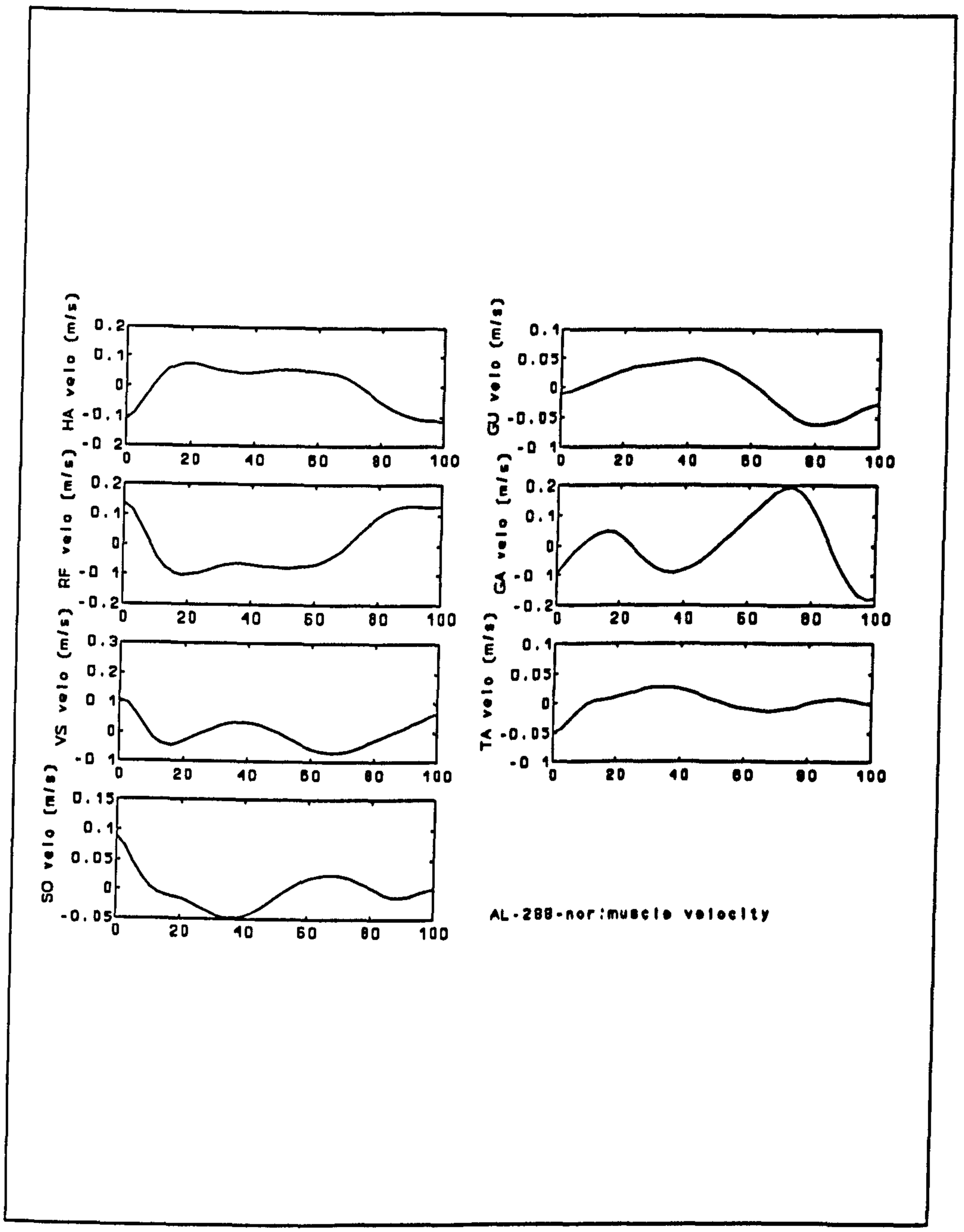

FIGURE 9.5.d Muscle velocity ranges in AL 288 in erect walking.

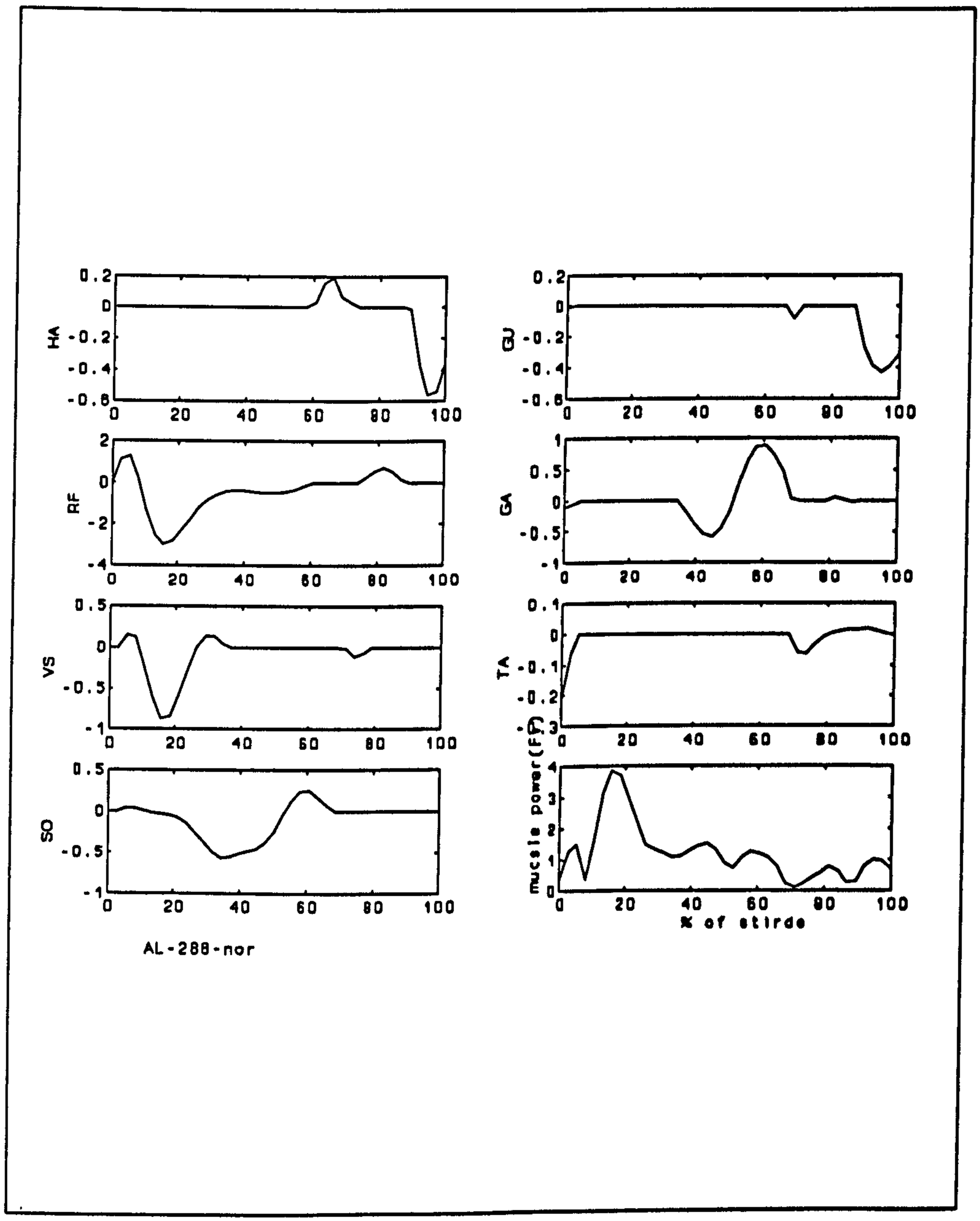

FIGURE 9.5.e Muscle powers in AL-288 in erect walking.

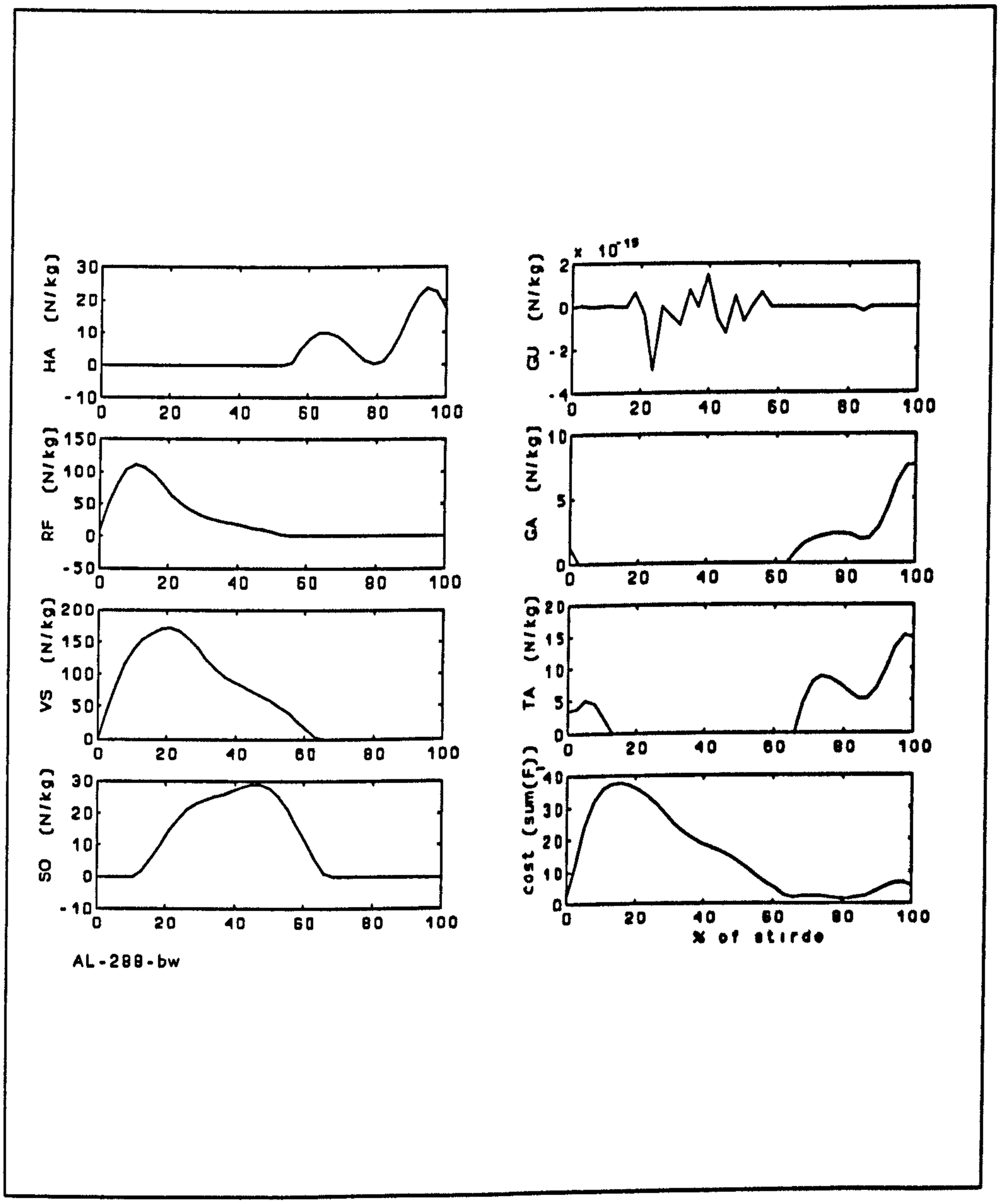

FIGURE 9.6.a Muscle forces in AL-288 in BHBK walking.

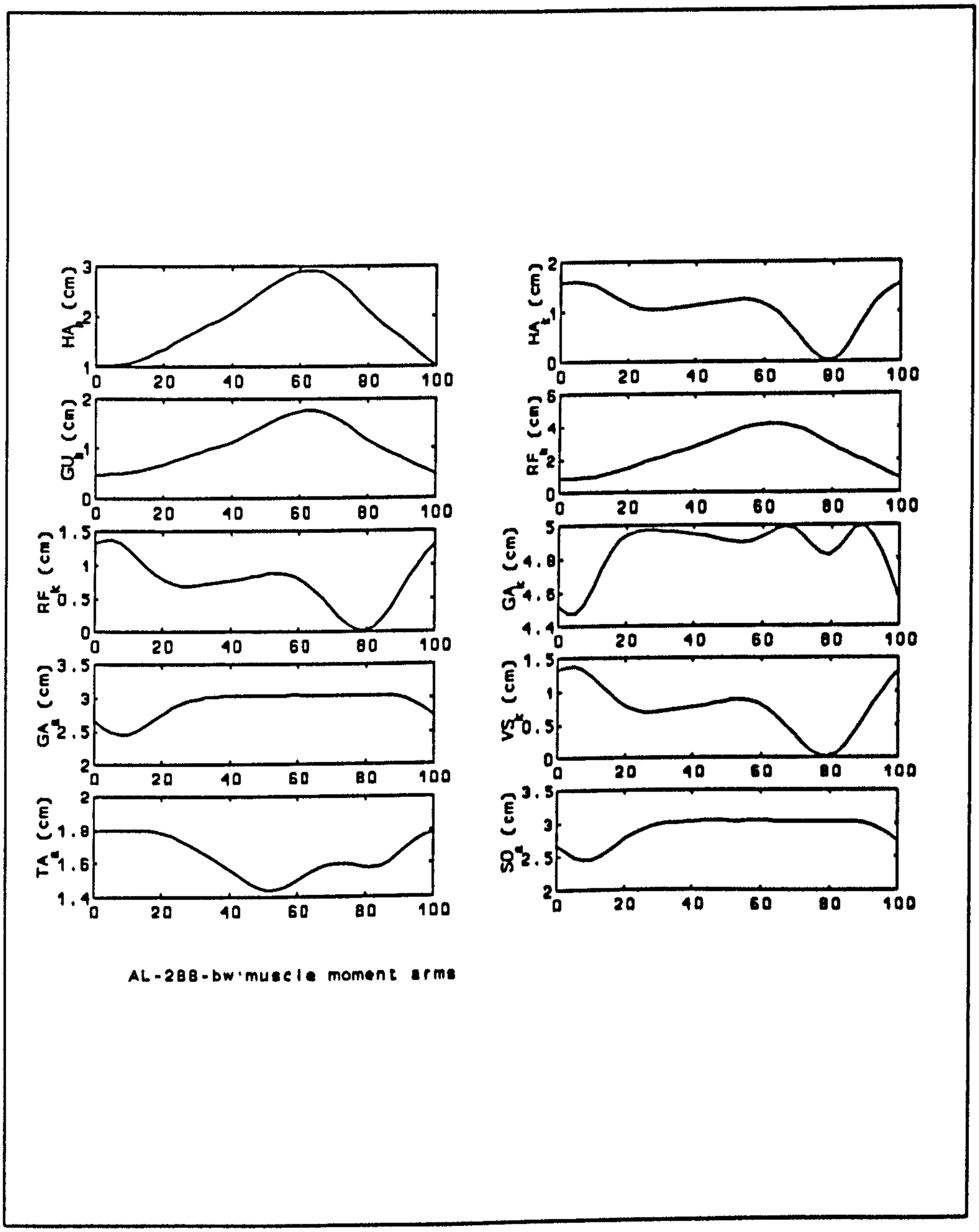

FIGURE 9.6.b Muscle moment arms in AL-288 in BIBK walking.

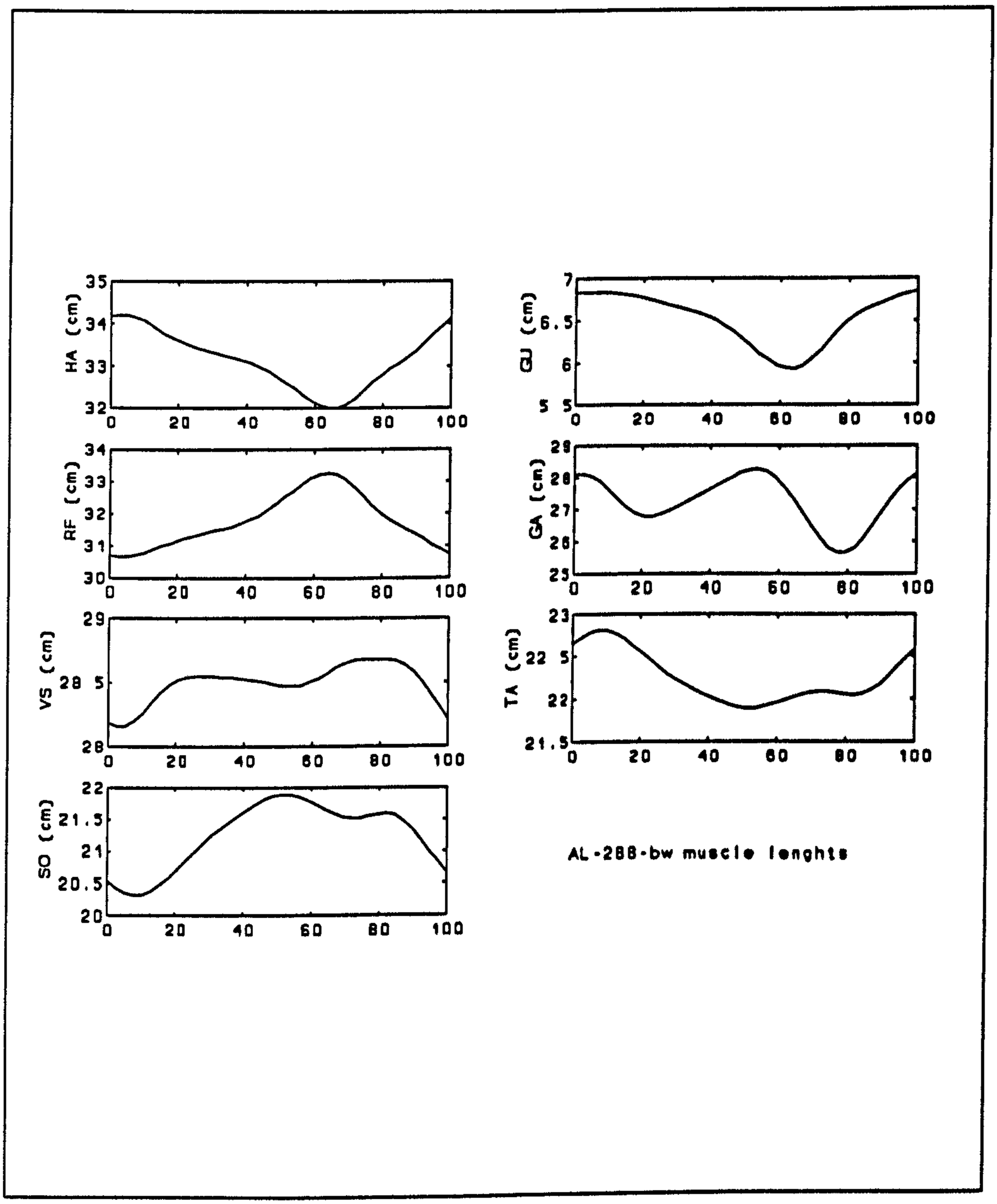

FIGURE 9.6.c Muscle length ranges in AL-288 in BHBK walking.

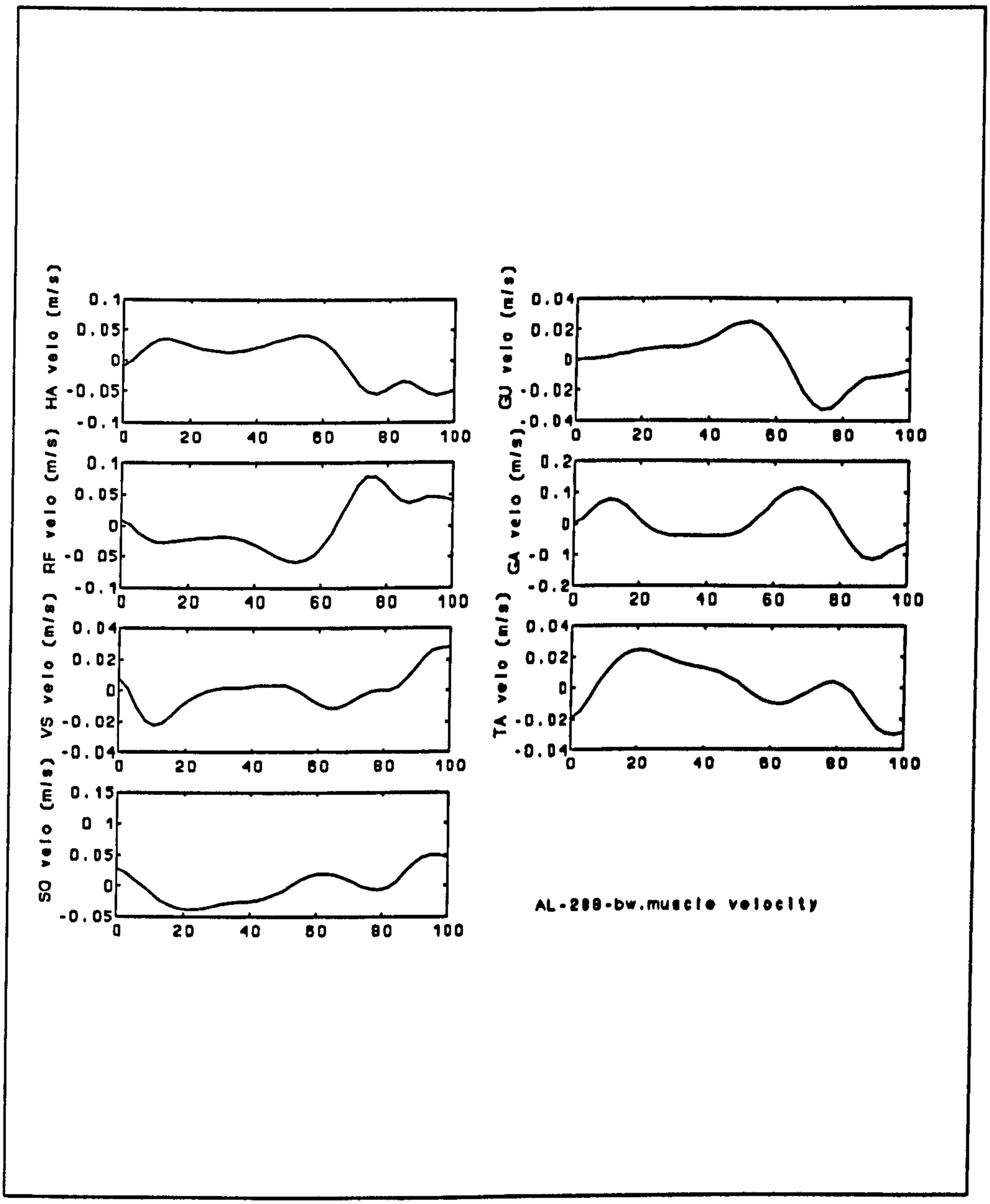

FIGURE 9.6.d Muscle velocities in AL-288 in BIIBK walking.

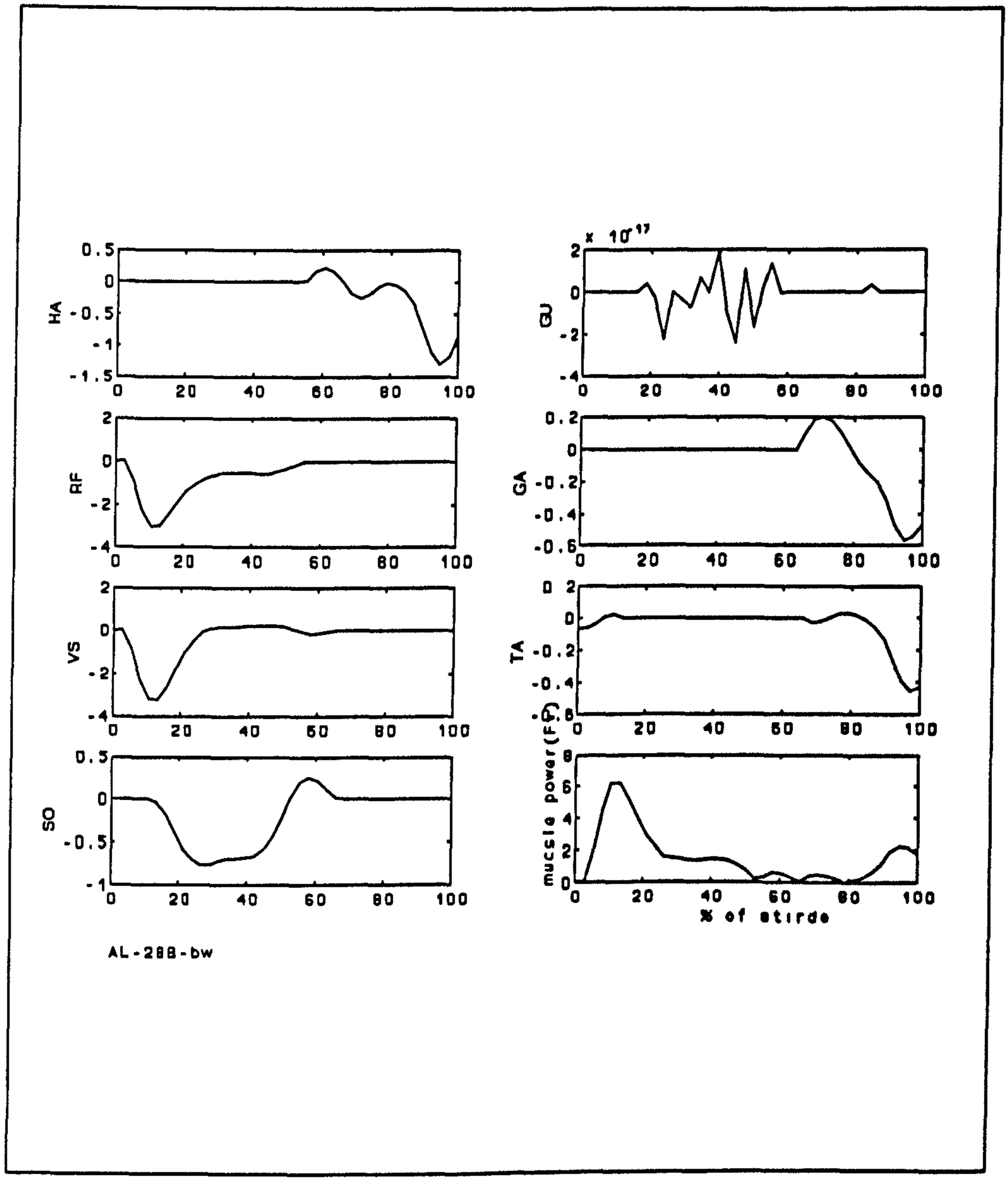

FIGURE 9.6.e Muscle powers in AL-288 in BHBK walking.

9.6 Discussion

9.6.1 Comparison with physiological experiments and force platform data

The pattern of total muscle forces (see Figs. 9.5.a and 9.6.a) in simulated erect and BHBK walking are similar to ground reaction force patterns recorded in measurements of real erect and BHBK walking respectively. Moreover, the simulated muscle force curves are similar to results in experimental EMG studies carried out during human erect and BHBK treadmill walking by another member of our research group (Carey, 1999). Thus, we can have some confidence in the validity of our findings.

9.6.2 General discussion of results from musculoskeletal modelling simulations

From Figure 9.5, 9.6 and 9.7, it is apparent that BHBK unloaded (BKW) and loaded (BLW) walking require larger muscle force and more power than erect walking, unloaded: NOR, SLO, FAS and loaded: NLW. Muscle forces may reach up to 4 times their levels in erect walking (see Fig 9.7.c). During BKW and BLW, muscle moment arms in the main muscles/muscle groups HA, GU, RF and VS are from 20% to 60% smaller than in erect walking, although a few muscles, such as GA, do obtain larger moment arms (see Fig. 9.7.b). Since the decrease in muscle moment arms occur in the main muscles which serve driving and balancing roles during walking, these muscles have to output rather large forces. At the same time, as muscles can only produce limited energy-per-unit-time (ie. power), muscle velocities have to decrease so that muscle output power can satisfy the kinematic requirements of the model. Therefore, during BHBK walking muscle velocities are lower than during erect walking (Fig. 9.7.d).

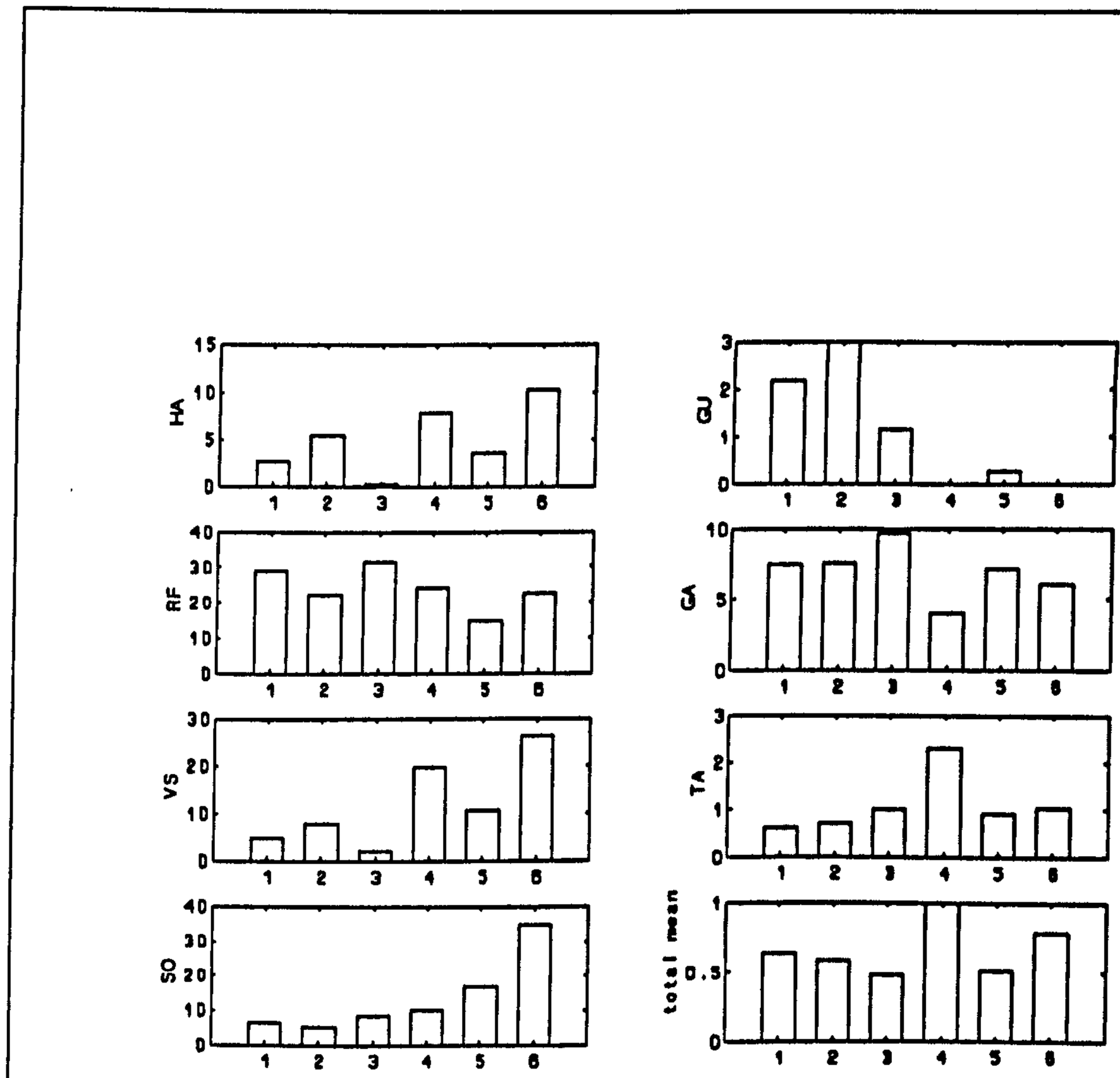

FIGURE 9.7.a The ABS_p variables in AL-288 simulation.

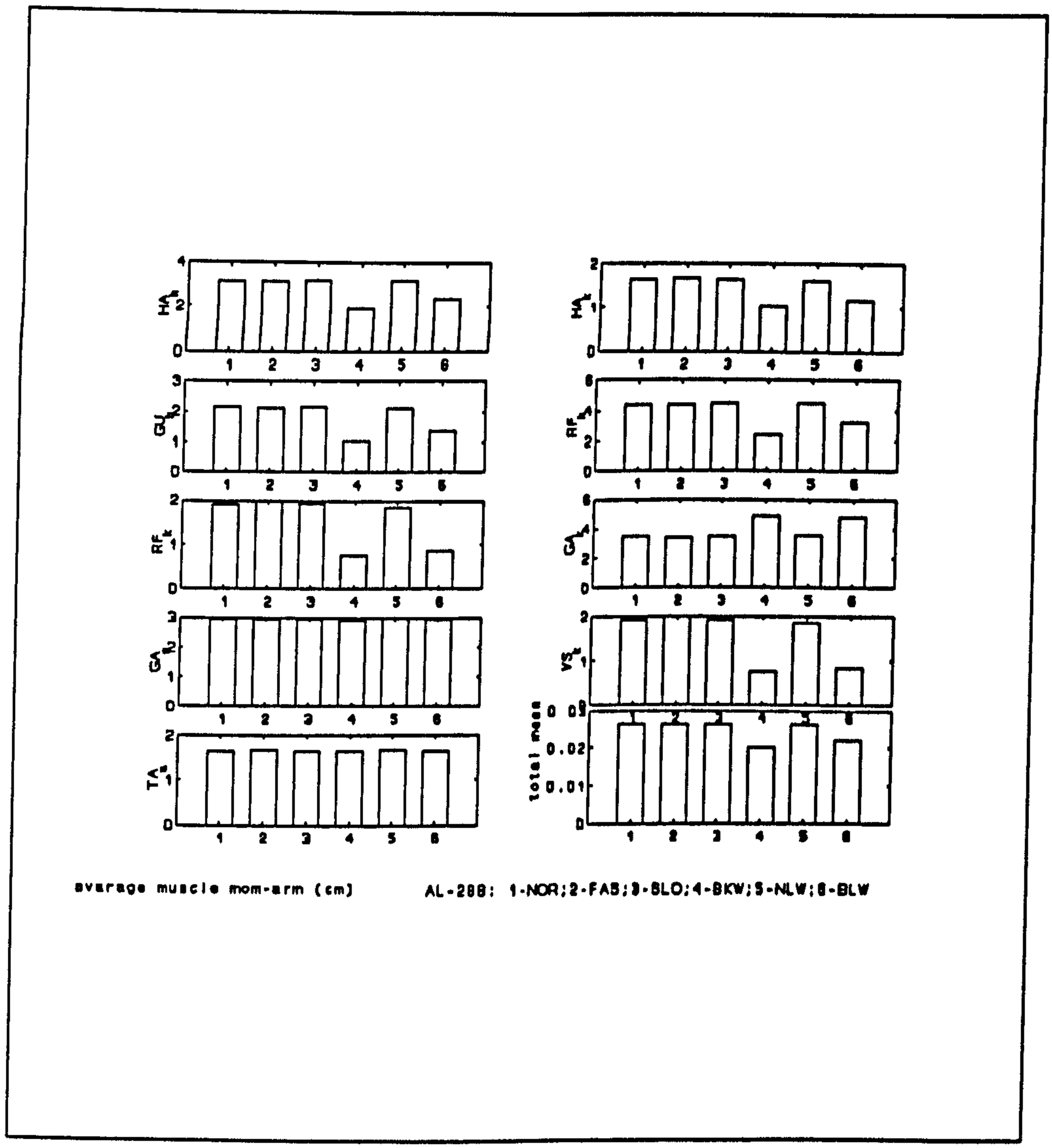

FIGURE 9.7.b The muscle mean_m_a variable in AL-288 simulation.

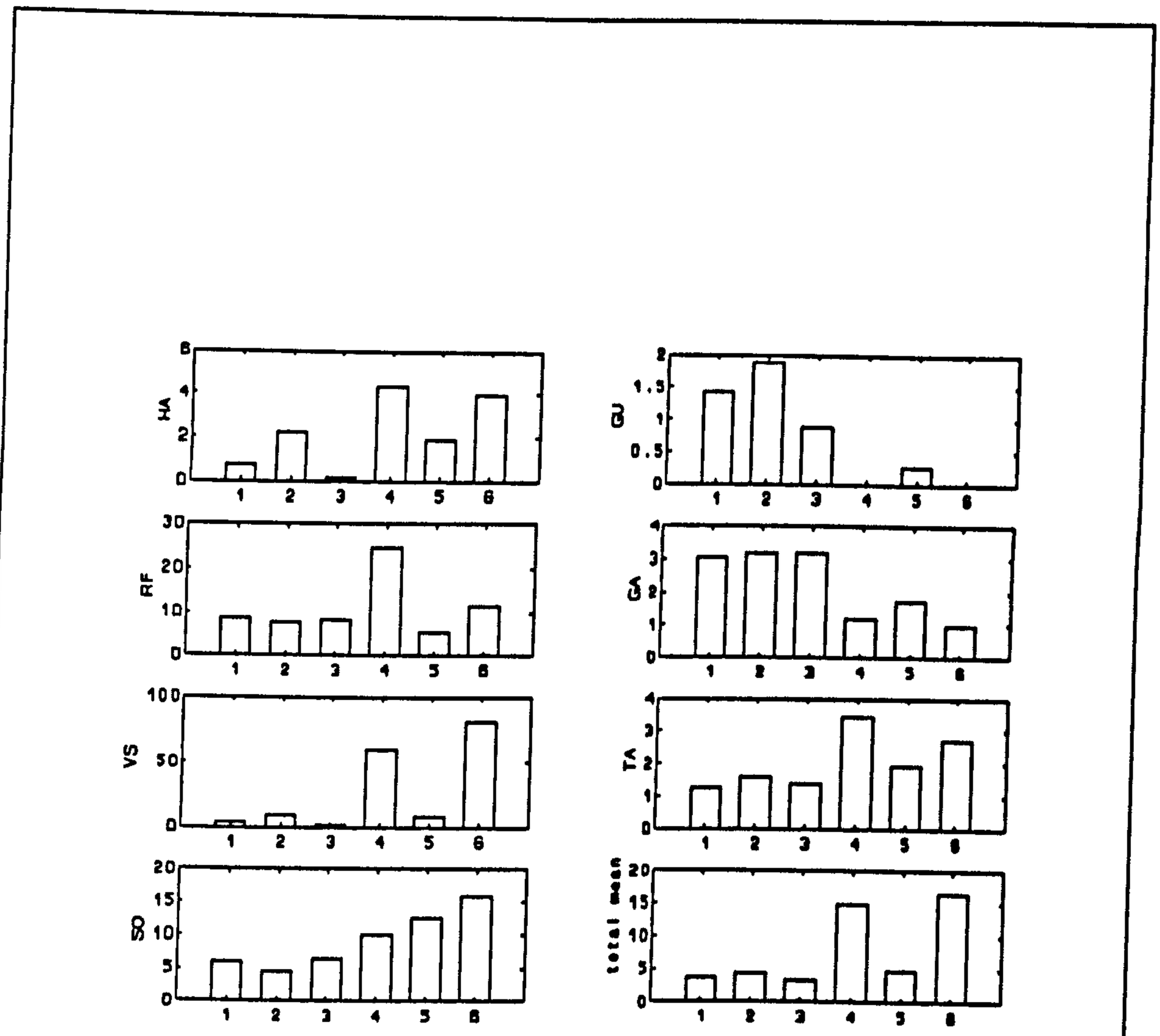

FIGURE 9.7.c The muscle mean_forces variable in AL-288 simulation.

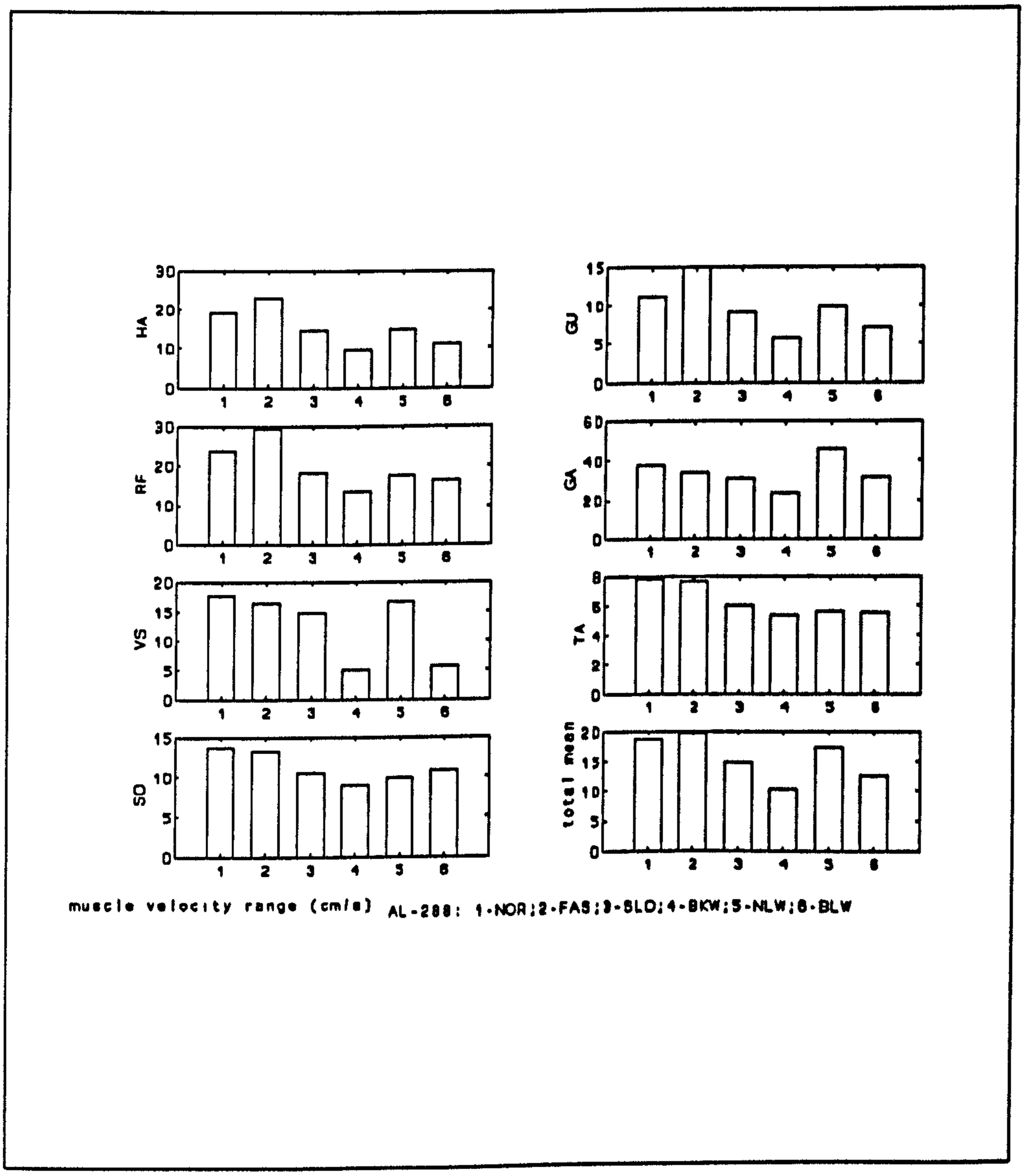

FIGURE 9.7.d Muscle velocity range in AL-288 simulation.

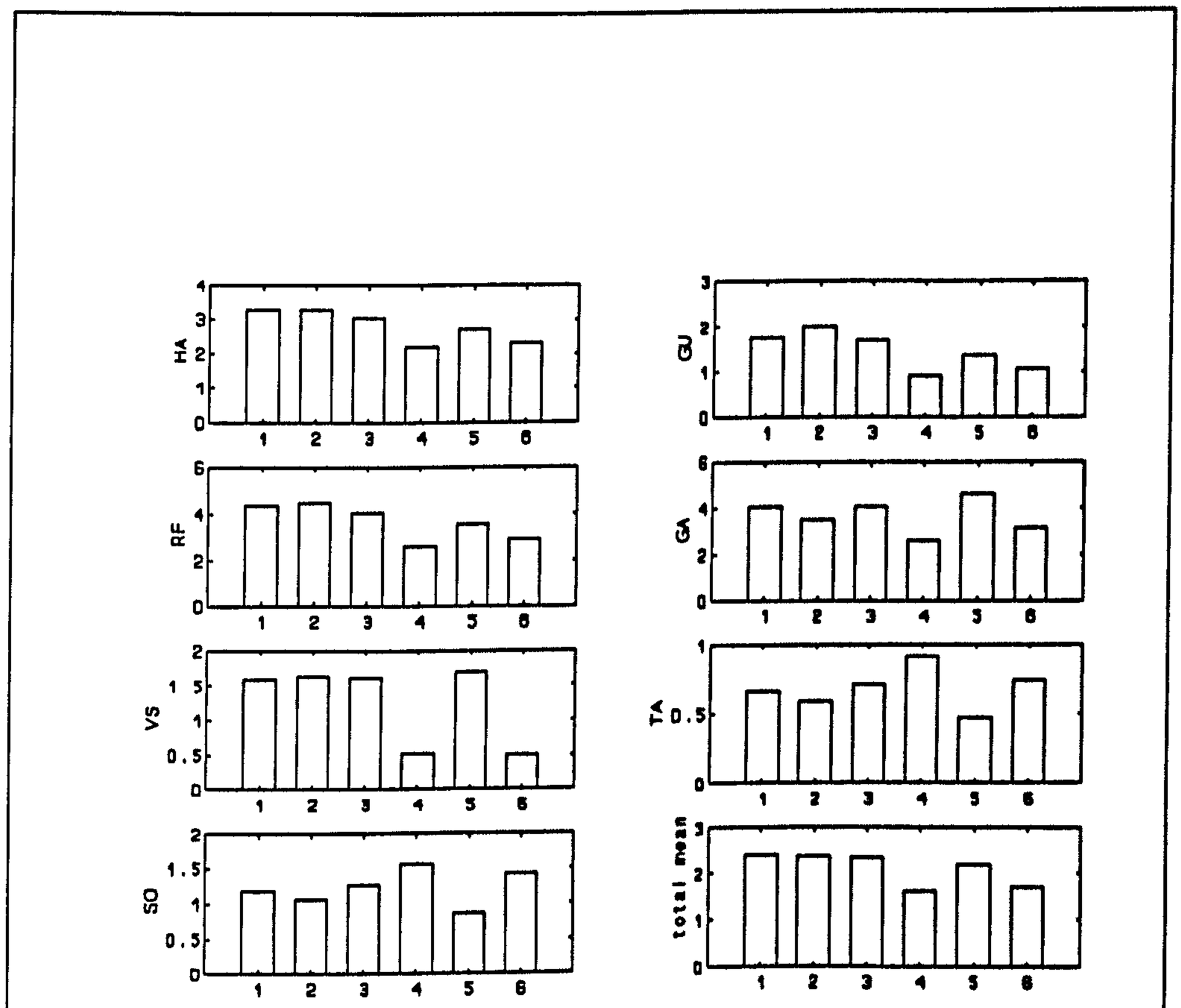

FIGURE 9.7.e Muscle length ranges in AL-288 simulation.

9.7 Conclusions

From the comparison of different modes of walking in AL-288-1, WT 15000 and modern adults, we may conclude that:

1) muscle forces are larger in BHBK walking than in erect walking;
2) muscles have to output more power in BHBK than in normal upright walking;
3) muscle moment arms will be smaller in BHBK than in erect walking;
4) muscle velocities are likely to be much smaller in BHBK walking because of biological limitations to muscles' output of mechanical power;
5) muscle length ranges will be smaller in BHBK walking

All these characteristics suggest that selection against BHBK walking would have been very strong, and it is only likely to have been adopted if overwhelming selective pressures would have been applied by other biological relationships. It is difficult to imagine what such overwhelming pressures could have been.

CHAPTER 10. SIZE, SHAPE AND POWER REQUIRED FOR MOTION: POSSIBLE CLUES TO THE EVOLUTION OF EARLY HOMINIDS

Ang set of ideas consistent among themselves and centered on the explanation of a natural phenomenon - this is what we mean by a theory - is useful, even at the moment of its own demise, when it suggests the new investigations that will lead to its replacement by something better.

Thomas A. McMahon (1984)

Abstract

The fossil record suggests that hominid stature and weight has shown a tendency to increase, but it is possible that robusticity is decreasing. This chapter explores possible relationships between size, power required for motion (PRM) and cycle-time, deriving relationships which indicate that PRM per mass per velocity is proportional to robusticity, but inversely proportional to stature. The results derived appear to be in agreement with general findings of physiological experiments. All other things being equal, if achievement of minimum PRM was the selective criterion, human stature might tend to increase slightly in the future but at a lower rate. If mobility and stability under loading were the selective criteria, there should be no size increase.

10.1 Changes in size in the fossil record

10.1.1 Size and weight

It is generally the case that hominids have overall become larger over time (Pilbeam and Gould 1974; Hill 1950), if 'size' is taken to be stature, diameter and body weight. For example, *A. afarensis*, AL-288-1 (3.6 Mya) had a estimated height 1.05 m and weight of 35 kg (Jungers 1982), but *H. erectus* WT-15000 (1.8 Mya), a 13 year old was 1.4-1.6 m high and weighed 40-50 kg though he was a only 13 year-old boy (Ohman et al. submitted ms.). Typical values for modern human adult males are 1.75 m and 75 kg and for females 1.65 m and 65 kg. However, children with similar stature to AL-288-1 may have a weight around 10 kg. This suggests that modern humans may be more slender than were early hominids. Table 10.1 collates approximate size values culled from the literature, but it must be emphasized that these are intended to be illustrative only, to serve as the dataset for an exploration of size relationships, and cannot purport to result from a detailed

survey.

If we assume that slenderness has been increasing over hominid evolution, we may

Table 10.1 Approximate size values for hominids

	age (Myr)	d (m)	L (m)	mass (kg)	R_p%
Australopitbecus afarensis					
AL288	3.6	0.19	1.05	30.0	9.082
AL333	3.6	0.26	1.42	78.0	9.312
Australopitbecus africanus					
Sts14	2.6	0.18	1.07	27.0	8.376
Paranthropus robustus					
Sk-82	1.7?	0.22	1.46	58.0	7.702
Paranthropus boisei					
Ke738	1.9	0.20	1.39	42.0	7.055
Ke993	1.5	0.25	1.33	64.0	9.305
K1503	1.9	0.22	1.33	51.0	8.307
K3728	1.9	0.19	1.43	40.0	6.599
Paranthropus?					
K1463	1.5	0.26	1.75	93.0	7.432
Homo habilis					
OH 62	1.8	0.23	1.09	44.0	10.399
Homo erectus					
WT 15000k	1.8	0.20	1.45	45.0	6.855
Modern humans					
Male	0.00	0.23	1.75	75.0	6.674
Female	0.00	0.20	1.60	50.0	6.233
Child-9	0.00	0.17	1.22	28.0	7.006

Note: d - any characteristic diameter, such as chest girth; L - any characteristic length, such as stature; mass- weight of subject; R_p- robusticity coefficient , d/L, slenderness.

investigate this phenomenon first of all by defining a coefficient of robusticity:

$$R_p = \frac{d}{L} \qquad (10.0)$$

where L - a characteristic length, such as stature or leg length; d - a characteristic diameter, such as chest girth or leg diameter

10.1.2 Tendency for Changing Robusticity

From the illustrative data in Table 10.1, it is possible to plot an approximate least squares regression curve for size variation (Fig. 10.1). This appears to show that while hominid stature and weight have been increasing, R_p has been decreasing. Inspection of Fig. 10.1, suggests that there should be some fossils at 2-3 Mya where R_p would be around 8.0. A possible candidate might be OH-62, where the R_p, on the basis of current reconstructions, is 10.4, a rather large value.

More to the point of the present study, why should size and weight of hominids change? Do these parameters have any functional significance for bipedalism?

fig 10.1

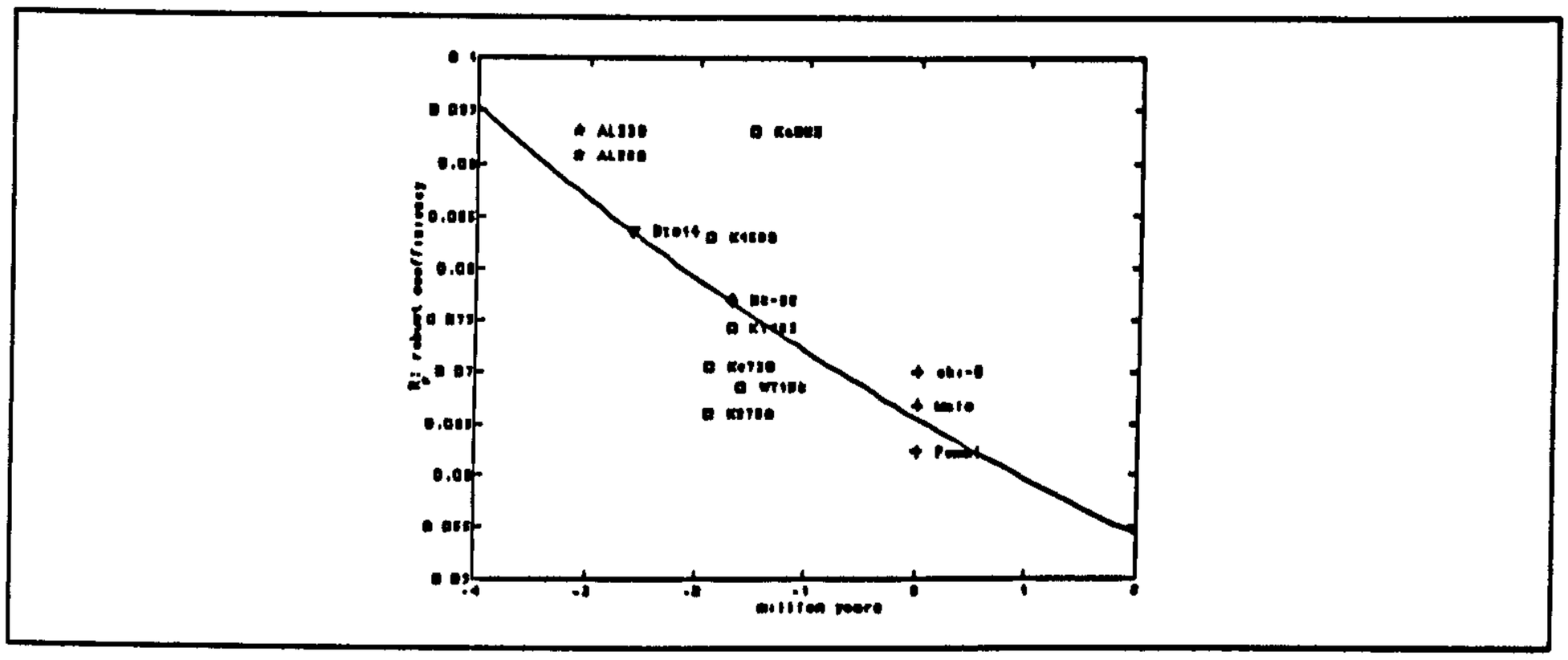

FIGURE 10.1.a Rp's tendency in last few million years. 0 million years express modern time, after the time the curve only gives only a possible tendency.

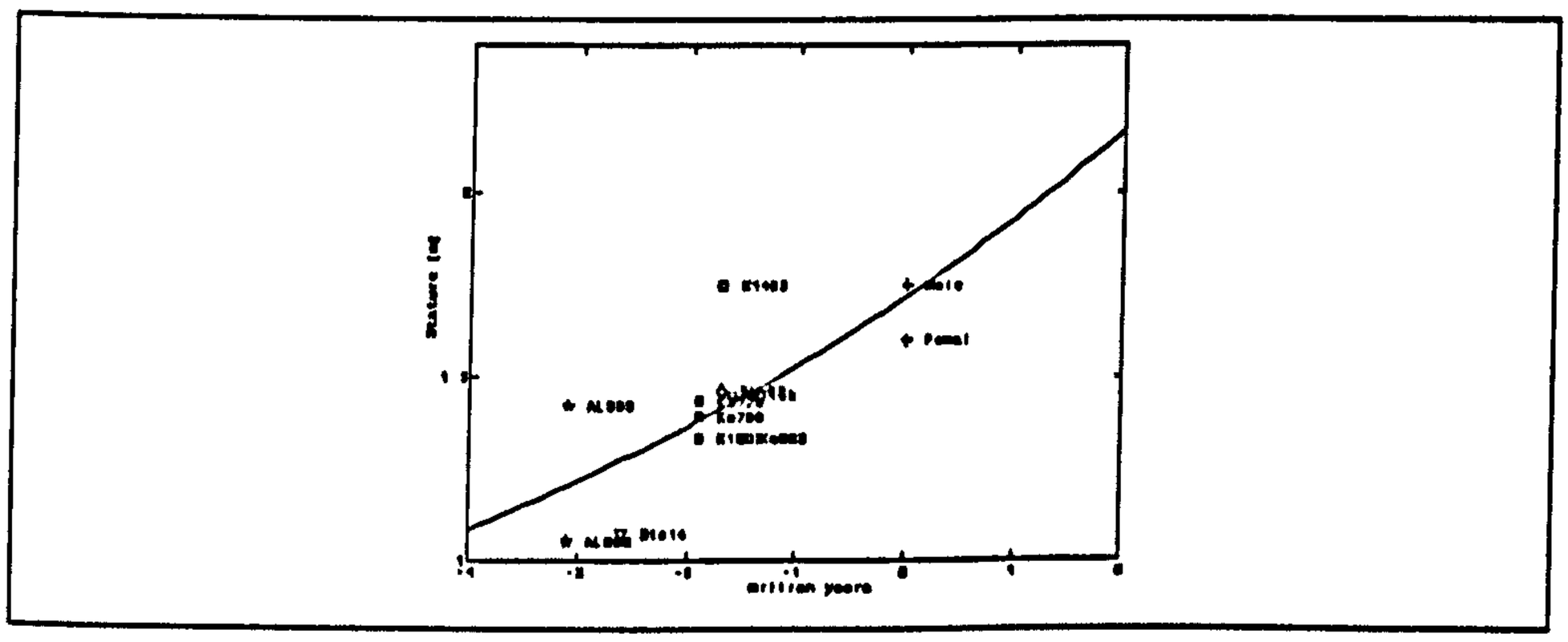

FIGURE 10.1.b Stuture's tendency in last few million years. After 0 million year expressed modern time, the curve gives only a possible tendency.

10.2 Dimensionless motive power and size

10.2.1 Assumptions concerning material density

I assume here that any given tissue will have the same density for different subjects at different times, approximately 1000 kg/m^3. In this case there is a general relation between size and mass:

$$\pi r^2 L\rho = m \qquad (10.1)$$

where r, L - characteristic radius and length; ρ - density; m - mass

10.2.2 Muscle power

Power required for motion is an important characteristic of locomotion. How much power does muscle output during motion? A simple model of the lower limb is presented in Fig.10 2, to clarify the relationship between internal forces produced by muscles and external forces from the environment. When there is a small change in the trunk/lower limb ('hip') joint angle, muscle length must also change. From Fig. 10.2, the internal moment produced by muscles should be proportional to the external moments produced by ground reaction forces. We have a series of proportional relationships:

$$F_m r \propto F_g L \qquad (10.2)$$

$$P_m \propto F_m \frac{\Delta L}{\Delta t} \qquad (10.3)$$

$$\Delta L \propto r \Delta 0 \qquad (10.4)$$

$$P_m \propto F_m r \frac{\Delta 0}{\Delta t} \qquad (10.5)$$

where F_m - muscle force; F_g - ground reaction force; Δt - small time interval; $\Delta 0$ - a

small change of joint angle; P_m - muscle power

From equations (10.2) and (10.5), muscle power should be:

$$P_m \propto F_g L \frac{\Delta\theta}{\Delta t} \qquad (10.6)$$

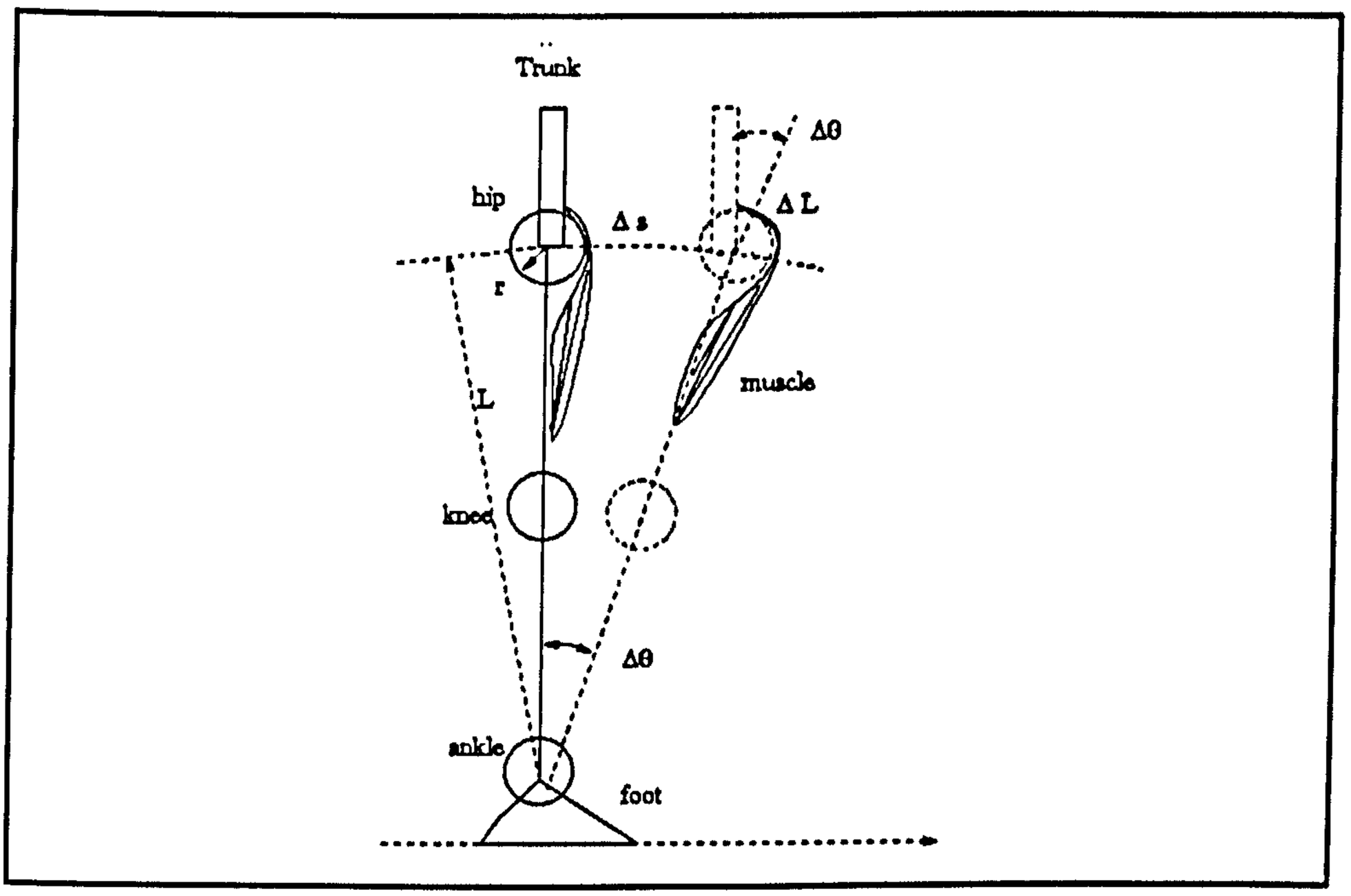

FIGURE 10.2. Relationship between the increase of muscle length and the increase of rotation angle. L - leg length; Δ0 - angle; r - joint radius or moment arm; s - displacement.

10.2.3 Mechanical motive power

In mechanics, a subject's power expenditure in moving should be:

$$P=F\cdot v \qquad (10.7)$$

If we only consider the effective part of power expenditure, i.e. that directed forwards, horizontal and level, (10.7) may be shown :

$$v=L\frac{\Delta\theta}{\Delta t} \qquad (10.8.1)$$

$$P\propto F_g L\frac{\Delta\theta}{\Delta t} \qquad (10.8)$$

Equation (10.8) has a similar form to equation (10.6), so that ignoring the efficiency of muscle work done, all muscle power should be equal to, or at least proportional to, external mechanical power.

10.2.4 Power expressed by fundamental variables

Since any physical variable can be expressed by the fundamental variables, mass, length and time, we can express (10.6) and (10.8) in terms of the basic variables. According to Newton's Laws:

$$F_g\propto Ma \qquad (10.9)$$

$$\because a=\frac{v_2-v_1}{\Delta t}=\frac{(s_2-s_1)-(s_1-s_0)}{\Delta t^2}\propto\frac{\Delta s}{(\Delta t)^2}$$

$$\because \Delta s\propto L\Delta\theta$$

$$\therefore F_g\propto M\frac{L\Delta\theta}{(\Delta t)^2} \qquad (10.10)$$

where a - acceleration (see Fig.10-2)

From equations (10.8) and (10.10) we obtain a relationship between PRM and length, time and mass:

$$P \propto M\frac{(L\Delta\theta)^2}{(\Delta t)^3} \qquad (10.11)$$

To compare PRM between different sized subjects, we may define a dimensionless power parameter: P/(Mgv) (Alexander, 1992), representing power expenditure per unit mass and per unit speed, and providing an expression of length, mass and time:

$$P_d \propto \frac{P}{Mgv} \propto \frac{L\Delta\theta}{(\Delta t)^2} \qquad (10.12)$$

where g - gravity constant.

Applying our assumptions to (10.12), in addition, we know that $\Delta t \propto L^2/d$ and $\Delta\theta \propto L/d$ (McMahon 1975, 1985), thus we arrive at a dimensionless power P_d expressed only in terms of length and mass:

$$P_d \propto \frac{d}{L^2} \propto \frac{R_p}{L} \qquad (10.13)$$

Or putting assumption (10.1) into (10.12) we obtain

$$P_d \propto \frac{1}{L}\sqrt{\frac{4M}{\pi\rho L^3}} \propto \sqrt{\frac{M}{L^5}} \qquad (10.14)$$

Equations (10.13) and (10.14) give the relationship of PRM, mass and size. Equation (10.13) implies that either an increase in stature or a decrease in the coefficient of robusticity will reduce power expenditure in moving a unit mass at a given speed. This is in agreement with observations from Table 10.1 and Fig. 1, showing that while stature has been increasing, the coefficient of robusticity

appears to have been decreasing. Equation (10.14) indicates that an increase in stature and a decrease in weight will result in a decrease in PRM. We can plot a graph (Fig. 10.3) which shows the relationship of the dimensionless power parameter P_d, mass M and characteristic length L. Note that both decrease of mass and increase in length may result in the decrease of PRM.

Equation (10.13) suggests that decrease in R_p and increase in stature lead to a decrease in PRM, and equation (10.14) further suggests that a decrease in mass and an increase in stature will also lead to a decrease in PRM.

From equations (10.13)-(10.14) and Fig.10.3, we may again suggest that an increase in stature and a decrease in the coefficient of robusticity will result in a decrease in PRM.

It should be noted that we cannot simplify the above by saying that an increase in size will lead to a decrease in PRM. Size includes length, diameter and weight. From our results, either an increase in length or a decrease in diameter enable a decrease in power. The three variables, d, L and mass are not independent and will tend to optimum proportions.

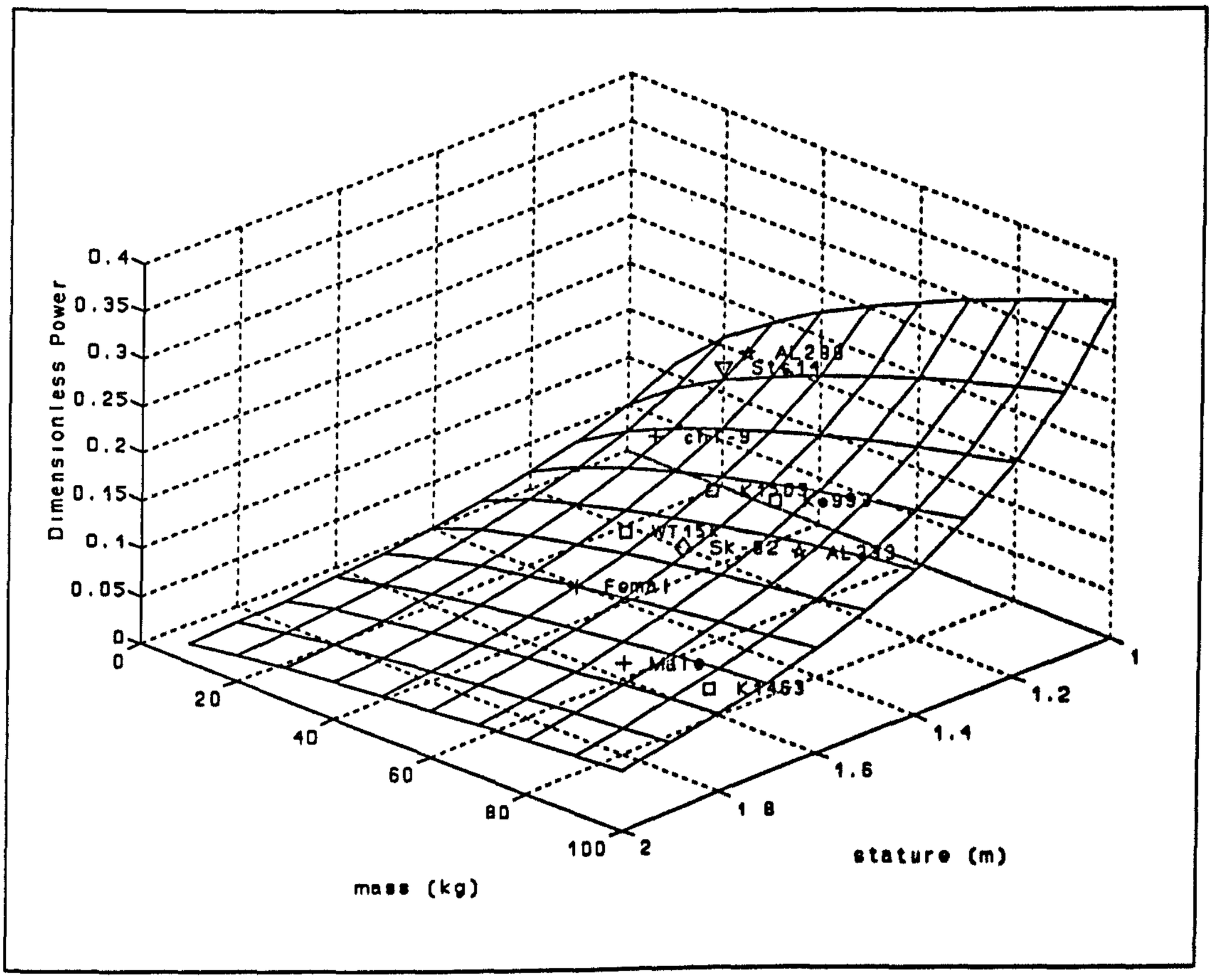

FIGURE 10.3 Dimensionless power and size.

TABLE 10.2.a Comparison of dimensionless motive power

subject	ages (Myr)	d (m)	L (m)	mass (kg)	R_p%	P_d(14)	P_d(13)
Australopithecus afarensis							
AL288	3.6	0.19	1.05	30.0	9.082	4.848	0.086
AL333	3.6	0.26	1.42	78.0	9.312	3.676	0.066
Australopithecus africanus							
Sts14	2.6	0.18	1.07	27.0	8.376	4.388	0.078
Paranthropus robustus							
Sk-82	1.7?	0.22	1.46	58.0	7.702	2.957	0.053
Paranthropus boisei							
Ke738	1.9	0.20	1.39	42.0	7.055	2.845	0.051
Ke993	1.5	0.25	1.33	64.0	9.305	3.922	0.070
K1503	1.9	0.22	1.33	51.0	8.307	3.501	0.062
K3728	1.9	0.19	1.43	40.0	6.599	2.586	0.046
Paranthropus?							
K1463	1.5	0.26	1.75	93.0	7.432	2.380	0.042
Homo habilis							
OH 62	1.8	0.23	1.09	44.0	10.399	5.348	0.095
Homo erectus							
WT15000	1.6	0.20	1.45	45.0	6.855	2.650	0.047
Modern Humans							
Male	0.00	0.23	1.75	75.0	6.674	2.138	0.038
Female	0.00	0.20	1.60	50.0	6.233	2.184	0.039
Child-9	0.00	0.17	1.22	28.0	7.006	3.219	0.057

TABLE 10.2.b Comparison of dimensionless power parameter

subject	ages	d %	L %	mass %	R_p %	$P_d(13)$ %	$P_d(14)$ %
Australopitbecus afarensis							
AL288	3.6	100.00	100.00	100.0	100.0	100.0	100.0
AL333	3.6	138.66	135.24	260.0	102.5	75.8	75.8
Australopitbecus africanus							
Sts14	2.6	93.98	101.90	90.0	92.2	90.4	90.4
Paranthropus robustus							
Sk-82	1.7	117.92	139.05	193.3	84.8	60.9	60.9
Paranthropus boisei							
Ke738	1.9	102.84	132.38	140.0	77.6	58.6	58.6
Ke993	1.5	129.78	126.67	213.3	102.4	80.8	80.8
K1503	1.9	115.85	126.67	170.0	91.4	72.2	72.2
K3728	1.9	98.95	136.19	133.3	72.6	53.3	53.3
Paranthropus?							
K1463	1.5	136.38	166.67	310.0	81.8	49.1	49.1
Homo habilis							
OH 62	1.8	118.86	103.81	146.7	114.5	110.3	110.3
Homo erectus							
WT 15000	1.8	104.22	138.10	150.0	75.4	54.6	54.6
Modern humans							
Male	0.00	122.47	166.6	250.0	73.4	44.1	44.1
Female	0.00	104.58	152.3	166.7	68.6	45.1	45.1
Child9	0.00	89.63	116.1	93.3	77.1	66.4	66.4

10.3 Power requirements of different subjects

10.3.1 Power comparison

Table 10.2 shows that AL-288-1 would have rather large P_d, but modern humans the smallest P_d. Figures 10.4.a and b, plotted from data in Table 10.2 show that modern humans also have the smallest PRM. The comparison in Fig. 10.4 shows the relationship between mass and length (from Jungers and Stern, 1983).

10.3.2 Comparison with physiological results

10.3.2.1 PRM

Since muscle power and external power appear to have similar expression (see equations (10.6) and (10.8)), equation (10.14) should be in agreement with results from physiological experiments. Under assumptions of geometry similarity, elastic similarity and static stress similarity (McMahon 1975 and 1984), results can be

TABLE 10.3 Comparison of dimensionless powers under different assumptions

	GS	ES	SS
$L \propto d^p$	p= 1/3	2/3	1/2
$L \propto M^k$	k= 1/3	1/4	1/5
$d \propto M^b$	b= 1/3	3/8	2/5
$P_d(14) \propto M^a$	a= -1/3	-1/8	0

Note: GS - geometric similarity; ES - elastic similarity; SS - static stress

obtained as below (Table 10.3).

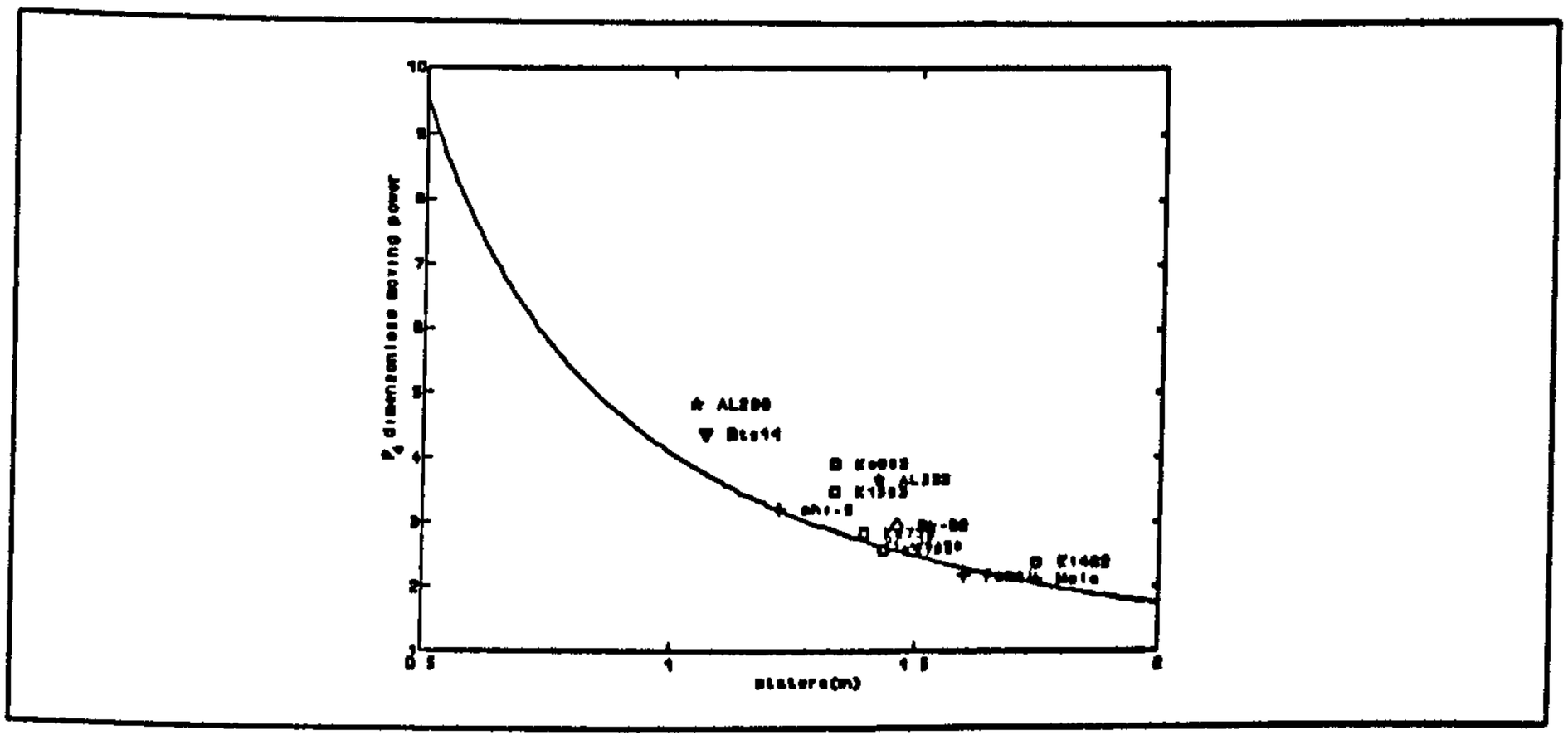

FIGURE 10.4.a The relationship between stature and MRP.

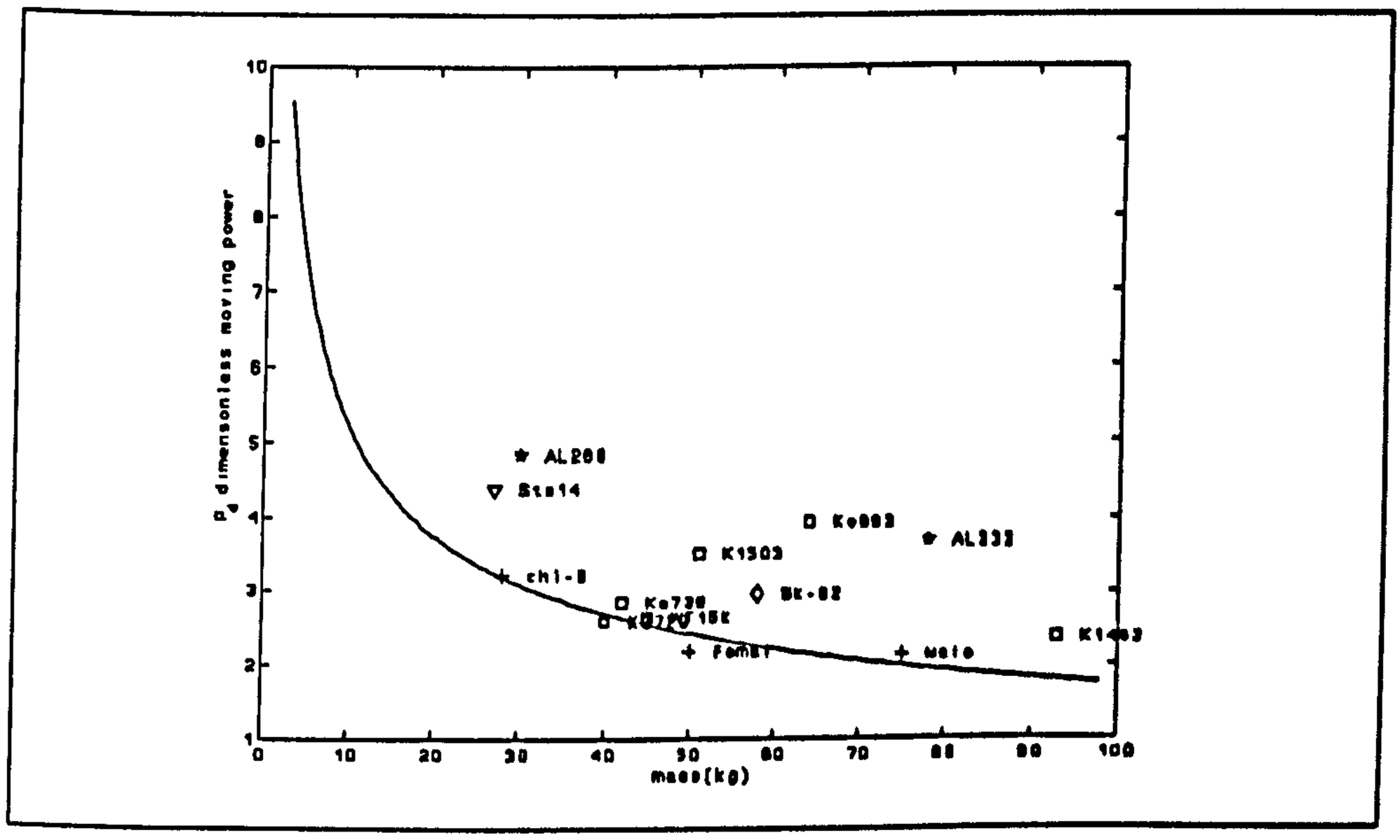

FIGURE 10.4.b THe relationship between mass and MPR.

From Table 10.3, if geometric similarity is applied to equations (10.13) and (10.14), dimensionless power should be proportional to $M^{-1/3}$.

Taylor et al (1970, 1980 and 1985) measured metabolic energy consumption in animals of different size (from 3 g to 3 tonnes), of different locomotor design (bipedal, quadrupedal and polypedal) and different locomotor behaviour (runners, walkers, hoppers, trotters and gallopers). They found that power per mass per velocity is proportional to $M^{-0.316}$. Full (1989) extended this research to smaller polypedal animals and found that metabolic power was proportional to $M^{-0.31}$. These experimental results are thus in broad agreement with my prediction from equations (10.13) and (10.14) that dimensionless power is proportional to $M^{-1/3}$. Thus, equations (10.13) and (10.14) may be used as general expressions.

10.3.2.2 Muscle force and external forces

We may estimate mass-specific external force according to equation (10.10). From this equation, estimation of mass-specific external force is similar to estimation of accceleration, so that mass-specific external force has a similar expression to P_d. Therefore, equation (10.13) and (10.14) are also applicable to external forces. According to the assumption of geometric similarity, F_g/M will be proportional to $M^{-1/3}$.

Similarly, by equation (10.2), (and still under the assumption of geometric similarity), mass-specific muscle force F_m is proportional to F_g. Therefore mass-specific muscle force $F_m/M \propto M^{-1/3}$. These results are good in agreement with Alexander (1985)'s data on maximum external forces and muscle forces for subjects ranging from 3 gm. insects to 3 tonne elephants and behaviours including walking, swimming, pulling, pushing, nipping and biting. Alexander found that both maximum mass-specific muscle force and maximum external force are proportional to $M^{-1/3}$, again confirming that the equations proposed here are meaningful.

10.4 Size - shape relations in humans

10.4.1 Possible predictions

If human PRM was to decrease, and given weights M_f and stature L_f according to (10.13) and (10.14) we have:

$$\frac{M_f}{L_f^5} < \frac{M_m}{L_m^5} \qquad (10.15)$$

Thus, on the basis of current values for male weight $M_m = 75$ kg and stature $L_{mc} = 1.75$ m, a height of 3 m would be accompanied by a weight of a maximum 1000 kg. This is clearly unrealistic, and such a weight could not possibly be supported by the lower limbs! (However, again from equation (10.15), M_f could decrease to a very low value while allowing the relationship to remain valid). The previous, unrealistic prediction requires further consideration, and the perspective of the relationship between loading stability and size may be a useful one.

10.4.2 Mechanics of materials and loading ability

10.4.2.1 Column stability and the mechanics of materials

From the mechanics of materials, if the lower limb or the whole body is considered as a column, its critical load P_{cr} should be:

$$P_{cr} = \frac{\pi^2 EI}{4L^2} \qquad (10.16)$$

where E - the modulus of elasticity of the material, and I- moments of inertia

where A-area of cross-section; σ_{cr}- critical stress

$$\because \quad I=\frac{\pi d^4}{64}$$

$$\therefore \quad P_{cr}=k_1\frac{d^4}{L^2}\propto R_p^2 d^2 \qquad (10.17)$$

$$\therefore \quad \sigma_{cr}\propto\frac{P_{cr}}{A}\propto\frac{d^2}{L^2}\propto R_p^2 \qquad (10.18)$$

Equation (10.18) implies that critical stress is proportional to the coefficient of robusticiy. In order to increase stability, a larger R_p is thus desirable. Data in Table 10.1 and 10.2 thus imply that loading stability of hominids is less now than it was for AL-288-1.

10.4.2.2 Loaded stability

From Table 10.4, the loaded stability of modern humans is only 60% of that of AL-288-1. This indicates that loaded stability has decreased while mobility has increased. Since we assume that the properties of biological materials are unchanged for any size, critical stress will tend towards a constant. From equation (10.18), R_p will do the same. Therefore, any tendency to become more slender and taller will be limited. When R_p reaches a constant, by the assumption of uniform of materials (equation 10.1), we have

$$\because \sigma_{cr}\propto R_p^2=const$$

$$\therefore R_p\propto\sqrt{\frac{M}{L^3}}=const \qquad (10.19)$$

This is geometric similarity. If we assume that modern humans have reached their critical stress (considering safety factors), we can expect continued geometric similarity.

10.4.3 Overview of mobility

Mobility may be described by the time spent in an action, for example, its cycle

TABLE 10.4 Comparison of loaded stability of different subjects

subject	Mya	d	L	mass	P_α%	σ_α%
Australopitbecus afarensis						
AL288	3.6	100.0	100.0	100.0	100.0	100.0
AL333	3.6	138.6	135.2	260.0	102.6	105.1
Australopitbecus africanus						
Sts14	2.6	93.9	101.9	90.0	92.2	85.0
Paranthropus robustus						
Sk-82	1.7	117.9	139.1	193.3	84.8	71.9
Paranthropus boisei						
Ke738	1.9	102.8	132.3	140.0	77.6	60.3
Ke993	1.5	129.7	126.6	213.3	102.4	104.9
K1503	1.9	115.8	126.6	170.0	91.4	83.6
K3728	1.9	98.9	136.2	133.3	72.6	52.7
K1463	1.5	136.3	166.6	310.0	81.8	66.9
Homo habilis						
OH-62	1.8	118.8	103.8	146.7	114.5	131.1
Homo erectus						
WT 15000	1.8	104.2	138.1	150.0	75.4	56.9
Modern humans						
Male	0.00	122.4	166.6	250.0	73.4	54.0
Female	0.00	104.5	152.3	166.7	68.6	47.1

time or frequency. It is likely to be another influence on size. If stature and weight are too great, actions will become too slow.

Let us consider two different size subjects, their characteristic lengths (mean stature or leg lengths) L_1 and L_2,, who complete a similar motion ($\Delta\theta_1 = \Delta\theta_2$) within cycle-time Δt_1 and Δt_2.. Their ratio of powers per unit mass and per unit velocity (equation 10.12) should be

$$\frac{P_1}{P_2} \propto \frac{L_1}{L_2} \frac{\Delta t_2^2}{\Delta t_1^2} \quad (10.20)$$

whatever form of similarity is applied.

Fig. 10.5 expresses the three-dimensional relationship between the ratios of powers, sizes and times. From function (10.10) and Fig. 10.5, it is very apparent that the ratio of powers increases with increase of L_1/L_2 and decreases with increase of $(\Delta t_1/\Delta t_2)^2$. In other words, if a subject is larger, that subject will take longer or require considerably increased energy to perform a given action.

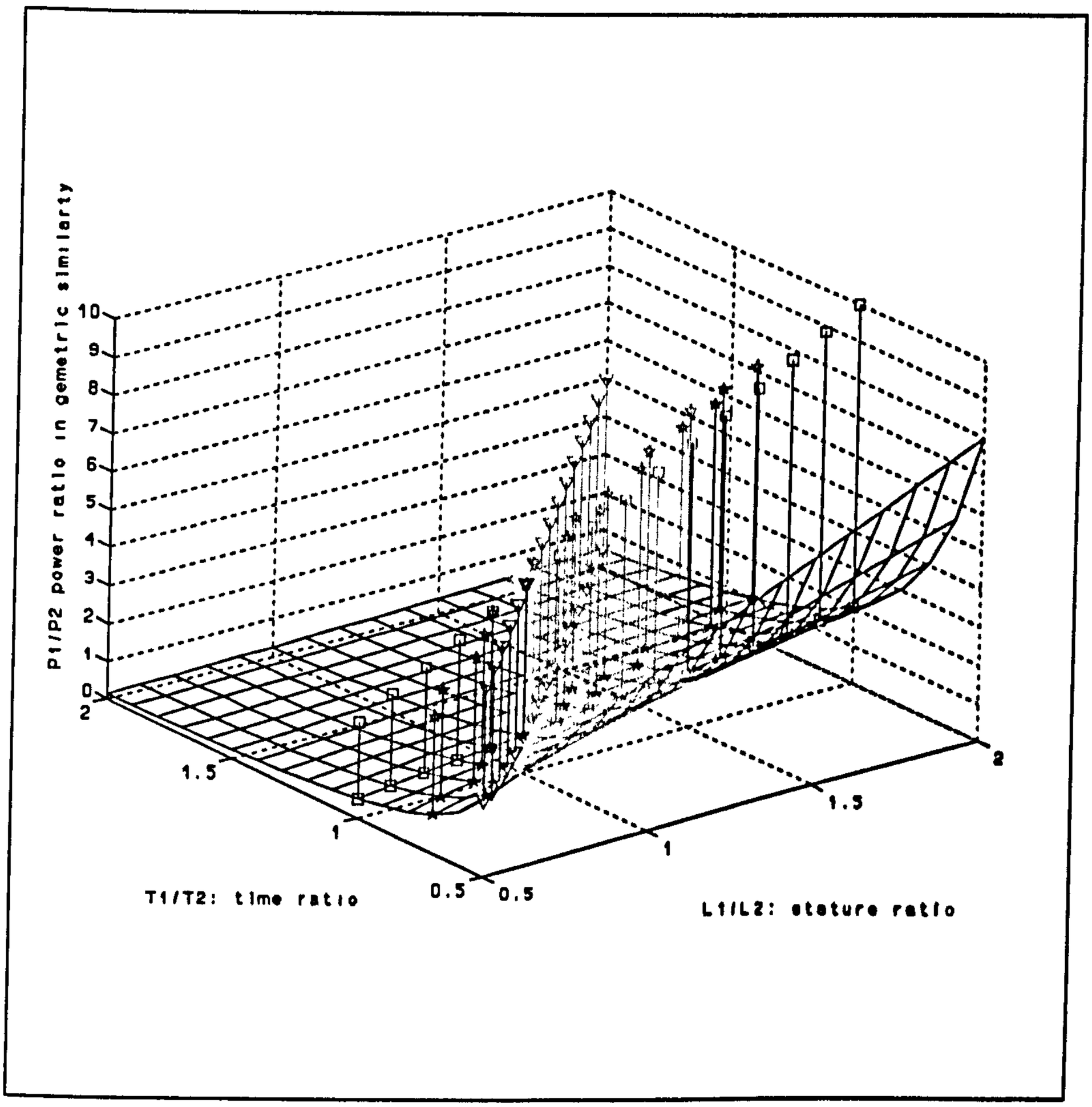

FIGURE 10.5 Relationship among power ratio, stature ratio and time ratios

TABLE 10.5.a Comparison of cycle-time under the iso-power assumption

Subject	Stature	Myr	Time%	Velo%
AL288	1.05	3.10	100.00	100.00
AL333	1.42	3.10	116.29	116.29
Sts14	1.07	2.60	100.95	100.95
Sk-82	1.46	1.70	117.92	117.92
Ke738	1.39	1.90	115.06	115.06
Ke993	1.33	1.50	112.55	112.55
K1503	1.33	1.90	112.55	112.55
K3728	1.43	1.90	116.70	116.70
K1463	1.75	1.70	129.10	129.10
WT15000	1.45	1.80	117.51	117.51
Male	1.75	0.00	129.10	129.10
Female	1.60	0.00	123.44	123.44
Child9	1.22	0.00	107.79	107.79

On the other hand, if the relationship between velocity V ($\propto L/\Delta t$) and power P is considered, a line of equivalent power ($P_1/P_2=1$) can be plotted (Fig 10.5). On the line of iso-power, V_1/V_2 increases very quickly with L_1/L_2 but increases relatively slowly with $\Delta t_1/\Delta t_2$. This means that while two subjects expend the same energy, the larger subject can obtain a faster velocity than to carry out a similar action at lower frequencies, or spend more energy than do smaller ones (Table 10.5.b). If modern humans perform an activity in the same time as AL-288-1, they expend 50-70% more energy, though their speed is 60-75% higher. Conversely, if smaller subjects have to act at the same velocity as larger subjects, they also need to expend more the smaller, although the larger will spend more time in each cycle of motion. Table 10.5 compares mobilities of different subjects. From Table 10.5.a, under the assumption of iso-power, modern humans have the advantage of 30-40% greater speed than AL-288-1 would have had, but spend 20-30% longer than AL-288-1 to

complete a cycle.

TABLE 10.5.b Comparison of powers under the iso-velocity assumption

Subjects	Stature	Myr	Time %	Power %
AL288	1.05	3.10	100.00	100.00
AL333	1.42	3.10	135.24	73.94
Sts14	1.07	2.60	101.90	98.13
Sk-82	1.46	1.70	139.05	71.92
Ke738	1.39	1.90	132.38	75.54
Ke993	1.33	1.50	126.67	78.95
K1503	1.33	1.90	126.67	78.95
K3728	1.43	1.90	136.19	73.43
K1463	1.75	1.70	166.67	60.00
WT15000	1.45	1.80	138.10	72.41
Male	1.75	0.00	166.67	60.00
Female	1.60	0.00	152.38	65.63
Child9	1.22	0.00	116.19	86.07

TABLE 10.5.c Comparison of power under the iso-time assumption

Subject	Stature	Myr	Velo%	Power%
AL288	1.05	3.10	100.00	100.00
AL333	1.42	3.10	135.24	135.24
Sts14	1.07	2.60	101.90	101.90
Sk-82	1.46	1.70	139.05	139.05
Ke738	1.39	1.90	132.38	132.38
Ke993	1.33	1.50	126.67	126.67
K1503	1.33	1.90	126.67	126.67
K3728	1.43	1.90	136.19	136.19
K1463	1.75	1.70	166.67	166.67
WT15000	1.45	1.80	138.10	138.10
Male	1.75	0.00	166.67	166.67
Female	1.60	0.00	152.38	152.38
Child9	1.22	0.00	116.19	116.19

Larger subjects have to perform a given action at lower frequencies, or spend more energy than a smaller subject (Table 10.5.b). For modern humans to perform an activity in the same time period as AL-288-1, they would have to expend 50-70% more energy, although their velocity is 60-75% higher. Contrarily, for smaller subjects to act at the same velocity as larger subjects, they have to expend more energy than the latter (Table 10.5.c).

Thus, the three variables: stature, velocity and time are not independent. Increase of subject size results in either an increase in cycle time, and it must be presumed that this will limit the tendency to size increase. A species-specific iso-power line seems

likely to exist. On the iso-time line, although $\Delta t_1/\Delta t_2=1$, P_1/P_2 increases very quickly with V_1/V_2 .

10.4.5 Discussion

If we hold stability unchanged, (in other words, Rp constant), from equations (10.13) and (10.14) we know that L (stature or leg length) should increase in order to decrease PRM.

$$\frac{M_m}{M_f}=\frac{d_m^2 L_m}{d_f^2 L_f} \qquad (10.21)$$

$$\therefore \frac{M_m}{M_f}=\frac{R_{pm}^2 L_m^3}{R_{pf}^2 L_f^3}=\frac{L_m^3}{L_f^3} \qquad (10.22)$$

Increase of stature will inevitably require increase of mass. Because of the continuity of material properties assumption, size and weight will increase according to geometric similarity. Equation (10.21) can be plotted as a figure (Figure 10.6). If decrease in PRM occurs over time, so should the increment rate of Pd should be also. Since:

$$\frac{dP_d}{dL} \propto -\frac{1}{L^2} \qquad (10.23)$$

the effect of this factor will decrease with increased stature (see Fig. 10.7).

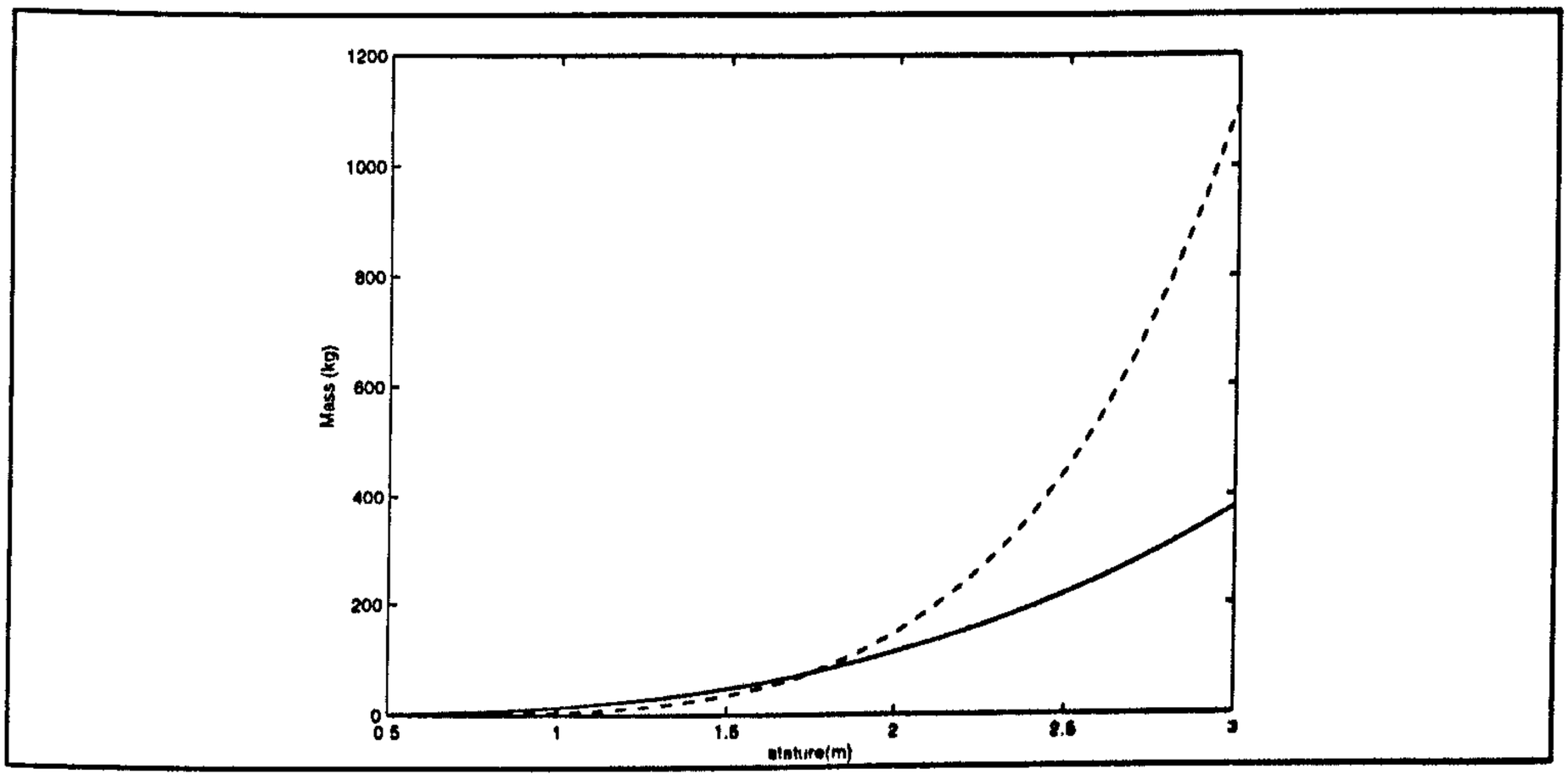

FIGURE 10.6 How human size might increase

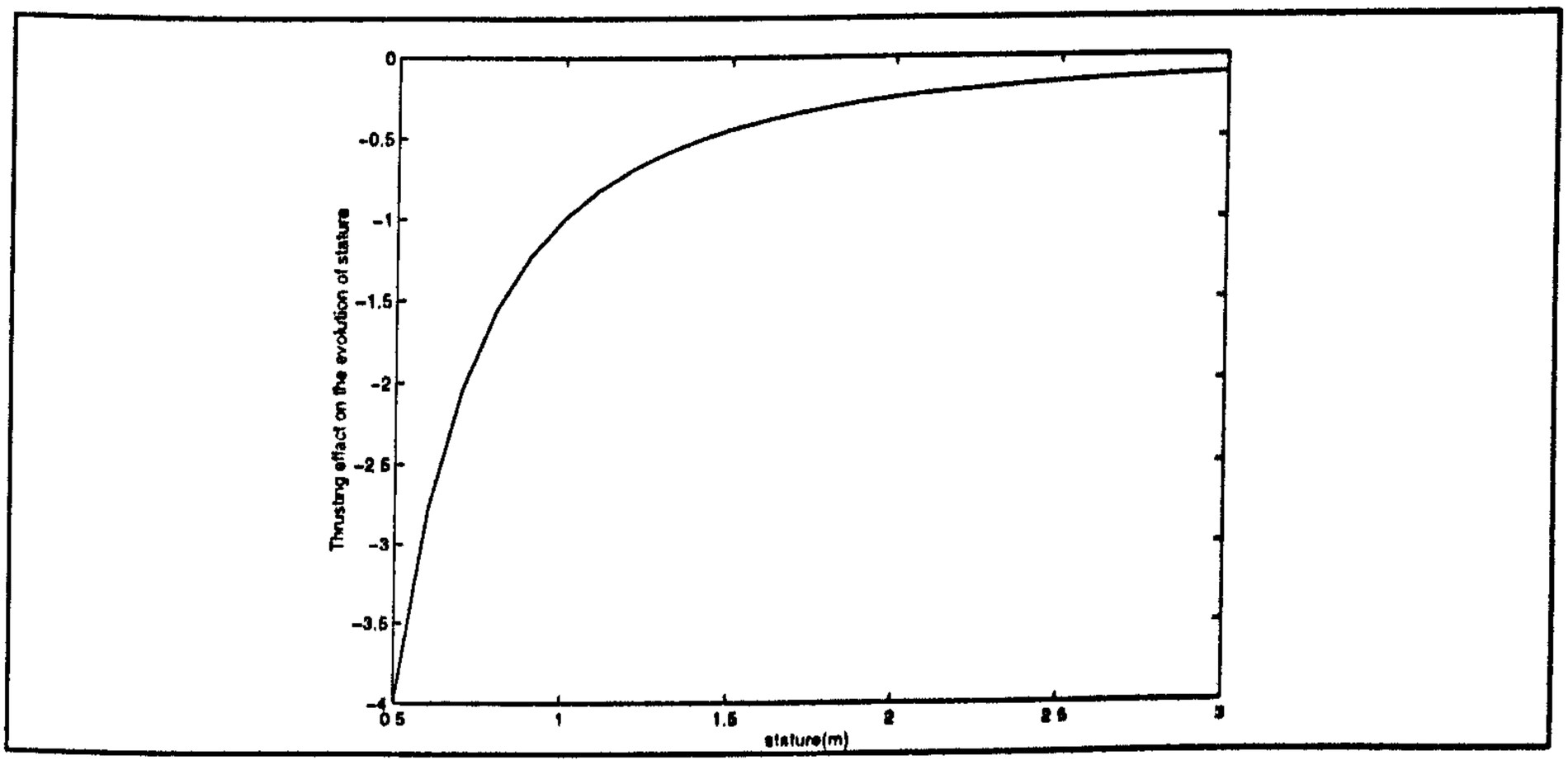

FIGURE 10.7 Increment rate of stature

CHAPTER 11 OVERALL CONCLUSIONS

I am like a child playing by the sea of knowledge.

I. Newton (1642-1727)

In Chapter 1, I stated that the major question posed in this thesis was: *'whether the acquisition of the longer-legged, shorter-trunked morphology of WT-15000 does indeed increase mechanical effectiveness in load-carrying'*.

Secondary goals were to provide new data on the comparative biomechanics (in particular, joint angles, joint velocities, joint torques, joint power and required energy) of unloaded erect and BHBK bipedalism in modern humans and the occasional bipedalism of the common chimpanzee, and to determine whether the skeletal proportions of early hominids were better suited to BHBK or erect walking, and to begin to estimate muscle forces for early hominids.

Using a range of techniques, including kinematic and kinetic measurements on the gait of living humans and other great apes, dynamic analysis, whole-body multi-rigid-segment dynamic modelling, studies of energy transformation at the segment and body centre of gravity, computational optimization and dynamic modelling of the mechanics of the musculoskeletal system (the latter two involving development of entirely new analytical tools) I have succeeded in addressing each of these goals. Some approaches, particularly prediction of muscle forces, are still at a preliminary stage, but I have demonstrated that they are feasible and can produce biologically meaningful results; other approaches, particularly the analysis of size and robusticity, remain to be tested on a better dataset, but these deficiencies are not easily remedied within the time and resources available.

Some of the more important findings are itemized below:

1) In general, the expenditure of energy is larger in BHBK than in erect walking. Both joint moments and powers are larger in BHBK than in erect walking, and the effectiveness of energy transformation is less in BHBK.

2) Work done is larger in BHBK than erect walking.

3) Analysis of multi-rigid-body model simulations of AL 288-1 and WT-15000 confirms that early hominids would also expend more energy in BHBK mode than in erect walking.

4) On a theoretical basis, it would appear that the need to coordinate swing frequencies of the upper to lower limbs, together with the need to carry objects in the hands, favours relatively shorter upper limbs, and may therefore explain why the humerofemoral index is lower in *Homo erectus* and modern humans than in *A. afarensis.*

5) According to computational simulations of early hominid bipedal walking, AL 288-1 would have expended more joint power per unit mass per unit velocity than WT-15000. This suggests that a relatively short upper body (trunk and upper limbs) would be selected for to enhance the effectiveness of bipedal walking.

6) According to computational simulation of hominid loaded walking, WT-15000 also had better carrying ability than did AL 288-1, confirming the hypothesis that transport of food or artefacts was likely to have been a factor selecting for the acquisition of a more 'modern' morphology. Transport of objects further increases the disadvantages of BHBK walking for AL-288-1 and other hominids. While WT-15000's morphology favours effective transport of light loads, carried over the shoulder or round the neck, the morphology of modern humans is better suited to hand transport and to transport of heavy loads.

7) According to a preliminary musculoskeletal modelling simulation, both muscle forces and powers per unit mass and per unit velocity are larger in BHBK than in erect walking.

8) According to theoretical biomechanical analysis of size, power per unit mass and per velocity may be less in larger species. This is in agreement with physiological experiments in the literature.

General significance

In experiments on 'bent-hip, bent-knee' walking, moments at the knee were not only much larger than in normal walking, but lasted much longer, almost the whole duration of stance. As a consequence of this and similar moments at the ankle and foot, total joint power for equal displacement of the mass centre was almost 1.5 times that in normal walking, and energy recovery (assessed, as above, using a particle mechanics approach) was *half* that in normal walking. Similarly, in computer simulations, normal unloaded walking by AL-288-1 incurred 56% of the power requirements it incurred in bent-hip, bent-knee unloaded walking. However, normal unloaded walking by WT-15000 incurred only 40% of its power requirements in bent-hip, bent-knee unloaded walking, so that the more modern body proportions of early *Homo*, with longer lower limbs and a shorter trunk actually increased the advantage, in terms of mechanical effectiveness, of erect walking relative to the advantage gained by *Australopithecus afarensis*. Conversely, this can be read to indicate that the cost of BHBK walking was relatively lower for *A. afarensis* than for early *Homo*.

Perhaps the most striking of our results for the dynamic response of our models during loaded walking was a comparison of normalized mechanical joint power requirements. It appears that BHBK walking would have been particularly disadvantageous to *A. afarensis* if this species had carried loads, however small. Models of WT-15000 have substantially lower relative power requirements for normal walking than *A. afarensis* whatever the relative size of the load. The WT-15000 models could carry a load of 20% of body weight at no greater relative cost than AL-288-1 incurred walking erect and unloaded. Thus, the shorter trunk but longer legs of WT-15000 do indeed serve to allow it to walk more effectively, loaded or unloaded, but are perhaps of particular significance in offering 'free' loading! In fact, the mechanical effectiveness of walking by the WT-15000 android is somewhat greater, carrying small loads, than for our modern human male adults,

although the advantage is reversed for loads above 40% body mass. Our detailed studies of the dynamic response of the AL-288-1 and WT-15000 models, and those representing modern humans indicates that one reason for the difference in performance of the models is the difference in the ratio of the length of the trunk and head to the lower limbs. The relatively long trunk and head of AL-288-1 results in high principal moments of inertia. Keeping lower limb length constant, moments at the hip then have to increase to maintain the stability of the upper body. (Although the head and trunk segment is longer in modern human adults than in both reconstructions of WT-15000, this cannot however completely explain the difference in performance).

Just as we found that energy transformation is more than halved in BHBK walking, our colleague Carey (1999) found that it leads to doubling of physiologic costs, and double the increase in core temperature that occurs over the same period in normal walking. Recovery of temperature after BHBK walking may be estimated to require 150% of activity time. Thus, if *A. afarensis* walked 'bent-hip, bent-knee' it is likely that activity time and hence ranging distances would have been small, and available food resources therefore limited. Erect walking, on the other hand, would have imposed lower costs, permitted longer activity periods and larger ranges — and by analogy to carnivores — permitted a more predatory ecology. Load carrying would only have accentuated the problems of BHBK walking. Acquisition of a more modern, long-legged, short-trunked morphology by WT-15000 would, on the other hand, have further enhanced the efficiency of erect walking, reduced the costs of carrying and therefore increased activity time.

Appendix:

Gaitlab: a purpose-written software package

A.1 Structure and functions of Gaitlab

To do basic biomechanical analysis, I have developed this special software. Gaitlab is comprised of modules, each of which serves a special function. Single or multiple modules can be run to serve the needs of any particular task. The interface is shown in Fig. A.1. Pressing different buttons gives access to different modules, and within each of these, there are different sub-modules The major functions available are listed in Table A.1.

Gaitlab is written in C and Matlab (R), and it can be run on both MS Windows/PC and UNIX workstation platforms.

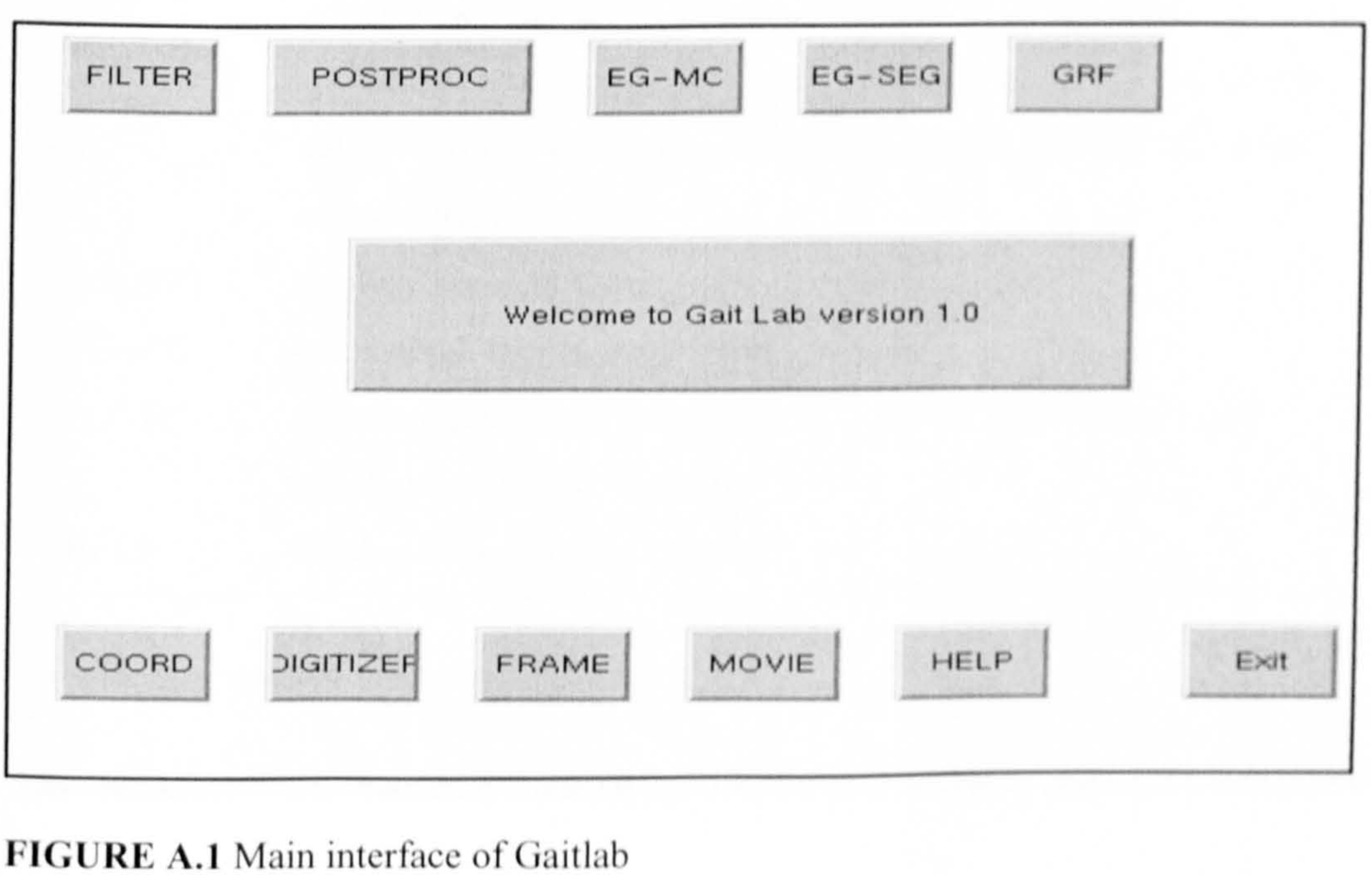

FIGURE A.1 Main interface of Gaitlab

TABLE A.1 The functions of modules of 'Gaitlab'

Module	Function
VIEWER	View single frames of a motion sequence
COORD	Build reference frame
DIGITIZER	Collect key coordinate points from a sequence of pictures;
FILTER	Digitize coordinates to provide data for analysis;
FRAME	Show a frame;
MOVIE	Show animation with superimposed ground reaction forces;
GRF	Analyze ground reaction force data from force platform, including combine 8 channels of raw data into three main forces; calculate major moments, force directions and path of the centre of pressure, etc.;
EG-SEG	Analyze segment energy ;
EG-MC	Analyze the energy at the centre of mass;
POSTPROC	Calculate joint angle, joint angular velocity, joint moment and (together with GRF module)
HELP	Explanation of use of modules.

Note: New modules are being developed.

A.2 A example of use of Gaitlab

We begin with a sequence of frames of recorded walking. The frames are captured one by one using a digital framestore controlled by other software packages written in our laboratory (eg. VC: (Savage, 1996) or DIGIT: Sellers, 1994). The frame may be viewed with module VIEWER

Using DIGITIZER, we can extract landmarks to be analyzed. Every single frame may be shown as a single stick figure (Fig.A.3). One by one, we may digitize every frame of a sequence and show these as a series of stick figures (Fig. A.4). The sequence may be animated using the MOVIE module.

The stick-figure data (Fig. A.5) may be rather noisy because of high frequency error produced during videography and digitizing, and cannot be completely avoided by any measurement means. In fact, bio-subject in motion at lower speed should not produce so high frequency of noises. The FILTER module improves the quality of the data considerably (see eg. Fig.A.5a).

At the same time, signals from a force platform can be analyzed by module GRF. In general, the raw data are comprised of signals from 8 channels (Fig.A.6). GRF converts these data into the three main forces and moments (Fig A.7), the direction of forces (Fig.A.8) and paths of the centre of pressure (Fig.A.9).

After GRF and FILTER have been run, POSTPROCess can be run to calculates joint angles (Fig.A.10), joint angular velocities (Fig.A.11), moments (Fig.A.12) and work done per unit time (power) (Fig.A.13). Of these, power is probably the most useful data, and forms the subject of several chapters of this thesis.

If energy is of particular interest, we may obtain information on energy fluctuation: modules E-SEG and E-MC provide analyses of fluctuations of kinetic and potential

energy (Fig.A.14) in segments and at the centre of mass.

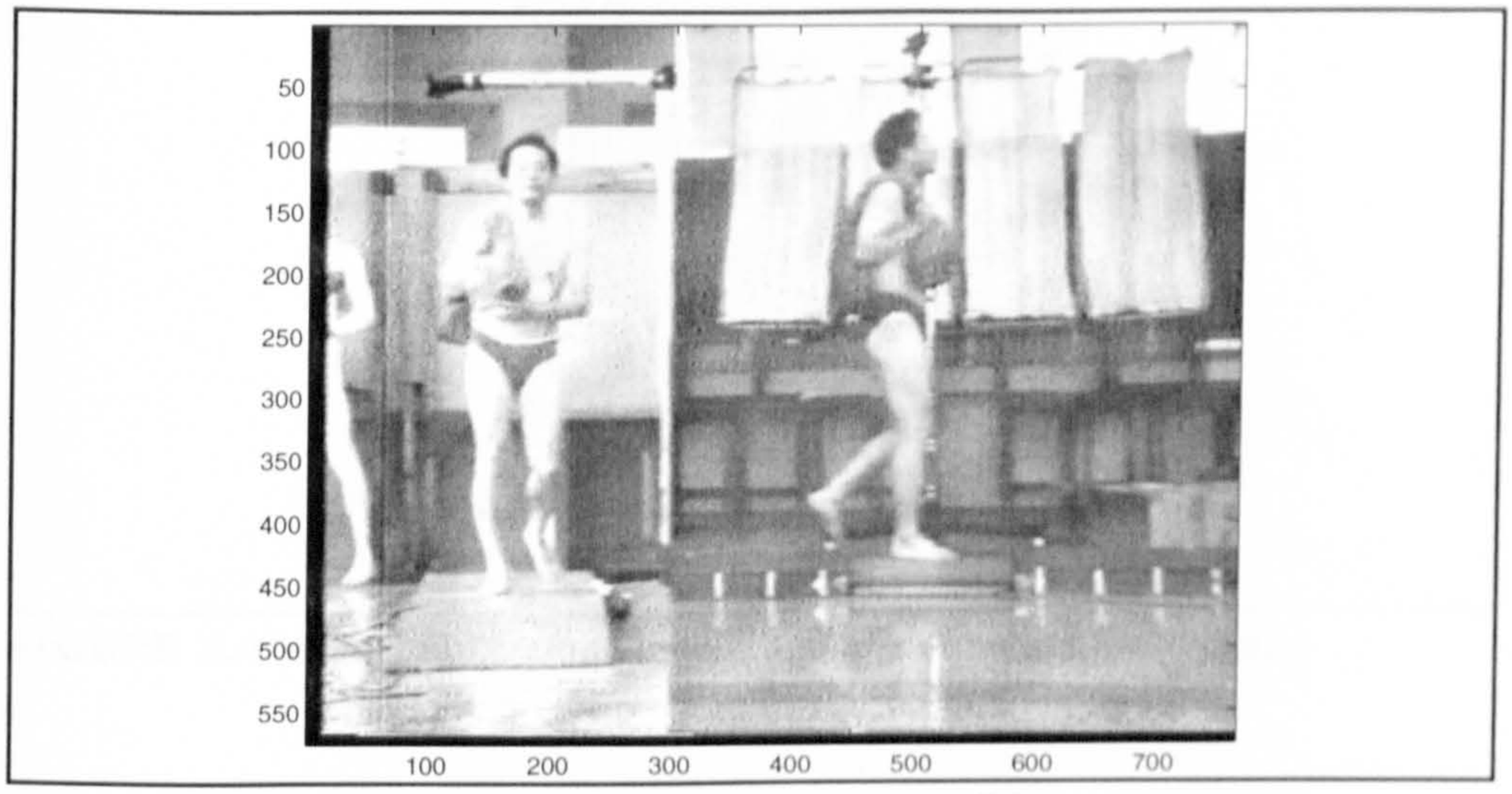

FIGURE A.2 A frame from a sequence of loaded walking

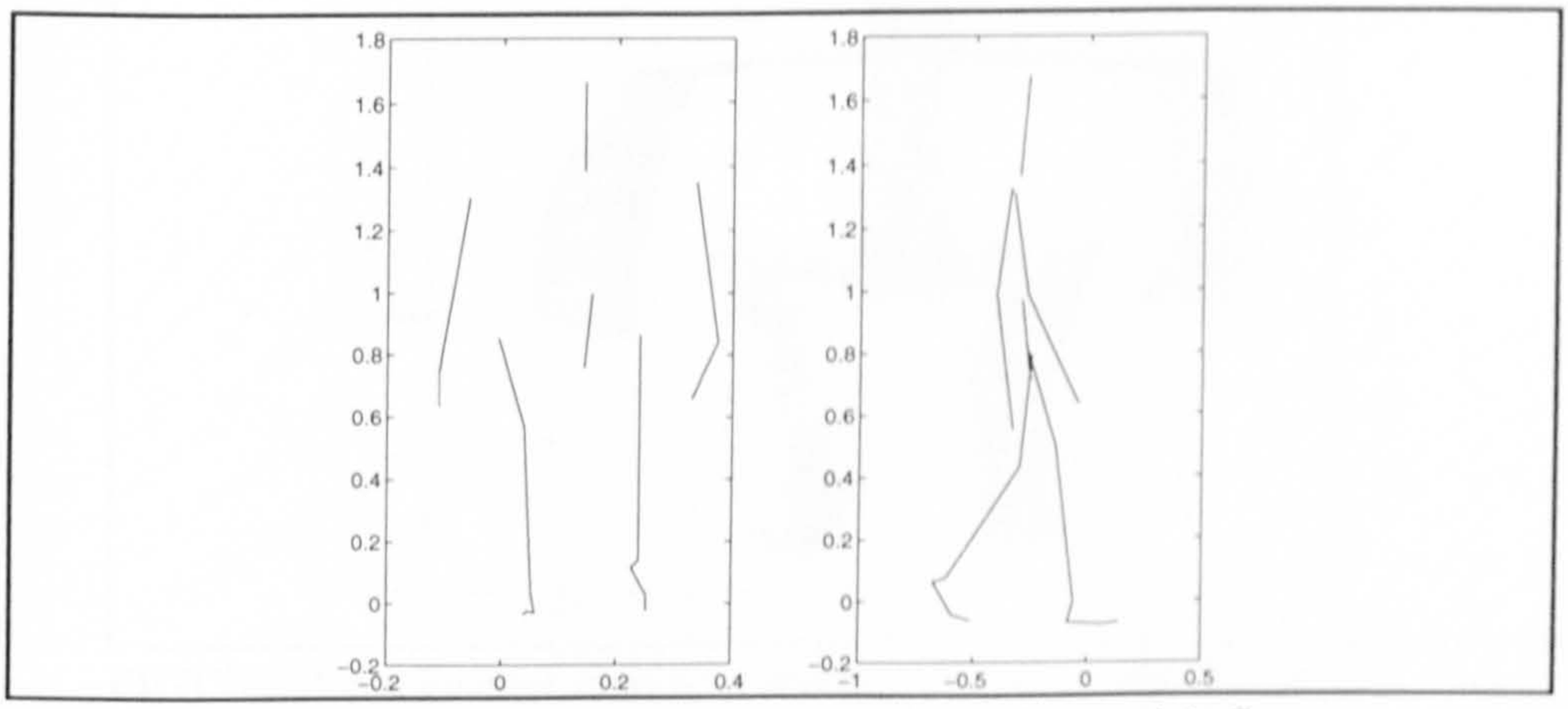

FIGURE A.3 A single frame of a sequence converted to a stick-figure representation

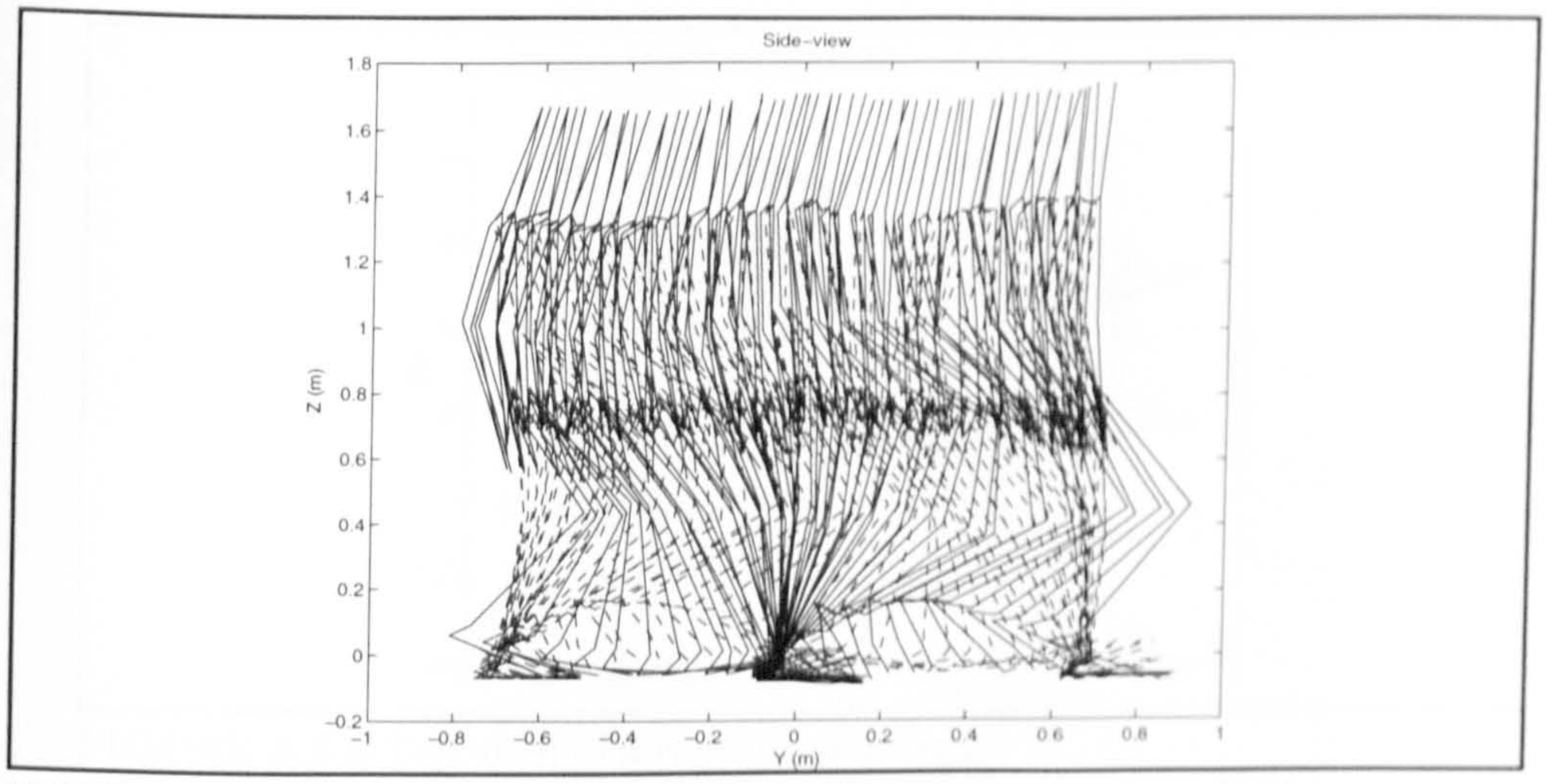

FIGURE A.4 A series of frames from a walking sequence (raw data).

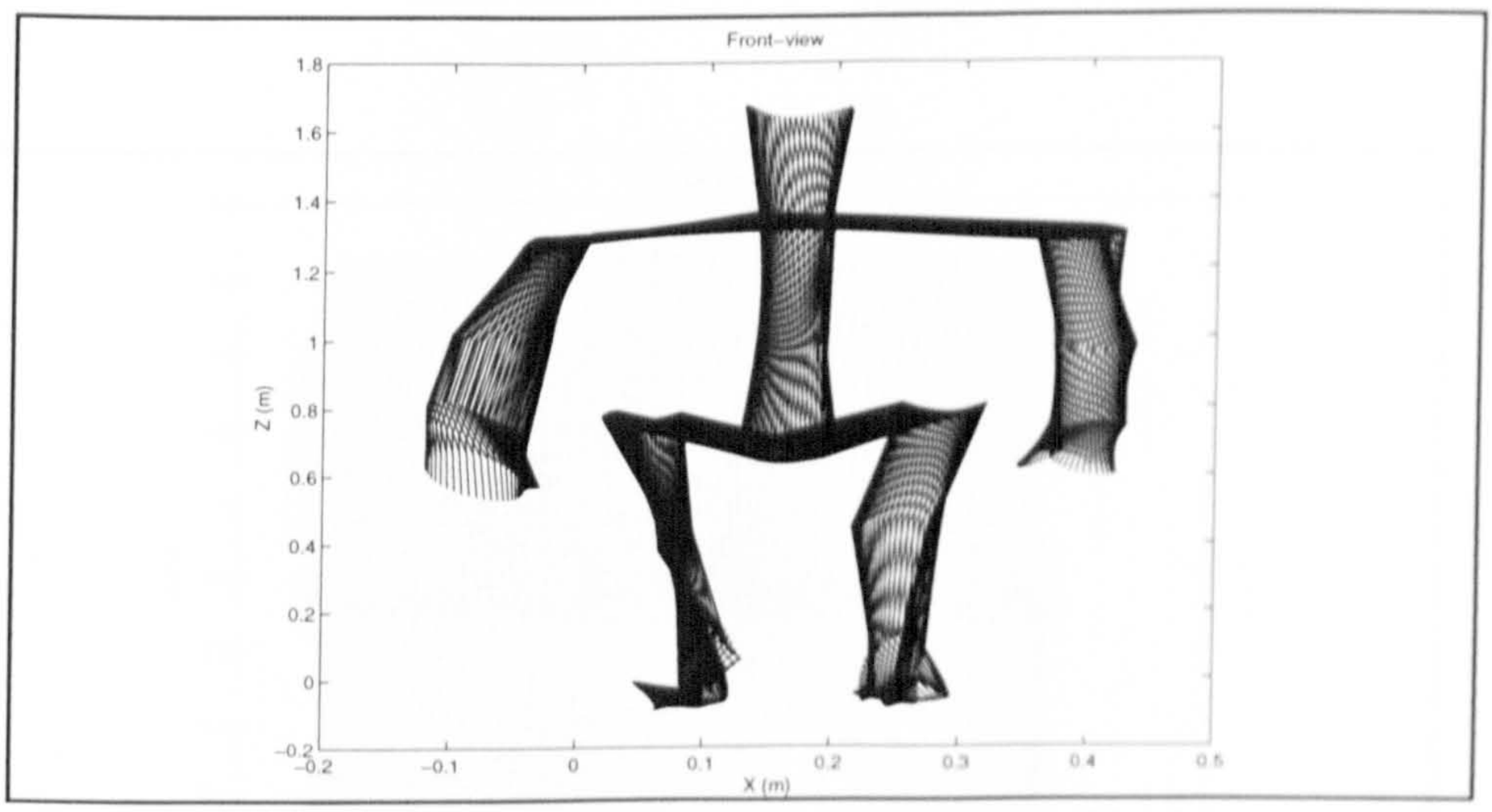

FIGURE A.5.a Frontal view of a walking sequence after filtering

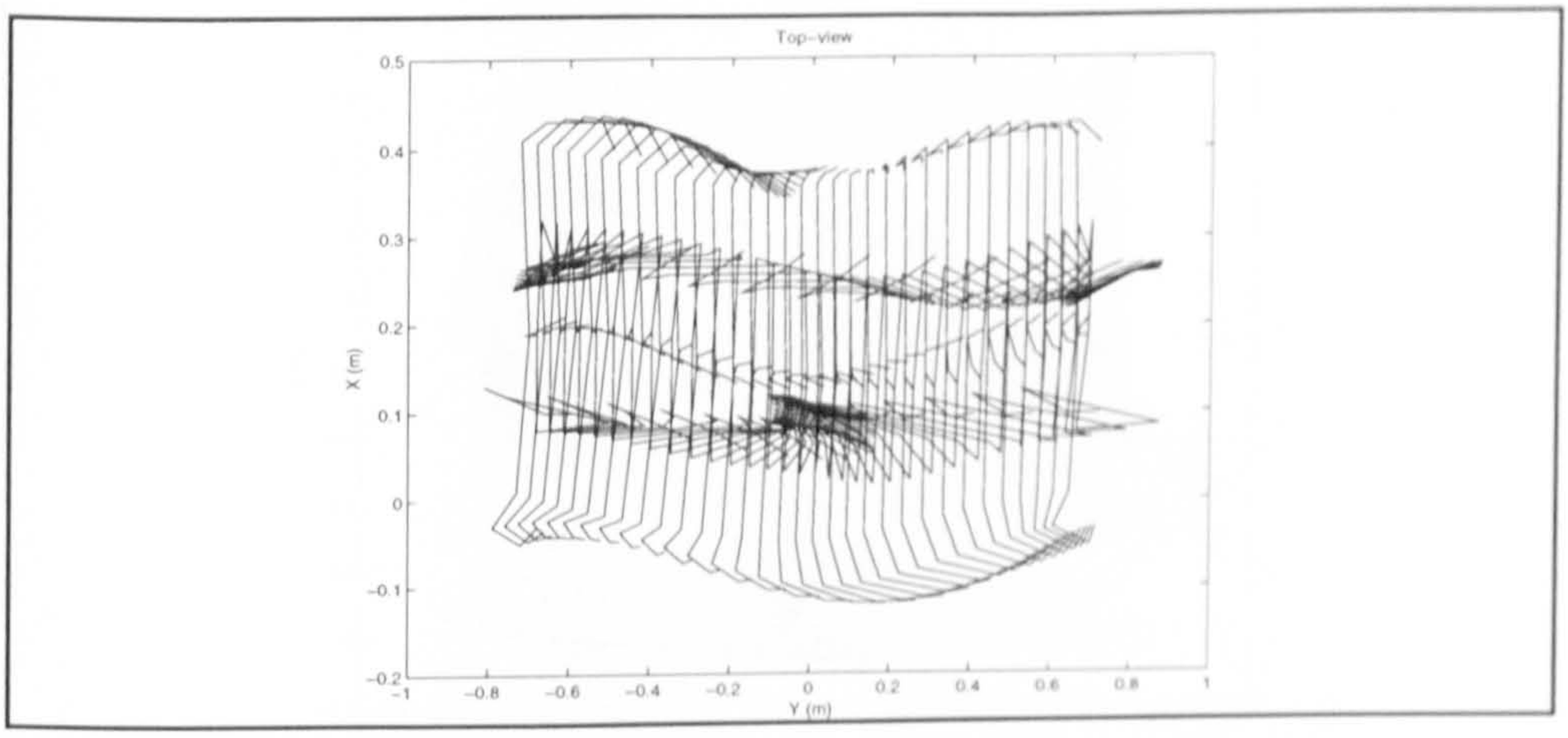

FIGURE A.5.b Top view of a walking sequence

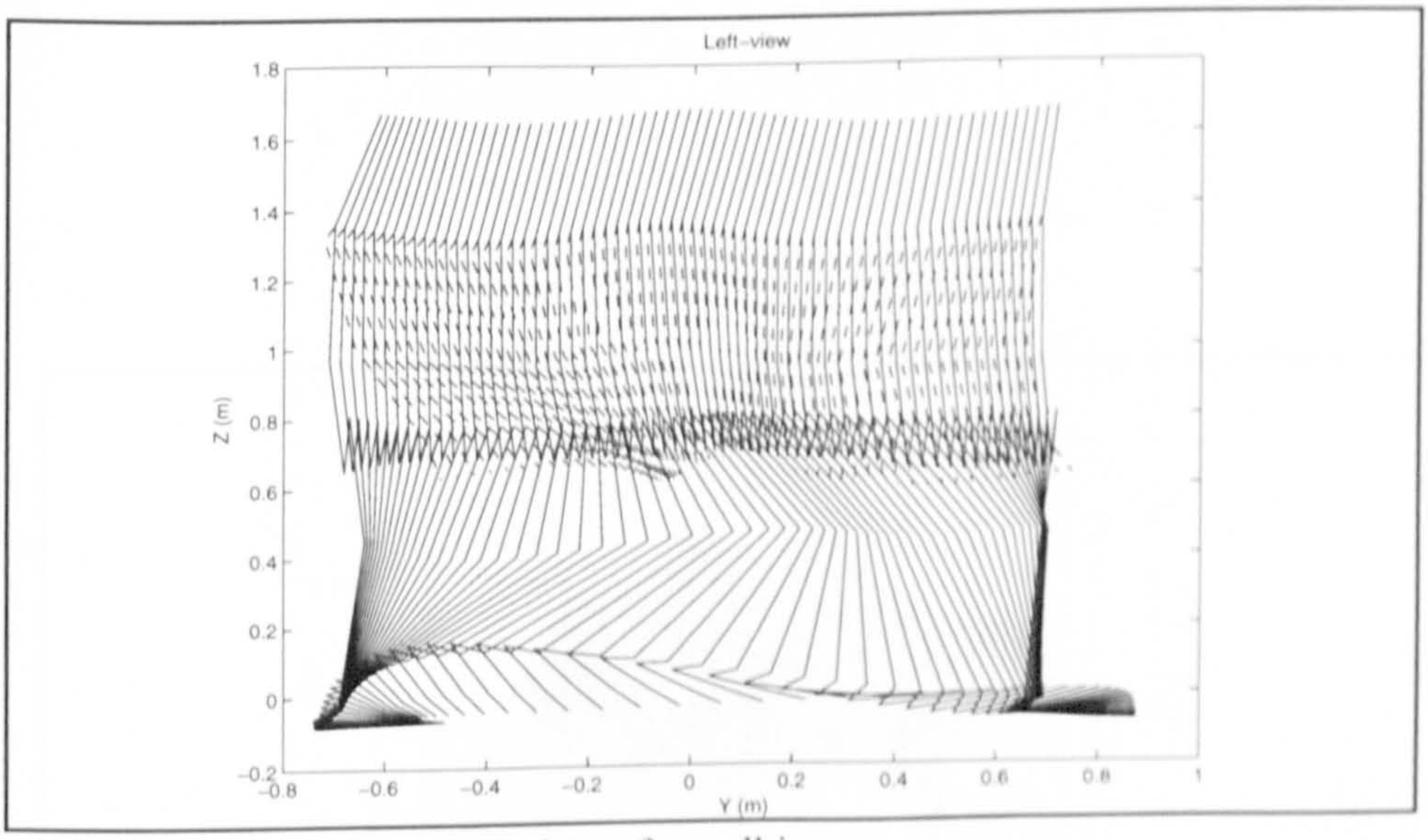

FIGURE A.5.c Left-sagittal view of a walking sequence

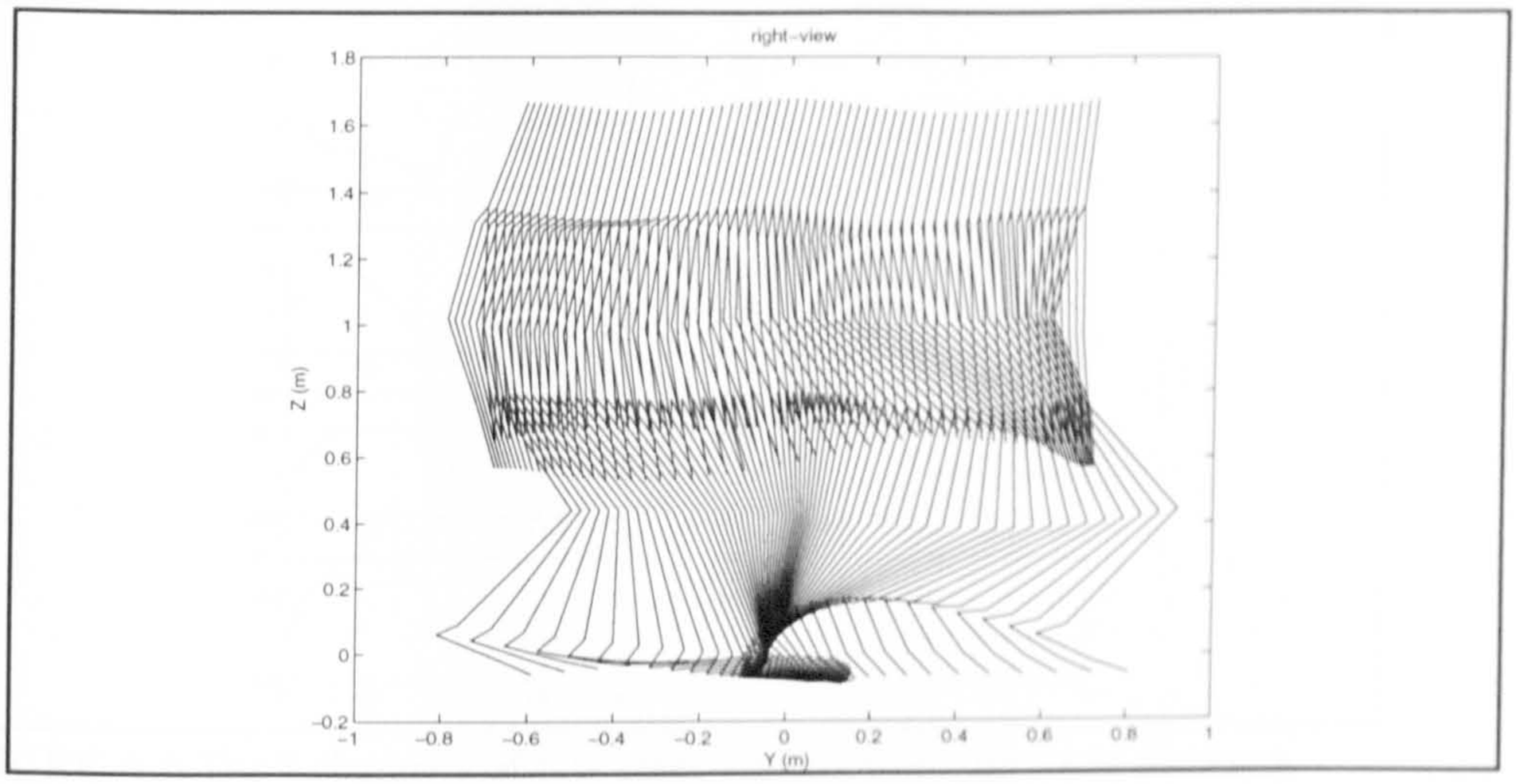

FIGURE A.5.d Right-sagittal view of a walking sequence

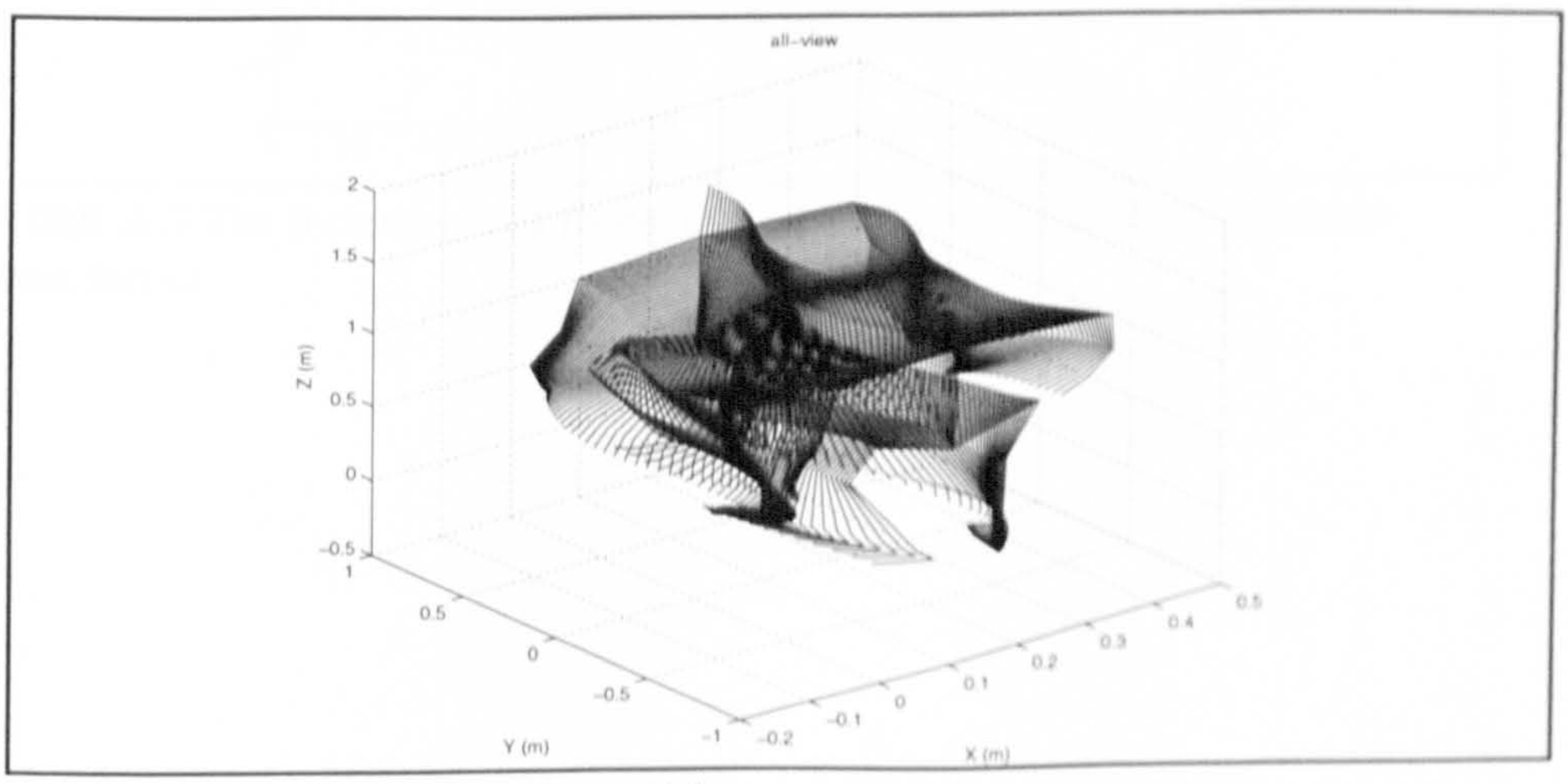

FIGURE A.5.e. 3D view of a walking sequence

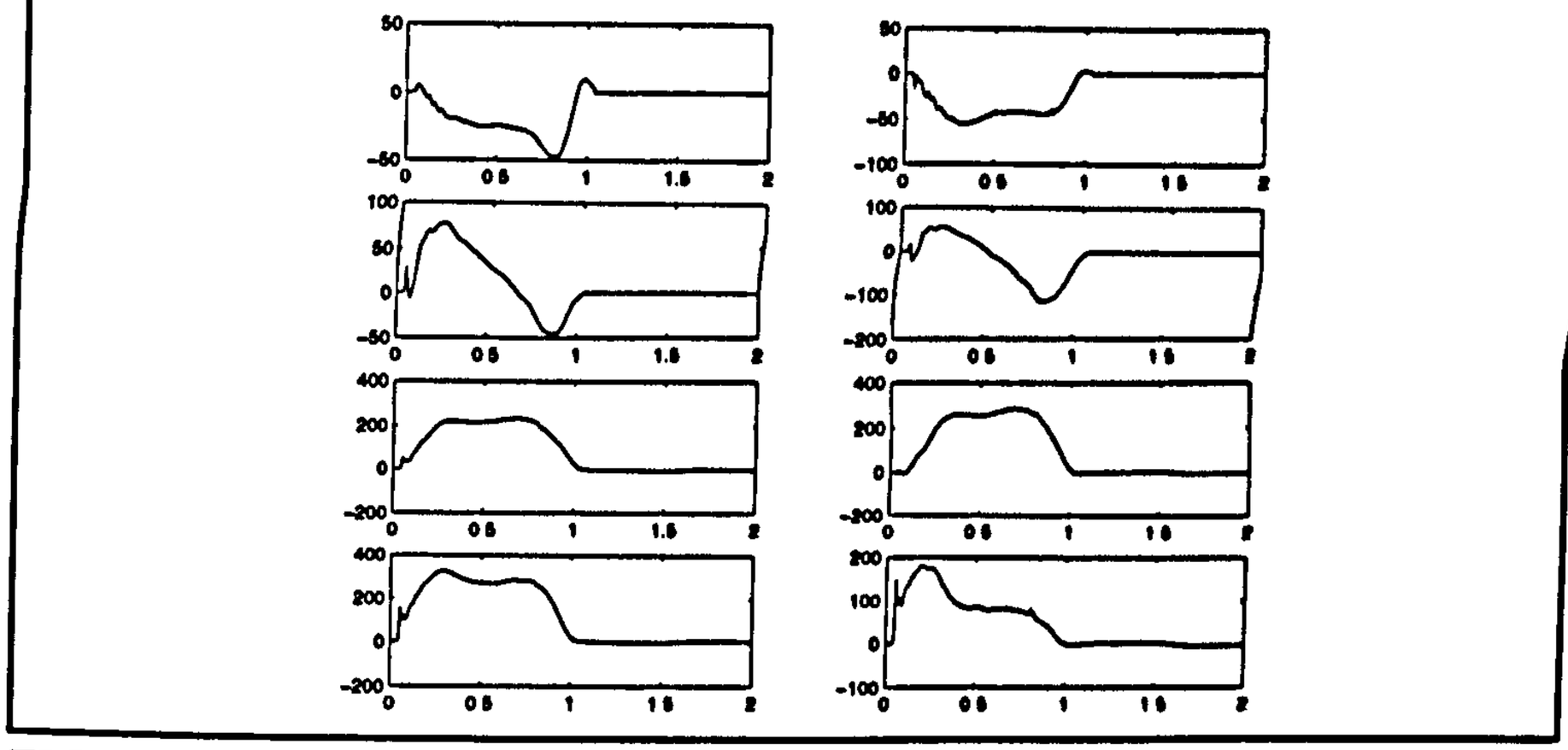

FIGURE A.6 The 8 channels of raw force signals from the force platform.

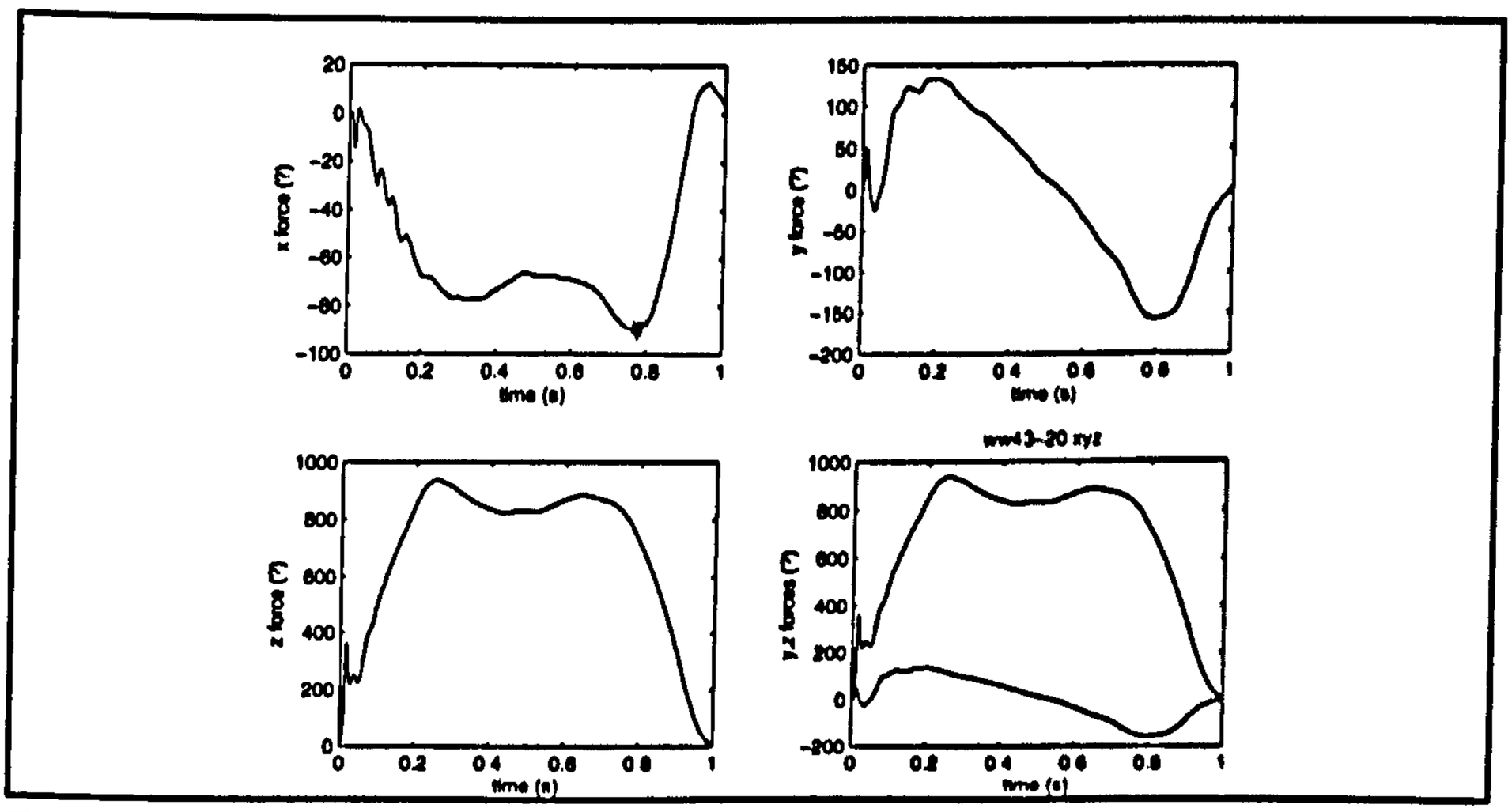

FIGURE A.7 The 8 channels of forceplate data resolved into the three main reaction forces

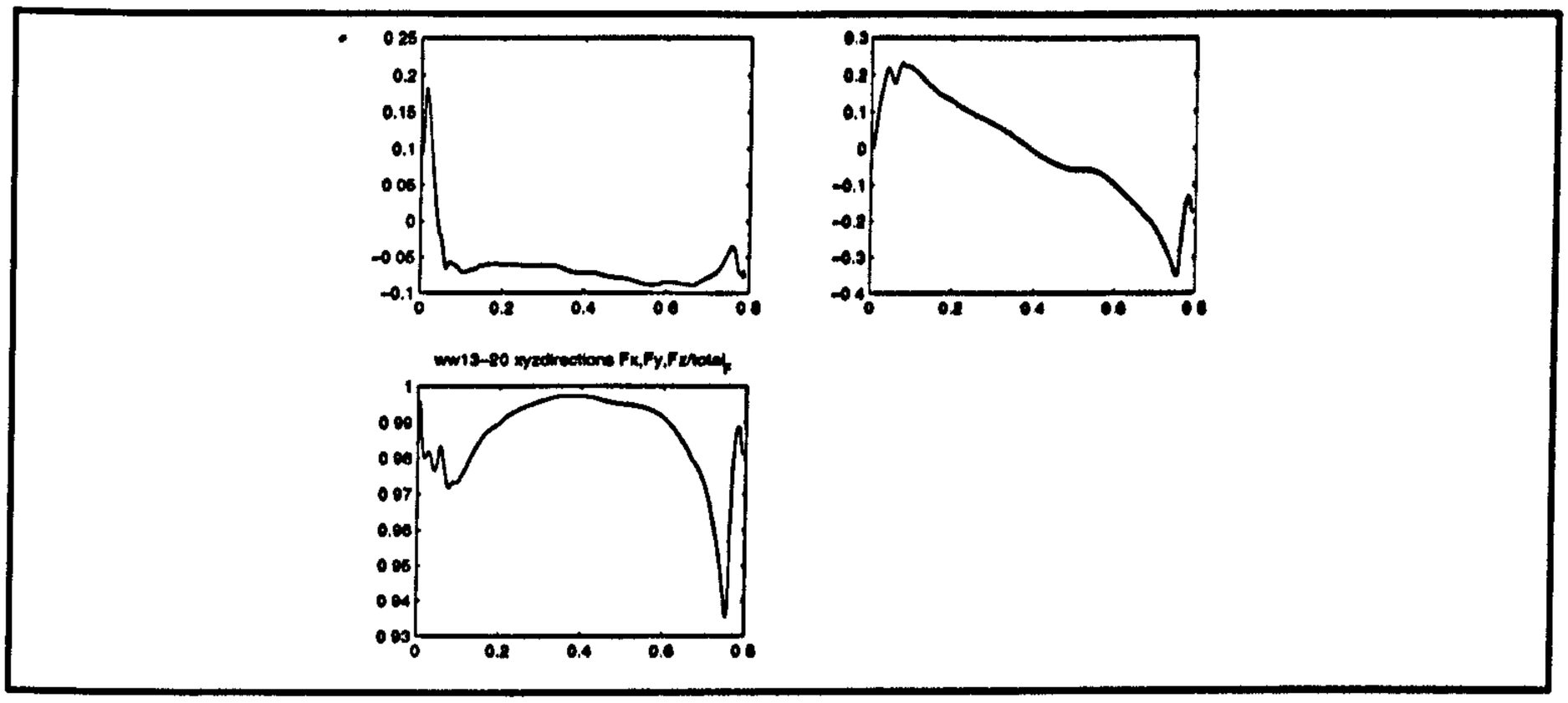

FIGURE A.8.a Directions of main forces (expressed by cosines)

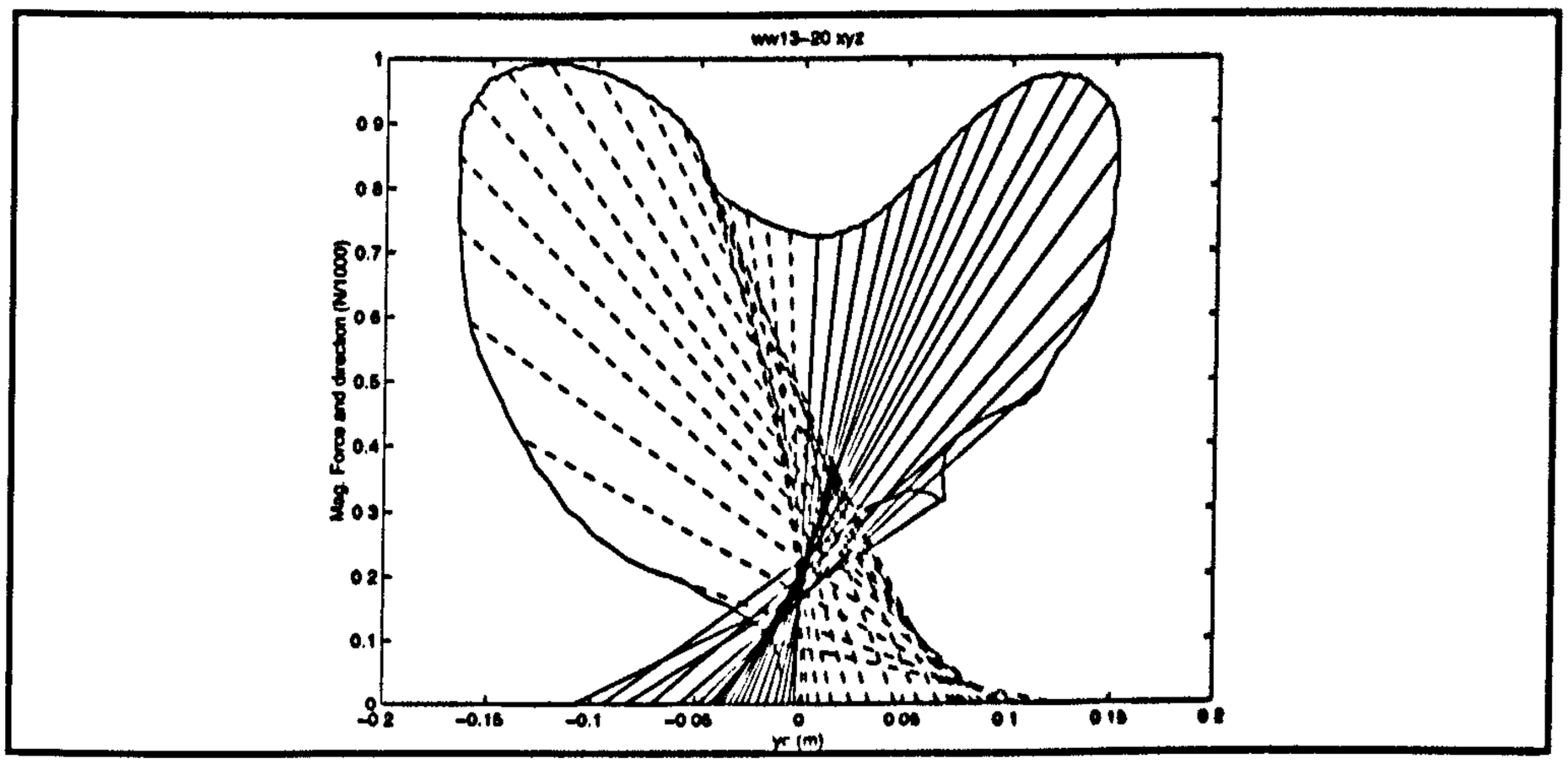

FIGURE A.8.b. Direction of Fy and Fz,-- Fy<0 and - Fy >0.

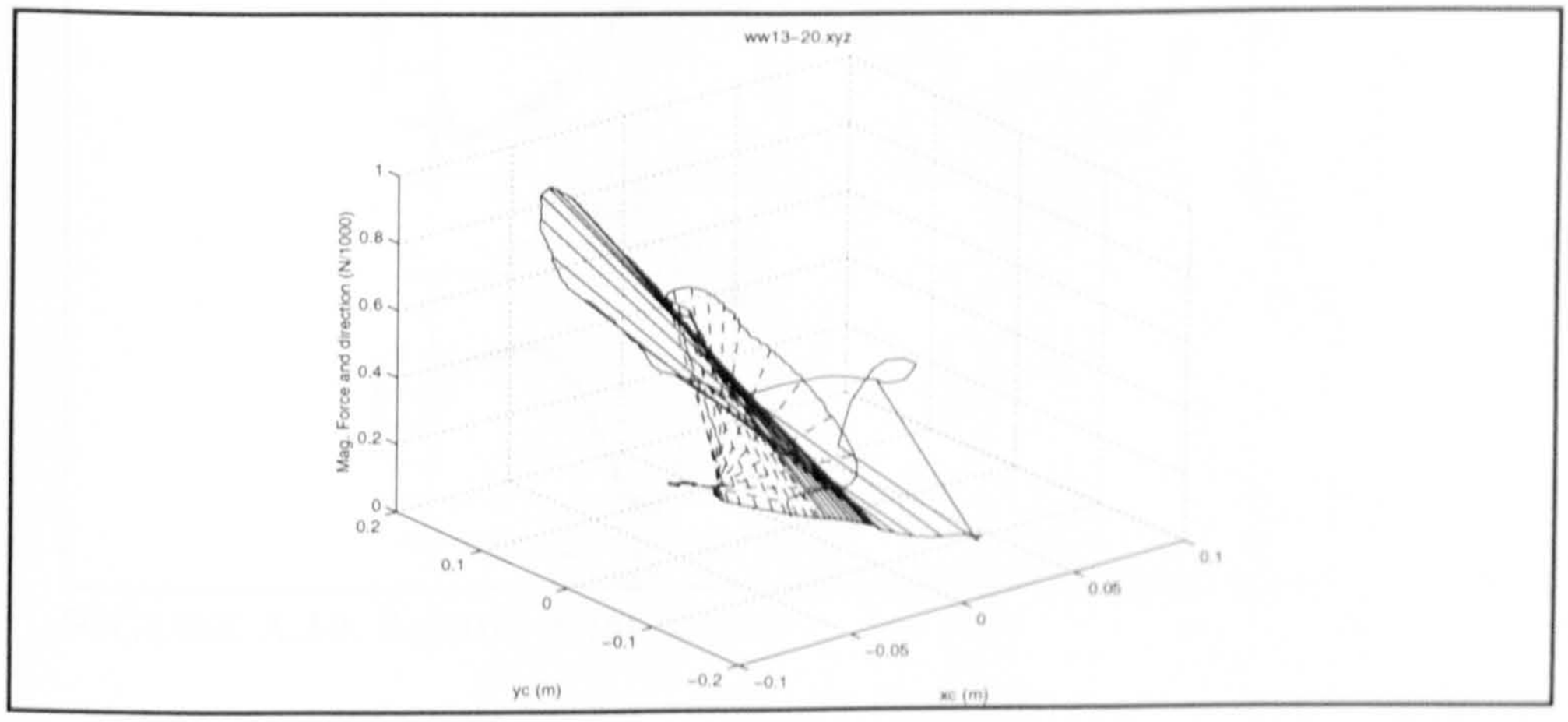

FIGURE A.8.c. 3D representation of the main force vector

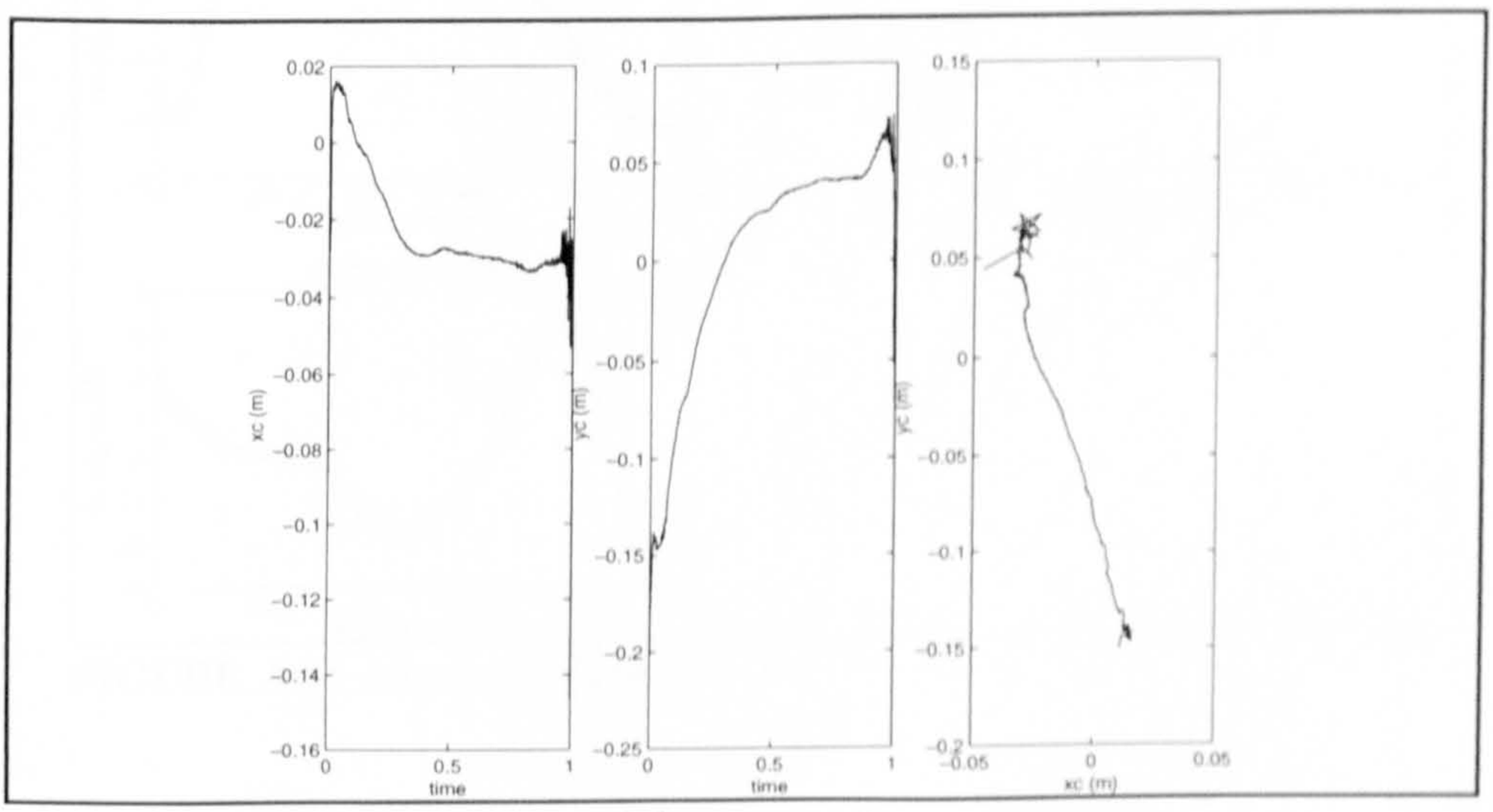

FIGURE A.9 Trace of the path of the centre of pressure

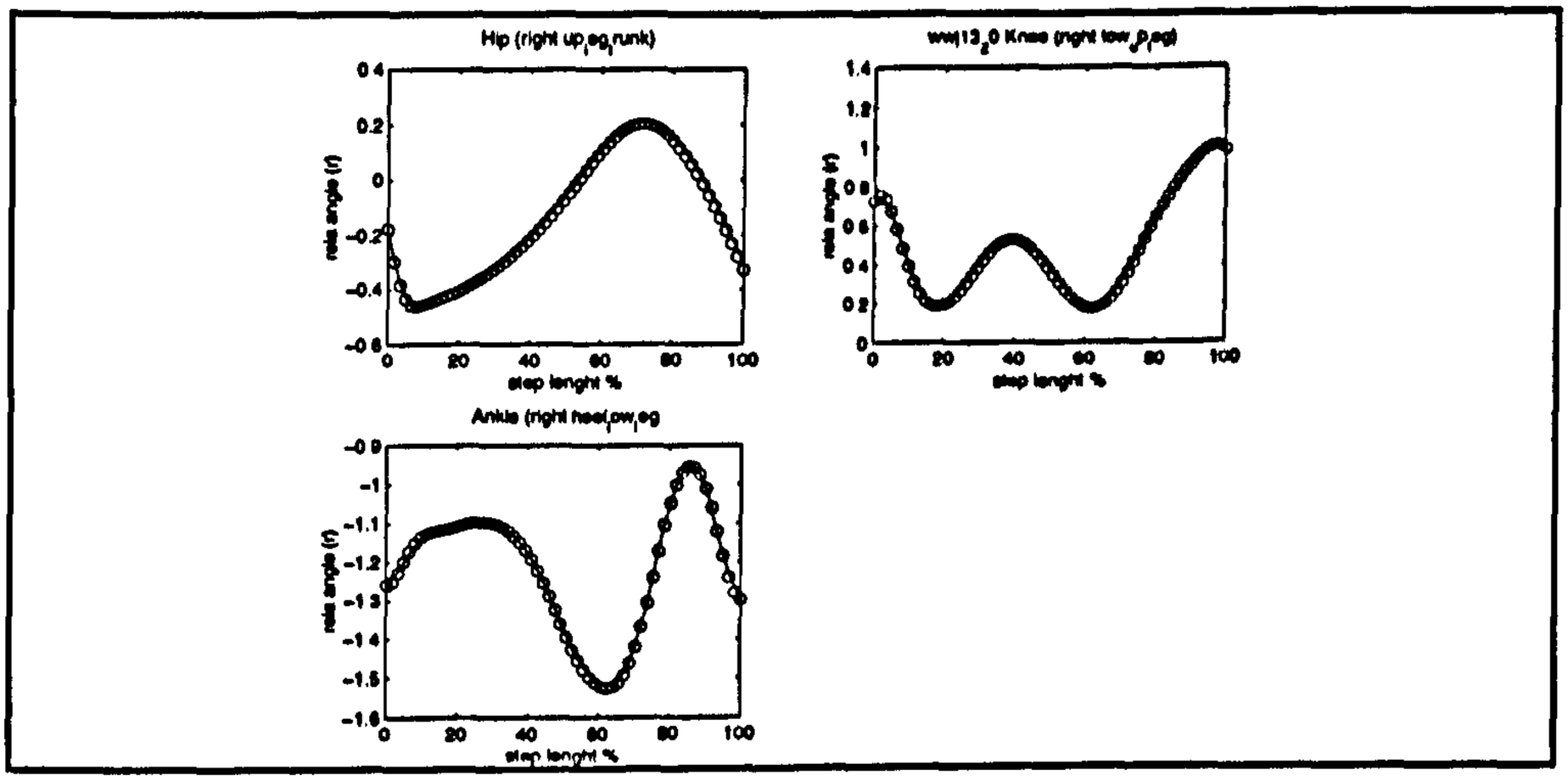

FIGURE A.10. Relative Joint Angles

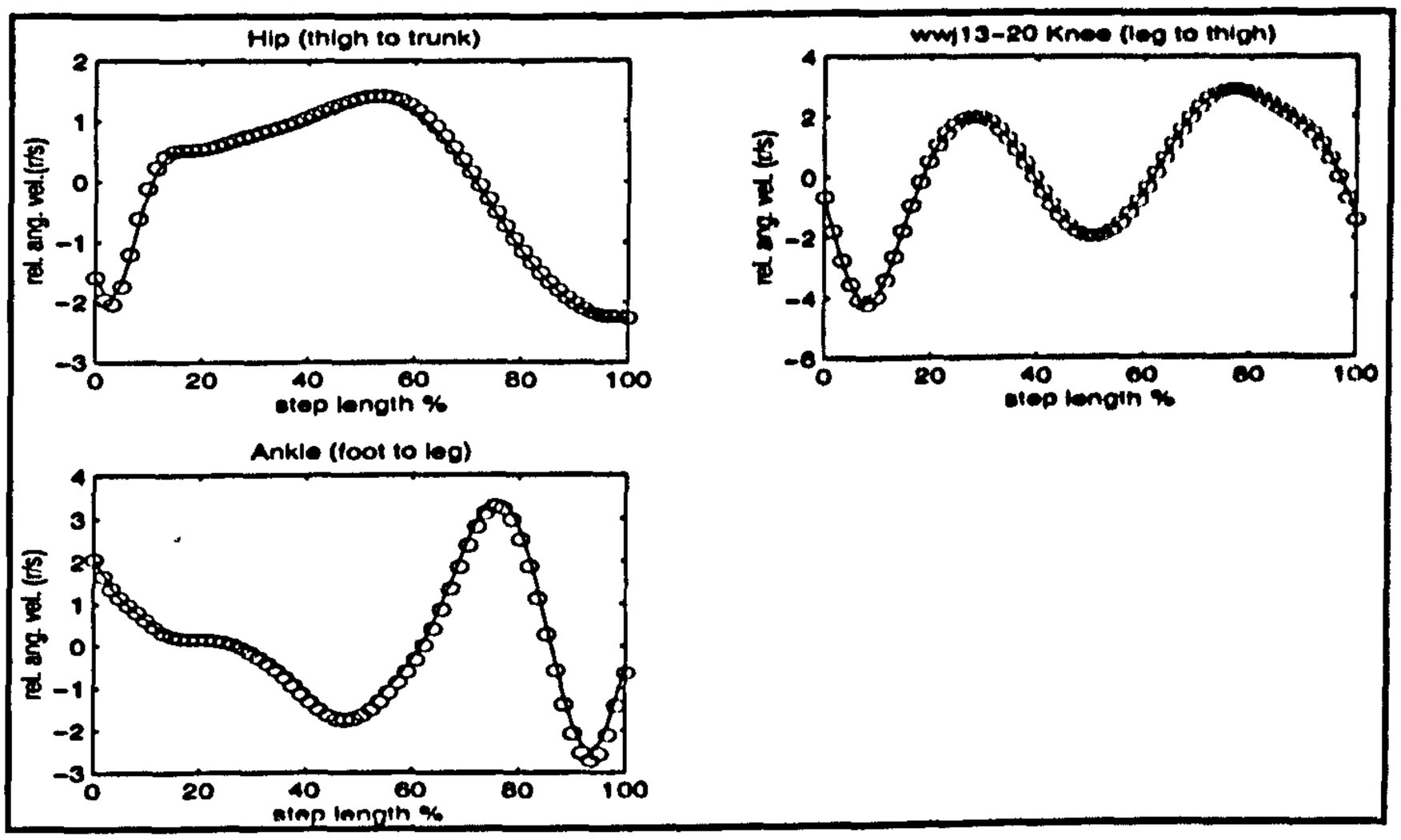

FIGURE A.11 Angular Velocities

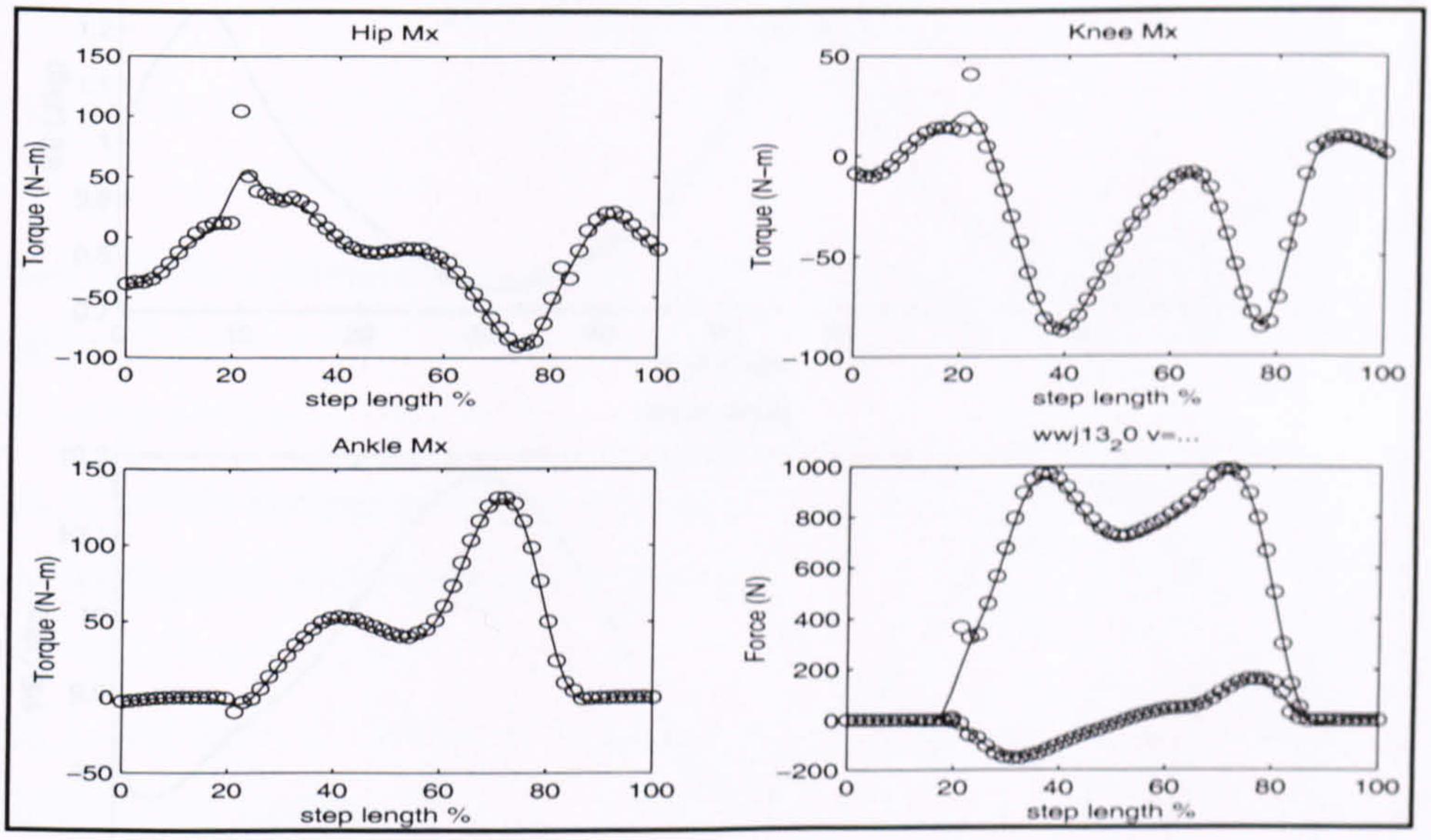

FIGURE A.12 Torques at joints

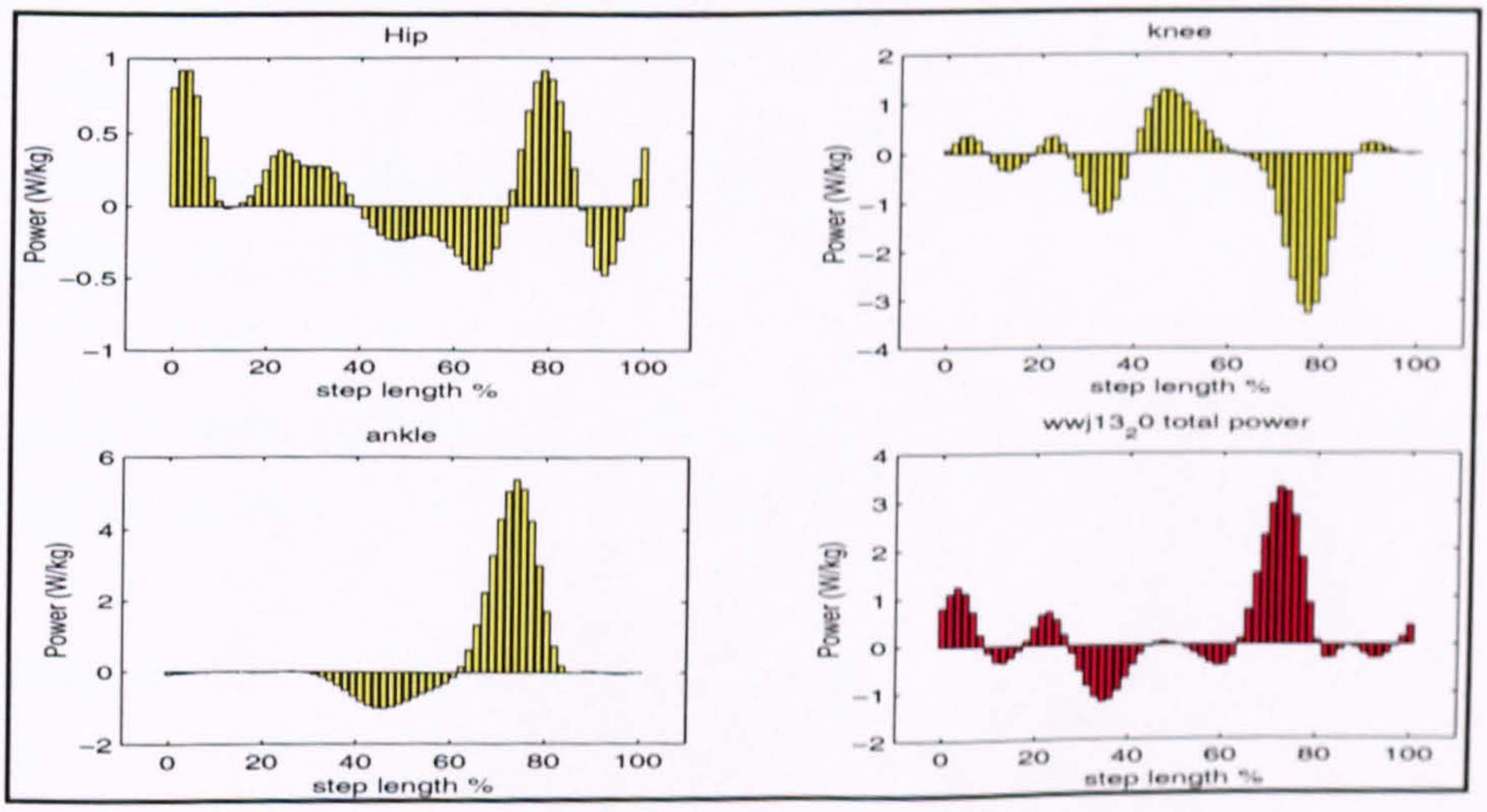

FIGURE A.13 Joint Powers

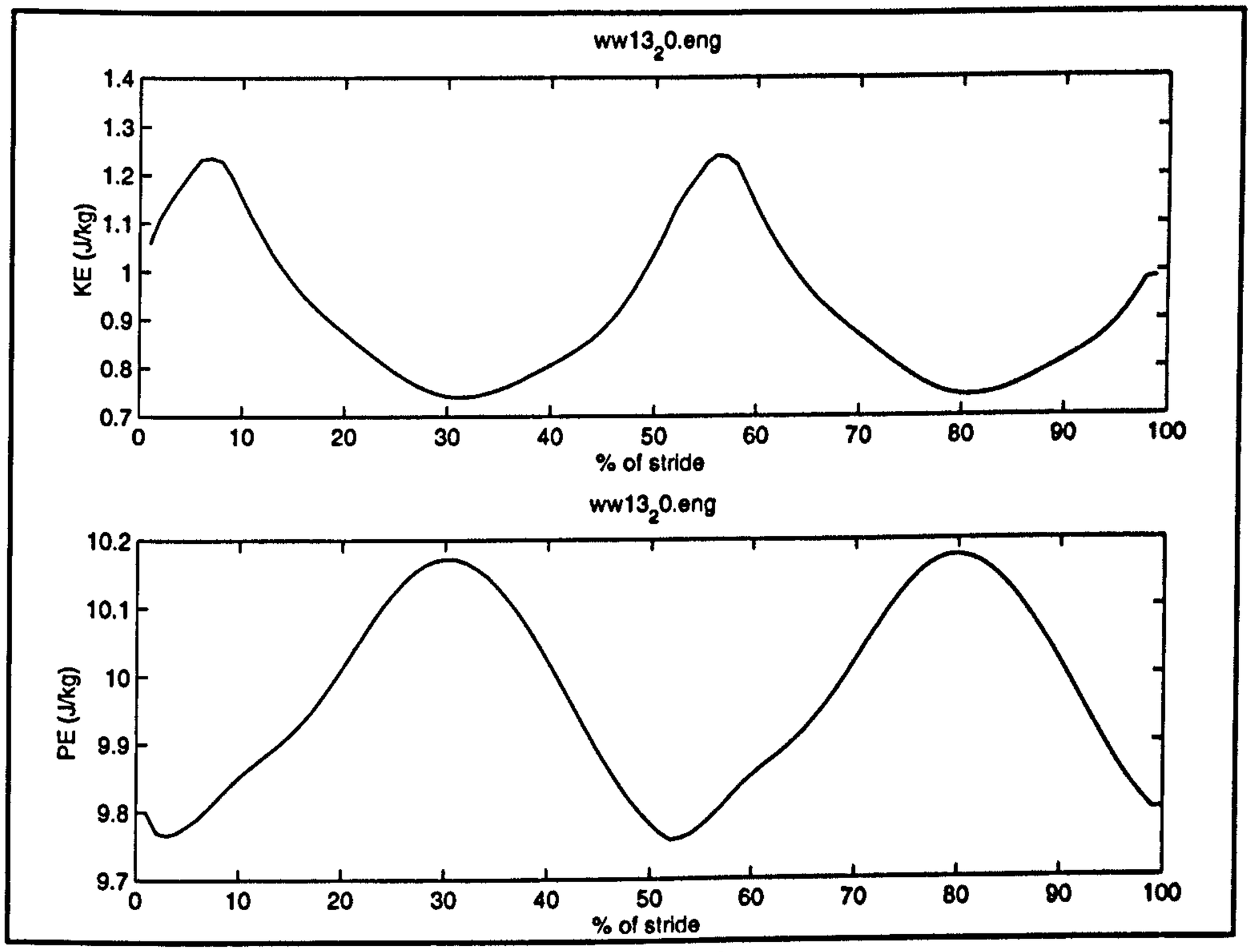

FIGURE A.14 Energy changes at the centre of mass

REFERENCES

ADAMS (1995) Automatic Dynamic Analysis of Mechanical System, Mechanical Dynamics, Inc.

Aiello, L. (1990) Patterns of stature and weight in human evolution. American Journal of Physical Anthropology, 81:186-187.

Aiello, L. and Dean, C. (1990) An introduction to human evolutionary anatomy. Academic Press, London.

Alexander, R. McN. (1968) Animal mechanics. Sidgwick and Jackson Ltd., London. Reedited (1983) by Blackwell Scientific Publication, Oxford.

Alexander, R. McN. (1980) Optimum walking techniques for quadrupeds and bipeds. *Zool.*, 192: 97-117.

Alexander, R. McN. (1984a) Elastic energy stores in running vertebrates. American Zoology, 24: 85-94.

Alexander, R. McN. (1984b) Walking and running. American Scientist, 72: 348-354.

Alexander, R. McN. (1985) The maximum forces exerted by animals. Journal of Experimental Biology, 115: 231-238.

Alexander, R. McN. (1991) Apparent Adaptation and Actual Performance. In:

Hecht, M.K., Wallace, B. and MacIntyre, R.J. (Eds.) Volutionary Biology, 25. New York: plenum, pp. 357-373.

Alexander , R. Mc.N. (1992) A model of bipedal locomotion on compliant legs. Phil. Trans. Roy. Soc. Lond. (B) 189-198.

Alexander, R. McN (eds) (1992) Mechanics of animal locomotion (in: Advances in Comparative and Environmental Physiology 11). Springer-Verlag Press, London.

Alexander, R. McN. and Goldspink, G. (1977) Mechanics and energetics of animal locomotion. Chapman and Hall Publish, London.

Alexander, R.McN. and Jayes, A.S. (1980) Fourier analysis of forces exerted in walking and running. Journal of Biomechanics 13, 383-390.

Apkarian, J. (1989) A three-dimensional kinematic and dynamic model of the lower limb. Journal of Biomechanics, 22: 143-155.

Basmajian, J. V. (1974) Muscle alive, their functions revealed by electromyography (3rd ed)., Williams and Wilkins Co., Baltimore.

Batholemew, G. A. and Birdsell, J. B. (1953). Ecology and the protohominids. *American Anthropol.*, 55: 481-498.

Bober, T. (1987) Factors influencing the angular velocity of a human limb segment. Journal of Biomechanics, 20: 511-521.

Broom, R. (1938a) The Pleistocene anthropoid apes of South Africa. Nature, 142: 377-379.

Broom, R. (1938b) Further evidence on the structure of South Africa Pleistocene anthropoids. Nature, 142: 897-899.

Broom, R. (1950) The genera and species of the South Africa Fossil ape-man. American Journal of Physical Anthropology, 8: 1-14.

Brown, F. Harris, J., Leakey, R. and Walker, A. (1985) Early Homo erectues skeleton from west Lake Turkana, Kenya. Nature, 316: 788-792.

Broom, R. and Schepers, G.W.H. (1946) The South Africa Fossil ape-man-the Australopithecinae. Transvaal Museum Memoir No. 4. Pretoria: South Africa.

Cappozzo, A. (1975) A general computing method for the analysis of human locomotion. Journal of Biomechanics, 8: 307-320.

Carey, T.S. (1999) Physiology of early hominid bipedalism. Thesis of Ph.D. The University of Liverpool.

Carrier, D. R. (1984) The energetic paradox of human running and hominid evolution. Curr. Anthrop., 25, 483-495.

Cavagna, G., Heglund, N. C. and Taylor, C. R. (1977) Mechanical work in terrestrial locomotion: two basic mechanisms for minimizing energy expenditure. American Journal of Physiology, 233(5): R243-R261.

Cavagna, G. A., Thys, H. and Zamboni, A. (1976) The sources of external work in level walking and running. Journal of Physiology, 262: 639-657.

Chandler, R. F., Clauser, C. E., McConville, J. T., Reynolds, H. M., Young, J. W. (1975) Investigation of the Inertial Properties of the Human Body. AMRL Tech.

Rep. 74 -137, Wright Patterson Air Force Base, Ohio.

Ciochon, R. L. and Fleagle, J. G. (1993) The human evolution source book, Prentice-Hall.

Clark, G. (1977) World prehistory (3rd ed.). Cambridge University Press, Cambridge.

Clark, J.D. (1980) The Plio-Pleistocene environmental and cultural sequence at Gadeb, northern Bale, Ethiopia. In: R.E. Leakey and B. Ogot, (Eds.) Proceedings of the 7th Panafrican Congress of Prehistory and Quaternary Studies. Nairobi: TILLMIAP) : pp. 189-193.

Clauser, C. E., McConville, J. T. and Young, J. W. (1969) Weight, Volume and Centre of Mass of Segments of the Human Body. Report AMRL-TR-69-70, Wright Patterson Air Force Base, Ohio.

Coolridge, H. J. (1933) Pan paniscus. Pigmy chimpanzee from South of the Congo River. American Journal of Physical Anthropology, 28: 1-57.

Crompton, R.H. and Gowlett J.A.J. (1993) Allometry and multidemensional from in Acheulean bifaces from Kilimbe, Kenya. Journal of Human Evolution, 25:175-199.

Crompton, R. H., Li, Y., Wang, W. J., Gunther, M. M. and Savage, R.(1998) The mechanical effectiveness of erect and "bent-knee,bent-hip" bipedal walking in Australopithecus Afarensis. Journal of Human Evolution, 35: 55-74.

Crowninshield, R. D. (1978) Use of optimization techniques to predict muscle forces. Journal of Biomechanical Engineering, 100: 88-92.

Dart, R. A. (1959) Adventures with the Missing Link. Harper: New York.

Day, R. A. (1986) Bipedalism: pressures, origins and modes. In B. Wood, L. Martin, and P. Andrews eds., "Major topics in primate and human evolution", Cambridge University Press: Cambridge, 188-202.

Day, M. H. (1977) Locomotor adaptation in man. Biol. Hum. Affairs, 42, 149-151.

Day, M. H. and Leakey, R. E. F. (1973) New evidence for the genus homo from East Rudolf, Kenya (I). American Journal of Physical Anthropology, 39: 341-354.

Darwin, C. (1871) The descent of Man and selection in relation to sex. John Murray, London.

Du Brul, E. L. (1962). – The general phenomenon of bipedalism. American Zoology, 2: 205-208.

Eickhoff, R. (1988). Origin of bipedalism – when, why, how and where? S. Afr. J. Sci., 84:486-488.

Eng, J. J. and Winter, D. A. (1995) Kinetic analysis of the lower limbs during walking: what information can be gained from a three-dimensional model? Journal of Biomechanics, 28(6): 753-758.

Etkin, W. (1954) Social behavior and the evolution of man's faculties. Am. Nat.,8: 129-142.

Fedak, M. A., and Seeherman, A. J. (1979) Reappraisal of energetics of locomotion shows identical cost in bipeds and quadrupeds including ostrich and horse. Nature, 282: 713-716.

Feldesman, M. R. and Lundy, J. K. (1988). Statues estimates for some African Plio-Pleistocene fossil hominids. Journal of Human Evolution, 17: 583-596.

Fifer, F. C. (1987) The adoption of bipedalism by the hominids: a new hypothesis. Hum. Evol., 2, 135-147.

Fleagle, J. G., Stern, J. T., Jungers, W. L., Susman, R. L., Vangor, A. K. and Wells, J. P. (1981) Climbing: a biomechanical link with brachiation and with bipedalism. In: Vertebrate Locomotion (M. H. Day, Ed.) ium of the Zoological Society of Londo. 48: 359-375.

Full, R. J. (1989) Mechanics and energetics of terrestrial locomotion: bipeds to polypods. Proceedings of the 10th Conference of the European Society for Comparative Physiology and biochemistry (edited by Wolfgang Wieser and Erich Gnaiger), 175-182. Published by Georg Thieme Verlag Stuttgart, New York.

Geist, V. (1978) Lifestrategies, human evolution, environmental design, Springer Verlag: New York.

Gowlett, J. A. J. (1982) Procedure and - form in a Lower Palaeolithic industry: stoneworking at-Kilombe, Kenya Studia Praehistorica Belgica 2: 101-109.

Guthrie, R. D. (1970) The evolution of human threat display organs. Evol. Biol., 4, 257-302.

Hardt, D. E. (1978a) A minimum energy solution for muscle force control during walking. Ph.D. thesis., MIT Dept. of Medical Engineering.

Hardt, D. E. (1978b) Determining muscle forces in the leg during normal human walking- an application and evolution of optimization methods. Journal of

Biomechanical Engineering, 100: 74-78.

Hardy, Y. A. (1960). Was man more aquatic in the past? New Scientist, 7, 642-645.

Harris, J.W.K. and Herbich, 1. (1978) Aspects of early Pleistocene hominid behaviour east of Lake Turkana, Kenya. In: Bishop, W.W. (Ed.) Geological, background to fossil man. Edinburgh: (Geol. Soc. London/Scottish Academic Press): pp. 529-548.

Hase, K. (1996) Neuro-musculo-skeletal models and the application of gene alrgtime to the evolution of bipedalism (in Japanses). Ph.D thesis, Keio University, Yokohama, Japan.

Hase, K. and Yamazaki, N. (1998) Computational evolution of human bipedal walking by a neuro-musculo-skeletal model. Proc. 3rd Int. Symp. on Artificial Life and Robotics, 174-177. Oita, Japan.

Hatze, H. (1977) A complete set of control equations for the muscleskeletal system. Journal of Biomechanics, 10: 799-805.

Hay, R .L. (1976) Geology of Olduvai Gorge. University of California Press, Berkeley.

Hewes, G. (1961) Food transport and the origin of hominid bipedalism. American Anthropologist, 63: 687-710.

Hill, A.V. (1938) The heat of shortening and dynamic constants of muscle. Proc. R. Soc. B. 126: 136-195.

Hill, A.V. (1950) The dimensions of animals and their muscular dynamics. Science

Progr. 38: 209-230.

Hirasaki, E. and Matano, S. (1996) Comparison of locomotor patterns and the cerebellar complex in Ateles and Macaca. Folia Primatologica, 66: 209-225.

Hof, A. L. and Berg, J. V. D. (1981) EMG to force processing I: an electrical analogue of the Hill muscle model. Journal of Biomechanics, 14(11): 747-758.

Hreljac, A. (1995) Determinants of the gait transition speed during human locomotion: kinematic factors. Journal of Biomechanics, 28: 669-677.

Hunt, K. D. (1990 Implications of chimpanzee positional behavior for the reconstruction of early hominid locomotion and posture. American Journal of Physical Anthroplogy, 81, 242.

Hunt, K.D. (1994) The evolution of human bipedality: ecology and functional morphology. Jounral of Human Evolution 26: 183-202.

Isaac, G. LI. (1972) Chronology and the tempo of cultural change during the Pleistocene. In Calibration of hominoid evolution (eds Bishop, W. W. and Miller, J. A.), Scottish Academic Press, Edinburgh.

Isaac, G. LI. (1978) Food sharing and huanam evolotion: archarologlical evodence from the plio pleostocene of east afroca. Journal of Anthropological Research, 34: 311-325.

Ishida, H., Kumakura, H. and Kondo, S. (1985) Primate bipedalism and quartpedalism: comparative electrography. In: *Primate Morphophysiology, Locomotion Analysis and Human Bipedalism* (S.Kondo, Ed.), 59-80. Tokyo: University of Tokyo Press.

Iwamoto, M. (1985) Bipedalism of Japanese monkeys and carrying models of hominization. In S, Kondo ed., "Primate morphophysiology, locomotor analyses, and human bipedalism". University of Tokyo Press: Tokyo, 251-260.

Jackson, K. M., Joseph, J. and Wyard, S.J. (1977) Sequential musclular contraction. Journal of Biomechanics, 10: 97-106.

Jacobs, R., Bobbert, M. F. and van Ingen Schenau, G. J. (1996) Mechanical Output from Individual Muscles during explosive leg extensions: the role of biarticular muscles. Journal of Biomechanics, 29(4): 513-523.

Jenkins, F. (1972) Chimpanzee bipedalism: cineradiographic analysis and implications for the evolution of gait. Science, 178: 887-879.

Jensen, R. K. (1989) Changes in segment inertia proportions between 4 and 20 years. Journal of Biomechanics, 22: 529-536.

Johanson, D. C., Lovejoy, C. O., Kimbel, W. H., White, T. D., Ward, S. C. Bush, M. E., Latimer, B. M. and Coppens, Y. (1982) Morphology of the Pliocene Partial hominid skeleton (AL 288-1) from the Hadar formation, Ethiopia. American Journal of Physical Anthropology, 57: 403-452.

Johanson, D. C., Masao, F. T., Eck, G. G., White, T. D., Walter, R. C., Kimbel, W. H., Asfaw, B., Manega, P., Nolessokia, P. and Suwa, G. (1987) New partial skeleton of Homo habilis from Olduvai Gorge, Tanzania. Nature, 327: 205-209.

Johanson, D. C. and White, T. D. (1979) A systematic assessment of early African hominids. Science, 202: 321-330.

Jolly, C. J. (1970) The seed-eaters: a new model of hominid differentiation based on

a baboon analogy. Man, 5, 1-26.

Joseph, J. (1975) Movements at the hip joint. Annals of the Royal College of Surgeons of England, 56: 192-201.

Jungers, W. L. (1982) Lucy's limbs: skeletal allometry and locomotion in Austral afarensis. *Nature*, 297: 676-678.

Jungers, W. L. (1985) Body size and scaling of limb proportions in primates. In: Size and scaling in Primate biology (Jungers, W.L. Ed.), pp. 345-381. New York: Plenum Press.

Jungers, W. L. (1987) Relative joint size and locomotor adaptations in the hominidea. *Ame. J. Physi. Anthro.*, 73:216-217.

Jungers, W. L. (1988) Lucy's length: stature reconsturction in Australopitbecus afarensis (AL 288-1) with implications for other smallbodied hominids. American Journal of Physical Anthropology, 76: 227-231.

Jungers, W. L. and Stern, J. T., Jr. (1983) Body proportions, skeletal allometry locomotion in the Hardar hominids: a reply to Wolpoff. Journal of Human Evolutio, 12:673-684.

Khalil, T. M. and Martinez, A. G. (1976) EMG models of mechanical torque. Biomechanics V-A. P. Komi, University Park Press, Baltimore: 233-239.

Kimura, T. (1986). Bipedal and Quadrupedal walking of Primates: Comparative Dynamics. In (S. Kondo, Ed.) Primate Morphophysiology, Locomotor Analyses and Bipedalism, pp. 81-104.. Tokyo: University of Tokyo Press.

Kimura, T. (1996) Centre of gravity of the body during the ontogeny of chimpanzee bipedal walking. Folia Primatol., 66: 126-136.

Kimura, T., Okada, M. and Ishida, H. (1979) Kinesiological characteristics of primate walking: its significance in human walking. In: Environment, Behaviour and Morphology: Dynamic Interactions in Primates (M. E. Morbeck, H. Preuschoft and N.Gomberg, Eds.), 297-311. New York: Gustav Fischer.

Kistle (1995) A registered trade make of Kistler Instrumente AG, Switzerland. Kistle Manual published in Switzerland.

Kohler, W. (1959) The Mentality of Apes. Vintage Books: New York.

Kortland, T. A. (1980) How might early hominids have defended themselves against large predators and food competitors 2 f. Hum. Evol., 9, 79-112.

Kumakura, H. (1989). Functional Analysis of the Biceps Femoris Muscle During Locomotor Behavior in Some Primates. American Journal of Physical Anthropology, 79: 379-391.

Kumakura, H. , Hrasaki, E. and Nakano, Y. (1996) Organization of the Epaxial Muscles in Terrestrial and Arboreal Primates. Folia Primatol., 66: 25-37.

Lancaster, J. (1978) Carrying and sharing in human evolution. Human Nature, 1: 82-89.

Latimer, B. (1991) Locomotor adaptations in *Australopithecus afarensis*: the issue of bipedality. In (Y. Coppens and B. Senut, Eds.) Origine(s) de la bipJdie chez les hominidJs, pp. 169-176, Paris: Editions du CRNS.

Latimer, B., and Lovejoy, C.O. (1989) The Calcaneus of Australopithecus afarensis. American Journal of Physical Anthroplogy. 78: 369-386.

Leakey, M.D., (1971) Olduvai Gorge, Vol. III: Excavations in Beds I and 11, 1960-1963. Cambridge (Cambridge University Press).

Leakey, M. D. (1979) Footprints in the Laetolil beds at Laetoki, north Tanzania. Nature 278: 317-323.

Leakey, M. D. and Hay, R. L. (1979) Pliocene footprints in the Laetolil beds at Laetoli, north Tanzania. Nature, 278: 317-323.

Li, Y. , Crompton, R. H., Alexander , R. McN. , Gunther, M. M. and Wang, W. J. (1996) Characteristics of ground reaction forces in normal and chimpanzee-like bipedal walking by human. Folia Primatologica, 66: 137-159.

Livingstone, F. B. (1962) Reconstructing man's Pliocene ancestor, American Anthropology. 64, 301-305.

Lovejoy, C. O. (1978) A biomechanical review of the locomotor diversity of early hominds, in early hominds of African. (C. Jolly, Ed.), 403-443. Duckworth, London.

Lovejoy, C. O. (1981) The origin of man. Science, 211, 341-350.

MacConaill, M. A. and Basmajian, J.V. (1977) Muscles and movements - a basis for human kinesiology. Robert and Krieger Publishing Co., Inc.

Marett, J. R. de la H. (1936) Race, Sex, and Environment. Bale: London.

Marzke, M. W. (1986) Tool use and the evolution of hominid hands and bipedality. In J. G Else and P. C. Lee eds., "Primate evolution", Cambridge University Press: Cambridge, 203-209.

Matlab (1984-) Registered trade mark of The MathWorks, Inc.

McGrew, W.C.(1993) Primate behavior - information, social knowledge, and the evolution of culture - QUIATT,D, REYNOLDS,V. Nature, 365 (No.6449), p.794.

McHenry, H. M. (1988) New estimates of body weight in early hominids and their significance to encephalization and megadontia in 'robust' australopithecines, In: Evolutionary History of the 'Robust' Australopithecines (F. E. Grine, Ed.), 133-148. New York: Aldine de Gruyter.

McHenry, H. M. (1992) Body size and proportions in early hominid. American Journal of Physical Anthropology 87: 407-431.

McHenry, H. M., and Temerin, L. A. (1979) The evolution of hominid bipedalism: evidence from the fossil record. Yearbook of Physical Anthropology 22: 105-131.

McMahon, T. A. (1975) Using body size to understand the structural design of animals: quadrupedal locomotion. Journal of Applied Physiology, 99: 619-627.

McMahon, T. A. (1984) Muscles, reflexes and locomotion. *Princeton University Press*, Princeton, New Jersey.

McMahon, T. A. (1985) The role of compliance in mammalian running gaits. Journal Experimental Biology 115: 263-282.

Merker, B. (1984) A note on hunting and hominid origins. American Anthropology

86, 112-114.

Montgomery, G. D. (1988) Rhythmical man: an alternative hypothesis to ape-human evolution. Speculations in Science and Technology, 11, 153- 159.

Morgan, E. (1982) The Aquatic Ape. Souvenir: London.

Napier, J. R. (1963) The locomotor functions of hominids. In (S. L. Washburn ed.): Classification and human evolution. Viking Fund Publications in Anthropology: New York, 178-189.

Napier, J.R. (1976) Primate locomotion. Oxford University Press, London..

Napier, J. R. and Napier, P. H. (1967) A handbook of living primates. Academic Press, London.

Morgan, E. (1972) The Descent of Woman. Souvenir Press, London.

Morrison, J. B. (1970) The mechanics of muscle function in locomotion. Journal of Biomechanics 3: 431-451.

Nigg, B. and Herzog, W. (1994) Biomechanics of the musculo-skeletal system. John Wiley and Sons Ltd., England.

Ohman, J. O., Wood, C. G., Wood., B. W., Crompton, R. H., Gunther, M. M. and Li, Y., Savage, R. and Wang, W.J. (1997, Manuscript submitted) Body size and shape of KNM-WT 15000 (Abstrct). Theoretical Anthropology Group (TAG) Annual Conference, p. 29-30.

Okada, M. (1985) Primate bipedal walking: comparative kinematics. In: Primate

Morphophysiology, Locomotion Analysis and Human Bipedalism (S. Kondo, Ed.), 47- 58. Tokyo: University of Tokyo Press.

Olney, S. J. (1991) Work and power in gait of stroke patients. Arch. Physical Medical Rehabiliation, 72:309-14.

Olney, S. J. and Winter, D. A. (1985) Prediction of knee and ankle moments of force in walking from EMG and kinematic data. Journal of Biomechanics, 18(1): 9-20.

Parker, S. T. (1987) A sexual selection model for hominid evolution. Hum. Evol., 2, 235-253.

Patriarco, A. G., Mann, R. W., Simonss, S. R. and Mansourss, J. M. (1981) An evaluation of the approaches of optimization models in the prediction of muscle forces during human gait. Journal of Biomechanics 14(8): 513-525.

Pilbeam, D. R. (1980) Major trends in human evolution. In: Current Angument on Early Man, (L. K. Konigsson. Ed.), 261-285. Pergamon Press, Oxford.

Pilbeam, D. and Gould, S. J. (1974) Size and scaling in human evolution. Science, 186: 892-900.

Preuschoft, H. (1970) Functional anatomy of the lower extremity. In: The Chimpanzee, (G. H. Bourne, Ed.), 3: 221-294. Basel: Karger.

Preuschoft, H. (1971a) Mode of locomation in subfossil giant lemurids from Madaga Proc.3rd Int.Congr.Primat.Zurich 1970, 79-90. Basel: Karger.

Preuschoft, H. (1971b) Body posture and mode of locomotion in early Pleistocene

Hominids. Folia Primat. 14:209-240.

Preuschoft, H. (1973) Functional anatomy of the upper extremity. In The Chimpanzee, 6, (Bourne G. H. Ed.), 34-120. Basel: Karger.

Preuschoft, H. (1978) Recent results concerning the biomechanics of man's acquisition of bipedality, in: Recent Advances in Primatology Evolution (Chivers and Joysey, Eds.), 3: 435-458. Academic Press, London.

Preuschoft, H. and Witte, H. (1991) Biomechanical reasons for the evolution of hominid body shape, in: Origines De La Bipedie Chez Les Hominides (Cahiers de Paleoanthropologie). Editions du CNRS, Paris.

Prost, J. H. (1980). Origin of bipedalism. American Journal of Physical Anthropology 52: 175-189.

Ravey, M. (1978) Bipedalism: an early warning system for Miocene hominoids. Science, 199, 372.

Reynolds, E. (1931) The evolution of the human pelvis in relation to the mechanics of the erect posture. Pap. Peabody Mus. American Journal of Archaeol. Ethnol., 11, 255- 334.

Reynolds, T. R. (1985) Stresses in the limbs of quadrupedal primates. American Journal of Physical Anthropology 67: 351-362.

Reynolds, T. R. (1987) Stride length and its determinants in humans, early hominid, primates and mammals. American Journal of Physical Anthropology, 46: 29-44.

Rodman, P. S. and McHenry, H. M. (1980) Bioenergetics and the origin of hominid

bipedalism. American Journal of Physical Anthropology 52: 103-106.

Rose, M. D. (1984) Food acquisition and the evolution of positional behavior: the case of bipedalism. In D.J. Chivers, B.A. Wood and A. Bilsborough eds., Food acquisition and processing in primates, Plenum Press: New York, 509-524.

Rose, M. D.(1991) The process of bipedalalization in hominids. In Y.Coppens and B.Senut (eds), Origine(s) de la bipedie chez les hominides: 37-48. Paris: CNRS.

Ruff, C.B. and Walker, A. (1993) in *The Nariokotome* Homo erectus Skeleton. Eds.by Walker A, Leakey R. Cambridge: Harvard University Press 234-265.

Savage, R. (1995) VC- an software on capturing pictures from video records. Internal manual in the Department of Huaman anatomy and Cell Biology, the University of Liverpool.

Schenau, G. J. van Ingen and Cavanagh, P. R. (1990) Power equations in endurance sports. Journal of Biomechanics 23: 865-881.

Schmid, P. (1983) Eine Rekonstrucktion des Skelettes von A.L. 288-1 (Hadar) und deren Konsequenzen. Folia Primatologica 40:283-306.

Schmitt, D., Stern, J.R. and Larson S.G. (1996) Compliant gait in humans: Implications for substrate reaction forces during australopithecine bipedalism. American Journal of Physical Anthropology. Suppl 22:209 (Abstract).

Schultz, A.H. (1937) Proportions, variability, and asymmetries of the long bones of the limbs and the clavicles in man and apes. Human Biology 9:281-328.

Seireg, A. and Arvikar, R.J. (1973) A mathematical model for evaluation of forces

in lower extremities of the musculoskeletal system. Journal of Biomechanics 6: 313-326.

Shipman, P. (1986) Scavenging or hunting in early hominoids: theoretical framework and tests. American Anthropology 88, 27-43.

Sigmon, B. A. (1971) Bipedal behavior and the emergence of erect posture in man. American Journal of Physical Anthropology 34, 55-60.

Simons, E. (1972) Primate Evolution. Macmillan, New York.

Sinclair, A. R. E., Leakey, M. D. and Norton-Griffiths, M. (1986) Migration and hominid bipedalism. Nature, 324, 307-308.

Stern, J. T. and Susman, R. L. (1983) The locomotion anatomy of Australopithecus afarensis. American Journal of Physical Anthropology 60:279-317.

Steudel, K. (1996) Limb morphology, bipedal gait, and the energetics of hominid locomotion. American Journal of Physical Anthropology 99: 345-355.

Susman, R.L., Stern, J.T. and Jungers, W.L. (1984) Arborcality and bipedality in the Hadarhominids. Folia Primatol. 43, 113-156.

Swisher, C.C., Curtis, G.H. Jacob, T., Getty, A.G., Suprijo, A. and Widaasmoro. (1994) Age of the Earliest Known Hominids in Java, Indonesia. Science 263: 1118-1121.

Szalay, F. (1975) Hunting-scavenging protohominids: a model for hominid origins. Man, 10, 420-429.

Tardieu, C. (1987) La centre du gravitJ pendant la marche.Paris: Editions du CRNS.

Tardieu, C., Aurengo, A. .and Tardieu B. (1993) New method of three-dimensional analysis of bipedal locomotion for the study of displacements of the body and body-parts centers of mass in man and non-human primates: evolutionary framework. American Journal of Physical Anthropology 90, 455-476.

Taylor, C. R., Schmidt-Nielsen, K. and Raab, J. L. (1970) Scaling of energetic cost of running to body size in mammals. American Journal of Physiology, 219: 1104-1107.

Taylor, C. R., Heglund, N. C., McMahon, T. A. and Lonney, T. R. (1980) Energetic cost of generating muscular force during running: a comparison of large and small animals. Journal of Experimental Biology, 86: 9-18.

Taylor, C. R. (1985) Force development doing sustained locomotion: a determinant of gait, speed and metabolic power. Journal of Experimental Biology, 115: 253-262.

Tuttle, R. H., Basmajian, J. V., and Ishida, H. (1979) Activities of pongid thigh muscles during bipedal behaviour. American Journal of Physical Anthropology, 50: 123-136.

Veerhaegen, M. (1985) The aquatic ape theory: evidence and a possible scenario. Med. Hypotheses, 16, 17-21.

Walker, A. C. and Leakey, R. E. (1986) Homo erectus skeleton from West Lake Turkana, Kenya. American Journal of Physical Anthropology, 69: 275 (Abstr.).

Walsh, E. G. and Wright, G. W. (1987) Inertia, resonant frequency, stiffness and kinetic energy of the human forearm. Quarterly Journal of Experimental Physiology, 72: 161-170.

Wang, W. J., Crompton, R. H., Li, Y., and Gunther, M. M. (1996) Comparison of the powers at the lower limb joints during walking at different velocities and their significance for a possible optimal walking velocity. The proceedings of the 1st International Conference on the Sport Engineering,p.71-76. Sheffield, U.K..

Washburn, S. L. (1967) Behavior and the origin of man. Proc. Roy. Anthropol. Inst., 3: 21-27.

Washburn, S. L. and Moore, R. (1980) Ape into Human. 2nd edn. Little, Brown and Co., Boston.

Washburn, S. L. and Lancaster, C. (1968) Hunting and human evolution. In: The Origns of Man, (I.DeVore, Ed.), 293-303. Aldine, Chicago.

Webb, D., Tuttle, R. H. and Baksh, M. (1994) Pendular activity of human upper limbs during slow and normal walking. American Journal of Physical Anthropology 93: 477-489.

Weiss, P. L. (1986) Position dependence of ankle joint dynamics-I:passive mechanics. Journal of Biomechanics 19: 727-735.

Wells, R.P. (1988) Mechanical energy costs of human movement: an approach to evaluating the transfer possibilities of two-joint muscles. Journal of Biomechanics, 21: 955-964.

Wescott, R. W. (1967) The exhibitionistic origin of human bipedalism. Man, 2,

630.

Wheeler, P.E. (1992) The thermoregulatory advantages of larger body size for hominids foraging in savannah environments. Journal of Human Evolution 23: 351-362.

Wheeler, P.E. (1993) The influence of stature and body form on hominid energy and water budgets: a comparison of Australopithecus and early Homo. Journal of Human Evolution 24: 13-28.

William, K. R. and Cavanagh, P. R. (1983) A model for calculation of mechanical power during distance running. Journal of Biomechanics, 16: 115-128.

William Sellers. (1994) Thesis PhD, the University of Liverpool.

Wilson, L. (1988) Petrography of the Lower Palaeolithic tool assemblage of the Caune de 11Arago (France). World Archaeology 19: 376-387.

Winter, D. A. (1979) A new definition of mechanical work done in human movement. Journal of Applied Physiology: Respirat Environ. Exercise Physiology 46(1): 79-83.

Winter, D. A. (1983) Energy generation and absorption at the ankle and knee during fast, natural and slow cadences. Clinical Orthopaedics and Related Research, 175: 147-154.

Winter, D. A. (1988) Biomechanics of belower-knee amputee gait. Journal of Biomechanics, 21: 361-367.

Winter, D. A. (1990) Biomechanics and motor control of human movement. John

Wile Sons, Inc. New York.

Winter, D. A. (1991) The biomechanics and motor control of human gait: normal, elderly and pathological (2nd ed.). University of Waterloo Press. Canada.

Witte, H., Preuschoft, H.and Recknagel, S. (1991) Human body proportions explained on the basis of biomechanical principles. Z. Morphol. Anthropol. 78(3):407-423.

Wolpoff, M. H. (1983a) Lucy's litter legs. Journal of Human Evolution, 12: 443-453.

Wolpoff, M. H. (1983b) Lucy's lower limbs: long enough for Lucy to be fully bipedal? Nature 304: 59-61.

Wood, B.A. (1994) Four legs good, two legs better. Nature, 363: 587-588.

Wrangham, R. W. (1980) Bipedal locomotion as a feeding adaptation in Gelada baboons and its implications for hominid evolution. Journal of Human Evolution, 9, 329-331.

Wundram, I. J. (1986) Cortical motor asymmetry and hominid feeding strategies. Human Evolution, 1:183-188.

Yaguramaki, N., Nishizawa, S., Adachi, K. and Endo, B. (1995) The relationship between posture and external forces in walking. Anthropol. Sci. 103:107-140..

Yamazaki, N. (1985) Primate bipedal walking: computer simulation. In: Primate Morphophysiology, Locomotion Analysis and Human Bipedalism (S.Kondo, Ed.), 59-80. Tokyo: University of Tokyo Press.

Yamazaki, N., Hase, K., Ogihara, N. and Hayamizu, N. (1996) Biomechanical analysis of the development of human bipedal walking by a neuro-musculo-skeletal model. Folia Primatol., 66: 253-271.

Zarrugh, M. Y. (1981) Power requirements and mechanical efficiency of treadmill walking. Journal of Biomechanics 14: 157-165.

Zihlman, A. L. and Cramer, D. L. (1978) A skeletal comparsion between pygmy (Pan paniscus) and common chimpanzees (Pan troglodytes). Folia Primatologica, 29: 86-94.

Zihlman, A. L. and Tanner, N. (1979) Gatherimg and the homind adaptation, in female hierarchiess, (T. Tiger and H.M. Fowler, Eds.), 163-194. Beresford Book Service, Chicago.

PAGE NUMBERING AS ORIGINAL

Related publications

Wang,W, Crompton, R.H, Gunther, M.M and Li.Y. (1998) The finite point method: a new computational method for modelling a multi-body android and simulating dynamics, and the application reconstruction of human walking. Presented in the Third World Congress of Biomechanics, August 1998, Osaka, Japan.

Wang,W,Crompton,R.H.,Wood, C., Gunther,M.M and Li.Y. (1998) The concept of positive and negative signs for work, power and energy, and their special meanings in biomechanics. The Proceedings of the 2nd International Conference of the Sports Engineering, July, 1998 (edited by Haak A), pp.225-232, AA Black Publish.

Wang,W,Crompton,R.H,Gunther,M.M, Li.Y and Wood,C (1998) Dynamic analysis of motion stability in different velocities and heights of the body centre of mass during loaded walking, and possible optimum area for different walking ways. The proceedings of the XVI International Symposium on Biomechanics in Sports, vol 1: 277-280, July, 1998, Konstanz, Germany.

Wang W, Crompton, R.H, Gunther,M.M and Li.Y. (1997) Energy transformation during erect and bent-knee walking by humans, and its significance for the evolution of human bipedalism. Submitted to American Journal of Physical Anthropology and in reviewing.

Wang,W, Crompton,R.H.,Li,Y. and Gunther,M.M (1996) The comparison of the powers at lower limb joints at different velocities and a possible optimum walking velocity. The proceedings of the First conference of Sports Engineering July 1996, Sheffield, U.K., pp.71-76, edited by Dr.Haak,A, AA Black Publish.

Crompton, R. H, Li.Y.,Wang W.J., Gunther,M.M and Savage,R.(1998) The mechanical effectiveness of erect and "bent-knee,bent-hip" bipedal walking in Australopithecus Afarensis. Journal of Human Evolution,35: 55-74.

Ohman, James C., Chris Wood, Bernard Wood, Robin H. Crompton, Michael M.Gunther, Li Yu, Russell Savage, and Weijie Wang (1997) Body size and shape of KNM-WT 15000. Abstracts, Theoretical Anthropology Group (TAG) Annual Conference 1997,p. 29-30.

Gunther,M.M,Li Y.,Crompton,R.H and Wang W.J. (1996) The evolution of bipedal walking: a biomechanical view. Primate Report, 44:14-15.

Crompton,R.H,Li.Y.,Alexander,R.McN.,Wang W.J.and Gunther,M.M(1996) Segment inertial properties of primate: new techniques for laboratory and field studies of locomotion. American Journal of Physical Anthropology, 99:547-570.

Li.Y.,Crompton,R.H,Alexander,R.McN.,Gunther,M.M and Wang W.J.(1996) Characteristics of ground reaction forces in normal and chimpanzee-like bipedal walking by human. Folia Primatologica, 66:137-152.